

University of Warwick institutional repository: <http://go.warwick.ac.uk/wrap>

A Thesis Submitted for the Degree of PhD at the University of Warwick

<http://go.warwick.ac.uk/wrap/77656>

This thesis is made available online and is protected by original copyright.

Please scroll down to view the document itself.

Please refer to the repository record for this item for information to help you to cite it. Our policy information is available from the repository home page.

**Towards sequence controlled functional polyesters:
Advances in the ring-opening (co)polymerisation of
large ring and ϵ -substituted lactones**

James Wilson

Submitted for the degree of Doctor of Philosophy



Department of Chemistry

May 2015

Table of Contents

Table of Contents	i
List of Figures, Schemes, and Tables	iv
List of Figures	iv
List of Schemes	xi
List of Tables	xii
Acknowledgments	xiv
Declaration of Authorship	xv
Publications	xvi
Abstract	xvii
List of Abbreviations	xix
List of Lactones	xxv
1 Introduction	1
1.1 Introduction	2
1.2 Ring-opening polymerisation	3
1.2.1 <i>Thermodynamics of ring-opening polymerisation</i>	3
1.2.2 <i>ROP catalysts</i>	5
1.2.3 <i>'Immortal' ring-opening polymerisation</i>	6
1.3 Lactone polymerisation	7
1.3.1 <i>Transesterification side reactions</i>	9
1.4 Pentadecalactone polymerisation	10
1.5 Pentadecalactone copolymerisation	13
1.5.1 <i>Copolymerisation with other non-substituted lactones</i>	13
1.5.2 <i>Copolymerisation with other monomers</i>	15
1.5.3 <i>Copolymers through functional initiation</i>	19
1.5.4 <i>PDL copolymers for post-polymerisation modification</i>	20
1.6 References	21
2 The 'immortal' ring-opening polymerisation of pentadecalactone by Mg(BHT) ₂ (THF) ₂	28
2.1 Introduction	29
2.2 Results and Discussion	30
2.2.1 <i>Synthesis of Mg(BHT)₂(THF)₂</i>	30
2.2.2 <i>Inert homopolymerisation of PDL</i>	31
2.2.3 <i>Non-inert polymerisation of PDL</i>	35
2.2.4 <i>Effects of solvent on polymerisation</i>	39
2.2.5 <i>'Immortal' polymerisation of PDL</i>	42
2.2.6 <i>'Immortal' polymerisation of εCL</i>	44
2.2.7 <i>'Immortal' polymerisation of δVL</i>	46
2.3 Conclusion	48

2.4	References	49
3	Synthesis of ω -pentadecalactone copolymers with independently tuneable thermal and degradation behaviour	51
3.1	Introduction	52
3.2	Results and Discussion	54
3.2.1	<i>Ring-Opening Homopolymerisations</i>	54
3.2.2	<i>Pentadecalactone copolymerisations</i>	57
3.2.3	<i>Sequential Polymerisation</i>	70
3.2.4	<i>Thermal Analysis</i>	74
3.2.5	<i>Crystallographic Analysis</i>	78
3.2.6	<i>Degradation Studies</i>	79
3.3	Conclusion	80
3.4	References	81
4	Synthesis and post-polymerisation modification of one-pot ω -pentadecalactone block- <i>like</i> copolymers	84
4.1	Introduction	85
4.2	Results and Discussion	87
4.2.1	<i>Homopolymerisation of menthide</i>	87
4.2.2	<i>Copolymerisation of PDL and MI</i>	91
4.2.3	<i>Triblock copolymers of PDL and MI</i>	103
4.2.4	<i>PDL block copolymers</i>	107
4.2.5	<i>Post polymerisation modification of P(PDL-co-DHC)</i>	110
4.3	Conclusion	113
4.4	References	113
5	Towards sequence control of lactone ROP: Copolymers from ϵ -substituted ϵ -lactones	115
5.1	Introduction	116
5.2	Results and Discussion	117
5.2.1	<i>MI copolymerisation with other lactones</i>	117
5.2.2	<i>Transesterification of ϵ-substituted ϵ-lactones</i>	122
5.2.3	<i>Terpolymerisation of ϵ-caprolactone, menthide and ω-pentadecalactone</i>	127
5.2.4	<i>ϵSL block copolymers</i>	134
5.2.5	<i>Sequence control of ϵ-substituted ϵCLs</i>	139
5.3	Conclusion	151
5.4	References	152
6	Conclusions	155
6.1	Conclusions	156
7	Experimental	158
7.1	Materials	159
7.2	Instrumental methods	159
7.3	Experimental procedures for Chapter 1	160
7.3.1	<i>Synthesis of $\text{Mg}(\text{BHT})_2(\text{THF})_2$</i>	160
7.3.2	<i>General procedure of δ-valerolactone polymerisation</i>	160
7.3.3	<i>General procedure of ϵ-caprolactone polymerisation</i>	161

7.3.4	General procedure of ω -pentadecalactone polymerisation	161
7.4	Experimental procedures for Chapter 2	162
7.4.1	Synthesis of η -caprylolactone	162
7.4.2	Synthesis of ω -dodecalactone	162
7.4.3	General procedure of lactone and ω -pentadecalactone copolymerization....	163
7.4.4	General Procedure of Degradation Studies	165
7.5	Experimental procedures for Chapter 3	165
7.5.1	Synthesis of menthide	165
7.5.2	Synthesis of dihydrocarvide	166
7.5.3	General procedure of menthide complexation	166
7.5.4	General procedure of menthide homopolymerization	167
7.5.5	General procedure of menthide and ω -pentadecalactone copolymerization.	167
7.5.6	General procedure of ω -pentadecalactone and ε -substituted ε -lactone copolymerization	168
7.5.7	General procedure for the transesterification of poly(menthide) and poly(ω - pentadecalactone)	170
7.5.8	General procedure for thiol-ene addition to P(PDL-co-DHC)	170
7.6	Experimental procedures for Chapter 4	172
7.6.1	Synthesis of ε -heptalactone	172
7.6.2	General procedure of menthide and non-substituted lactone copolymerization 172	
7.6.3	General procedure of menthide and ε -substituted ε -lactone copolymerization 174	
7.6.4	General procedure for the transesterification of poly(menthide) and poly(ε - caprolactone)	175
7.6.5	General procedure for the transesterification of poly(menthide) and poly(ε - heptalactone)	176
7.7	References	176

List of Figures, Schemes, and Tables

List of Figures

Figure 1.1 Small ring lactones and corresponding standard enthalpies and entropies of ring-opening.	4
Figure 1.2 Differences between ‘immortal’ ROP and ‘classical’ ROP.	6
Figure 1.3 Examples of substituted lactones and macrolactones.	8
Figure 1.4 Examples of organocatalysts for ROP.	12
Figure 1.5 Examples of organometallic catalysts used in ROP.	13
Figure 1.6 Organometallic catalysts with the ability to polymerise ω -pentadecalactone. ...	15
Figure 1.7 Examples of unsaturated macrolactones.	16
Figure 2.1 ^1H NMR spectrum of $\text{Mg}(\text{BHT})_2(\text{THF})_2$ (400 MHz, C_6D_6 , 298 K).	31
Figure 2.2 ^1H NMR spectrum of DP20 PPDL produced using $\text{Mg}(\text{BHT})_2(\text{THF})_2$ as a catalyst (400 MHz, 298 K, CDCl_3).	32
Figure 2.3 Kinetic plot for the polymerisation of ω -pentadecalactone using $\text{Mg}(\text{BHT})_2(\text{THF})_2$ as a catalyst at 80 °C in toluene with $[\text{PDL}]_0:[\text{BnOH}]_0:[\text{cat.}]_0 = 50:1:1$ and initial monomer concentration = 1 M.	33
Figure 2.4 M_n and \mathcal{D}_M changes over monomer conversion in the homopolymerisation of ω -pentadecalactone at 80 °C in toluene with $[\text{PDL}]_0:[\text{BnOH}]_0:[\text{cat.}]_0 = 50:1:1$ and initial monomer concentration = 1 M.	34
Figure 2.5 SEC chromatograms of poly(ω -pentadecalactone) at various targeted DPs.	35
Figure 2.6 a) Kinetic plot and b) change in M_n and \mathcal{D}_M against monomer conversion for the polymerisation of ω -pentadecalactone in a non-inert environment, using $\text{Mg}(\text{BHT})_2(\text{THF})_2$ as a catalyst at 80 °C in toluene with $[\text{PDL}]_0:[\text{BnOH}]_0:[\text{cat.}]_0 = 50:1:1$ and initial monomer concentration = 1 M.	36
Figure 2.7 SEC chromatograms for the evolution of molecular weight distribution throughout polymerisation of PDL in non-inert conditions, targeting a DP of 20.	37
Figure 2.8 a) MALDI-TOF of DP10 PPDL produced in a dry argon environment b) MALDI-TOF of DP10 PPDL produced in non-inert conditions.	38
Figure 2.9 SEC chromatograms for DP 20 PPDL produced in various solvents.	40
Figure 2.10 SEC chromatographs of DP 50 PPDL produced in various ratios of hexanes : toluene.	42
Figure 2.11 SEC chromatograph for the molecular weight distribution of targeted DP100 PCL using 0.1 eq. $\text{Mg}(\text{BHT})_2(\text{THF})_2$ catalyst with respect to benzyl alcohol initiator.	45
Figure 2.12 SEC chromatographs of DP 100 PVL produced with varying molar ratios of $\text{Mg}(\text{BHT})_2(\text{THF})_2$ catalyst.	47

Figure 3.1 a) Kinetic plot for the homopolymerisation of η -caprylolactone using $\text{Mg}(\text{BHT})_2(\text{THF})_2$ as a catalyst at 80 °C in toluene with $[\eta\text{CL}]_0:[\text{BnOH}]_0:[\text{cat.}]_0 = 50:1:1$, total monomer concentration = 1 M. b) Changes in M_n and \bar{D}_M over monomer conversion for the same polymerisation.....	55
Figure 3.2 a) Kinetic plot for the homopolymerisation of dodecalactone using $\text{Mg}(\text{BHT})_2(\text{THF})_2$ as a catalyst at 80 °C in toluene with $[\text{DDL}]_0:[\text{BnOH}]_0:[\text{cat.}]_0 = 50:1:1$, total monomer concentration = 1 M. b) Changes in M_n and \bar{D}_M over monomer conversion for the same polymerisation.....	56
Figure 3.3 Kinetic plots for the copolymerisations of ω -pentadecalactone with a) dodecalactone, b) η -caprylolactone, c) ϵ -caprolactone and d) δ -valerolactone. All reactions at 80 °C in toluene with $[\text{PDL}]_0:[\text{M}]_0:[\text{BnOH}]_0:[\text{cat.}]_0 = 50:50:1:1$, total initial monomer concentration = 2 M.....	60
Figure 3.4 M_n against conversion for the copolymerisation of δ -valerolactone and ω -pentadecalactone at 2 M in toluene at 80 °C with $[\delta\text{VL}]_0:[\text{PDL}]_0:[\text{BnOH}]_0:[\text{Mg}(\text{BHT})_2(\text{THF})_2]_0$ of 50:50:1:1. M_n and \bar{D}_M determined by SEC against poly(styrene) standards.	61
Figure 3.5 Quantitative ^{13}C NMR spectra of the carbonyl region during copolymerisations of ω -pentadecalactone with δ -valerolactone (125 MHz, CDCl_3 , 298 K).	62
Figure 3.6 M_n against conversion for the copolymerisation of ϵ -caprolactone and ω -pentadecalactone at 2 M in toluene at 80 °C with $[\epsilon\text{CL}]_0:[\text{PDL}]_0:[\text{BnOH}]_0:[\text{Mg}(\text{BHT})_2(\text{THF})_2]_0$ of 50 : 50 : 1 : 1. M_n and \bar{D}_M determined by SEC against poly(styrene) standards.....	64
Figure 3.7 Quantitative ^{13}C NMR spectra of the carbonyl region during copolymerisations of ω -pentadecalactone with ϵ -caprolactone (125 MHz, CDCl_3 , 298 K).....	64
Figure 3.8 Quantitative ^{13}C NMR spectra of the carbonyl region after 24 h of transesterification of PPDL with PCL (top) and PVL (bottom) (125 MHz, CDCl_3 , 298 K).....	66
Figure 3.9 Quantitative ^{13}C NMR spectra of the carbonyl region during copolymerisations of ω -pentadecalactone with η -caprylolactone (125 MHz, CDCl_3 , 298 K).....	67
Figure 3.10 M_n against conversion for the copolymerisation of η -caprylolactone and ω -pentadecalactone at 2 M in toluene at 80 °C with $[\eta\text{CL}]_0:[\text{PDL}]_0:[\text{BnOH}]_0:[\text{Mg}(\text{BHT})_2(\text{THF})_2]_0$ of 50:50:1:1. M_n and \bar{D}_M determined by SEC against poly(styrene) standards.	67
Figure 3.11 M_n against conversion for the copolymerisation of dodecalactone and ω -pentadecalactone at 2 M in toluene at 80 °C with $[\text{DDL}]_0:[\text{PDL}]_0:[\text{BnOH}]_0:[\text{Mg}(\text{BHT})_2(\text{THF})_2]_0$ of 50:50:1:1. M_n and \bar{D}_M determined by SEC against poly(styrene) standards.	69
Figure 3.12 Quantitative ^{13}C NMR spectra of the carbonyl region during copolymerisations of ω -pentadecalactone with dodecalactone (125 MHz, CDCl_3 , 298 K).....	69
Figure 3.13 Quantitative ^{13}C NMR spectra of the carbonyl region during the sequential polymerisation of a) ϵ -caprolactone followed by ω -pentadecalactone and b) ω -pentadecalactone followed by ϵ -caprolactone compared to c) the one-pot copolymerisation of ϵ -caprolactone and ω -pentadecalactone (125 MHz, CDCl_3 , 298 K).	71

Figure 3.14 Quantitative ^{13}C NMR spectra of the carbonyl region of polymers formed by a) the one-pot copolymerisation of δ -valerolactone and ω -pentadecalactone compared to the sequential polymerisation of b) δ -valerolactone followed by ω -pentadecalactone and c) ω -pentadecalactone followed by δ -valerolactone (125 MHz, CDCl_3 , 298 K).....	72
Figure 3.15 DSC thermograms of poly(ω -pentadecalactone-co- ϵ -caprolactone) T_m at 1, 2, 4, 6 and 8 h during copolymerisation of an equimolar mixture of ϵ -caprolactone and ω -pentadecalactone.	74
Figure 3.16 Quantitative ^{13}C NMR spectra of DP100 PDL copolymers with varying PDL mol% a) P(PDL-co- δ VL), b) P(PDL-co- ϵ CL), c) P(PDL-co- η CL) and d) P(PDL-co-DDL) (125 MHz, CDCl_3 , 298 K).	75
Figure 3.17 DSC thermograms (second heating curve, between 0 and 100 °C) showing the T_m for a) P(PDL-co- δ VL), b) P(PDL-co- ϵ CL), c) P(PDL-co- η CL) and d) P(PDL-co-DDL) at various molar ratios of PDL at DP100.	76
Figure 3.18 DSC thermograms (second cooling curve, between 0 and 100 °C) showing the T_c for a) P(PDL-co- δ VL), b) P(PDL-co- ϵ CL), c) P(PDL-co- η CL) and d) P(PDL-co-DDL) at various molar ratios of PDL at DP100.	76
Figure 3.19 DSC thermograms showing a) the T_m (second heating curve, between 0 and 100 °C) and b) the T_c (second cooling curve, between 0 and 100 °C) for PPDL at various DPs. ...	77
Figure 3.20 WAXD diffractograms of DP100 a) P(PDL-co- δ VL), b) P(PDL-co- ϵ CL), c) P(PDL-co- η CL) and d) P(PDL-co-DDL) with varying molar ratio feed of monomers.	78
Figure 3.21 Average mass loss of PDL copolymers studied in accelerated degradation conditions (5 M NaOH, 38 °C).	80
Figure 4.1 ^1H NMR spectra showing significant chemical shift changes between a) menthine, b) $\text{Mg}(\text{BHT})_2(\text{THF})_2/\text{BnOH}/\text{menthine}$ complex and c) poly(menthine) (400 MHz, toluene- d_8 , 298 K).	88
Figure 4.2 a) Kinetic plot for the homopolymerisation of menthine using $\text{Mg}(\text{BHT})_2(\text{THF})_2$ as a catalyst at 80 °C in toluene with $[\text{M}]_0 : [\text{BnOH}]_0 : [\text{cat.}]_0 = 50 : 1 : 1$, total monomer concentration = 1 M. b) Changes in M_n and D_M over monomer conversion for the same reaction. M_n and D_M determined by SEC against poly(styrene) standards.....	89
Figure 4.3 SEC chromatogram of the molecular weight distribution of the resultant polymer from the homopolymerisation of menthine at 1 M in toluene at 80 °C, with $[\text{M}]_0 : [\text{BnOH}]_0 : [\text{cat.}]_0 = [50] : 1 : 1$. Molecular weight determined against poly(styrene) standards and CHCl_3 (0.5% Net_3) as eluent.....	90
Figure 4.4 ^1H NMR spectra of the α -methylene signals observed during the copolymerisation of menthine and pentadecalactone at 1 : 1 mol%, targeting a total DP of 100 (400 MHz, 298 K, CDCl_3).	92
Figure 4.5 Kinetic plot for the copolymerisation of menthine and pentadecalactone, conducted at 80 °C in toluene with $[\text{PDL}]_0 : [\text{M}]_0 : [\text{BnOH}]_0 : [\text{cat.}]_0 = 50 : 50 : 1 : 1$, total monomer concentration = 2 M.....	92

Figure 4.6 Changes in M_n and D_M over total monomer conversion for the copolymerisation of menthide and ω -pentadecalactone using $Mg(BHT)_2(THF)_2$ as a catalyst at 80 °C in toluene with $[MI]_0 : [BnOH]_0 : [cat.]_0 = 50 : 1 : 1$, total monomer concentration = 2 M. M_n and D_M determined by SEC against poly(styrene) standards.	94
Figure 4.7 Quantitative ^{13}C NMR spectra of the carbonyl region during copolymerisation of ω -pentadecalactone with menthide (125 MHz, $CDCl_3$, 298 K)	96
Figure 4.8 DOSY NMR spectra of P(PDL-co-MI) (500 MHz, 298 K, $CDCl_3$).....	96
Figure 4.9 Quantitative ^{13}C NMR spectra of the carbonyl region for the transesterification of PPDL and PMI (125 MHz, $CDCl_3$, 298 K).	97
Figure 4.10 SEC chromatograms for the molecular weight distribution of PPDL, PMI and the resultant material from the attempted transesterification of both polymers. Molecular weights determined by poly(styrene) standards and $CHCl_3$ (0.5% Net_3) as eluent.	98
Figure 4.11 Quantitative ^{13}C NMR spectra of DP100 P(PDL-co-MI) copolymers with varying PDL mol% (125 MHz, $CDCl_3$, 298 K).....	100
Figure 4.12 a) DSC thermograms (second heating curve, between 0 °C and 100 °C) of the T_m at various molar ratios of DP 100 P(ω -pentadecalactone-co- menthide). b) DSC thermograms (second cooling curve, between 0 °C and 100 °C) of the T_m at various molar ratios of DP 100 P(ω -pentadecalactone-co- menthide).	102
Figure 4.13 Kinetic plot for the sequence controlled copolymerisation of menthide and pentadecalactone, conducted at 80 °C in toluene with $[PDL]_0 : [MI]_0 : [BnOH]_0 : [cat.]_0 = 50 : 50 : 1 : 1$, total monomer concentration = 1 M, MI injected into reaction mixture at $t = 3$ h.	103
Figure 4.14 Quantitative ^{13}C NMR spectra of the carbonyl region of the diblock copolymer P(PDL ₅₀ -co-MI ₅₀) and triblock copolymers P(PDL ₂₅ -co-MI ₅₀ -co-PDL ₂₅) and P(PDL ₅₀ -co-MI ₅₁₀₀ -co-PDL ₂₅) respectively (125 MHz, $CDCl_3$, 298 K).....	105
Figure 4.15 SEC chromatograms of the molecular weight distribution of a) P(PDL ₅₀ -co-MI ₅₀), b) P(PDL ₂₅ -co-MI ₅₀ -co-PDL ₂₅) and c) P(PDL ₅₀ -co-MI ₁₀₀ -co-PDL ₅₀). Molecular weights determined by poly(styrene) standards and $CHCl_3$ (0.5% Net_3) as eluent.....	106
Figure 4.16 Quantitative ^{13}C NMR spectra of the carbonyl region of copolymerisations of ω -pentadecalactone with a) ϵ -heptalactone; b) ϵ -decalactone; c) menthide and d) dihydrocarvide at 1 : 1 mol% monomers and total DP of 100 (125 MHz, $CDCl_3$, 298 K).	108
Figure 4.17 DOSY NMR spectra of a) P(PDL-co- ϵ HL), b) P(PDL-co- ϵ DL), c) P(PDL-co-MI) and d) P(PDL-co-DHC) (500 MHz, 298 K, $CDCl_3$).	109
Figure 4.18 1H NMR spectrum for P(PDL-co-DHC) in the region of $\delta = 5.4$ -3.9 ppm illustrating preservation of the alkene post-polymerisation (400 MHz, $CDCl_3$, 298 K).....	110
Figure 4.19 1H NMR spectra for a) P(PDL-co-DHC) and thiol-ene addition products b) P(PDL-co-DHCME), c) P(PDL-co-DHCBM) and P(PDL-co-DHCDT), with unique resonances highlighted to show conversion (a, b, d; 400 MHz, $CDCl_3$, 298 K. c; 400 MHz, CD_2Cl_2 , 298 K).	111

Figure 4.20 SEC chromatograms of P(PDL- <i>co</i> -DHC) and the resultant polymers from thiol-ene addition of benzyl mercaptan (P(PDL- <i>co</i> -DHCBM)), dodecanethiol (P(PDL- <i>co</i> -DHCDT)) and mercaptoethanol (P(PDL- <i>co</i> -DHCME)).	112
Figure 5.1 DOSY NMR spectra of a) P(MI- <i>co</i> - δ VL), b) P(MI- <i>co</i> - ϵ CL), c) P(MI- <i>co</i> - ζ HL) and d) P(MI- <i>co</i> - η CL) (500 MHz, 298 K, CDCl ₃).	119
Figure 5.2 Possible transesterification side reactions in the copolymerisation of δ -valerolactone and menthide.	120
Figure 5.3 Quantitative ¹³ C NMR spectra of the carbonyl region for copolymers of menthide with a) ω -pentadecalactone; b) η -caprylolactone; c) ζ -heptalactone; c) ϵ -caprolactone and d) δ -valerolactone at 1 : 1 mol% monomers with an total DP of 100 (125 MHz, CDCl ₃ , 298 K).	121
Figure 5.4 SEC chromatogram of the resultant polymer mixture of the transesterification of DP 5 PCL and DP 50 PMI at 1 M in toluene at 80 °C, using Mg(BHT) ₂ (THF) ₂ as a catalyst. Molecular weight determined against poly(styrene) standards using CHCl ₃ (0.5% NEt ₃) as eluent.	125
Figure 5.5 Quantitative ¹³ C NMR spectra of the carbonyl region for the resultant material from the transesterification of poly(ϵ -caprolactone) and poly(menthide) (125 MHz, CDCl ₃ , 298 K).	125
Figure 5.6 SEC chromatograms for the molecular weight distribution of P ϵ HL, PMI and the resultant material from the attempted transesterification of both polymers. Molecular weights determined by poly(styrene) standards and CHCl ₃ (0.5% NEt ₃) as eluent.	127
Figure 5.7 Quantitative ¹³ C NMR spectra of the carbonyl region for the resultant material from the transesterification of poly(ϵ -heptalactone) and poly(menthide) (125 MHz, CDCl ₃ , 298 K).	127
Figure 5.8 Kinetic plot for the terpolymerisation of ϵ -caprolactone, menthide and pentadecalactone, conducted at 80 °C in toluene with [ϵ CL] ₀ : [PDL] ₀ : [MI] ₀ : [BnOH] ₀ : [cat.] ₀ = 50 : 50 : 50 : 1 : 1, total monomer concentration = 1 M.	128
Figure 5.9 Quantitative ¹³ C NMR spectra of the carbonyl region for the one-pot terpolymerisation of equimolar quantities of ϵ -caprolactone, menthide and pentadecalactone with an initial concentration of [ϵ CL] ₀ : [MI] ₀ : [PDL] ₀ : [BnOH] ₀ : [cat.] ₀ = 50 : 50 : 50 : 1 : 1, total initial monomer concentration = 1 M (125 MHz, CDCl ₃ , 298 K).	130
Figure 5.10 Quantitative ¹³ C NMR spectra of the carbonyl region for the one-pot terpolymerisation of equimolar quantities of ϵ -caprolactone, menthide and pentadecalactone with an initial concentration of [ϵ CL] ₀ : [MI] ₀ : [PDL] ₀ : [BnOH] ₀ : [cat.] ₀ = 10 : 50 : 50 : 1 : 1, total initial monomer concentration = 1 M (125 MHz, CDCl ₃ , 298 K).	131

Figure 5.11 Quantitative ^{13}C NMR spectra of the carbonyl region for the copolymerisation of equimolar quantities of menthide and pentadecalactone with a timed injection of ϵ -caprolactone and an initial concentration of $[\epsilon\text{CL}]_0 : [\text{MI}]_0 : [\text{PDL}]_0 : [\text{BnOH}]_0 : [\text{cat.}]_0 = 50 : 50 : 50 : 1 : 1$. Injection of ϵCL at $t = 16$ h and total initial monomer concentration = 1 M (125 MHz, CDCl_3 , 298 K).....	133
Figure 5.12 Kinetic plot for the copolymerisation of ϵ -heptalactone and menthide at 80 °C in toluene with $[\epsilon\text{HL}]_0 : [\text{MI}]_0 : [\text{BnOH}]_0 : [\text{cat.}]_0 = 50 : 50 : 1 : 1$, total initial monomer concentration = 1 M.....	134
Figure 5.13 Evolution of M_n and \bar{D}_M over total monomer consumption for the copolymerisation of ϵ -heptalactone and menthide at 80 °C in toluene with $[\epsilon\text{HL}]_0 : [\text{MI}]_0 : [\text{BnOH}]_0 : [\text{cat.}]_0 = 50 : 50 : 1 : 1$, total initial monomer concentration = 1 M. M_n and \bar{D}_M determined by SEC against poly(styrene) standards.....	135
Figure 5.14 Molecular weight distribution of polymeric species in the copolymerisation of ϵ -heptalactone and menthide at 80 °C in toluene with $[\epsilon\text{HL}]_0 : [\text{MI}]_0 : [\text{BnOH}]_0 : [\text{cat.}]_0 = 50 : 50 : 1 : 1$, total initial monomer concentration = 1 M.	136
Figure 5.15 Quantitative ^{13}C NMR spectra of the carbonyl region for the one-pot copolymerisation of ϵ -heptalactone and menthide at 1 : 1 mol% with initial concentration of $[\epsilon\text{HL}]_0 : [\text{MI}]_0 : [\text{BnOH}]_0 : [\text{cat.}]_0 = 50 : 50 : 1 : 1$, total initial monomer concentration = 1 M (125 MHz, CDCl_3 , 298 K).....	137
Figure 5.16 Kinetic plot for the copolymerisation of ϵ -decalactone and menthide at 80 °C in toluene with $[\epsilon\text{DL}]_0 : [\text{MI}]_0 : [\text{BnOH}]_0 : [\text{cat.}]_0 = 50 : 50 : 1 : 1$, total initial monomer concentration = 1 M.....	137
Figure 5.17 Evolution of M_n and \bar{D}_M over total monomer consumption for the copolymerisation of ϵ -heptalactone and menthide at 80 °C in toluene with $[\epsilon\text{HL}]_0 : [\text{MI}]_0 : [\text{BnOH}]_0 : [\text{cat.}]_0 = 50 : 50 : 1 : 1$, total initial monomer concentration = 1 M. M_n and \bar{D}_M determined by SEC against poly(styrene) standards.....	138
Figure 5.18 Kinetic plot for the sequence controlled copolymerisation of menthide and ϵ -heptalactone, conducted at 80 °C in toluene with $[\text{MI}]_0 : [\epsilon\text{HL}]_0 : [\text{BnOH}]_0 : [\text{cat.}]_0 = 100 : 10 : 1 : 1$, total monomer concentration = 1 M, ϵHL injected into reaction mixture at $t = 3$ h.	140
Figure 5.19 SEC chromatogram for poly(ϵ -heptalactone-co-menthide) in CHCl_3 . Molecular weight determined against poly(styrene) standards.....	140
Figure 5.20 DOSY NMR spectra of the resultant polymer from sequence controlled injection of 10 eq. ϵHL into a DP 100 homopolymerisation of MI at 50% MI conversion (500 MHz, 298 K, CDCl_3).	140
Figure 5.21 Increase in DP over 30 min after injection of ϵHL for the copolymerisation of MI and ϵHL , conducted at 80 °C in toluene with $[\text{MI}]_0 : [\epsilon\text{HL}]_0 : [\text{BnOH}]_0 : [\text{cat.}]_0 = 100 : 10 : 1 : 1$, total monomer concentration = 1 M, ϵHL injected into reaction mixture at $t = 3$ h.	141

Figure 5.22 Quantitative ^{13}C NMR spectra of the carbonyl region for the sequential control copolymerisation of ϵHL and MI with $[\epsilon\text{HL}]_0 : [\text{MI}]_0 : [\text{BnOH}]_0 : [\text{cat.}]_0 = 10 : 100 : 1 : 1$, with ϵHL injection after 3 h and a total initial monomer concentration of 1 M (125 MHz, CDCl_3 , 298 K).	142
Figure 5.23 Kinetic plot for the sequence controlled copolymerisation of menthide and ϵ -decalactone, conducted at 80 °C in toluene with $[\text{MI}]_0 : [\epsilon\text{DL}]_0 : [\text{BnOH}]_0 : [\text{cat.}]_0 = 100 : 10 : 1 : 1$, total monomer concentration = 1 M, ϵDL injected into reaction mixture at $t = 3$ h.....	142
Figure 5.24 Increase in DP over 200 min after injection of ϵDL for the copolymerisation of MI and ϵDL , conducted at 80 °C in toluene with $[\text{MI}]_0 : [\epsilon\text{DL}]_0 : [\text{BnOH}]_0 : [\text{cat.}]_0 = 100 : 10 : 1 : 1$, total monomer concentration = 1 M, ϵDL injected into reaction mixture at $t = 3$ h.....	143
Figure 5.25 SEC chromatogram for poly(ϵ -decalactone- <i>co</i> -menthide). Molecular weight determined against poly(styrene) standards.....	144
Figure 5.26 Quantitative ^{13}C NMR spectra of the carbonyl region for the sequential control copolymerisation of ϵDL and MI with $[\epsilon\text{DL}]_0 : [\text{MI}]_0 : [\text{BnOH}]_0 : [\text{cat.}]_0 = 10 : 100 : 1 : 1$, with ϵDL injection after 3 h and a total initial monomer concentration of 1 M (125 MHz, CDCl_3 , 298 K).	145
Figure 5.27 Kinetic plot for the sequence-controlled block copolymerisation of menthide and ϵ -heptalactone, conducted at 80 °C in toluene with $[\text{MI}]_0 : [\epsilon\text{HL}]_0 : [\text{BnOH}]_0 : [\text{cat.}]_0 = 50 : 50 : 1 : 1$, with a further 20 eq. ϵHL added at $t = 5.33$ h and total initial monomer concentration = 1 M.....	147
Figure 5.28 Increase in DP throughout the sequence-controlled block copolymerisation of MI and ϵHL , conducted at 80 °C in toluene with $[\text{MI}]_0 : [\epsilon\text{HL}]_0 : [\text{BnOH}]_0 : [\text{cat.}]_0 = 50 : 20 : 1 : 1$, with a further 20 eq. ϵHL added at $t = 5.33$ h and total monomer concentration = 1 M.	147
Figure 5.29 Quantitative ^{13}C NMR spectra of the carbonyl region for the sequence-controlled block copolymerisation of menthide and ϵ -heptalactone using $\text{Mg}(\text{BHT})_2(\text{THF})_2$ as a catalyst at 80 °C in toluene with $[\text{MI}]_0 : [\epsilon\text{HL}]_0 : [\text{BnOH}]_0 : [\text{cat.}]_0 = 50 : 20 : 1 : 1$, with a further 20 eq. ϵHL added at $t = 5$ h and total monomer concentration = 1 M. (125 MHz, CDCl_3 , 298 K).	148
Figure 5.30 Changes in M_n and \bar{D}_M over total monomer conversion for the sequence-controlled block copolymerisation of menthide and ϵ -heptalactone using $\text{Mg}(\text{BHT})_2(\text{THF})_2$ as a catalyst at 80 °C in toluene with $[\text{MI}]_0 : [\epsilon\text{DL}]_0 : [\text{BnOH}]_0 : [\text{cat.}]_0 = 50 : 20 : 1 : 1$, with a further 20 eq. ϵHL added at $t = 5$ h and total monomer concentration = 1 M. M_n and \bar{D}_M determined by SEC against poly(styrene) standards.	149
Figure 5.31 Molecular weight distribution of polymeric species in the the sequence-controlled block copolymerisation of menthide and ϵ -heptalactone using $\text{Mg}(\text{BHT})_2(\text{THF})_2$ as a catalyst at 80 °C in toluene with $[\text{MI}]_0 : [\epsilon\text{DL}]_0 : [\text{BnOH}]_0 : [\text{cat.}]_0 = 50 : 20 : 1 : 1$, with a further 20 eq. ϵHL added at $t = 5$ h and total monomer concentration = 1 M. Molecular weights determined by SEC against poly(styrene) standards.....	150

List of Schemes

Scheme 1.1 Baeyer-Villiger oxidation of cyclic ketones into lactones.	8
Scheme 1.2 a) Intermolecular and b) intramolecular transesterification side reactions during lactone polymerisation.	9
Scheme 1.3 Copolymerisation of ϵ -caprolactone and ω -pentadecalactone.	13
Scheme 1.4 Copolymerisation of PDL with 1-oxa-8-aza-cyclotetradecan-9,14-dione (top) and <i>p</i> -dioxanone (bottom).	15
Scheme 1.5 Copolymerisation of ω -pentadecalactone with γ -benzoyloxy- ϵ -caprolactone (top) and γ -methacryloyloxy- ϵ -caprolactone (bottom).	18
Scheme 1.6 Copolymerisation of ω -pentadecalactone with ethyl 3-(4-(hydroxymethyl)piperidin-1-yl)propanoate.	18
Scheme 1.7 Copolymerisation of ω -pentadecalactone with ϵ -decalactone.	19
Scheme 2.1 One-pot synthesis of $\text{Mg}(\text{BHT})_2(\text{THF})_2$	30
Scheme 2.2 Homopolymerisation of PDL by $\text{Mg}(\text{BHT})_2(\text{THF})_2$	31
Scheme 2.3 Homopolymerisation of ϵ -caprolactone catalysed by $\text{Mg}(\text{BHT})_2(\text{THF})_2$	44
Scheme 2.4 Homopolymerisation of δ -valerolactone catalysed by $\text{Mg}(\text{BHT})_2(\text{THF})_2$	46
Scheme 3.1 Homopolymerisation of various lactones catalysed by $\text{Mg}(\text{BHT})_2(\text{THF})_2$	54
Scheme 3.2 Copolymerisation of pentadecalactone with other lactones catalysed by $\text{Mg}(\text{BHT})_2(\text{THF})_2$	58
Scheme 3.3 Sequential polymerisation of ω -pentadecalactone, followed by δ -valerolactone or ϵ -caprolactone.	70
Scheme 4.1 Polymerisation of menthide catalysed by $\text{Mg}(\text{BHT})_2(\text{THF})_2$	87
Scheme 4.2 Potential complex formed by $\text{Mg}(\text{BHT})_2(\text{THF})_2$ and the first ring-opened unit of MI using BnOH as an initiator (298 K, CDCl_3 , 298 K).	88
Scheme 4.3 Copolymerisation of menthide and pentadecalactone in catalysed by $\text{Mg}(\text{BHT})_2(\text{THF})_2$	91
Scheme 4.4 Sequence controlled copolymerisation of PDL and MI through the timed injection of MI into a PDL homopolymerisation.	103
Scheme 4.5 Copolymerisation of MI and PDL with bifunctional initiator 1,4-benzenedimethanol.	104
Scheme 4.6 Copolymerisation of an ϵ -substituted ϵ -lactone (ϵSL) with ω -pentadecalactone using $\text{Mg}(\text{BHT})_2(\text{THF})_2$ as a catalyst to form block-like copolymers.	107
Scheme 4.7 Thiol-ene addition of a thiol onto P(PDL-co-DHC).	110
Scheme 5.1 Copolymerisation of menthide with non-substituted lactones catalysed by $\text{Mg}(\text{BHT})_2(\text{THF})_2$	117

Scheme 5.2 Copolymerisation of menthide and pentadecalactone with timed injection of ϵ -caprolactone.	132
Scheme 5.3 Copolymerisation of menthide with an ϵ -substituted ϵ -lactone.	134
Scheme 5.4 Sequence control polymerisation of ϵ -substituted ϵ CLs.	139
Scheme 5.5 Copolymerisation of menthide with an ϵ -substituted ϵ -lactone with sequential addition of ϵ -heptalactone to produce a tetrablock-like copolymer.	146

List of Tables

Table 2.1 Synthesis of DP 50 PPDL using different solvents in non-inert conditions.	40
Table 2.2 Synthesis of DP 50 PPDL in hexanes at different temperatures in inert conditions ^a	41
Table 2.3 Synthesis of DP 50 PPDL using different solvent ratios of hexanes and toluene. .	42
Table 2.4 ‘Immortal’ ring-opening polymerisation results for varied $\text{Mg}(\text{BHT})_2(\text{THF})_2$ concentrations polymerising PDL ^a	44
Table 2.5 ‘Immortal’ ring-opening polymerisation results for varied $\text{Mg}(\text{BHT})_2(\text{THF})_2$ concentrations polymerising ϵ CL ^a	46
Table 2.6 ‘Immortal’ ring-opening polymerisation results for varied $\text{Mg}(\text{BHT})_2(\text{THF})_2$ concentrations polymerising δ VL ^a	48
Table 3.1 Copolymerisation of PDL and δ VL at 1:1 mol% targeting DP100.....	62
Table 3.2 Copolymerisation of PDL and ϵ CL at 1:1 mol% targeting DP100.....	65
Table 3.3 Copolymerisation of PDL and η CL at 1:1 mol% targeting DP100.....	68
Table 3.4 Copolymerisation of PDL and DDL at 1:1 mol% targeting DP100.	70
Table 3.5 Copolymerisation of PDL with another lactone at varied monomer ratio feeds targeting DP100.	77
Table 4.1 Copolymerisation of 1 : 1 mol% $[\text{PDL}]_0 : [\text{MI}]_0$ targeting various DPs.....	99
Table 4.2 Copolymerisation of PDL and MI at varying monomer molar feed ratio targeting DP 100.....	100
Table 4.3 Copolymerisations of PDL and MI at 1 : 1 mol% with varying DP and initiator...	106
Table 4.4 Copolymerisation of pentadecalactone with an equimolar ratio of ϵ -substituted ϵ -lactone monomer, targeting a total DP of 100.....	110
Table 4.5 Thiol-ene addition to P(PDL-co-DHC).....	112
Table 5.1 Copolymerisations of menthide with a linear lactone at 1 : 1 mol% targeting an overall DP of 100.....	118
Table 5.2 Relative integrals of carbonyl diad resonances for copolymers of menthide and a linear lactone at 1 : 1 mol% targeting an overall DP of 100	120

Table 5.3 Homopolymerisations of ϵ -substituted ϵ -lactones targeting an overall DP of 50124	
Table 5.4 Terpolymerisations of ϵ CL, PDL and MI	129
Table 5.5 Terpolymer carbonyl diads formed from the sequential polymerisation of PDL and MI followed by ϵ CL.....	133
Table 5.6 Copolymerisation of MI with an equimolar ratio of ϵ -substituted ϵ -lactone monomer, targeting a total DP of 100.....	139

Acknowledgments

I'm not one for breaking tradition, so.... Firstly, thank you to Prof. Andrew Dove for the opportunity to do a PhD in the Dove group. The advice and guidance over the past four years has been invaluable and really appreciated, even with the jibes about my pescetarianism and inability to look at blood. Thanks also to Infineum UK Ltd and the EPSRC for the joint funding, especially the former who have always offered helpful advice on my project regardless of the deviation from their project goals.

Next up to thank is the wonderful Dove group, regardless of the moods I've been in over the past four years, you've all been a joy to work with and made my time in the group the most fun possible. Special thanks have to go to Ruairí for being a great lab partner/drinking buddy/housemate, but just remember; you're still a bad man, Ruairí Brannigan. Also thanks to Becky. I had to write this as a contractual agreement for the MALDI-TOF data in chapter 2. But seriously, thanks Becky for being a good friend. I have to keep this to one page under APD rule, so I'll just say special mentions to Ed, Annette, Craig, Ian and Robin. Thanks next to the O'Reilly group, especially Dan, Dafni, Beth, Alice and Anne; I'm glad we're all allowed to talk to each other after that first year of awkwardness.

On a personal note, thanks to my amazing partner, Danielle. Sticking by me for all of this hasn't been exactly easy, but I'm very glad she did and I can't wait for our next adventure together. Thanks should go to my mother, Yvonne, as well and not just from me, but the entire Dove group for the regular cake and brownie supply that kept us fuelled or at risk of diabetes. As for the rest of my family, thanks for making the effort to learn about what I've been researching. I realise I can bore you senseless, but the effort hasn't gone unnoticed. Good luck reading through this!

Declaration of Authorship

This thesis is submitted to the University of Warwick in support of my application for the degree of Doctor of Philosophy. It has been composed by myself and has not been submitted in any previous application for any degree. The work presented (including data generated and data analysis) was carried out by the author except in the cases outlined below:

- The MALDI-TOF MS data in Chapter 2 was obtained by Dr Rebecca Williams (University of Warwick);
- The DSC data in Chapters 3 and 4 was obtained and analysed by Dr Anaïs Pitto-Barry and Ruairí Brannigan (University of Warwick);
- The WAXD data in Chapter 3 was obtained by Cathrin Kirchhoefer (University of Warwick);
- The quantitative ^{13}C NMR and DOSY NMR data in chapters 2, 3, 4 and 5 were obtained by Dr Ivan Prokes, Edward Tunnah and Rob Perry (University of Warwick).

Publications

'Immortal' ring-opening polymerisation of ω -pentadecalactone by $\text{Mg}(\text{BHT})_2(\text{THF})_2$, J. A. Wilson, S. A. Hopkins, P. M. Wright and A. P. Dove, *Polym. Chem.*, 2014, 2691-2694 (**Chapter 2**).

Synthesis of ω -pentadecalactone copolymers with independently tunable thermal and degradation behavior, J. A. Wilson, S. A. Hopkins, P. M. Wright and A. P. Dove, *Macromolecules*, 2015, 950-958 (**Chapter 3**).

Abstract

This thesis reports studies into the ring-opening polymerisation (ROP) of large ring lactones (macrolactones) and ϵ -substituted ϵ -lactones (ϵ SLs). Additionally, the copolymerisations of these monomers with other lactones were investigated in order to determine the conditions that define the sequencing of lactone copolymers. The ability to produce one-pot lactone copolymers with tuneable properties is explored and carried forward to introduce functional groups for post-polymerisation functionalisation. The ability to produce sequence controlled block copolymers using only lactone monomers is also outlined for the first time in this thesis.

Chapter 1 provides an overview for the current published literature on the ROP of macrolactones, including the factors that affect macrolactone polymerisation and copolymerisation with a variety of other monomers.

In Chapter 2, the ‘immortal’ ROP (iROP) of the macrolactone, ω -pentadecalactone (PDL), is demonstrated with the use of a Mg catalyst. The technique is shown to be achievable in a non-inert environment, with no undesired side reactions affecting the properties of the final polymers compared to polymers produced in an inert environment. Furthermore, the catalyst is demonstrated to be able to ‘immortally’ polymerise smaller ring lactones.

Chapter 3 describes the copolymerisation of PDL with a variety of lactones of smaller ring-sizes. The sequencing of the copolymers is characterised throughout the copolymerisation using quantitative ^{13}C NMR spectroscopy and demonstrates the randomisation of the polymer sequencing in each case. The thermal and crystalline properties of the copolymers is explored and optimised in order to produce PDL copolymers with independently tuneable thermal and degradative properties.

In Chapter 4, the copolymerisation of PDL with the ϵ SL, menthide (MI), is examined and shown to produce a copolymer with a block-like sequencing. This sequencing is demonstrated in the case of PDL copolymerisation with other ϵ SL monomers. This discovery is then used in order to produce a block copolymer of PDL with an alkene

functionalised ϵ SL. The ability of this copolymer to undergo post-polymerisation modification is demonstrated through thiol-ene addition onto the pendent alkene groups.

Chapter 5 goes on to use MI in copolymerisations with other non-substituted lactones in order to determine the factors that affect the sequencing of ϵ SL copolymers. The production of macrolactone/ ϵ SL copolymers with a random sequencing is then attempted. The sequencing of copolymers produced from two ϵ SLs is also demonstrated to produce block-like copolymers. As a consequence of the large difference in reactivity between ϵ SLs, the potential for sequence controlled lactone copolymers is established.

A general summary of Chapters 2 - 5 is presented in Chapter 6, with the concluding findings outlined.

List of Abbreviations

4MeCL	4-Methylcaprolactone
AcetCL	γ -Acetyloxy- ϵ -caprolactone
AcrCL	γ -Acryloyloxy- ϵ -caprolactone
Amb	Ambrettolide
AROP	Anion ring-opening polymerisation
ATRP	Atom transfer radical polymerisation
BDM	1,4-Benzenedimethanol
BenzCL	γ -Benzoyloxy- ϵ -caprolactone
BHT	2,6-di- <i>tert</i> -butyl-4-methylphenoxide
BnOH	Benzyl alcohol
CALB	<i>Candida Antarctica</i> lipase B
cat.	Catalyst
cEA	Cyclic ester amide
CROP	Cationic ring-opening polymerisation
CTA	Chain transfer agent
DBU	1,8-diazabicycloundec-7-ene
DDL	Dodecalactone
DES	Diethyl sebacate

DHC	Dihydrocarvide
DHCBM	Benzylmercaptan dihydrocarvide
DHCDT	Dodecanethiol dihydrocarvide
DHCME	Mercaptoethanol dihydrocarvide
\bar{D}_M	Dispersity
DMTA	Dynamic mechanical thermal analysis
DOSY	Diffusion-ordered spectroscopy
DP	Degree of polymerisation
DPP	Diphenyl phosphine
DSC	Differential scanning calorimetry
EHMPP	Ethyl 3-(4-(hydroxymethyl)piperidin-1-yl)propanoate
eROP	Enzymatic ring-opening polymerisation
f	Mole fraction
FRP	Free radical polymerisation
Gbl	Globalide
GPC	Gel-permeation chromatography
HDL	Hexadecalactone
HEA	Hydroxyethyl acrylate
HEMA	Hydroxyethyl methacrylate

I	Initiator
iROP	Immortal' ring-opening polymerisation
k_d	Rate of depolymerisation
k_p	Rate of polymerisation
L	Lactone
LDPE	Low-density polyethylene
M	Monomer
m/z	mass-to-charge ratio
MALDI-ToF MS	Matrix-assisted LASER desorption-ionisation time of flight mass spectrometry
mCPBA	<i>meta</i> -Chloroperoxybenzoic acid
McrCL	γ -Methacryloyloxy- ϵ -caprolactone
MDEA	<i>N</i> -Methyldiethanolamine
MI	Menthide
M_n	Number-average molecular weight
M_p	Molecular weight at peak
MS	Mass spectrometry
M_w	Weight-average molecular weight
NMR	Nuclear magnetic resonance
P(η CL)	Poly(η -caprylolactone)

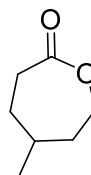
PCL	Poly(ϵ -caprolactone)
PDDL	Poly(dodecalactone)
PDL	ω -pentadecalactone
pDO	<i>para</i> -Dioxanone
PEGMA	Poly(ethylene glycol) methacrylate
PLA	Poly(lactide)
PMI	Poly(menthide)
PPDL	Poly(ω -pentadecalactone)
PS	Poly(styrene)
PVL	Poly(δ -valerolactone)
P ϵ DL	Poly(ϵ -decalactone)
P ϵ HL	Poly(ϵ -heptalactone)
P ϵ SL	Poly(ϵ -substituted ϵ -lactone)
R	Gas constant
RAFT	Reversible addition-fragmentation chain transfer
RI	Refractive index
ROCOP	Ring-opening copolymerisation
ROMP	Ring-opening metathesis polymerisation
ROP	Ring-opening polymerisation

RT	Room temperature
SEC	Size-exclusion chromatography
T	Temperature
TBD	1,5,7-Triazabicyclo[4.4.0]dec-5-ene
T_c	Crystallisation temperature
T_g	Glass transition temperature
THF	Tetrahydrofuran
T_m	Melting temperature
TMC	Trimethylene carbonate
TMP	Trimercapto propionate
TOF	Turn-over frequency
TON	Turn-over number
UV	Ultraviolet
WAXD	Wide-angle X-ray diffraction
ZROP	Zwitterionic ring-opening polymerisation
α Cl ϵ CL	α -Chloro- ϵ -caprolactone
β PL	β -Propiolactone
γ BL	γ -Butyrolactone
δ	Chemical shift

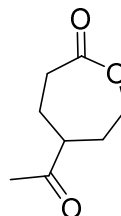
δDL	δ -Decalactone
ΔG_{RO}	Gibbs free energy of ring-opening
ΔH_{RO}	Enthalpy of ring-opening
ΔS_{RO}	Entropy of ring-opening
δVL	δ -Valerolactone
ϵCL	ϵ -Caprolactone
ϵDL	ϵ -Decalactone
ϵHL	ϵ -Heptalactone
ϵSL	ϵ -Substituted ϵ -caprolactone
ζHL	ζ -Heptalactone
ηCL	η -Caprylolactone

List of Lactones

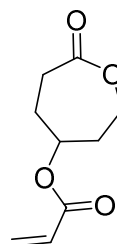
4MeCL 4-Methylcaprolactone



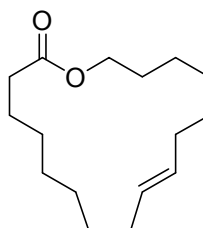
AcetCL γ -Acetyloxy- ϵ -caprolactone



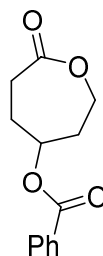
AcrCL γ -Acryloyloxy- ϵ -caprolactone



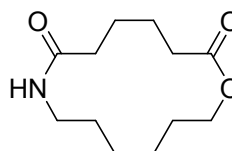
Amb Ambrettolide



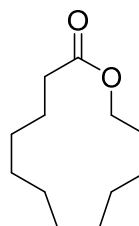
BenzCL γ -Benzoyloxy- ϵ -caprolactone



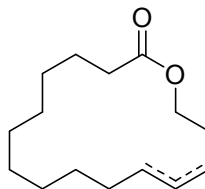
cEA Cyclic ester amide



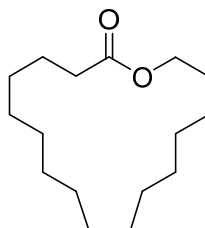
DDL Dodecalactone



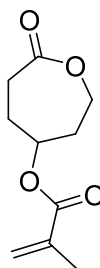
Gbl Globalide



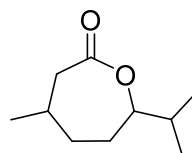
HDL Hexadecalactone



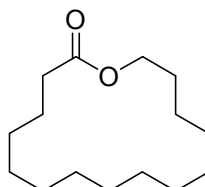
McrCL γ -Methacryloyloxy- ϵ -caprolactone



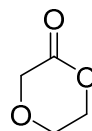
MI Menthide



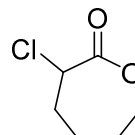
PDL ω -pentadecalactone



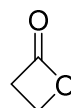
pDO para-Dioxanone



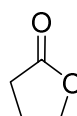
α Cl ϵ CL α -Chloro- ϵ -caprolactone



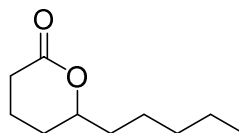
β PL β -Propiolactone



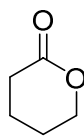
γ BL γ -Butyrolactone



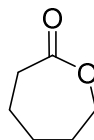
δ DL δ -Decalactone



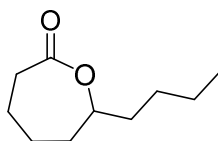
δ VL δ -Valerolactone



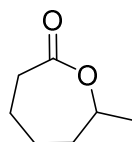
ϵ CL ϵ -Caprolactone



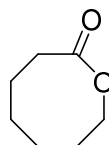
ϵ DL ϵ -Decalactone



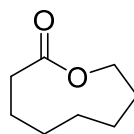
ϵ HL ϵ -Heptalactone



ζ HL ζ -Heptalactone



η CL η -Caprylolactone



1 Introduction

1.1 Introduction

The synthesis of polyesters has become increasingly popular since the 1930 discovery of the first synthetic polyester by Carothers *et al.*, with a multitude of new materials produced since then to encompass a wide range of targeted properties. Originally the majority of these polymers were produced from non-renewable sources, significantly fossil fuels. However with the moving of global conscience towards renewable/degradable polymers and increasing cost of raw materials, trends in research have now shifted towards a more “eco-friendly” outlook. Production of polyesters can occur through various methods, such as step-growth polycondensation, ring-opening polymerisation (ROP) and free radical polymerisation (FRP). Whilst step-growth polycondensation of diols and diacids is often the most industrially viable method of polyester production, there is little control over the monomer conversion, molecular weights and dispersities achieved in the final polymer. This is most evident with the fact that 50% monomer conversion produces largely dimers. Polycondensations often require high temperature to promote esterification and long reaction times in order to reach high conversion and high molecular weight. This greatly lowers the amount of control over the materials produced, which are generally very disperse and only achieve low molecular weights. Thus, in order to maintain control of the growth of polymer chains during polymerisation, targeting specific molecular weights and maintaining low dispersities with a high degree of accuracy, ROP techniques are generally employed. More predictable and higher molecular weight polymers are possible with narrow dispersities and higher end-group fidelities through the use of ROP rather than polycondensation and as such, research has turned towards ROP for polyester production. However, industrial production of polylactide (PLA) is currently one of the few commercially viable products from ROP.

1.2 Ring-opening polymerisation

Polymerisation by the ring-opening of cyclic monomers has been studied for a large variety of monomers, including cyclic alkenes,^{1, 2} epoxides,^{3, 4} carbonates,^{5, 6} lactides,^{5, 7-9} lactones,^{5, 10-30} *N*-carboxyanhydrides,³¹⁻³³ *O*-carboxyanhydrides,^{34, 35} *etc.* In order to polymerise these monomers, a range of controlled ROP techniques have been developed such as ring-opening metathesis polymerisation (ROMP),^{1, 2} cationic ROP (CROP),³⁶ anionic ROP (AROP),³⁷ enzymatic ROP (eROP),^{29, 30, 38, 39} 'immortal' ROP (iROP)^{26-28, 40, 41} and ring-opening copolymerisation (ROCOP).⁴² However, not all cyclic molecules can be ring-opened, even if they contain a functional group suitable for ROP, as a consequence of the thermodynamics of ring-opening polymerisation.

1.2.1 Thermodynamics of ring-opening polymerisation

Through the assumption that every polymer chain end exhibits the same activity, regardless of degree of polymerisation, the Gibbs free-energy of ring-opening can be abbreviated to:

$$\Delta G_{RO} = \Delta H_{RO}^{\circ} - T(\Delta S_{RO}^{\circ} + R \ln[M])$$

where ΔG is the Gibbs free-energy, ΔH° is the standard enthalpy of ring-opening, T is the temperature, ΔS° is the standard entropy of ring-opening, R is the gas constant and $[M]$ is the concentration of monomer. If the Gibbs free-energy is positive, the ring-opening cannot thermodynamically occur and the ring remains closed. In order for a ring-opened monomer to polymerise, a mechanism for ring-opening and attaching another monomer is required, generally facilitated by a catalyst.

Polymerisation and depolymerisation reactions generally occur at the same time in ROP and the growth of the polymer chain only proceeds if the rate of polymerisation (k_p) is greater than the rate of depolymerisation (k_d). A decrease in the concentration of monomer during ROP would allow for more depolymerisation reactions to occur, this

increases the available monomer for polymerisation and eventually equilibrium between the concentration of monomer and polymer is reached. As a consequence of the equilibrium between the monomer and the polymer, a critical concentration of monomer exists, below which polymerisation cannot occur as equilibrium is shifted in favour of the monomer and depolymerisation becomes more likely to occur. This is accounted for in the equation above, but generally does not apply to oligomeric polymers of 20 repeat units or below.

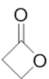
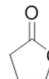
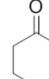
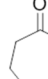
				
	β -Propiolactone (β PL)	γ -Butyrolactone (γ BL)	δ -Valerolactone (δ VL)	ϵ -Caprolactone (ϵ CL)
ΔH_{RO}° (kJ.mol ⁻¹)	-82.3	5.1	-27.4	-28.8
ΔS_{RO}° (J.mol ⁻¹ .K ⁻¹)	-74.0	-29.9	-65.0	-53.9

Figure 1.1 Small ring lactones and corresponding standard enthalpies and entropies of ring-opening.

With the majority of lactones (cyclic esters), especially small ring lactones (4-, 6- and 7-membered rings), conformational ring-strain provides an exothermic release when ring-opened and gives a highly negative ΔH_{RO}° that allows polymerisation (Figure 1.1).⁴³ In the case of the 5-membered γ -butyrolactone (γ BL), the positive enthalpy and negative entropy of ROP lead to an overall positive ΔG_{RO}° and so polymerisation is not achievable. The conformation of poly(γ -butyrolactone) is helical with ester linkages in close proximity to one another, facilitating ring-closing depolymerisation back into the more energetically favourable, envelope conformation of a γ BL monomer. Furthermore, γ BL contains very little ring-strain on the ester functionality in the envelope conformation as a consequence of the bond angles of the ester being close to the lowest achievable free-energy state.⁴⁴ Not all γ -butyrolactone derivatives are unable to polymerise through ROP, α -functionalised γ BL derivatives have been shown to copolymerise with ϵ -caprolactone (ϵ CL), although poor incorporation of the γ -butyrolactone is achieved and homopolymerisation has yet to be realised.⁴⁵ Analysis of the carbonyl diad resonances by ¹³C NMR spectroscopy revealed no

adjacent γ -butyrolactone repeat units were present in the final polymer; this is likely a consequence of depolymerisation immediately after incorporation of the second γ -butyrolactone unit. The entropy of small ring lactones increases throughout polymerisation as a consequence of the limited free movement of the monomer once it is incorporated into the chain. Hence, in order to limit the effect of entropy on the polymerisation, reactions are often carried out at low temperatures and high concentrations. For example in the polymerisation of δ -decalactone (δ DL), the reaction is kept at 0 °C or below, with polymerisation unachievable at higher temperatures.¹⁷

As the size of the lactone ring increases, the strain in the ring decreases as more conformations are available to limit strained bond angles in the ring. Large lactones, known as macrolactones, are defined as lactones with larger ring sizes where the ring-strain can be said to be 'strainless', *i.e.* ring-strain is so low that ΔH_{RO}° becomes a positive value.⁴⁶ In these cases, polymerisation can still occur as long as there is an entropic gain (ΔS_{RO}° is positive as a consequence of increased entropy from less hindered chain rotation). Therefore, unlike with small ring lactones, the polymerisation of macrolactones is assisted by higher temperatures and lower concentrations. Hence, the polymerisations of macrolactones, such as ω -pentadecalactone (PDL), have been accomplished at high temperatures.

1.2.2 ROP catalysts

Catalysts involved in ROP can be divided into three categories; inorganic, organic and enzymatic. Inorganic catalysts have been shown to polymerise monomers through mechanisms such as co-ordination insertion or metathesis, and can contain metal centres including Mg,^{13, 26} Al,^{47, 48} Sn,^{8, 49-51} Ru²¹ and Fe.⁵² The main advantages of using inorganic catalysts are the ability to tailor both the metal and ligand in order to find optimum (or desired) conditions for polymerisation. However, the major disadvantage is the intrinsic use of metal, which can be costly or have negative side effects in applications (*e.g.* toxicity in

biomaterials) as a consequence of the difficulty in removing catalyst post-polymerisation. Organocatalysts such as guanidines,^{12, 53-57} amidines,^{53, 57-59} phosphazenes^{37, 57} and *N*-heterocyclic carbenes^{7, 60, 61} have all been used in ROP for many different types of monomer. As a consequence of most organocatalysts being either acidic or basic, they can be removed through simple washing methods, materials produced from these catalysts are often biocompatible.⁵³ However, the versatility of the catalysts is limited, with little area for modification of catalyst in order to tailor conditions. Enzymes such as lipases and proteases have exhibited the ability to catalyse polymerisation at high monomer concentrations, when equilibrium favours the polymerisation route.^{11, 16, 23, 25, 39} Materials can therefore be produced from completely renewable sources and with the availability of some enzymes immobilised on resin beads, easy removal *via* simple gravity filtration is possible. However, the mechanisms by which these enzymes catalyse polymerisation are very dependent on factors such as high monomer concentration to prevent depolymerisation and require water in order to function, which can lead to side reactions.^{18, 29}

1.2.3 'Immortal' ring-opening polymerisation

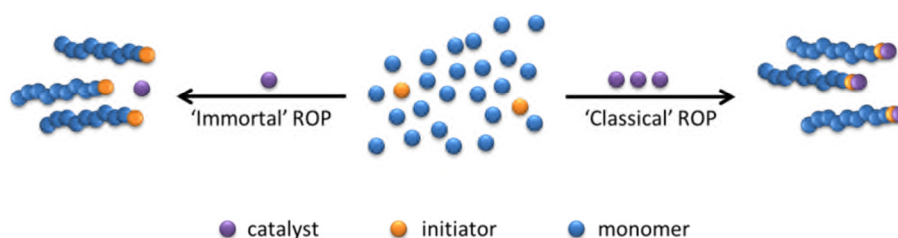


Figure 1.2 Differences between 'immortal' ROP and 'classical' ROP.

Most ROP techniques initiate through the interaction of the catalyst with the initiator to form a complex, such as a metal-alkoxide, and polymerise one chain at a time.⁶ However, this means the resulting polymers are defined not only from the molar ratio of monomer-to-initiator but also initiator-to-catalyst and thus monomer-to-initiator-to-catalyst ratio. Therefore, for most ROP techniques, an equimolar quantity of catalyst is usually required in order to form a catalyst/initiator complex (*e.g.* metal alkoxide) from which only one polymer chain can grow. In 1985, Inoue *et al.* coined the term 'immortal' ROP (iROP) for

use in ROP reactions where the quantity of catalyst did not affect the molecular weight of the resulting polymers and a lower than equimolar quantity of catalyst with respect to initiator could be used.^{3, 28} Hence, one catalytic unit can polymerise multiple chains at the same time (Figure 1.2). This means that polymers produced by iROP have molecular weights purely defined by the ratio of monomer-to-initiator. Typically iROP catalysts have a significantly higher turn-over number (TON) and turn-over frequency (TOF) than non-‘immortal’, or ‘classical’, ROP catalysts. As a lower quantity of catalyst is required than ‘classical’ ROP, cost benefits arising for the industrial viability of ROP and lower toxicity in materials from reduced catalyst loading has led to recent research into iROP increasing, with the technique being applied to epoxies, lactide, lactones and carbonates.⁴¹ The catalysts used in these cases have all been inorganic, with Al, Ca or Zn metal centres and phenolate, porphyrin or phenoxides ligands, which increases control through steric hindrance of the initiator to the metal centre as a consequence of their bulky composition.^{3, 5, 6, 26-28}

1.3 Lactone polymerisation

Polyesters produced from lactones have been of interest in biomaterials research since the use of polylactides in sutures and the natural sourcing of many lactones providing a cheap, renewable feedstock. Lactones are cyclic esters that can be found in varying sizes, from the smallest lactone, α -acetolactone, to macrolactones such as the sixteen-membered ring PDL. They can also incorporate other functional groups as seen with the alkene-functionalised ambrettolide (Amb), alkyl chain functionalised ϵ -decalactone or halo-functionalised α -chloro- ϵ -caprolactone (Figure 1.3). A large quantity of lactones can be found naturally in various plants and animals, where they are used for numerous applications including taste (limonine in lemons), scent (δ -decalactone (δ DL)) and chemical messaging (PDL). The renewability of naturally occurring lactones has resulted in the commercial extraction of some lactones for industrial use. For example, PDL can be sourced

from deer and due to its occurrence in the male body as a pheromone in sweat, is used in industry as a fragrance.⁶²

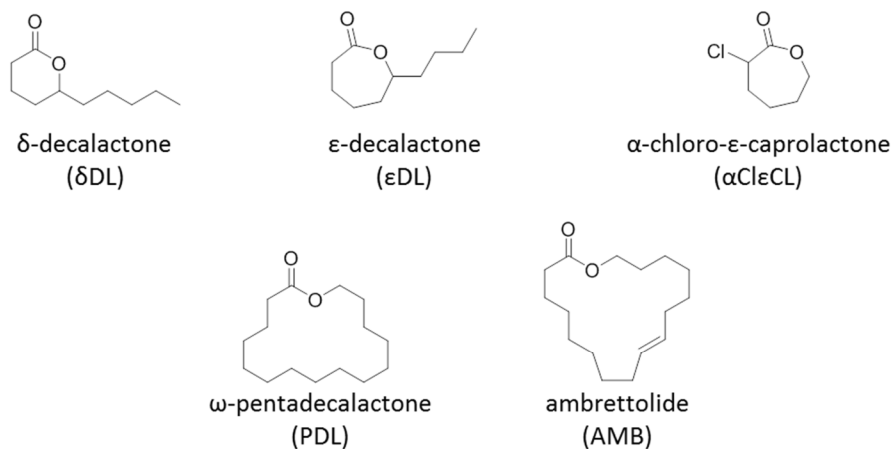
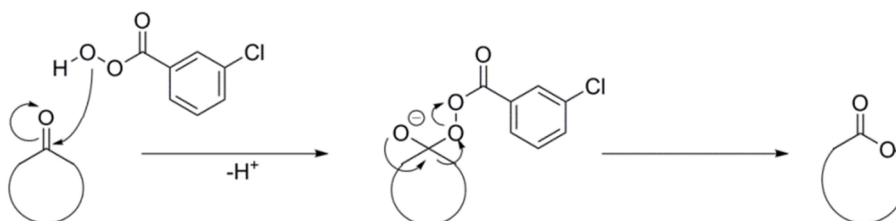


Figure 1.3 Examples of substituted lactones and macrolactones.

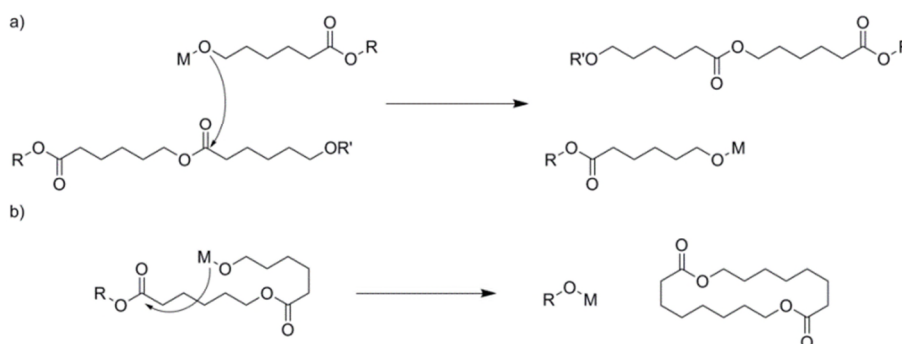
Lactones can also be produced from other renewable feedstocks through relatively simple synthesis. Cyclic ketones are the most common precursor in lactone synthesis as the ketone functionality provides an easy access point for oxidation. The first example of oxidation of a cyclic ketone into a lactone came in 1899, with Baeyer and Villiger demonstrating the oxidation of the naturally occurring camphor and menthone into the lactones, camphide and menthine respectively (Scheme 1.1). The reaction occurs in the presence of peroxy acids, which initially attack the carbonyl before a Criegee rearrangement to form a lactone and acid. Baeyer-Villiger oxidation, as it became known, has been exhibited for numerous other lactones in the 115 years since, generally with good (*ca.* 70%) yields.⁶³ Lactones can also be produced from ring-closure reactions; however these methods are more challenging than Baeyer-Villiger oxidation and often require very dilute conditions in order to avoid polymerisation.⁶⁴



Scheme 1.1 Baeyer-Villiger oxidation of cyclic ketones into lactones.

1.3.1 Transesterification side reactions

An inherent risk with all ROP is transesterification side reactions, which can be either intermolecular or intramolecular (Scheme 1.2). Intermolecular transesterification occurs between the chain end of one polymer chain and the ester linkage of another chain that results in the former chain extending and the latter chain shortening, increasing dispersity. Intramolecular transesterification occurs between the chain end of the polymer chain and its own ester linkage that results in a shorter linear chain and a cyclic species, also increasing dispersities. In the case of small ring lactones, such as δ -valerolactone (δ VL) or ϵ CL, the mechanism of ROP is much more preferable to transesterification, which means the rate of polymerisation is much higher than that of transesterification. Therefore, transesterification does not generally occur during polymerisation until either high conversion or a long reaction time is achieved. Control of the polymerisation is therefore achievable as long as the reaction is terminated before transesterification side reactions take place. High conversions are also avoided with lactones as a consequence of the equilibrium between monomer and polymer in lactones, as low monomer concentration would therefore shift the equilibrium in favour of depolymerisation.²² This has been observed experimentally with ϵ CL catalysed by 1,5,7-triazabicyclo[4.4.0]dec-5-ene (TBD) or co-catalysed by 1,8-diazabicycloundec-7-ene (DBU) and thiourea.^{53, 65}



Scheme 1.2 a) Intermolecular and b) intramolecular transesterification side reactions during lactone polymerisation.

As a consequence of the thermodynamics of macrolactones, the energy required for ROP is very similar to that of transesterification, thus it is possible to have both

transesterification and polymerisation occurring concurrently, observed experimentally with macrolactones often exhibiting large dispersities. Furthermore, recent work has shown that in the case of 'strainless' macrolactones, transesterification not only occurs in conjunction with polymerisation but occurs before polymerisation.⁴⁶ The formation of cyclic species occurs before the polymerisation of linear chains and, due to the equilibrium in the system between monomer and polymer, cyclic species are always present in polymerisation. This also means there is a critical concentration of monomer that is required in order to polymerise linear chains, below which only cyclic species are formed through transesterification.

1.4 Pentadecalactone polymerisation

PDL is a monomer commonly found in nature making it an ideal candidate for a renewably sourced material. The monomer itself is a sixteen-membered ring macrolactone with no side chains or functional groups. Poly(pentadecalactone) (PPDL) is an interesting material as a consequence of its long repeat unit length giving the polymer a repeating 15-carbon alkyl chain. This not only means that polymerisation of PDL is a quick, effective route to generating high molecular weight polymers, but the long aliphatic backbone introduces strong crystallinity. In fact, the crystallinity exhibited by PPDL is very high, leading to the polymer displaying high mechanical and tensile strength properties that are comparable to low-density poly(ethylene) (LDPE).⁶⁶⁻⁶⁸ The crystallinity also affects the melting and crystallisation temperatures (T_m and T_c) of the polymer, which are very high (T_m = 95 °C) compared to poly(ϵ -caprolactone) (PCL) (T_m = 57 °C).⁶⁹ The glass transition temperature of PPDL is difficult to measure through calorimetric measures (*e.g.* differential scanning calorimetry (DSC)) and can only be observed through dynamic mechanical testing (*e.g.* dynamic mechanical thermal analysis (DMTA)). This is a consequence of the high crystallinity leading to a large intensity in the T_m and T_c , which mask the T_g , even using slow heating or rapid cooling techniques.²⁹

The recurring ester linkage present is an ideal centre for hydrolytic degradation, similar to that of other polymerised lactones.^{45, 67, 70-73} However, degradation has proven difficult as a consequence of the high hydrophobicity of the alkyl chain contributing strongly to the prevention of attack on the ester, thus PPDL has only been shown to degrade enzymatically or in highly acidic or basic conditions.³⁰ The use of PPDL as a homopolymer for biomedical application is unfeasible, however, as the human body does not contain enzymes in the body capable of degrading PPDL.¹⁹

As a consequence of this large ring size, PDL exhibits very low ring-strain which leads to a $\Delta H_{RO}^{\circ} = +3 \text{ kJ.mol}^{-1}$. The driving force for polymerisation is therefore entropy (ΔS_{RO}°), which is a negative value ($-23 \text{ J.mol}^{-1}.\text{K}^{-1}$) as a consequence of gain in free rotation and therefore produces a positive value for the term, $-T\Delta S_{RO}^{\circ}$. Higher temperatures are required compared to strained lactones with ROP driven by enthalpy in order to produce a negative Gibbs free energy of polymerisation, allowing polymerisation to occur. As mentioned above, the thermodynamics of PDL polymerisation means that transesterification side reactions occur concurrently with polymerisation and cyclic species are present throughout polymerisation.

The polymerisation of PDL was first conducted in 1996 through eROP using Novozyme 435, immobilised *Candida antarctica* Lipase B (CALB) on acrylic resin.⁷⁴ Water is intrinsically required for the enzyme to function, however water can also initiate polymerisation of PDL leading to low end-group fidelity when using another initiator. Furthermore, the eROP of PDL is known to occur through the initial co-ordination of the monomer to the enzyme, rather than with other catalysts, with which the initiating species usually coordinates first.¹⁸ This therefore means transesterification side reactions and initiation from water can occur concurrently with polymerisation from the start of the reaction, resulting in increased overall molecular weight dispersity and low end-group fidelity.

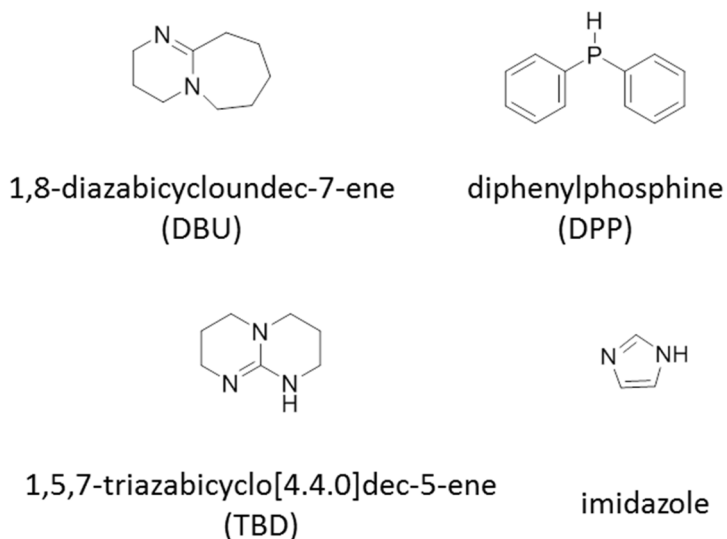


Figure 1.4 Examples of organocatalysts for ROP.

An extensive study was recently carried out into the polymerisation of PDL by commercially available organocatalysts (Figure 1.4).¹² The results of the study showed that only TBD can successfully polymerise PDL to high conversions, with other organocatalysts showing either no polymerisation or only oligomer formation. However, more inorganic catalysts have been shown to polymerise PDL than organocatalysts. Organometallic catalysts with metal centres of Al,^{42, 47, 49} Sn,⁴⁹ Ca,⁷⁵ Zn,^{54, 75} La, Nd and Y¹⁹ have all displayed the ability to polymerise PDL. These catalysts have shown the ability to polymerise PDL to high molecular weights efficiently, although dispersities still broaden as a consequence of cyclic species formation. Furthermore, the quantity of catalyst required for the polymerisation is usually equimolar with initiator as a catalyst/chain transfer agent (CTA) complex is generated in order to propagate polymerisation. This meant most PPDL molecular weights were defined by the molar ratio of monomer-to-initiator-to-catalyst as is common in 'classical' ROP. Recently, the use of novel Al and Zn catalysts have shown iROP can be achieved with PDL and lower catalytic loading allows for molecular weight to be defined solely by the molar ratio of monomer-to-initiator (Figure 1.5).⁴⁰ The catalysts have all required stringent drying techniques to be applied to all reagents before polymerisation can progress and also required an inert environment, which can be very expensive when

increased to an industrial scale. Furthermore, the cost of production of these catalysts (particularly the lanthanide catalysts) can be high.

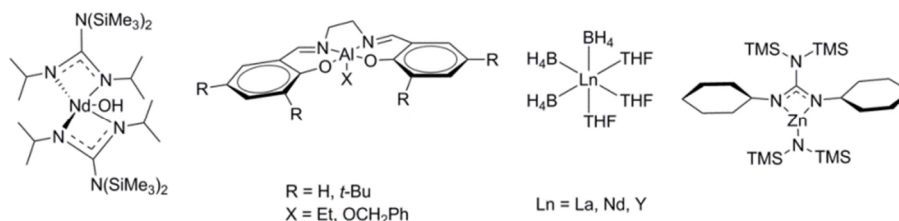
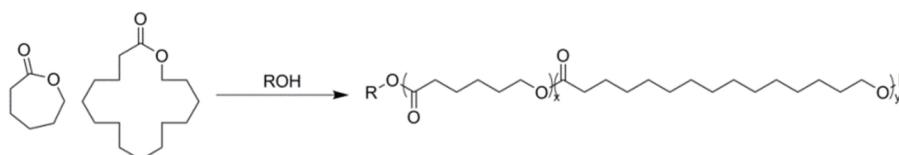


Figure 1.5 Examples of organometallic catalysts used in ROP.

1.5 Pentadecalactone copolymerisation

Due to the high processing temperatures and lack of functional groups in PPDL homopolymerisations, the material has limited application. However, copolymers of PDL with other monomers, such as lactones and carbonates, has been researched in order to keep the useful properties of PDL (*e.g.* tensile strength) and introduce new features (*e.g.* lower crystallinity, low processing temperatures, improved degradability) and making more industrially relevant materials.

1.5.1 Copolymerisation with other non-substituted lactones



Scheme 1.3 Copolymerisation of ϵ -caprolactone and ω -pentadecalactone.

The copolymerisation of PDL with ϵ CL to produce random copolymers has been well documented through enzymatic, organic and inorganic catalyst based ROP (Scheme 1.3).^{12, 16, 76, 77} Copolymerisations of PDL and ϵ CL by eROP were observed to form polymers that were completely random in architecture. Kinetic studies of the copolymerisation showed that although PDL monomer was consumed at a greater rate than ϵ CL, transesterification side reactions occurring concurrently produced random and not gradient copolymers.¹⁶ Sequential polymerisation techniques were also attempted in order to produce block copolymers, however transesterification side reactions still occurred and random

copolymers were formed. TBD catalysed copolymerisations of PDL and ϵ CL also produced completely random copolymers, however, copolymerisation was shown to occur with ϵ CL incorporation occurring faster than PDL, which contrasts with eROP copolymerisation.¹² The consumption of ϵ CL occurs quicker than PDL as a consequence of the more favourable thermodynamics, whereas in eROP, the high hydrophobicity of PDL over ϵ CL concentrates the monomer at the enzyme active site, promoting preferential consumption. The resulting materials of TBD catalysed copolymerisation were still random in architecture as a result of concurrent transesterification. In both TBD and enzyme catalysed ROP, when the sequential polymerisation was attempted, transesterification side reactions caused the formation of random copolymers instead of the expected block copolymers.

Through varying the molar ratio of PDL-to- ϵ CL and measuring the T_m and T_c of the polymers through differential scanning calorimetry (DSC), it was discovered that a linear relationship between molar ratio and T_m/T_c exists, such that as the content of one lactone increases, the T_m and T_c change linearly towards the T_m and T_c of the respective lactone homopolymer.^{12, 16, 76} The blending of PCL and PPDL homopolymers in the presence of catalyst has also been attempted for both eROP and ROP catalysed by TBD. In both cases it was shown that the resulting materials produced were completely random copolymers based on the molar ratio of PDL and ϵ CL in the system.^{40, 78} The use of organocatalyst ROP is preferable over eROP as a consequence of the higher activity of the catalyst leading to lower polymerisation times and better control through accurate measurement of catalytic loading that ultimately leads to higher molecular weight polymers.

Copolymerisations of PDL and ϵ CL by inorganic catalysts of 2-(((2-dimethylamino)ethyl)imino)methyl)-4,6-bis(1,1-dimethylethyl)-phenol with Zn, Ca or Al metal centres have also yielded similar results to TBD, with one-pot polymerisations progressing through initially polymerising only ϵ CL before incorporating PDL concurrently with transesterification to produce random copolymers (Figure 1.6).⁴⁰ As also observed

with TBD and CALB, when PCL and PPDL are mixed in the presence of some inorganic catalysts, the resulting materials are random copolymers as a consequence of transesterification side reactions.

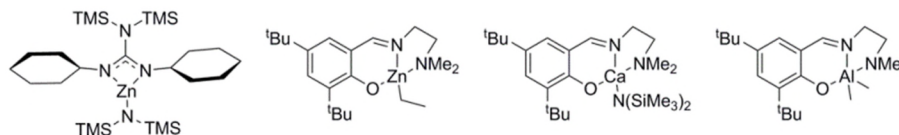
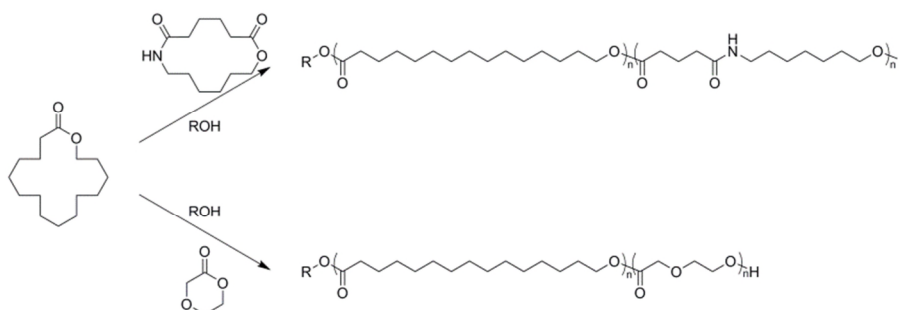


Figure 1.6 Organometallic catalysts with the ability to polymerise ω -pentadecalactone.

1.5.2 Copolymerisation with other monomers

Copolymerisation through eROP of PDL with the lactones *p*-dioxanone (pDO)⁷⁹ and 1-oxa-8-aza-cyclotetradecan-9,14-dione (a cyclic ester amide (cEA)),³⁹ a 14-membered ring lactone with amide functionality also in the ring, have been studied (Scheme 1.4). P(PDL-co-pDO), as with P(PDL-co- ϵ CL), is a random copolymer as a result of transesterification side reactions occurring during the polymerisation. The introduction of the ether functionality in the polymer backbone is beneficial in terms of assisting drug encapsulation in the network, whilst the similarity to P(PDL-co- ϵ CL) affords the polymer with the ability to tailor degradability for controlled release. Copolymers of PDL and cEA proceed with ring-opening only occurring at the cyclic ester as a consequence of the enzyme catalyst.³⁹ The resultant copolymer contained random monomer sequencing as a consequence of transesterification side reactions and lower melting temperature than PPDL homopolymer, however neither pre- or post-polymerisation functionalisation at the amide has been documented.



Scheme 1.4 Copolymerisation of PDL with 1-oxa-8-aza-cyclotetradecan-9,14-dione (top) and *p*-dioxanone (bottom).

The copolymerisation of PDL with the carbonate trimethylene carbonate (TMC) through eROP resulted in polymers formed displaying random architecture, despite different rates of incorporation of monomers.⁴⁹ As a consequence of hydrophobic interactions between PDL and the enzyme catalyst, PDL was consumed rapidly in comparison to TMC, similar to the copolymerisation of PDL and ϵ CL using eROP. The random sequencing of the copolymer is surprising in the fact that other than through eROP, copolymerisations of TMC and PDL either produce TMC homopolymers or block copolymers. Furthermore, the random copolymers also exhibited a significant increase in crystallinity compared to that of the carbonate homopolymer, whilst processing temperatures were kept low. Functionalised carbonates have also been synthesised and used in copolymerisations with PDL. Tartaric acid can be used to form a ketal diester from the secondary alcohol groups, which followed by reduction and phosgene-based ring-closure of the ester functionalities, producing a carbonate monomer with a pendent five-membered ketal ring. Copolymerisation with PDL through eROP produces random copolymers, similar to PDL/TMC copolymerisation. Post-polymerisation deprotection of the ketal is possible and introduces two hydroxyl groups per carbonate repeat unit into the polymer backbone, with the aim of accelerating degradation, but also as a site for post-polymerisation functionalisation.⁸⁰ The copolymerisation of PDL with oxo-crown ethers has also been demonstrated to produce random copolymers, with the extra ether functionalities introduced providing better regions for degradation, although this was at the cost of cocrystallinity and led to phase separation.^{81, 82}

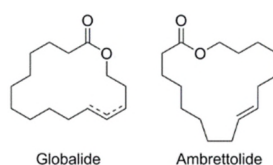


Figure 1.7 Examples of unsaturated macrolactones.

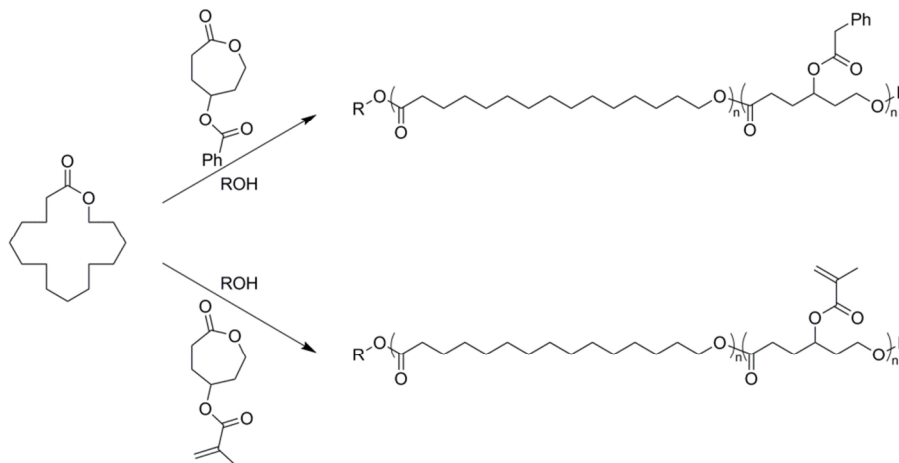
Another route to introducing functionality into PPDL is the use of ambrettolide (Amb), the unsaturated analogue of hexadecalactone (HDL), in copolymerisation (Figure 1.7). The

alkene functionality in the ring is an ideal target for modification before or after polymerisation for oxidation or thiol-ene addition. The introduction of epoxy functionality to Amb by *m*CPBA is able to be polymerised by CALB, as well as copolymerised with PDL.^{30,}

⁸³ This does produce copolymers of lower crystallinity, however the epoxy group is very stable and unsuitable for further reactions. Globalide (GL), an unsaturated PDL with alkene functionality in the ring at C11 or C12, has also been used to produce functionalised PPDL. Copolymerisation with ϵ CL through eROP produces materials similar to P(PDL-*co*- ϵ CL) but with reduced crystallinity as a consequence of the unsaturation. Thiol-ene addition of trimercapto propionate (TMP) using UV activated radical initiation crosslinked the polymers to significantly decrease the crystallinity of the network.⁸⁴

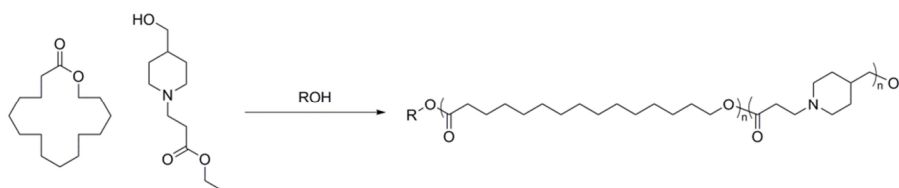
In order to introduce more complex functionalities to PDL copolymers, monomers with pendent chain functionalities have been used with PDL in copolymerisations. The simplest monomer with which to introduce side chain functionality is 4-methylcaprolactone (4MeCL). The copolymerisation of 4MeCL with GL produced materials of much lower crystallinity than P(PDL-*co*- ϵ CL).⁸³ Post-polymerisation crosslinking of the alkene in the backbone of P(GL-*co*-4MeCL) produced completely amorphous materials. The use of γ -substituted- ϵ -caprolactones, such as 4MeCL, is a common method for introduction of side chain functionalities; commercially available monomers, such as γ -acyloxy- ϵ -caprolactones, have been used for copolymerisation with PDL. PDL has successfully copolymerised with γ -methacryloyloxy- ϵ -caprolactone (McrCL) and γ -benzoyloxy- ϵ -caprolactone (BenzCL) to produce random copolymers with pendent methacrylate and benzoyl functionalities respectively (Scheme 1.5).³⁹ The pendent methacrylate group is thus available post-polymerisation for crosslinking *via* FRP, atom transfer radical polymerisation (ATRP) or reversible addition fragmentation chain transfer (RAFT) polymerisation, whilst the benzoyl functionality is an available site for ester deprotection and post-polymerisation functionalisation. However, not all γ -substituted- ϵ -caprolactones can copolymerise with

PDL, monomers such as γ -acetyloxy- ϵ -caprolactone (AcetCL) and γ -acryloyloxy- ϵ -caprolactone (AcrCL) preferentially rearrange to form γ -butyrolactones that cannot copolymerise (see above).



Scheme 1.5 Copolymerisation of ω -pentadecalactone with γ -benzoyloxy- ϵ -caprolactone (top) and γ -methacryloyloxy- ϵ -caprolactone (bottom).

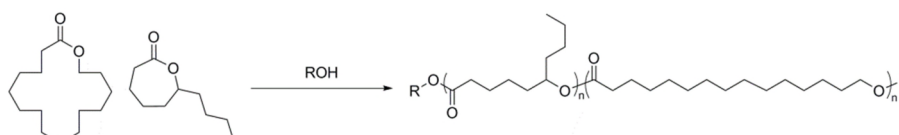
Another interesting PDL copolymer is produced from enzyme-catalysed copolymerisation with ethyl 3-(4-(hydroxymethyl)piperidin-1-yl)propanoate (EHMPP) (Scheme 1.6). Whilst the kinetics of the copolymerisation show the reaction occurs through a step-growth polymerisation mechanism, the material itself possesses interesting properties. Both monomers exhibit semi-crystalline behaviour, however they do not cocrystallise.⁸⁵ This means that varying the monomer feed ratio of the copolymerisation alters the crystallinity of the resulting material such that a minimum T_m is observed close to equimolar incorporation and T_m increases as the copolymer incorporation tends towards that of either homopolymer. This contrasts with cocrystalline PDL copolymers, where the minimum T_m is observed at a low incorporation of one monomer.^{12, 66, 86}



Scheme 1.6 Copolymerisation of ω -pentadecalactone with ethyl 3-(4-(hydroxymethyl)piperidin-1-yl)propanoate.

Terpolymers incorporating PDL have also been documented, with the terpolymerisation of PDL, diethyl sebacate (DES) and *N*-methyldiethanolamine (MDEA).⁸⁷ Through a mixture of ROP and polycondensation, in the presence of CALB, completely random terpolymers are formed that display increasing thermal stability with higher PDL content. Furthermore, the terpolymer showed crystallisation between PDL segments, but not cocrystallisation with the DES or MDEA chain segments.

Most recently, production of one-pot PDL block copolymers with other functionalised lactones has been realised through the use of the inorganic catalyst zinc 2-(((2-dimethylamino)ethyl)imino)methyl)-4,6-bis(1,1-dimethylethyl)-phenol.^{54, 75} Copolymers with the ϵ -substituted caprolactone, ϵ -decalactone (ϵ DL), have been shown to only form block copolymers with PDL, through the polymerisation of solely ϵ DL followed by the polymerisation of PDL (Scheme 1.7). The presence of the alkyl side chain adjacent to the ester means PDL would initiate from a secondary alcohol, which is very thermodynamically unfavourable and only occurs after complete consumption of the ϵ DL. The side chain is also likely to prevent transesterification side reactions between blocks as a consequence of steric hindrance.



Scheme 1.7 Copolymerisation of ω -pentadecalactone with ϵ -decalactone.

1.5.3 Copolymers through functional initiation

Polymers with inherent functionalities have also been used as macroinitiators for PDL in order to introduce sites for post-polymerisation functionalisation (*e.g.* crosslinking, thiol-ene addition). The first copolymer of this nature was poly(butadiene-*b*-pentadecalactone) produced through eROP of a monohydroxy-terminated poly(butadiene) macroinitiator, which introduces alkene functionality to the main chain backbone.⁸⁸ Conversely, the use of 2-hydroxyethyl methacrylate (HEMA) and 2-hydroxyl acrylate (HEA) as a PDL initiator to

produce graftable PPDL macromonomers has been demonstrated as a consequence of the initiating end-group being a (meth)acrylate.⁸⁹ In the case of HEMA-initiated PPDL, FRP of the macromonomer resulted in PPDL brushes. Similarly a short-chain poly(ethylene glycol) methacrylate (PEGMA) can initiate PDL eROP, followed by FRP to produce brush copolymers. Analysis of both HEMA and PEGMA end-group PPDL polymer brushes by wide-angle x-ray diffraction (WAXD) and DSC showed decreased crystallinity as a consequence of the lower conformational ability of the brush.⁹⁰ However, transacylation side reactions, as well as transesterification side reactions, have been shown to transfer the methacrylate end-group intermolecularly during polymerisation. This therefore produces PPDL with 0, 1 or 2 methacrylate end-groups, increasing dispersity and lowering end-group fidelity.⁸⁹ Whilst quicker reaction times have been shown to decrease the effect of transacylation, thereby increasing end-group fidelity, some transacylation always occurs and only low molecular weight PPDL is possible.

Similarly to HEMA, 6-mercapto-1-hexanol has been used as a PDL initiator to afford PPDL with a thiol end-group.⁹¹ Telechelic polymers were then produced by reacting the polymer with γ -thiobutyrolactone and crosslinked PPDL networks produced by thiol-ene addition with dialkenes. Telechelic PPDL has also been produced through the use of the difunctional initiator, adipic acid, to produce carboxy-terminated PPDL at both chain ends, which were reacted with glycidol resulting in epoxy-terminated telechelic PPDL.³⁸ Telechelic epoxy-PPDL could then be used alone or in conjunction with other epoxies to produce networks.

1.5.4 PDL copolymers for post-polymerisation modification

As previously mentioned, attempts to produce block copolymers of PDL with other non-substituted lactones using organic or enzymatic catalysts through sequential polymerisation have been unsuccessful. However, unlike with TBD or eROP, the sequential copolymerisation of ϵ CL and PDL using ‘immortal’ Zn or Ca catalysts has resulted in block

copolymers. Through the initial homopolymerisation of PDL, followed by the addition of ϵ CL through injection, block copolymers were observed that did not change to a random architecture over time. This meant that even at low monomer concentrations, transesterification side reactions were not energetically favourable and thus no randomisation of the chain occurs.⁴⁰

1.6 References

1. C. W. Bielawski and R. H. Grubbs, *Prog. Polym. Sci.*, 2007, **32**, 1-29.
2. D. Smith, E. B. Pentzer and S. T. Nguyen, *Polym. Rev. (Philadelphia, PA, U. S.)*, 2007, **47**, 419-459.
3. S. Asano, T. Aida and S. Inoue, *J. Chem. Soc., Chem. Commun.*, 1985, 1148-1149.
4. Y. Li, J. Hong, R. Wei, Y. Zhang, Z. Tong, X. Zhang, B. Du, J. Xu and Z. Fan, *Chem. Sci.*, 2015, **6**, 1530-1536.
5. N. Ajellal, J.-F. Carpentier, C. Guillaume, S. M. Guillaume, M. Helou, V. Poirier, Y. Sarazin and A. Trifonov, *Dalton Trans.*, 2010, **39**, 8363-8376.
6. S. M. Guillaume and J.-F. Carpentier, *Catal. Sci. Tech.*, 2012, **2**, 898-906.
7. F. Nederberg, E. F. Connor, T. Glausser and J. L. Hedrick, *Chem. Commun.*, 2001, 2066-2067.
8. M. Ryner, K. Stridsberg, A.-C. Albertsson, H. von Schenck and M. Svensson, *Macromolecules*, 2001, **34**, 3877-3881.
9. X. Lou, C. Detrembleur and R. Jérôme, *Macromol. Rapid Commun.*, 2003, **24**, 161-172.
10. A. K. Acharya, Y. A. Chang, G. O. Jones, J. E. Rice, J. L. Hedrick, H. W. Horn and R. M. Waymouth, *J. Phys. Chem. B*, 2014, **118**, 6553-6560.
11. K. S. Bisht, L. A. Henderson, R. A. Gross, D. L. Kaplan and G. Swift, *Macromolecules*, 1997, **30**, 2705-2711.

12. M. Bouyahyi, M. P. F. Pepels, A. Heise and R. Duchateau, *Macromolecules*, 2012, **45**, 3356-3366.
13. H.-J. Fang, P.-S. Lai, J.-Y. Chen, S. C. N. Hsu, W.-D. Peng, S.-W. Ou, Y.-C. Lai, Y.-J. Chen, H. Chung, Y. Chen, T.-C. Huang, B.-S. Wu and H.-Y. Chen, *J. Polym. Sci., Part A: Polym. Chem.*, 2012, **50**, 2697-2704.
14. H. Kikuchi, H. Uyama and S. Kobayashi, *Polym. J.*, 2002, **34**, 835-840.
15. H. Kim, J. V. Olsson, J. L. Hedrick and R. M. Waymouth, *ACS Macro Lett.*, 2012, **1**, 845-847.
16. A. Kumar, B. Kalra, A. Dekhterman and R. A. Gross, *Macromolecules*, 2000, **33**, 6303-6309.
17. M. T. Martello, A. Burns and M. Hillmyer, *ACS Macro Lett.*, 2011, **1**, 131-135.
18. Y. Mei, A. Kumar and R. Gross, *Macromolecules*, 2003, **36**, 5530-5536.
19. Y. Nakayama, N. Watanabe, K. Kusaba, K. Sasaki, Z. Cai, T. Shiono and C. Tsutsumi, *J. Appl. Polym. Sci.*, 2011, **121**, 2098-2103.
20. S. Namekawa, S. Suda, H. Uyama and S. Kobayashi, *Int. J. Biol. Macromol.*, 1999, **25**, 145-151.
21. A. Valente, P. Zinck, A. Mortreux, M. Visseaux, P. J. G. Mendes, T. J. L. Silva and M. H. Garcia, *J. Mol. Catal. A: Chem.*, 2011, **346**, 102-110.
22. L. van der Mee, F. Helmich, R. de Bruijn, J. A. J. M. Vekemans, A. R. A. Palmans and E. W. Meijer, *Macromolecules*, 2006, **39**, 5021-5027.
23. L. Zhang, X. Deng and Z. Huang, *Biotechnol. Lett.*, 1996, **18**, 1051-1054.
24. I. van der Meulen, E. Gubbels, S. Huijser, R. Sablong, C. E. Koning, A. Heise and R. Duchateau, *Macromolecules*, 2011, **44**, 4301-4305.
25. I. K. Varma, A.-C. Albertsson, R. Rajkhowa and R. K. Srivastava, *Prog. Polym. Sci.*, 2005, **30**, 949-981.

26. J. A. Wilson, S. A. Hopkins, P. M. Wright and A. P. Dove, *Polym. Chem.*, 2014, **5**, 2691-2694.
27. T. L. Yu, C. C. Wu, C. C. Chen, B. H. Huang, J. C. Wu and C. C. Lin, *Polymer*, 2005, **46**, 5909-5917.
28. M. Endo, T. Aida and S. Inoue, *Macromolecules*, 1987, **20**, 2982-2988.
29. M. L. Focarete, M. Scandola, A. Kumar and R. A. Gross, *J. Polym. Sci., Part B: Polym. Phys.*, 2001, **39**, 1721-1729.
30. I. van der Meulen, M. de Geus, H. Antheunis, R. Deumens, E. A. J. Joosten, C. E. Koning and A. Heise, *Biomacromolecules*, 2008, **9**, 3404-3410.
31. G. J. M. Habraken, A. Heise and P. D. Thornton, *Macromol. Rapid Commun.*, 2012, **33**, 272-286.
32. S. H. Wibowo, A. Sulistio, E. H. H. Wong, A. Blencowe and G. G. Qiao, *Chem. Commun.*, 2014, **50**, 4971-4988.
33. P. Thornton, R. Brannigan, J. Podporska, B. Quilty and A. Heise, *J. Mater. Sci.: Mater. Med.*, 2012, **23**, 37-45.
34. R. J. Pounder, D. J. Fox, I. A. Barker, M. J. Bennison and A. P. Dove, *Polym. Chem.*, 2011, **2**, 2204-2212.
35. O. Thillaye du Boullay, C. Bonduelle, B. Martin-Vaca and D. Bourissou, *Chem. Commun.*, 2008, 1786-1788.
36. M. Basko, A. Duda, S. Kazmierski and P. Kubisa, *J. Polym. Sci., Part A: Polym. Chem.*, 2013, **51**, 4873-4884.
37. H. J. Yang, J. B. Xu, S. Pispas and G. Z. Zhang, *Macromolecules*, 2012, **45**, 3312-3317.
38. M. Eriksson, L. Fogelstrom, K. Hult, E. Malmstrom, M. Johansson, S. Trey and M. Martinelle, *Biomacromolecules*, 2009, **10**, 3108-3113.
39. C. Vaida, H. Keul and M. Moeller, *Green Chem.*, 2011, **13**, 889-899.
40. M. Bouyahyi and R. Duchateau, *Macromolecules*, 2014, **47**, 517-524.

41. T. Aida, *Prog. Polym. Sci.*, 1994, **19**, 469-528.
42. M. P. F. Pepels, M. Bouyahyi, A. Heise and R. Duchateau, *Macromolecules*, 2013, **46**, 4324-4334.
43. A. Duda and A. Kowalski, in *Handbook of Ring-Opening Polymerization*, Wiley-VCH Verlag GmbH & Co. KGaA, 2009, pp. 1-51.
44. K. N. Houk, A. Jabbari, H. K. Hall and C. Alemán, *J. Org. Chem.*, 2008, **73**, 2674-2678.
45. L. M. Orozco-Castellanos, A. Marcos-Fernández and A. Martínez-Richa, *Polym. Adv. Technol.*, 2011, **22**, 430-436.
46. M. P. F. Pepels, P. Souljé, R. Peters and R. Duchateau, *Macromolecules*, 2014, **47**, 5542-5550.
47. Y. Wang and M. Kunioka, *Macromol. Symp.*, 2005, **224**, 193-206.
48. Y. Watanabe, T. Yasuda, T. Aida and S. Inoue, *Macromolecules*, 1992, **25**, 1396-1400.
49. A. Kumar, K. Garg and R. A. Gross, *Macromolecules*, 2001, **34**, 3527-3533.
50. W. Zhu, A. Nese and K. Matyjaszewski, *J. Polym. Sci., Part A: Polym. Chem.*, 2011, **49**, 1942-1952.
51. R. Mahadev Patil, A. A. Ghanwat, S. Ganugapati and R. Gnaneshwar, *J. Macromol. Sci., Part A: Pure Appl. Chem.*, 2015, **52**, 114-123.
52. M.-Z. Chen, H.-M. Sun, W.-F. Li, Z.-G. Wang, Q. Shen and Y. Zhang, *J. Organomet. Chem.*, 2006, **691**, 2489-2494.
53. B. G. G. Lohmeijer, R. C. Pratt, F. Leibfarth, J. W. Logan, D. A. Long, A. P. Dove, F. Nederberg, J. Choi, C. Wade, R. M. Waymouth and J. L. Hedrick, *Macromolecules*, 2006, **39**, 8574-8583.
54. L. Jasinska-Walc, M. R. Hansen, D. V. Dudenko, A. Rozanski, M. Bouyahyi, M. Wagner, R. Graf and R. Duchateau, *Polym. Chem.*, 2014.
55. M. T. Martello, A. Burns and M. Hillmyer, *ACS Macro Lett.*, 2012, **1**, 131-135.

56. R. C. Pratt, B. G. G. Lohmeijer, D. A. Long, R. M. Waymouth and J. L. Hedrick, *J. Am. Chem. Soc.*, 2006, **128**, 4556-4557.
57. C. G. Jaffredo, J.-F. Carpentier and S. M. Guillaume, *Macromolecules*, 2013, **46**, 6765-6776.
58. F. Suriano, O. Coulembier and P. Dubois, *React. Funct. Polym.*, 2010, **70**, 747-754.
59. P. Lecomte, C. Detrembleur, X. Lou, M. Mazza, O. Halleux and R. Jérôme, *Macromol. Symp.*, 2000, **157**, 47-60.
60. F. Nederberg, E. F. Connor, M. Möller, T. Glauser and J. L. Hedrick, *Angew. Chem., Int. Ed. Engl.*, 2001, **40**, 2712-2715.
61. S. Naumann, F. G. Schmidt, W. Frey and M. R. Buchmeiser, *Polym. Chem.*, 2013, **4**, 4172-4181.
62. D. McGinty, C. S. Letizia and A. M. Api, *Food Chem. Toxicol.*, 2011, **49**, **Supplement 2**, S193-S201.
63. A. Baeyer and V. Villiger, *Ber. Bunsen-Ges. Phys. Chem.*, 1899, **32**, 3625-3633.
64. R. J. Williams, A. P. Dove and R. K. O'Reilly, *Polym. Chem.*, 2015, **6**, 2998-3008.
65. A. P. Dove, *Chem. Commun.*, 2008, 6446-6470.
66. J. Cai, C. Liu, M. Cai, J. Zhu, F. Zuo, B. S. Hsiao and R. A. Gross, *Polymer*, 2010, **51**, 1088-1099.
67. I. Castilla-Cortázar, J. Más-Estellés, J. M. Meseguer-Dueñas, J. L. Escobar Ivirico, B. Marí and A. Vidaurre, *Polym. Degrad. Stab.*, 2012, **97**, 1241-1248.
68. M. de Geus, I. van der Meulen, B. Goderis, K. van Hecke, M. Dorsch, H. van der Werff, C. E. Koning and A. Heise, *Polym. Chem.*, 2010, **1**, 525-533.
69. Y. S. Chun, Y. J. Kyung, H. C. Jung and W. N. Kim, *Polymer*, 2000, **41**, 8729-8733.
70. X. F. L. Christopher, M. S. Monica, T. Swee-Hin and W. H. Dietmar, *Biomed. Mater.*, 2008, **3**, 034108.
71. W.-J. Lin, *J. Biomed. Mater. Res., Part A*, 1999, **47**, 420-423.

72. G. G. Pitt, M. M. Gratzl, G. L. Kimmel, J. Surles and A. Sohindler, *Biomaterials*, 1981, **2**, 215-220.
73. K.-S. C. S.-Y. Lin, H.-H. Teng, M.-J. Li, *J. Microencapsulation*, 2000, **17**, 577-586.
74. H. Uyama, H. Kikuchi, K. Takeya and S. Kobayashi, *Acta Polym.*, 1996, **47**, 357-360.
75. L. Jasinska-Walc, M. Bouyahyi, A. Rozanski, R. Graf, M. R. Hansen and R. Duchateau, *Macromolecules*, 2015, **48**, 502-510.
76. G. Ceccorulli, M. Scandola, A. Kumar, B. Kalra and R. A. Gross, *Biomacromolecules*, 2005, **6**, 902-907.
77. J. Zotzmann, M. Behl, Y. Feng and A. Lendlein, *Adv. Funct. Mater.*, 2010, **20**, 3583-3594.
78. A. Kumar and R. A. Gross, *J. Am. Chem. Soc.*, 2000, **122**, 11767-11770.
79. Z. Jiang, H. Azim, R. A. Gross, M. L. Focarete and M. Scandola, *Biomacromolecules*, 2007, **8**, 2262-2269.
80. R. Wu, T. F. Al-Azemi and K. S. Bisht, *Macromolecules*, 2009, **42**, 2401-2410.
81. P. C. M. M. Magusin, B. Mezari, L. van der Mee, A. R. A. Palmans and E. W. Meijer, *Macromol. Symp.*, 2005, **230**, 126-132.
82. L. Van Der Mee, J. Antens, B. Van De Kruijs, A. R. A. Palmans and E. W. Meijer, *J. Polym. Sci., Part A: Polym. Chem.*, 2006, **44**, 2166-2176.
83. I. van der Meulen, Y. Li, R. Deumens, E. A. J. Joosten, C. E. Koning and A. Heise, *Biomacromolecules*, 2011, **12**, 837-843.
84. M. Claudino, I. van der Meulen, S. Trey, M. Jonsson, A. Heise and M. Johansson, *J. Polym. Sci., Part A: Polym. Chem.*, 2012, **50**, 16-24.
85. L. Martino, M. Scandola and Z. Jiang, *Polymer*, 2012, **53**, 1839-1848.
86. J. A. Wilson, S. A. Hopkins, P. M. Wright and A. P. Dove, *Macromolecules*, 2015, **48**, 950-958.
87. I. Voevodina, M. Scandola, J. Zhang and Z. Jiang, *RSC Adv.*, 2014, **4**, 8953-8961.

88. A. Kumar, R. A. Gross, Y. Wang and M. A. Hillmyer, *Macromolecules*, 2002, **35**, 7606-7611.
89. Y. Xiao, M. Takwa, K. Hult, C. E. Koning, A. Heise and M. Martinelle, *Macromol. Biosci.*, 2009, **9**, 713-720.
90. B. Kalra, A. Kumar, R. A. Gross, M. Baiardo and M. Scandola, *Macromolecules*, 2004, **37**, 1243-1250.
91. M. Takwa, N. Simpson, E. Malmström, K. Hult and M. Martinelle, *Macromol. Rapid Commun.*, 2006, **27**, 1932-1936.

2 The 'immortal' ring-opening polymerisation of pentadecalactone by $\text{Mg}(\text{BHT})_2(\text{THF})_2$

2.1 Introduction

Ring-opening polymerisation (ROP) of large ring lactones is of great interest as a consequence of the properties that these materials exhibit, such as high tensile strength.¹⁻⁵ However, high molecular weight polymers produced from macrocyclic lactones were difficult to achieve until the turn of the century as a consequence of inorganic catalysts manipulating the enthalpy of breaking ring-strain to drive polymerisation.⁶⁻⁸ Whilst this method is ideal for smaller (4-6 ring) lactones with high ring-strain, 14-16 ring lactones are sufficiently large to not exhibit strain and are thus commonly hard to polymerise using such catalysts.

Recent studies have shown that a range of species are able to polymerise the 16-membered cyclic lactone, ω -pentadecalactone (PDL). Poly(pentadecalactone) (PPDL) contains a long 14-carbon length chain per repeat unit, which gives the polymer a highly hydrophobic and crystalline nature leading to tensile properties similar to that of low density poly(ethylene) (LDPE).^{9, 10} Furthermore, the recurring ester group of the chain makes the polymer susceptible to degradation under hydrolytic conditions.^{11, 12} Amongst the species reported to mediate this entropy-driven process are yttrium, zinc and aluminium catalysts,^{7, 13} as well as organocatalysts and enzymes.^{1, 14-18}

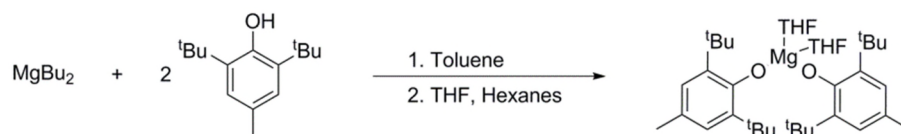
Social and economic pressures have pushed studies toward finding 'greener', less environmentally damaging processes of material production. Currently, ROP catalysts are often dependent on rigorously dry and inert environments, the implementation of which increases the cost and time of the total process. The presence of water in particular can be problematic for end-group fidelity and transesterification side reactions with water, leading to polymers of high dispersity and diverse properties.¹⁹ Organic and enzymatic catalysts both initiate ROP from any excess water present; however organometallic catalysts can be tailored through ligand variation to negate the effects of water, although are commonly deactivated under such conditions. Polymerisations would therefore be performed in inert

atmospheres, the degassing of which can be time consuming and costly, depending on the environment (*i.e.* Ar or N₂), or quantity of degas cycles. The ideal catalyst for use in a commercially viable process would therefore maintain high end group fidelity, have a high throughput before poisoning and be produced from renewable or inexpensive, commercially available compounds. 'Immortal' ring-opening catalysts as pioneered by Carpentier, Guillaume and coworkers meet such demands through acting as 'true' catalysts, allowing low quantities of catalyst with respect to monomer, ignoring any impurity present in the reaction mixture and maintaining a high monomer turnover number.^{7, 8, 20, 21} Whilst the ROP of pentadecalactone has been shown to be catalysed by the small range of catalysts described above, so far none have been shown to polymerise in the presence of water without water initiation and water-based transesterification side reactions taking place.

A recent report has shown the ability of the metallorganic catalyst, magnesium 2,6-di-tert-butyl-4-methylphenoxide (Mg(BHT)₂(THF)₂), to catalyse the ROP of ϵ -caprolactone (ϵ CL) under "air" conditions, *i.e.* the reagents used were not dried prior to use in an oxygen-rich (air) environment.²² The work in this chapter investigates the 'immortal' ring-opening polymerisation of PDL using Mg(BHT)₂(THF)₂. Furthermore, for the first time the successful polymerisation of PDL is shown to occur in atmospheric conditions, without drying reagents beforehand, yet still maintaining high end-group fidelity.

2.2 Results and Discussion

2.2.1 Synthesis of Mg(BHT)₂(THF)₂



Scheme 2.1 One-pot synthesis of Mg(BHT)₂(THF)₂.

The synthesis of Mg(BHT)₂(THF)₂ was replicated in line with the previous report from the Ittel group (Scheme 2.1).²³ Briefly, under an argon environment, ⁿBu₂Mg was reacted with 2

molar equivalents of 2,6-di-*tert*-butyl-4-methylphenol (BHT) in toluene. The solvent was removed and pentane was added in excess, followed by 2 molar equivalents of tetrahydrofuran. Following the reaction, all solvents were again removed and the white solid was dried under vacuum overnight before being stored in a glovebox. The structure of the catalyst was confirmed by ^1H and ^{13}C NMR spectroscopy, with the resonances corresponding to complexed BHT and THF being around 0.2 ppm downfield to the non-complexed reagents in deuterated benzene (C_6D_6) (Figure 2.1).

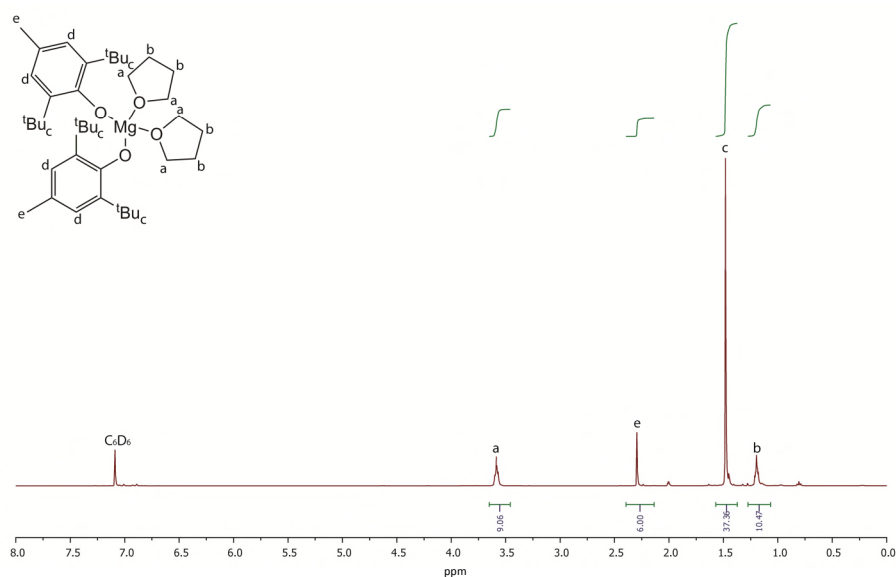
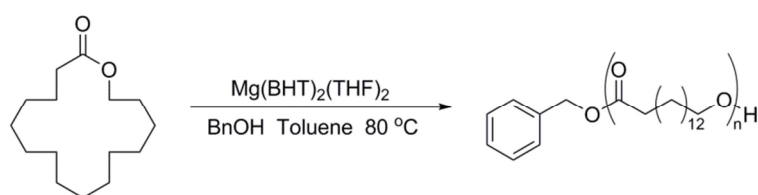


Figure 2.1 ^1H NMR spectrum of $\text{Mg}(\text{BHT})_2(\text{THF})_2$ (400 MHz, C_6D_6 , 298 K).

2.2.2 Inert homopolymerisation of PDL



Scheme 2.2 Homopolymerisation of PDL by $\text{Mg}(\text{BHT})_2(\text{THF})_2$.

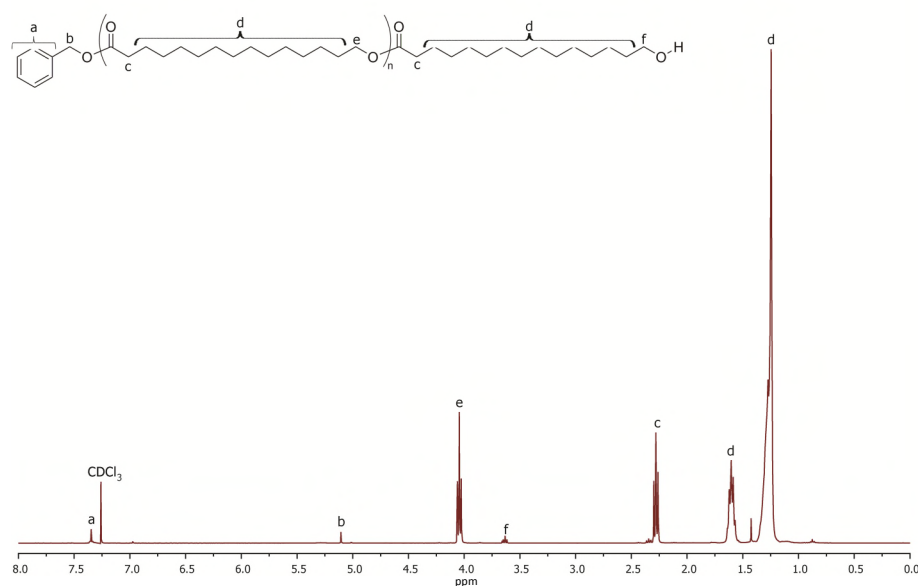


Figure 2.2 ^1H NMR spectrum of DP20 PPDL produced using $\text{Mg}(\text{BHT})_2(\text{THF})_2$ as a catalyst (400 MHz, 298 K, CDCl_3).

$\text{Mg}(\text{BHT})_2(\text{THF})_2$ has previously been studied as a catalyst for the ROP of ϵCL .²² PDL is a much larger (16-membered) cyclic molecule compared to ϵCL (7-membered cyclic molecule) with a lower ring-strain that results from its greater flexibility. Thus, polymerisation is driven through the entropic gain of rotation from ring-opening rather than ring-strain enthalpy, resulting in longer reaction times to reach full conversion. The catalytic activity of $\text{Mg}(\text{BHT})_2(\text{THF})_2$ in the ROP of PDL, using benzyl alcohol as an initiator, was studied (Scheme 2.2). The reactions were generally undertaken in 75 wt.% toluene at 80 °C in order to maintain the poorly soluble monomer and polymer in solution. Monomer conversion was monitored during the polymerisation using ^1H NMR spectroscopy by monitoring the disappearance of the monomer $\text{CH}_2\text{OC}=\text{O}$ resonance ($\delta = 4.15$ ppm) and appearance of the polymer $\text{CH}_2\text{OC}=\text{O}$ resonance ($\delta = 4.05$ ppm) in agreement with previous literature.²⁴ The polymer was purified through precipitation into excess methanol and underwent centrifugation to remove any PDL monomer present. Analysis of the resultant polymer by ^1H NMR spectroscopy allowed for the calculation of the degree of polymerisation (DP) through the ratio of the benzyl methylene resonance ($\delta = 5.11$ ppm) to the α -methylene resonance of PPDL ($\delta = 4.05$ ppm) (Figure 2.2). PDL polymerisation

kinetics were indicative of first order kinetics, maintaining the number of active chains, and conversion was maintained throughout the reaction, displaying no solvation effects decreasing the rate (Figure 2.3). It was observed that the equilibrium of polymerisation was reached at 94% monomer conversion, after which no further monomer consumption occurred and dispersities notably broadened as a consequence of continued transesterification.

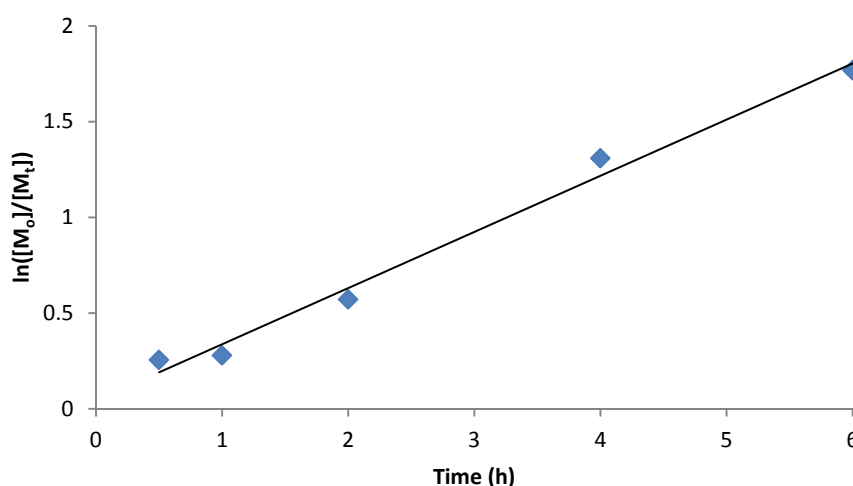


Figure 2.3 Kinetic plot for the polymerisation of ω -pentadecalactone using $\text{Mg}(\text{BHT})_2(\text{THF})_2$ as a catalyst at 80 °C in toluene with $[\text{PDL}]_0:[\text{BnOH}]_0:[\text{cat.}]_0 = 50:1:1$ and initial monomer concentration = 1 M.

The viscosity of the solution noticeably increased throughout the reaction. Regular aliquots were taken and quenched using acidified methanol (5% 1 M HCl), dissolved into chloroform and precipitated in excess methanol. Analysis of the aliquot samples by size-exclusion chromatography (SEC) showed steady growth of the polymer with M_n increasing proportionally to monomer conversion (Figure 2.4). This shows the controlled growth of the polymer chains with no termination side reactions occurring and suggests that all chains were growing at the same rate. Notably, the dispersity of these polymers was consistently greater than 2 which indicated that significant transesterification occurred alongside ROP during the polymerisation process. Furthermore, the M_n observed throughout the reaction was noticeably skewed toward lower molecular weights as a consequence of the evolution of low molecular weight cyclic species, which were present

even at low conversions and contributed to the large dispersities observed. The evolution of low molecular weight cyclic species is a consequence of the transesterification side reactions that occur concurrently with polymerisation, namely the transesterification back-biting of the active chain end reacting with an ester linkage of its own chain to form a shortened chain and a cyclic species. Following deconvolution of the chromatograms with an idealised Gaussian fit, the cyclic oligomer fraction was able to be estimated at about 12% of all polymer species. These cyclic species were easily removed through fractionation in methanol; however as a consequence of their presence, increase in M_n over conversion appears skewed with an apparent high molecular weight at 0% conversion.

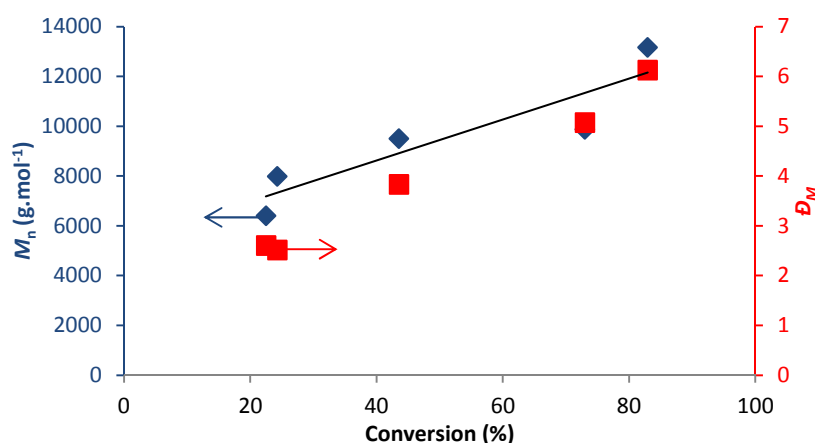


Figure 2.4 M_n and \overline{DP}_n changes over monomer conversion in the homopolymerisation of ω -pentadecalactone at 80 °C in toluene with $[PDL]_0:[BnOH]_0:[cat.]_0 = 50:1:1$ and initial monomer concentration = 1 M.

Polymerisations of PDL at 1 M concentration in toluene at 80 °C, with benzyl alcohol as initiator and $Mg(BHT)_2(THF)_2$ as catalyst, were also performed targeting DPs of 10, 25, 50 and 100, in order to prove the catalyst could produce PPDL of various molecular weights. Analysis of the reaction mixture at the end time point by 1H NMR spectroscopy showed that in all cases, monomer conversions of $\geq 94\%$ were achieved. Analysis of the resultant polymers by SEC demonstrated increasing molar mass in line with increased targeted degrees of polymerisation (Figure 2.5). As observed in the kinetics of the polymerisation, low molecular weight cyclic species were present in the final polymer that constituted up to 12% of all polymeric materials formed, as measured by deconvolution.

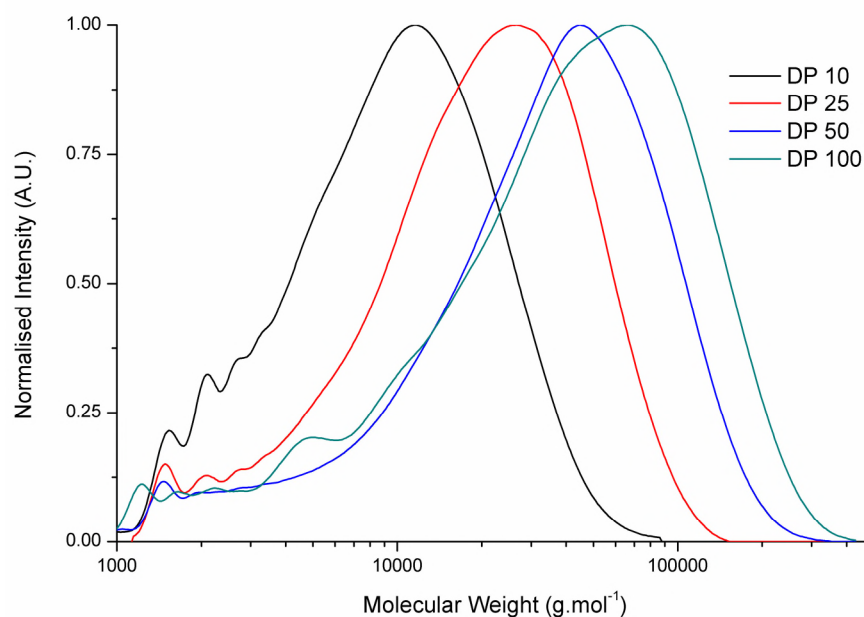


Figure 2.5 SEC chromatograms of poly(ω -pentadecalactone) at various targeted DPs.

2.2.3 Non-inert polymerisation of PDL

Further polymerisations were performed without prior drying or degassing of monomer, initiator or solvent and in an oxygen-rich (air) environment. The kinetics of the polymerisation were followed by ^1H NMR spectroscopy and shown to no longer exhibit completely linear rate behaviour, with an initially slow PDL conversion as a consequence of the competing reaction of $\text{Mg}(\text{BHT})_2(\text{THF})_2$ with the residual water present (Figure 2.6a). However, the monomer conversion at the end of the polymerisation was found to be identical to that of an inert polymerisation.

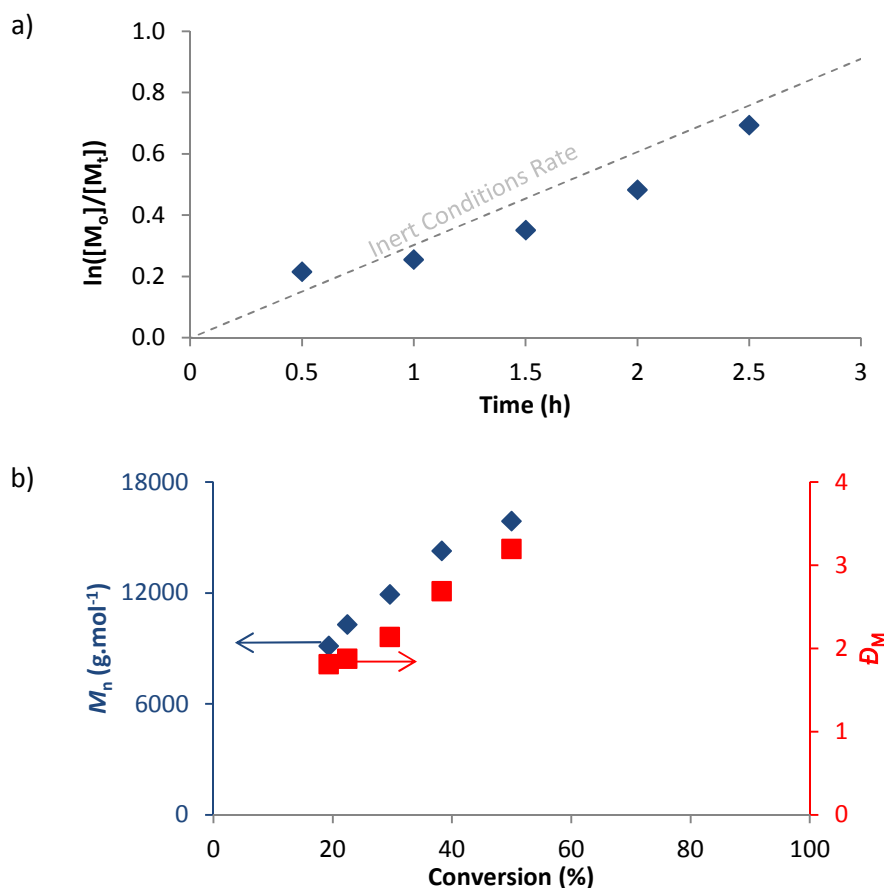


Figure 2.6 a) Kinetic plot and b) change in M_n and D_M against monomer conversion for the polymerisation of ω -pentadecalactone in a non-inert environment, using $\text{Mg}(\text{BHT})_2(\text{THF})_2$ as a catalyst at 80 °C in toluene with $[\text{PDL}]_0:[\text{BnOH}]_0:[\text{cat.}]_0 = 50:1:1$ and initial monomer concentration = 1 M.

Furthermore, the non-inert polymerisations produced polymers similar to those produced in inert conditions, with comparable yield, dispersity (D_M) and theoretical molecular weight based on monomer conversion. Analysis of samples taken during the polymerisation by SEC showed the linear increase of molecular weight with increasing monomer conversion (Figure 2.6b), thus controlled growth of polymer chains. Again, cyclic species were found to be present at low conversion and remained throughout the polymerisation (Figure 2.7). Deconvolution of the SEC chromatogram for the final polymer sample showed the quantity of cyclic species to be around 12% of all polymer species, similar to the quantity of cyclic species observed during polymerisation in inert conditions.

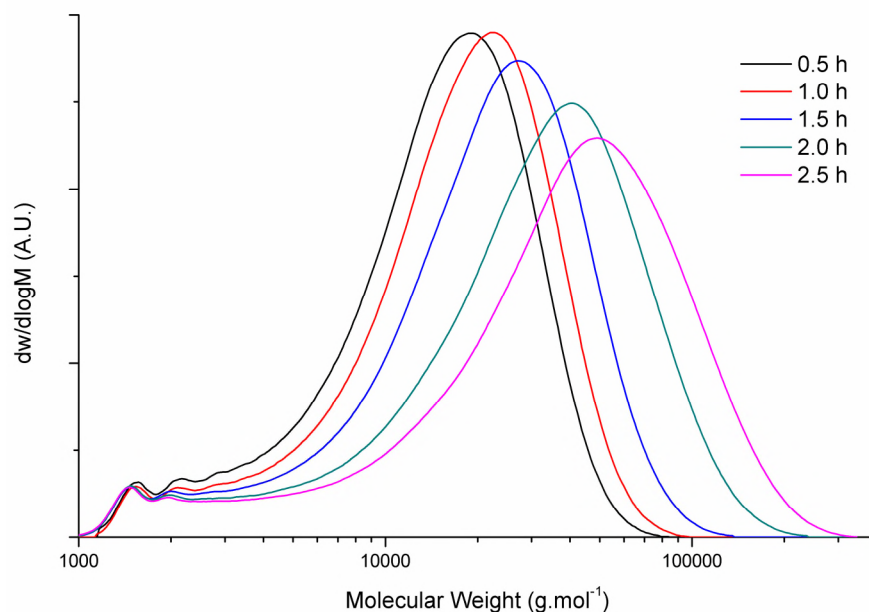


Figure 2.7 SEC chromatograms for the evolution of molecular weight distribution throughout polymerisation of PDL in non-inert conditions, targeting a DP of 20.

The presence of water in the ROP of lactones can lead to transesterification and water-initiating side reactions, which ultimately lower end-group fidelity. Therefore, the end-group fidelity of polymers produced in polymerisations targeting DP 10 PPDL in both inert and non-inert conditions was quantified through matrix-assisted laser desorption/ionization - time of flight (MALDI-TOF) mass spectrometry (Figure 2.8). Higher DP PPDL was not used for analysis by MALDI-TOF mass spectrometry as a consequence of the high molecular weight repeat unit making the polymer difficult to ionise and pass along the detector. A single distribution was observed for both polymer sets, with an average difference in mass/charge (m/z) of 240.38 between peaks that is attributable to the mass of one PDL unit. The distribution of the molecular weights in both inert and non-inert conditions was equivalent to the equation $m/z = 240.38n + 108.14$, where n is the DP. The m/z constant value of 108.14 shows the distribution is directly attributable to a polymer species initiating from a benzyl alcohol group. No further distributions were found to indicate polymers formed from other initiating species, such as water. However, water initiation would result in the formation of a carboxylic acid end-group, which can be

difficult to detect as a consequence of ionisation and therefore may be present in a low quantity. It can thus be assumed the catalyst is largely selectively initiating the ROP with benzyl alcohol in preference to water. Hence, when the catalyst reacts with residual water in non-inert conditions, water is effectively eliminated from the reaction mixture. The activity of the catalyst also decreases, as observed through ^1H NMR spectroscopy and can therefore be assumed to be poisoned as a consequence of reacting with water.

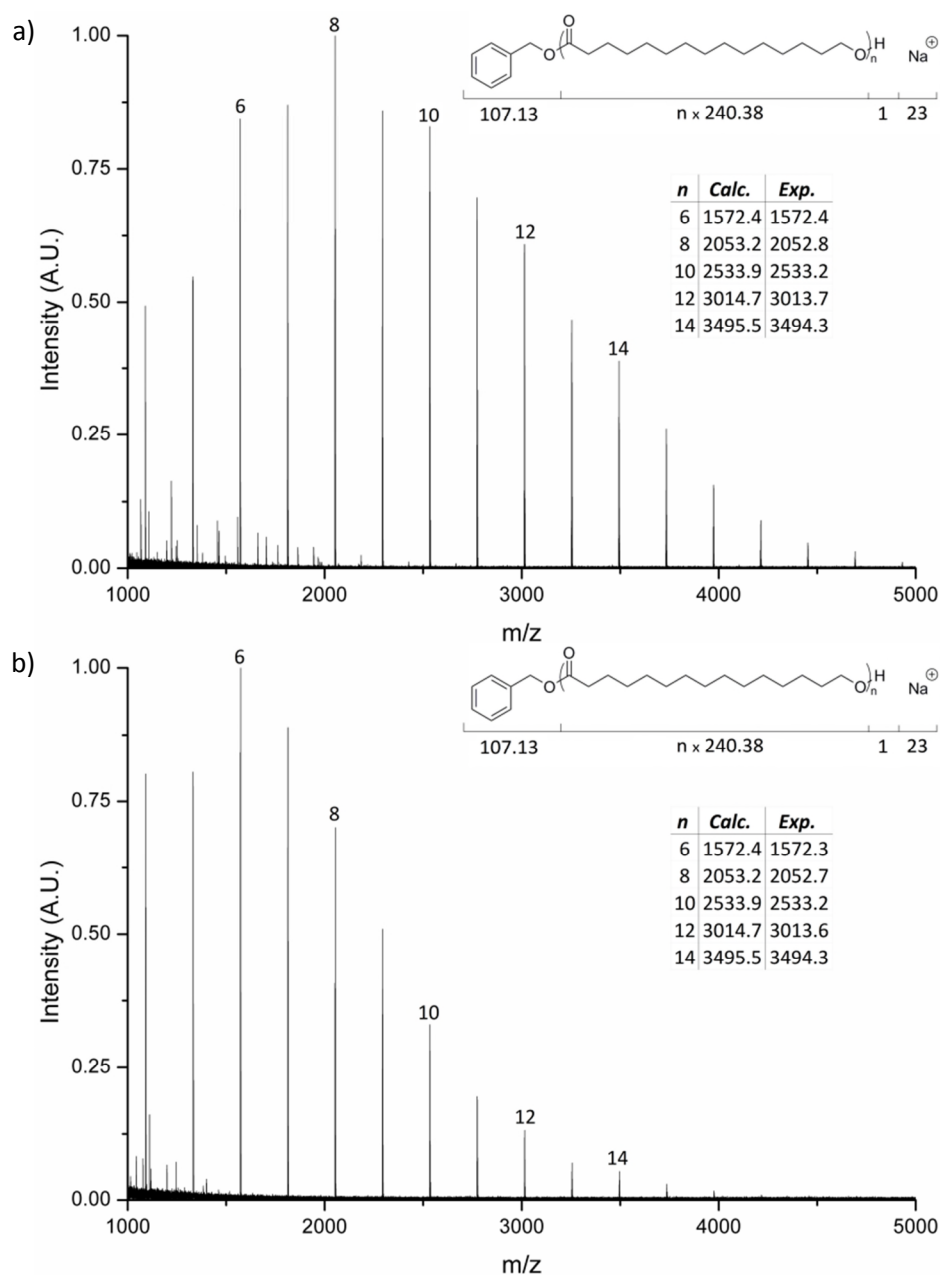


Figure 2.8 a) MALDI-TOF of DP10 PPDL produced in a dry argon environment b) MALDI-TOF of DP10 PPDL produced in non-inert conditions.

2.2.4 *Effects of solvent on polymerisation*

The conditions under which this ROP could be conducted were extended. To this end, the replacement of toluene with a more hydrophobic solvent was investigated. PDL is soluble in hexanes, however PPDL is insoluble in hexanes. To this end, the polymerisation of PDL at 1 M in hexanes at 80 °C, with benzyl alcohol as initiator and $\text{Mg}(\text{BHT})_2(\text{THF})_2$ as catalyst was conducted targeting a DP of 20 (Table 2.1). As expected, the liquid polymer formed became immiscible with hexanes and formed a visibly phase separated mixture, with solidified polymer forming immediately upon removal from the heat source. However, after 6 h of polymerisation the consumption of PDL was found to be 94% by ^1H NMR spectroscopy, with molecular weight distributions (Figure 2.9), dispersities and yields comparable to those formed in the same conditions using toluene as solvent. Thus, the ROP of PDL in hexanes yielded comparable results to those observed with toluene, despite the lack of solubility of the polymer in hexanes even at elevated temperatures.

In a further experiment, bulk polymerisation was investigated at 100 °C, the further elevated temperature was required to maintain the monomer and polymer in the melt phase. A polymerisation targeting DP 20 with benzyl alcohol as initiator and $\text{Mg}(\text{BHT})_2(\text{THF})_2$ as a catalyst in bulk PDL was attempted. After 6 h, 95% monomer conversion was determined by ^1H NMR spectroscopy, similar to 1 M polymerisations in toluene and hexanes. SEC analysis showed polymer distributions similar to those produced in solvated conditions, however a secondary distribution was prominent at lower molecular weights, attributable to an increase in the presence of cyclic species. This could be a consequence of poor solubility of the benzyl alcohol initiator in liquid PDL or the result of poor accessibility to the propagating chain end, with polymerisation occurring through initiation by the catalyst to form a zwitterion that ring-closes to form a cyclic polymer species similar to zwitterionic ROP (ZROP) of δ -valerolactone (δVL).²⁵

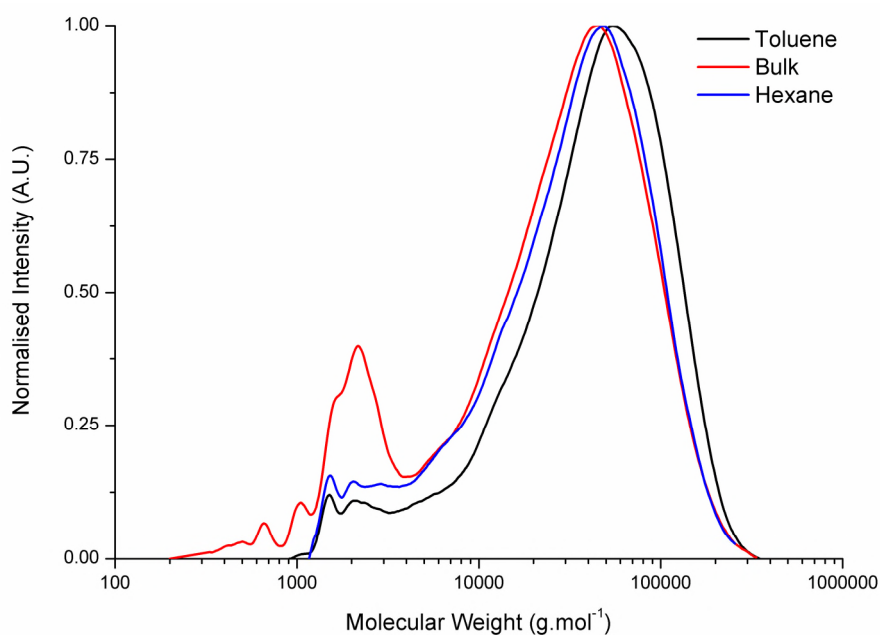


Figure 2.9 SEC chromatograms for DP 20 PPDL produced in various solvents.

Table 2.1 Synthesis of DP 50 PPDL using different solvents in non-inert conditions.

Solvent ^a	[M] : [I]	Time (h)	Conversion ^b (%)	M_p^c (kDa)	M_n^c (kDa)	M_w^c (kDa)	\mathcal{D}_M^c
Toluene	50 : 1	6	95	54.1	17.4	57.3	3.29
Hexane	50 : 1	6	94	48.5	14.3	47.0	3.29
Bulk	50 : 1	6	95	45.5	9.0	41.9	4.66

^a All reactions in solvent with [PDL] = 1 M at 80 °C, except in bulk ([PDL] = 3.8 M) at 100 °C.

^b Determined by ¹H NMR spectroscopy. ^c Determined by size-exclusion chromatography.

In order to determine whether the temperature of the polymerisation could control the molecular weight growth of PPDL in hexanes through the precipitation of solid PPDL at earlier timepoints during polymerisation, homopolymerisations of PDL were conducted at 40 °C and 60 °C for 6 hours at 1 M in hexanes, with benzyl alcohol as initiator and Mg(BHT)₂(THF)₂ as catalyst, targeting a DP of 50. For both polymerisations, a solid polymer precipitate was observed after a short period of time, which continued to increase in quantity as the polymerisation continued. Analysis of the reaction mixture after 6 hours by ¹H NMR spectroscopy showed lower overall monomer conversion than observed with the same polymerisation at 80 °C, as expected. Analysis of the polymer by SEC revealed similar molecular weight distributions to polymers formed in melt conditions (80 °C). The lack of a sharp high molecular weight drop in the distribution indicates the polymer chains continued to grow despite precipitation. Polymerisation is likely to occur through partial

solubilisation of the polymer chain end, which allows propagation to occur before reprecipitation. The dispersity of the molecular weight distribution remained similar to high temperature polymerisation and low molecular weight cyclic species were still present, thus no control over molecular weight can be achieved from control of temperature alone (Table 2.2).

Table 2.2 Synthesis of DP 50 PPDL in hexanes at different temperatures in inert conditions^a.

Temperature (°C)	Time (h)	Conversion ^b (%)	M_p^c (kDa)	M_n^c (kDa)	M_w^c (kDa)	M_n^b (kDa)	\bar{D}_M^c
40	48	46	17.0	7.8	19.2	5.2	2.47
60	24	86	29.4	12.3	29.6	9.7	2.40
80	6	83	33.7	14.3	33.5	10.6	2.34

^a All reactions in solvent with [PDL] = 1 M. ^b Determined by ¹H NMR spectroscopy. ^c Determined by size-exclusion chromatography.

Controlling the solubility of the polymer at higher molecular weights during polymerisation at low (60 °C) temperature would allow for control over the overall molecular weight distribution. In order to determine whether the solubility can be used to control molecular weight distribution, the homopolymerisations of PDL were conducted at 60 °C at 1 M in a hexane/toluene mixture, with benzyl alcohol as initiator and Mg(BHT)₂(THF)₂ as catalyst, targeting a DP of 50. The ratio of hexanes : toluene was varied in order to determine an ideal mixture ratio for controlled growth of PPDL and as such, ratios of 25 : 75, 50 : 50 and 75 : 25 hexanes : toluene were tested (Table 2.3). Polymerisations were heated at 60 °C for a period of 6 h, after which monomer conversion was determined by ¹H NMR spectroscopy and molecular weight determined by SEC analysis. During polymerisations at 50 : 50 and 75 : 25 hexanes : toluene, a white precipitate was observed after 1 h of polymerisation, which continued to increase in quantity as the polymerisation progressed.

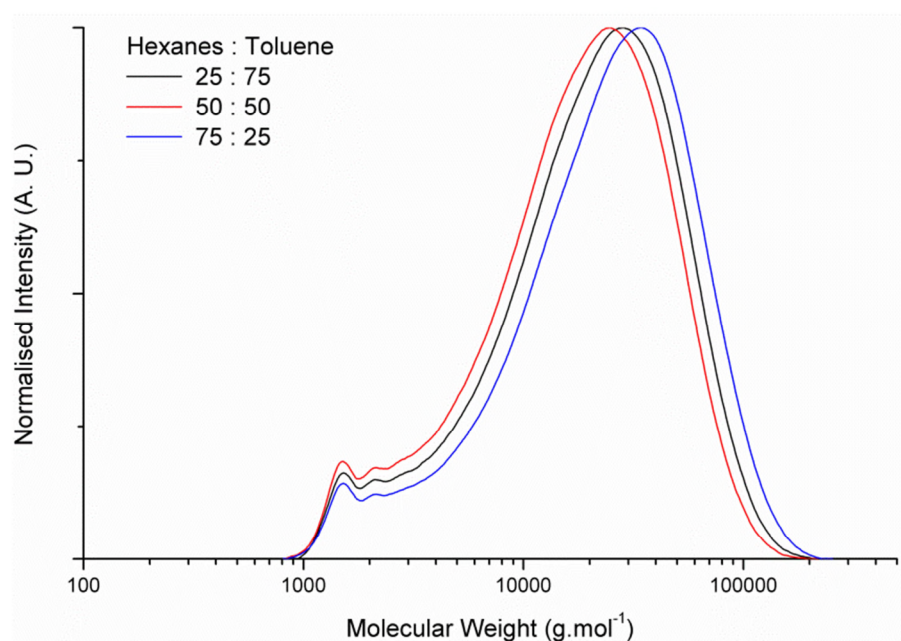
Table 2.3 Synthesis of DP 50 PPDL using different solvent ratios of hexanes and toluene.

Hexanes : Toluene	Time (h)	Conversion ^b (%)	M_p^c (kDa)	M_n^c (kDa)	M_w^c (kDa)	\mathcal{D}_M^c
25 : 75	6	60	28.4	10.7	27.6	2.58
50 : 50	6	58	34.6	12.0	32.4	2.70
75 : 25	6	74	24.9	9.6	24.4	2.54

^a All reactions in solvent with [PDL] = 1 M at 60 °C. ^b Determined by ¹H NMR spectroscopy.

^c Determined by size-exclusion chromatography.

For each solvent ratio tested, the degree of monomer conversion was lower than the conversion observed in homopolymerisations of PDL at 80 °C for pure toluene or hexanes polymerisation (between 55% and 75%), however the SEC analysis of each of the resultant copolymers showed large dispersities with low molecular weight cyclic species still present similar to homopolymerisations of PDL at 80 °C (Figure 2.10). No sharp high molecular weight drop was observed for any solvent ratio, which indicates the precipitation of the polymer did not affect the growth of the PPDL chain.

**Figure 2.10** SEC chromatographs of DP 50 PPDL produced in various ratios of hexanes : toluene.

2.2.5 'Immortal' polymerisation of PDL

Polymerisation of PDL in non-inert conditions still produced PPDL with similar molecular weight properties to PDL polymerisation in inert conditions, despite the catalyst being partially poisoned by residual water. This strongly indicates that the molar equivalents of catalyst required to successfully polymerise PDL is less than the molar equivalents of

initiator, typical of 'immortal' ROP catalysts. In order to investigate the 'immortal' ring-opening polymerisation (iROP) behaviour of $\text{Mg}(\text{BHT})_2(\text{THF})_2$ under inert conditions, the catalyst loading was decreased by an order of magnitude in a sequence of reactions until no observable polymerisation occurred (Table 2.4). It was observed that a monomer-to-catalyst molar ratio of 200 : 1 underwent successful polymerisation reaching the targeted degree of polymerisation (DP) of 200. Increasing the quantity of initiator, such that the initiator-to-catalyst molar ratio became 10 : 1 resulted in complete monomer conversion and the production of DP 20 PPDL. This shows the polymerisation can occur at lower catalyst-to-initiator molar ratios than 1 : 1 and thus is not a 'classical' ROP method. The catalyst can polymerise multiple chain ends concurrently and maintain controlled growth of each chain, typical of 'immortal' ROP catalysts. Reducing the monomer concentration to a monomer-to-initiator-to-catalyst molar ratio of 1000 : 10 : 1 (*i.e.* a targeted DP of 100 with 0.1 mol% catalyst) severely reduced the rate of polymerisation, with only 36% monomer conversion achieved over 48 h. This is a consequence of impurities present in the reaction mixture poisoning the catalyst, which are minimal at higher catalyst loading, but have significant effect at lower catalyst concentrations. Further reduction of the monomer-to-initiator-to-catalyst molar ratio to 10000 : 100 : 1 showed no polymerisation activity after 24 h. Complete loss of catalytic activity with polymerisations at an initiator-to-catalyst molar ratio of 100 : 1 occurs as a consequence of the quantity of impurities with respect to catalyst becoming too great and poisoning all the catalyst in the mixture.

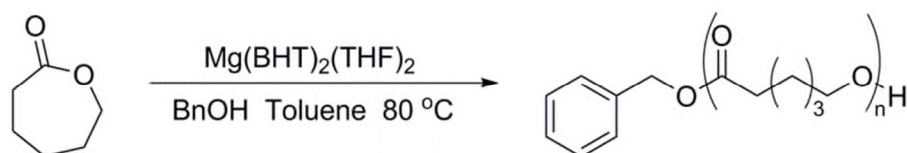
Table 2.4 'Immortal' ring-opening polymerisation results for varied $\text{Mg}(\text{BHT})_2(\text{THF})_2$ concentrations polymerising PDL^a.

[M] : [I] : [cat.]	[M] : [I]	Time (h)	Conversion ^b (%)	M_p^c (kDa)	M_n^c (kDa)	M_w^c (kDa)	\bar{D}_M^c
100 : 1 : 1	100 : 1	15	95	99.7	33.3	84.3	2.53
200 : 1 : 1	200 : 1	19	82	195.4	89.1	176.5	1.98
200 : 10 : 1	20 : 1	19	99	20.8	9.9	20.9	2.11
1000 : 10 : 1	100 : 1	48	36	42.1	17.3	41.5	2.39
10000 : 100 : 1	100 : 1	24	0	-	-	-	-

^a All polymerisations conducted in dry conditions using 75 wt% toluene. ^b Determined by ¹H NMR spectroscopy. ^c Determined by size-exclusion chromatography.

The results indicate 'truer' catalytic behaviour in the polymerisation, which pertains to the degree of active chains being greater than the quantity of catalyst; hence the chain can activate and deactivate reversibly by chain transfer, requiring low catalyst loading. Very recently, a catalyst study from the Duchateau group has also shown that immortal ROP of PDL is possible with a range of aluminium, zinc and calcium species.¹⁷ Herein, we have demonstrated that $\text{Mg}(\text{BHT})_2(\text{THF})_2$ enables the synthesis of relatively high molecular weight PPDL, perhaps on account of lower degrees of transesterification under the conditions employed.

2.2.6 'Immortal' polymerisation of ϵCL



Scheme 2.3 Homopolymerisation of $\epsilon\text{-CL}$ catalysed by $\text{Mg}(\text{BHT})_2(\text{THF})_2$.

The 'immortal' catalytic ability of $\text{Mg}(\text{BHT})_2(\text{THF})_2$ in the ROP of ϵCL at 80 °C and a monomer concentration of 1 M in toluene, initiated from benzyl alcohol with a monomer-to-initiator ratio of 100 : 1, was also explored (Scheme 2.3). The quantity of $\text{Mg}(\text{BHT})_2(\text{THF})_2$ used was systematically decreased in line with the study of the ROP of PDL. $\text{Mg}(\text{BHT})_2(\text{THF})_2$ was shown to mediate the ROP of ϵCL at a reduced molar ratio with respect to initiator of 10 : 1, with no loss of catalytic activity (Table 2.5). The homopolymerisation of ϵCL with a targeted DP of 500 at reduced catalyst loading ([I] : [cat.] being 10 : 1) was found to reach a total monomer conversion of 89% after 24 h, indicating an achievable turnover number

(TON) of ~ 4450 for the ROP of ϵ CL catalysed by $\text{Mg}(\text{BHT})_2(\text{THF})_2$. SEC analysis of the resultant poly(ϵ -caprolactone) (PCL) showed comparable dispersities to polymers produced with an equimolar ratio of initiator : catalyst, and a monomodal molecular weight distribution (Figure 2.11). A small low molecular weight shoulder is observed as a consequence of some transesterification at higher temperatures. This differs to the homopolymerisation of PDL using $\text{Mg}(\text{BHT})_2(\text{THF})_2$ as a catalyst as a consequence of the strained nature of ϵ CL negating the formation of low molecular weight cyclic species before producing linear polymer chains. Reduction of the initiator-to-catalyst molar ratio to 100 : 1 showed that, similarly to PDL homopolymerisation attempts at this concentration, polymerisation does not occur as a consequence of catalyst deactivation by impurities present in the solution.

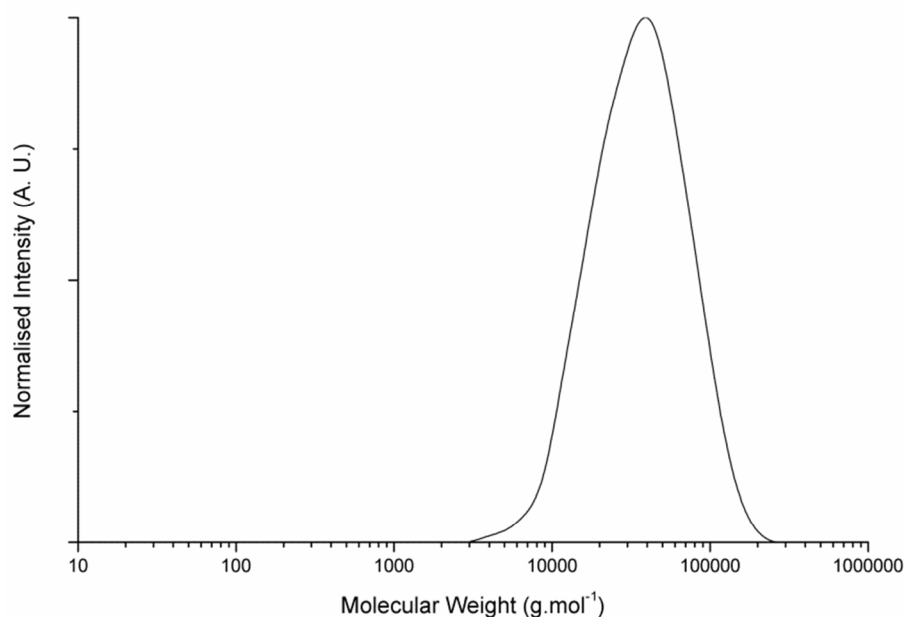


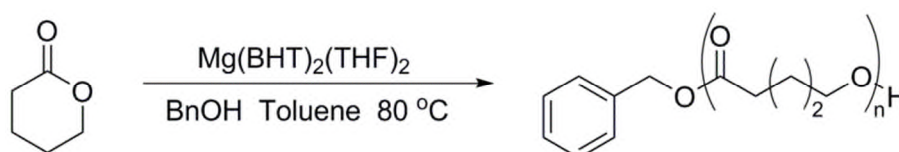
Figure 2.11 SEC chromatograph for the molecular weight distribution of targeted DP100 PCL using 0.1 eq. $\text{Mg}(\text{BHT})_2(\text{THF})_2$ catalyst with respect to benzyl alcohol initiator.

Table 2.5 'Immortal' ring-opening polymerisation results for varied $\text{Mg}(\text{BHT})_2(\text{THF})_2$ concentrations polymerising ϵCL^a .

$[\text{M}] : [\text{I}] : [\text{cat.}]$	$[\text{M}] : [\text{I}]$	Time (h)	Conversion ^b (%)	M_p^c (kDa)	M_n^c (kDa)	M_w^c (kDa)	\bar{D}_M^c
100 : 1 : 1	100 : 1	0.5	99	38.3	23.8	41.6	1.75
1000 : 10 : 1	100 : 1	0.5	99	39.6	27.4	43.9	1.60
5000 : 10 : 1	500 : 1	24	89	25.8	18.2	30.9	1.70
10000 : 100 : 1	100 : 1	24	0	-	-	-	-

^a All polymerisations conducted in dry conditions at 1 M in toluene. ^b Determined by ^1H NMR spectroscopy. ^c Determined by size-exclusion chromatography.

2.2.7 'Immortal' polymerisation of δVL



Scheme 2.4 Homopolymerisation of δ -valerolactone catalysed by $\text{Mg}(\text{BHT})_2(\text{THF})_2$.

The 'immortal' ROP ability of $\text{Mg}(\text{BHT})_2(\text{THF})_2$ was further explored through the homopolymerisation of δVL (Scheme 2.4). The homopolymerisation of δVL at 1 M in toluene was conducted at 80 °C with benzyl alcohol as initiator and $\text{Mg}(\text{BHT})_2(\text{THF})_2$ as catalyst, targeting an initial monomer-to-initiator ratio of 100 : 1. The quantity of catalyst used was systematically lowered from an initial 1 : 1 molar ratio of initiator : catalyst. The homopolymerisation of δVL occurred rapidly in comparison to the homopolymerisation of ϵCL under the same conditions, with a visible increase in viscosity within moments of the start of polymerisation. However, unlike other homopolymerisations, the equilibrium of polymerisation was reached at a much lower monomer conversion and only a maximum of 82% monomer conversion was achieved. The low conversion before equilibrium for the homopolymerisation of δVL is expected as a consequence of thermodynamics that leads to $[\text{M}]_{\text{eq}} = 3.9 \times 10^{-1} \text{ mol.L}^{-1}$ (at 298 K) for δVL homopolymerisation, an order of magnitude higher than that of ϵCL homopolymerisation ($[\text{M}]_{\text{eq}} = 5.1 \times 10^{-2} \text{ mol.L}^{-1}$ at 298 K). This does mean that higher conversions can be accessed for δVL homopolymerisations through higher initial monomer concentrations or polymerisation at a lower temperature.

The homopolymerisation of δ VL was found to proceed until equilibrium with a reduced initiator-to-catalyst ratio of 10 : 1. SEC analysis of the polymer produced showed a monomodal distribution with low dispersity ($\mathcal{D}_M = 1.31$) (Figure 2.12). The lack of a low molecular weight shoulder in the molecular weight distribution showed that no low molecular weight cyclic species were formed as a consequence of the strained nature of δ VL avoiding the thermodynamic formation of these cyclic species. As observed with a 1 : 1 initiator-to- catalyst ratio, the equilibrium of polymerisation was reached at a relatively low monomer conversion with respect to the homopolymerisation of ϵ CL and PDL, with a maximum conversion observed at 82% (Table 2.6).

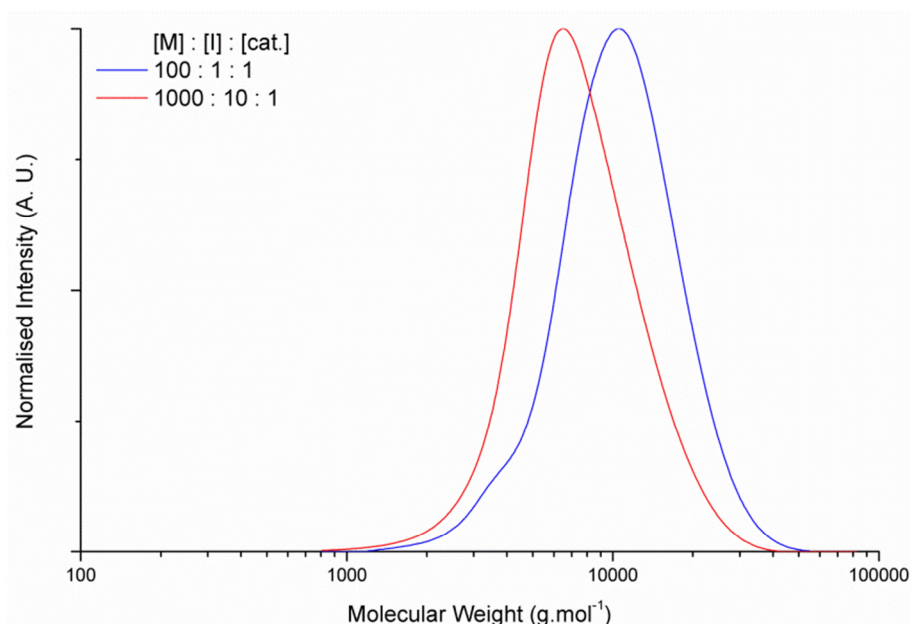


Figure 2.12 SEC chromatographs of DP 100 PVL produced with varying molar ratios of $\text{Mg}(\text{BHT})_2(\text{THF})_2$ catalyst.

In order to determine the turnover number (TON) of the catalyst in the homopolymerisation of δ VL, a solution of 1 M δ VL in toluene at 80 °C was polymerised using benzyl alcohol as initiator, $\text{Mg}(\text{BHT})_2(\text{THF})_2$ as a catalyst and targeting a DP of 500 with an initiator-to-catalyst ratio of 10 : 1. After 48 h of polymerisation, a monomer conversion of 51% was determined by ^1H NMR spectroscopy, indicating a total monomer TON of ~ 2550 for the catalyst $\text{Mg}(\text{BHT})_2(\text{THF})_2$.

Table 2.6 'Immortal' ring-opening polymerisation results for varied $\text{Mg}(\text{BHT})_2(\text{THF})_2$ concentrations polymerising δVL^a .

$[\text{M}] : [\text{I}] : [\text{cat.}]$	$[\text{M}] : [\text{I}]$	Time (h)	Conversion ^b (%)	M_p^c (kDa)	M_n^c (kDa)	M_w^c (kDa)	\bar{D}_M^c
100 : 1 : 1	100 : 1	0.5	80	10.6	8.9	11.7	1.32
100 : 1 : 1	100 : 1	1	82	11.5	10.2	14.0	1.36
1000 : 10 : 1	100 : 1	0.5	82	6.4	6.4	8.4	1.31
5000 : 10 : 1	500 : 1	48	51	7.2	7.2	9.6	1.33
10000 : 100 : 1	100 : 1	24	0	-	-	-	-

^a All polymerisations conducted in dry conditions at 1 M in toluene. ^b Determined by ^1H NMR spectroscopy. ^c Determined by size-exclusion chromatography.

Reduction of the concentration of $\text{Mg}(\text{BHT})_2(\text{THF})_2$ catalyst to a molar ratio of 100 : 1 initiator : catalyst showed no evidence of polymerisation over the course of 24 h. This is in line with observations from the homopolymerisations of both ϵCL and PDL using $\text{Mg}(\text{BHT})_2(\text{THF})_2$ as a catalyst and is a consequence of the impurities in the system poisoning the small amount of catalyst present in the experiment, thus preventing polymerisation.

2.3 Conclusion

Magnesium 2,6-di-*tert*-butyl-4-methylphenoxide ($\text{Mg}(\text{BHT})_2(\text{THF})_2$) has been successfully demonstrated to catalyse ω -pentadecalactone (PDL) through 'immortal' ring-opening polymerisation (iROP) for the first time. Characterisation of the poly(PDL) (PPDL) produced through this method exhibited good control over the molecular weights, with targetable degrees of polymerisation. Cyclic species were shown to be an inherent issue with PDL polymerisation, in line with other recent literature. The polymers produced exhibited no initiation or transesterification with water when reagents were not dried prior to use and polymerisations were conducted in non-inert atmospheres. The iROP of both PDL, ϵ -caprolactone (ϵCL) and δ -valerolactone (δVL) were also shown to be successful for catalyst : initiator ratios above 1 : 10; however polymerisations below this molar ratio proved unsuccessful as a consequence of catalytic deactivation by impurities present in the polymerisation mixture.

2.4 References

1. M. L. Focarete, M. Scandola, A. Kumar and R. A. Gross, *J. Polym. Sci., Part B: Polym. Phys.*, 2001, **39**, 1721-1729.
2. Z. Jiang, H. Azim, R. A. Gross, M. L. Focarete and M. Scandola, *Biomacromolecules*, 2007, **8**, 2262-2269.
3. B. Lebedev and A. Yevstropov, *Makromol. Chem.*, 1984, **185**, 1235-1253.
4. M. de Geus, I. van der Meulen, B. Goderis, K. van Hecke, M. Dorschu, H. van der Werff, C. E. Koning and A. Heise, *Polym. Chem.*, 2010, **1**, 525-533.
5. N. Simpson, M. Takwa, K. Hult, M. Johansson, M. Martinelle and E. Malmström, *Macromolecules*, 2008, **41**, 3613-3619.
6. A. P. Dove, *Chem. Commun.*, 2008, 6446-6470.
7. N. Ajellal, J.-F. Carpentier, C. Guillaume, S. M. Guillaume, M. Helou, V. Poirier, Y. Sarazin and A. Trifonov, *Dalton Trans.*, 2010, **39**, 8363-8376.
8. S. M. Guillaume and J.-F. Carpentier, *Catal. Sci. Tech.*, 2012, **2**, 898-906.
9. J. Cai, C. Liu, M. Cai, J. Zhu, F. Zuo, B. S. Hsiao and R. A. Gross, *Polymer*, 2010, **51**, 1088-1099.
10. G. Ceccorulli, M. Scandola, A. Kumar, B. Kalra and R. A. Gross, *Biomacromolecules*, 2005, **6**, 902-907.
11. I. van der Meulen, M. de Geus, H. Antheunis, R. Deumens, E. A. J. Joosten, C. E. Koning and A. Heise, *Biomacromolecules*, 2008, **9**, 3404-3410.
12. J. Zotzmann, M. Behl, Y. Feng and A. Lendlein, *Adv. Funct. Mater.*, 2010, **20**, 3583-3594.
13. I. van der Meulen, E. Gubbels, S. Huijser, R. Sablong, C. E. Koning, A. Heise and R. Duchateau, *Macromolecules*, 2011, **44**, 4301-4305.
14. M. Bouyahyi, M. P. F. Pepels, A. Heise and R. Duchateau, *Macromolecules*, 2012, **45**, 3356-3366.

15. H. Uyama, H. Kikuchi, K. Takeya and S. Kobayashi, *Acta Polym.*, 1996, **47**, 357-360.
16. A. Kumar, B. Kalra, A. Dekhterman and R. A. Gross, *Macromolecules*, 2000, **33**, 6303-6309.
17. M. Bouyahyi and R. Duchateau, *Macromolecules*, 2014, **47**, 517-524.
18. L. Jasinska-Walc, M. R. Hansen, D. V. Dudenko, A. Rozanski, M. Bouyahyi, M. Wagner, R. Graf and R. Duchateau, *Polym. Chem.*, 2014.
19. S. Namekawa, S. Suda, H. Uyama and S. Kobayashi, *Int. J. Biol. Macromol.*, 1999, **25**, 145-151.
20. T. L. Yu, C. C. Wu, C. C. Chen, B. H. Huang, J. C. Wu and C. C. Lin, *Polymer*, 2005, **46**, 5909-5917.
21. T. Aida, *Prog. Polym. Sci.*, 1994, **19**, 469-528.
22. H.-J. Fang, P.-S. Lai, J.-Y. Chen, S. C. N. Hsu, W.-D. Peng, S.-W. Ou, Y.-C. Lai, Y.-J. Chen, H. Chung, Y. Chen, T.-C. Huang, B.-S. Wu and H.-Y. Chen, *J. Polym. Sci., Part A: Polym. Chem.*, 2012, 2697-2704.
23. J. Calabrese, M. A. Cushing and S. D. Ittel, *Inorg. Chem.*, 1988, **27**, 867-870.
24. M. Eriksson, L. Fogelstrom, K. Hult, E. Malmstrom, M. Johansson, S. Trey and M. Martinelle, *Biomacromolecules*, 2009, **10**, 3108-3113.
25. A. K. Acharya, Y. A. Chang, G. O. Jones, J. E. Rice, J. L. Hedrick, H. W. Horn and R. M. Waymouth, *J. Phys. Chem. B*, 2014, **118**, 6553-6560.

3 Synthesis of ω -pentadecalactone copolymers with independently tuneable thermal and degradation behaviour

3.1 Introduction

The mechanical and thermal properties of poly(ω -pentadecalactone), PPDL, and its copolymers¹⁻⁹ have resulted in a recent increase in the interest in the ring-opening polymerisation (ROP) of ω -pentadecalactone (PDL) and other macrolactone monomers. As a consequence of the long alkyl chain backbone of PPDL copolymers and the crystallinity they exhibit, interest has increased annually in their application in semicrystalline polymer brushes and networks,^{5, 8, 10-12} biomedical materials⁷ and as part of shape-memory materials.¹³ The ability to source PDL from renewable feedstocks provides a potentially 'greener' route to the production of LDPE-like polymers. As a consequence of the hydrophobicity of the alkyl chain surrounding the ester repeat unit in the polymer backbone, degradation by hydrolysis in highly basic or acidic conditions has not been successful.⁷ While some enzymatic methods have been found to degrade PPDL, the enzymes applied are not naturally present in the human body.¹⁴ PPDL has been shown to degrade at high temperature (425 °C)¹ and also exhibited partial mass loss in compost (18% over 280 days).¹⁴ Hence, in order to produce PDL-based materials with enhanced biodegradability profiles, the monomer must be copolymerised with a more readily degradable comonomer.

ϵ -Caprolactone (ϵ CL) and δ -valerolactone (δ VL) are smaller ring lactones, which through ROP have been used to produce biodegradable materials. The smaller alkyl chains in the backbone of poly(ϵ -caprolactone) (PCL) and poly(δ -valerolactone) (PVL) exhibit less hydrophobicity and crystallinity than PPDL and therefore allow hydrolysis in weaker acid or base conditions.¹⁵⁻¹⁸ Furthermore, PCL and PVL have lower melting and crystallisation temperatures (T_m and T_c respectively) than PPDL and thus can be processed at lower temperatures. Previous studies have shown the statistical copolymerisation of PDL and ϵ CL produces random copolymers, which are statistically quantifiable through analysis of the polymer carbonyl resonances using ¹³C NMR spectroscopy.^{6, 9, 19} These copolymers display

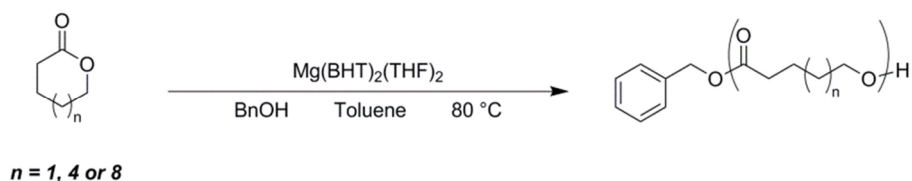
cocrystallinity with T_m and T_c linearly dependent on the molar ratio of PDL:εCL units. The kinetics of the copolymerisation of PDL and εCL have been studied with the use of different catalysts and although in each case, random copolymers are produced, the copolymerisation proceeds with different rates of consumption for each monomer. By ^1H NMR spectroscopic measurement, PDL is shown to polymerise more rapidly than εCL when *Candida antarctica* Lipase B (CALB) is applied as a catalyst,²⁰ however as a consequence of extensive transesterification side reactions, random copolymers are produced.¹⁹ Conversely, with the organic catalyst 1,5,7-triazabicyclo[4.4.0]dec-5-ene (TBD), rates of homopolymerisation predict the fast consumption of εCL compared to PDL, leading to gradient copolymers, although transesterification side reactions were again reported to cause the formation of random copolymers in practice.^{9, 21, 22}

PDL has been copolymerised with other monomers (*e.g.* *p*-dioxanone, dialkyl carbonates) to produce degradable copolymers for biomaterials.^{3, 4, 23, 24} In each of these cases, PDL was found to randomly copolymerise with the other monomers and cocrystallise to a higher degree than expected from the molar ratio of PDL present. The rate of degradation of the copolymers was proportional to the composition, with copolymers that contain less PDL and more comonomer degrading more rapidly.

This chapter demonstrates the application of $\text{Mg}(\text{BHT})_2(\text{THF})_2$ in the copolymerisation of PDL with other lactone monomers across a range of ring sizes in order to access degradable materials with a range of thermal and degradation properties. A clear correlation between the thermal properties of the resulting copolymers and monomer composition is demonstrated, which was exploited to produce copolymers with targeted thermal properties but different rates of degradation.

3.2 Results and Discussion

3.2.1 Ring-Opening Homopolymerisations



Scheme 3.1 Homopolymerisation of various lactones catalysed by $\text{Mg(BHT)}_2(\text{THF})_2$.

The synthesis of $\text{Mg(BHT)}_2(\text{THF})_2$ was undertaken as reported previously.^{25, 26} The catalyst has been previously shown to catalyse the ROP of both ω -pentadecalactone (PDL), ϵ -caprolactone and δ -valerolactone (Chapter 2). In order to quantify the effect of lactone ring size on the rate of ROP, homopolymerisations of η -caprylolactone (η CL) and ω -dodecalactone (DDL) were carried out in comparable conditions to the ROP of PDL and ϵ CL using $\text{Mg(BHT)}_2(\text{THF})_2$ as a catalyst. Whilst δ VL, ϵ CL and PDL are all commercially available, η CL and DDL were prepared through the Baeyer-Villiger oxidation of cyclooctanone and cyclododecalatone respectively with *meta*-chloroperoxybenzoic acid (*m*CPBA).²⁰

The homopolymerisations of η CL and DDL were carried out using $\text{Mg(BHT)}_2(\text{THF})_2$ as catalyst in an equimolar ratio to the benzyl alcohol initiator with a total monomer concentration of 1 M in toluene at 80 °C with a targeted degree of polymerisation (DP) of 50 (Scheme 3.1).

In comparison to the δ VL and ϵ CL homopolymerisations, η CL and DDL homopolymerisations took much longer to reach equilibrium and required heating to 80 °C. This difference in polymerisation activity is a result of smaller ring size monomers (δ VL and ϵ CL) having large, negative enthalpies of ring-opening as a result of ring strain; whereas larger ring monomers (η CL, DDL and PDL) have a lower enthalpy and hence can be polymerised by entropy-driven processes.

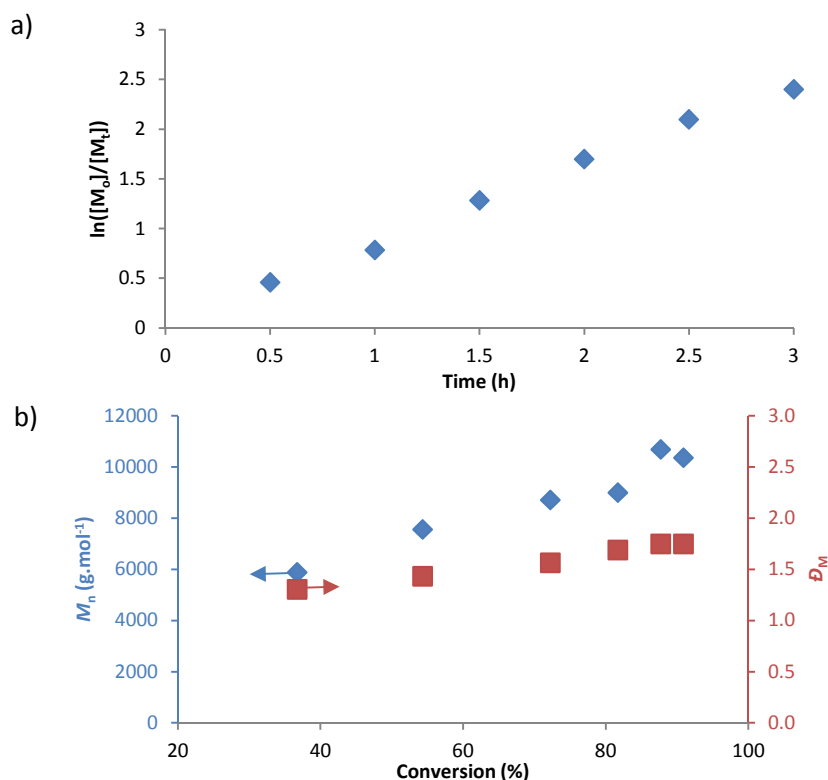


Figure 3.1 a) Kinetic plot for the homopolymerisation of η -capryl lactone using $\text{Mg}(\text{BHT})_2(\text{THF})_2$ as a catalyst at 80 °C in toluene with $[\eta\text{CL}]_0:[\text{BnOH}]_0:[\text{cat.}]_0 = 50:1:1$, total monomer concentration = 1 M. b) Changes in M_n and D_M over monomer conversion for the same polymerisation.

The homopolymerisation of ηCL was conducted at 1 M in toluene at 80 °C using benzyl alcohol as initiator, $\text{Mg}(\text{BHT})_2(\text{THF})_2$ as catalyst and targeting a DP of 50. The polymerisation was monitored throughout by ^1H NMR spectroscopy and SEC. The monomer conversion was determined by ^1H NMR spectroscopy by the disappearance of the monomer $\text{CH}_2\text{OC}=\text{O}$ resonance ($\delta = 4.32$ ppm) and appearance of the polymer $\text{CH}_2\text{OC}=\text{O}$ resonance ($\delta = 4.08$ ppm). Following the kinetics of the polymerisation through this method presented linear consumption of ηCL , indicative of first order kinetics (Figure 3.1a). The number of active chains and monomer conversion throughout the polymerisation was therefore maintained, with no termination side reactions or solvation effects decreasing the rate of polymerisation. The propagation rate (k_p) was determined to be $k_p = 0.014 \text{ s}^{-1}$. Equilibrium of polymerisation was reached after 5 h at 98% monomer conversion, after which the dispersity of the polymer increased from $D_M = 1.85$ at 5 h to $D_M = 2.7$ at 6 h as a

consequence of prevailing transesterification side reactions. Dispersities remained low ($\mathcal{D}_M < 2$) throughout the polymerisation, with no low molecular weight skew observed by SEC analysis, indicating cyclic species are not formed during the polymerisation (Figure 3.1b). Whilst η CL exhibits less ring strain than δ VL and ϵ CL, there is sufficient strain for the energy of ROP to be lower than the energies associated with transesterification side reactions. Polymerisation is thus favoured until equilibrium, after which transesterification side reactions can occur as observed by the broadening of dispersity.

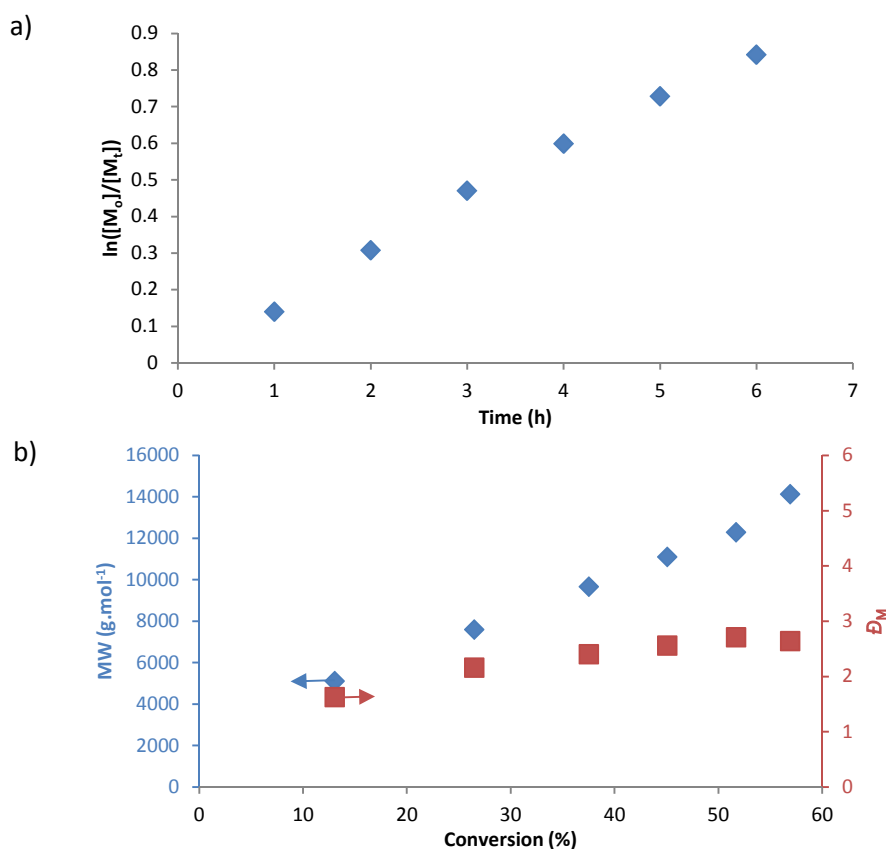


Figure 3.2 a) Kinetic plot for the homopolymerisation of dodecalactone using $\text{Mg}(\text{BHT})_2(\text{THF})_2$ as a catalyst at 80 °C in toluene with $[\text{DDL}]_0:[\text{BnOH}]_0:[\text{cat.}]_0 = 50:1:1$, total monomer concentration = 1 M. b) Changes in M_n and \mathcal{D}_M over monomer conversion for the same polymerisation.

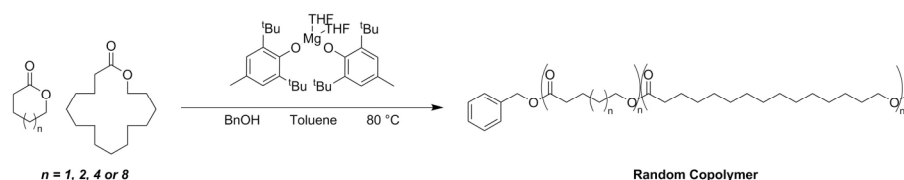
The homopolymerisation of DDL at 1 M in toluene was conducted at 80 °C, with a targeted DP of 50, benzyl alcohol as initiator and $\text{Mg}(\text{BHT})_2(\text{THF})_2$ as catalyst. Determination of monomer conversion during polymerisation was achieved by ^1H NMR spectroscopy by monitoring the disappearance of the monomer $\text{CH}_2\text{OC}=\text{O}$ resonance ($\delta = 4.17$ ppm) and the

appearance of the polymer $\text{CH}_2\text{OC}=\text{O}$ resonance ($\delta = 4.07$ ppm). First order kinetics were observed for the consumption of monomer throughout the polymerisation, with no termination side reactions or solvation effects altering the rate of polymerisation (Figure 3.2a). The observed k_p was much slower than the homopolymerisation of ηCL in the same conditions, with $k_p = 0.002 \text{ s}^{-1}$. Analysis of samples taken throughout the polymerisation by SEC showed a low molecular weight shoulder as a consequence of the formation of low molecular weight cyclic species. The cyclic species were present throughout the polymerisation, indicative of a strainless ring monomer undergoing ROP. Dispersities above 2 were observed as a consequence of the low molecular weight cyclic species (Figure 3.2b). Equilibrium of polymerisation was achieved at 89% monomer conversion, after which monomer consumption ceased and transesterification side reactions broadened the dispersity of the polymer significantly ($\mathcal{D}_M > 3$).

Comparison of the rates of polymerisation of δVL , ηCL and DDL showed a clear trend with the rate of polymerisation decreasing with increasing ring size. This is expected as a consequence of the effect of ring strain on the thermodynamics of ROP, where smaller rings exhibit greater ring strain and a larger, negative enthalpy of ring-opening. Conversely, larger rings exhibit low ring strain and therefore have a low or positive enthalpy of ring-opening and hence require more energy to propagate polymerisation.

3.2.2 Pentadecalactone copolymerisations

In order to investigate PDL copolymerisation with lactones of different sizes and the range of physical properties that these copolymer materials exhibit, PDL was copolymerised with δVL , ϵCL , ηCL and DDL (Scheme 3.2). The ROP of lactones catalysed by $\text{Mg}(\text{BHT})_2(\text{THF})_2$ is ‘immortal’ and achievable in non-inert ‘air’ conditions, however in order to provide consistency and comparability with literature, all reactions were performed in dry, inert environments.²⁶



Scheme 3.2 Copolymerisation of pentadecalactone with other lactones catalysed by $\text{Mg}(\text{BHT})_2(\text{THF})_2$.

As a first study, δVL was used as the comonomer for the copolymerisation of PDL with another lactone. The homopolymerisation of δVL is considerably faster than the homopolymerisation of PDL, thus the copolymerisation of δVL and PDL was predicted to take place through the rapid polymerisation of δVL followed by the slower polymerisation of PDL. As transesterification side reactions can occur in ROP, the final polymer may possess a random sequence of repeat units. The copolymerisation of an equimolar mixture of δVL and PDL was undertaken at an overall monomer concentration of 2 M in toluene at 80 °C, with a targeted DP of 100. Aliquots were taken periodically and the overall monomer conversion was followed by ^1H NMR spectroscopy and SEC. After 5 min of polymerisation the α -methylene resonance at $\delta = 4.35$ ppm, attributable to δVL , had been significantly reduced, which coincided with the appearance of a resonance at $\delta = 4.05$ ppm, the α -methylene resonance of either poly(δ -valerolactone) (PVL) or poly(ω -pentadecalactone) (PPDL). It should be noted that individual monomer conversion could not be monitored by ^1H NMR spectroscopy as a consequence of the α -methylene resonance for all poly(lactone)s tested appearing at $\delta = 4.05 \pm 0.01$ ppm and the overlapping of the remaining methylene resonances over the region of $\delta = 2\text{--}3$ ppm. The integration of the α -methylene resonance of PDL remained constant between 0 min and 5 min of polymerisation, which indicates that the polymer produced was a pure PVL chain. As PDL began to be incorporated into the chain, the PDL α -methylene resonance decreased over time. The incorporation of PDL was observed to be significantly slower than δVL , resulting in the overall monomer conversion slowing from 40% within the first 5 min, increasing to 58% over the next 24 h, an increase of only 18% (Figure 3.3d). Clearly, the copolymerisation

progresses through the rapid conversion of δ VL followed by the slow incorporation of PDL. This is probably a consequence of the transesterification of PVL being energetically preferable over the ROP of PDL and thus severely slowing the rate of monomer consumption. SEC analysis of the copolymerisation showed two distinct gradients in number-average molecular weight (M_n) growth (Figure 3.4). A shallow gradient was observed until 50% overall monomer consumption as a consequence of the incorporation of the relatively low molecular weight δ VL monomer, after which a steeper gradient was observed once the incorporation of larger molecular weight PDL began. Dispersities of samples taken during the copolymerisation increased significantly during the incorporation of PDL as a consequence of not only transesterification side reactions, but also the unavoidable formation of cyclic species during the polymerisation of strainless macrolactones, such as PDL, which leads to low molecular weight tailing being observed in SEC analysis.²⁷

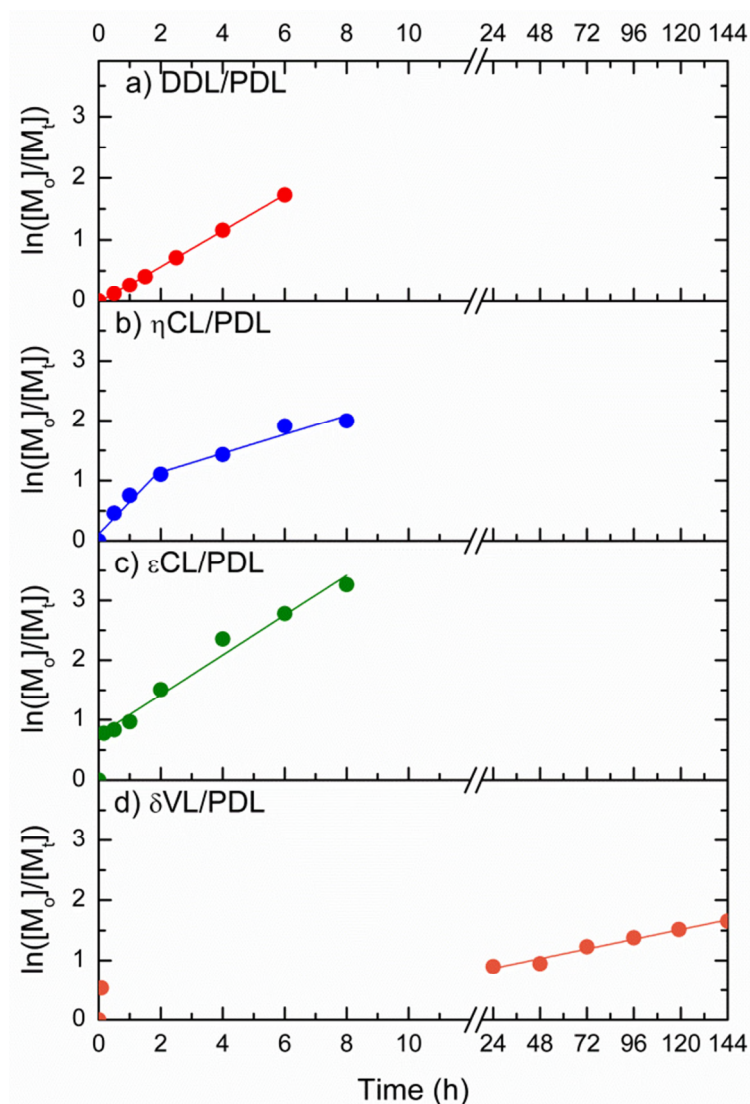


Figure 3.3 Kinetic plots for the copolymerisations of ω -pentadecalactone with a) dodecalactone, b) η -caprylolactone, c) ϵ -caprolactone and d) δ -valerolactone. All reactions at 80 °C in toluene with $[PDL]_0:[M]_0:[BnOH]_0:[cat.]_0 = 50:50:1:1$, total initial monomer concentration = 2 M.

The characterisation of monomer sequencing in the polymer chain, by the integration of the carbonyl region in quantitative ^{13}C NMR spectroscopy, is important in order to determine whether transesterification side reactions have occurred. At 40% overall monomer conversion ($t = 5$ min), only one carbonyl diad resonance was observed at $\delta = 173.4$ ppm that corresponds to a δ VL carbonyl adjacent to a δ VL repeat unit ($\delta\text{VL}^*-\delta\text{VL}$, where * represents the observed carbonyl) (Figure 3.5). As PDL is incorporated into the polymer chain, three additional carbonyl diad resonances appear that correspond to $\delta\text{VL}^*-\text{PDL}$, $\text{PDL}^*-\delta\text{VL}$ and PDL^*-PDL ($\delta = 173.5, 174.0$ and 174.1 ppm respectively). The relatively

rapid appearance of carbonyl diad resonances $\delta\text{VL}^*\text{-PDL}$ and $\text{PDL}^*\text{-}\delta\text{VL}$ compared to $\text{PDL}^*\text{-PDL}$ show that transesterification side reactions occurred faster than the incorporation of PDL. Hence, during the copolymerisation the majority of PDL incorporated onto the chain end is transesterified into the main chain before another PDL unit is incorporated. As the amount of PDL in the polymer chain increases, the probability of transesterification leading to two adjacent PDL repeat units ($\text{PDL}^*\text{-PDL}$) increases. At any time throughout the copolymerisation, the probability of an $\text{A}^*\text{-B}$ diad resonance being observed is equivalent to $P(\text{A}^*\text{-B}) = f_{\text{A}} \times f_{\text{B}}$, where f_{A} and f_{B} are the mole fractions of monomers A and B respectively (Table 3.1);^{3, 28} this is only observed in copolymers with a completely random architecture.

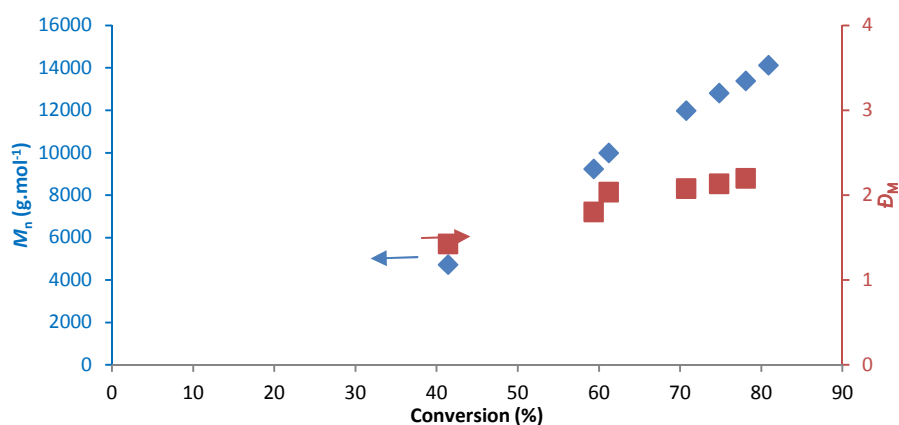


Figure 3.4 M_n against conversion for the copolymerisation of δ -valerolactone and ω -pentadecalactone at 2 M in toluene at 80 °C with $[\delta\text{VL}]_0:[\text{PDL}]_0:[\text{BnOH}]_0:[\text{Mg}(\text{BHT})_2(\text{THF})_2]_0$ of 50:50:1:1. M_n and \bar{D}_M determined by SEC against poly(styrene) standards.

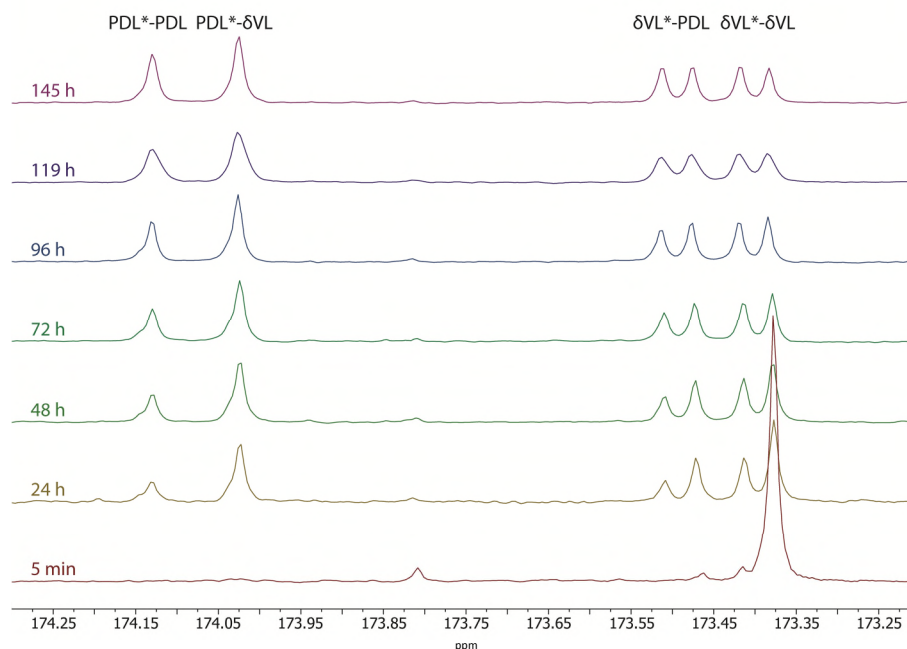


Figure 3.5 Quantitative ^{13}C NMR spectra of the carbonyl region during copolymerisations of ω -pentadecalactone with δ -valerolactone (125 MHz, CDCl_3 , 298 K).

Table 3.1 Copolymerisation of PDL and δ VL at 1:1 mol% targeting DP100.

Time (h)	Conversion ^a (%)	M_n^b (GPC) (kDa)	M_w^b (GPC) (kDa)	D_M^b	M_n^c (NMR) (kDa)	Diads ^d			
						PDL*- PDL	PDL*- δ VL	δ VL*- PDL	δ VL*- δ VL
0.08	41	8.5	12.0	1.42	4.7	0.00 (0.00)	0.00 (0.00)	0.03 (0.00)	0.97 (1.00)
24	59	9.5	17.2	1.80	9.2	0.09 (0.07)	0.24 (0.20)	0.23 (0.20)	0.44 (0.53)
48	61	9.1	18.5	2.04	10.0	0.12 (0.09)	0.26 (0.21)	0.25 (0.21)	0.37 (0.49)
72	71	10.1	21.1	2.08	12.0	0.16 (0.14)	0.26 (0.23)	0.27 (0.23)	0.31 (0.40)
96	75	12.0	25.6	2.13	12.8	0.18 (0.17)	0.27 (0.24)	0.27 (0.24)	0.28 (0.35)
119	78	12.9	28.4	2.20	13.4	0.18 (0.18)	0.28 (0.24)	0.26 (0.24)	0.28 (0.34)
145	81	14.2	31.7	2.23	14.1	0.21 (0.19)	0.27 (0.25)	0.26 (0.25)	0.26 (0.31)

^aTotal monomer conversion determined by ^1H NMR spectroscopy. ^bDetermined by SEC in CHCl_3 against poly(styrene) standards. ^cDetermined by end-group analysis by ^1H NMR spectroscopy. ^dDetermined by quantitative ^{13}C NMR spectroscopy, with * defining the carbonyl analysed and numbers in parentheses are theoretical values based on composition by the equation $P(A^*-B) = f_a \times f_b$.

The copolymerisation of an equimolar mixture of ϵ CL and PDL with an overall monomer concentration of 2 M in toluene at 80 °C with a targeted DP of 100 was also performed. Aliquots were taken periodically and overall monomer conversion determined by ^1H NMR spectroscopy and molecular weight growth followed by SEC analysis. The copolymerisation of ϵ CL and PDL was found to occur in a similar fashion to the copolymerisation of δ VL and PDL, with the fast consumption of the small ring lactone (in this case ϵ CL) followed by the slower incorporation of PDL (Figure 3.3c). The resulting polymers were determined to be completely random copolymers by quantitative ^{13}C NMR spectroscopic analysis as a consequence of transesterification side reactions. SEC analysis of samples taken during the copolymerisation again showed two distinct trends of growth as a result of the lower molecular weight ϵ CL being polymerised first, followed by a greater molecular weight increase as a consequence of PDL addition into the polymer chain (Figure 3.6). Dispersities were high ($D_M > 2$), similar to the copolymerisation of PDL and δ VL, as a consequence of the unavoidable formation of cyclic species already mentioned. The incorporation of PDL was much more rapid than observed with the copolymerisation δ VL and PDL, with complete monomer consumption occurring within a few hours rather than 14 days under the same conditions. Indeed, whilst no PDL was observed within the chain before all δ VL was consumed, some PDL was incorporated before complete consumption of ϵ CL. This behaviour may be the result of the reduced steric hindrance of δ VL in comparison to PDL, such that the catalyst favours transesterification of δ VL over the ROP of PDL. Integration of the carbonyl diad resonances in quantitative ^{13}C NMR spectra of the copolymers throughout the evolution of the polymerisation (Figure 3.7) showed the evolution of an almost pure PCL chain at 50% overall monomer conversion, which transformed into a completely random copolymer through transesterification side reactions as PDL was incorporated on to the polymer chain end, as was also observed for the copolymerisation of δ VL and PDL (Table 3.2). Interestingly, the copolymerisation shows opposite behaviour

to that of enzymatic ROP, where PDL is the first monomer consumed and δ CL is incorporated afterwards during transesterification.¹⁹

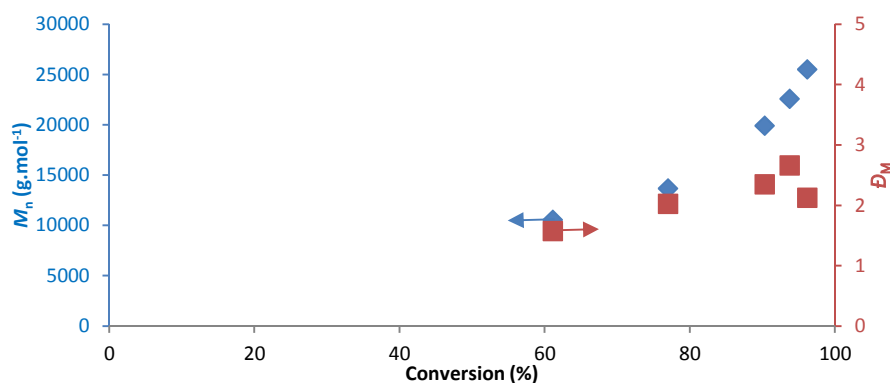


Figure 3.6 M_n against conversion for the copolymerisation of ϵ -caprolactone and ω -pentadecalactone at 2 M in toluene at 80 °C with $[\epsilon\text{CL}]_0 : [\text{PDL}]_0 : [\text{BnOH}]_0 : [\text{Mg}(\text{BHT})_2(\text{THF})_2]_0$ of 50 : 50 : 1 : 1. M_n and \bar{D}_M determined by SEC against poly(styrene) standards.

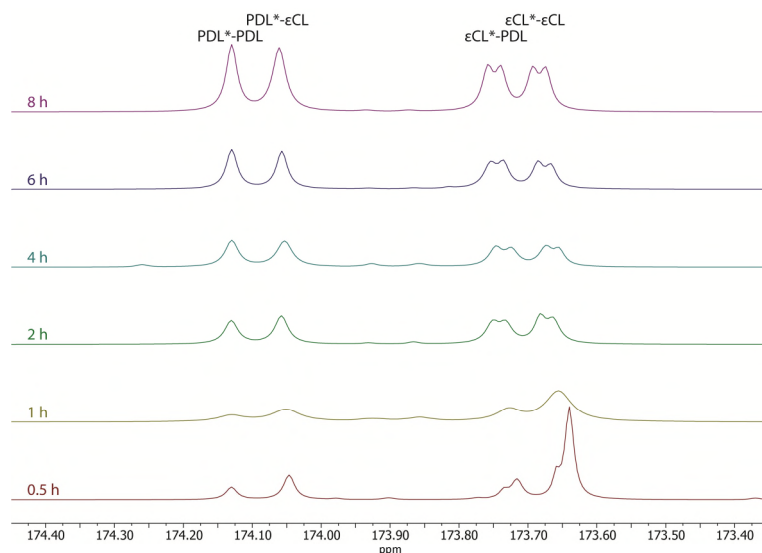


Figure 3.7 Quantitative ^{13}C NMR spectra of the carbonyl region during copolymerisations of ω -pentadecalactone with ϵ -caprolactone (125 MHz, CDCl_3 , 298 K).

Table 3.2 Copolymerisation of PDL and ϵ CL at 1:1 mol% targeting DP100.

Time (h)	Conversion (%)	M_n^a (GPC) (kDa)	M_w^a (GPC) (kDa)	\bar{D}_M^a	M_n^b (NMR) (kDa)	Diads ^c			
						PDL*- PDL	PDL*- ϵ CL	ϵ CL*- PDL	ϵ CL*- ϵ CL
0.5	57	18.1	30.1	1.67	8.3	0.08 (0.06)	0.16 (0.19)	0.18 (0.19)	0.58 (0.56)
1	61	13.4	32.5	2.42	9.5	0.12 (0.10)	0.16 (0.21)	0.25 (0.21)	0.48 (0.48)
2	77	17.2	43.1	2.50	14.0	0.18 (0.18)	0.22 (0.24)	0.27 (0.24)	0.33 (0.34)
4	90	21.5	62.1	2.90	15.6	0.22 (0.22)	0.25 (0.25)	0.28 (0.25)	0.25 (0.28)
6	94	23.8	67.0	2.82	16.5	0.23 (0.23)	0.23 (0.25)	0.28 (0.25)	0.27 (0.27)
8	96	23.1	66.7	3.00	16.9	0.23 (0.23)	0.26 (0.25)	0.26 (0.25)	0.26 (0.27)

^aDetermined by SEC in CHCl_3 against poly(styrene) standards. ^bDetermined by end-group analysis by ^1H NMR spectroscopy. ^cDetermined by quantitative ^{13}C NMR spectroscopy, with * defining the carbonyl analysed and numbers in parentheses are theoretical values based on composition.

The incorporation of PDL in the copolymerization of PDL and ϵ CL is more rapid than the observed incorporation of PDL in the copolymerization of PDL and δ VL. This could be a consequence of the stronger chelation of δ VL onto $\text{Mg}(\text{BHT})_2(\text{THF})_2$ that hinders the addition of PDL onto the polymer chain. In order to determine the effect of δ VL chelation, the transesterification of PVL and PPDL was compared to the transesterification of PCL and PPDL at 100 °C, using $\text{Mg}(\text{BHT})_2(\text{THF})_2$ as a catalyst. After 24 h the transesterification of PCL and PPDL produced polymers with full random sequencing determined by quantitative ^{13}C NMR spectroscopy (Figure 3.8). However, the transesterification of PVL and PPDL after 24 h showed incomplete randomization of the polymer chains when analyzed by quantitative ^{13}C NMR spectroscopy. Thus, the strength of the chelation of δ VL onto the Mg catalyst limits the availability of the catalyst for transesterification and ROP.

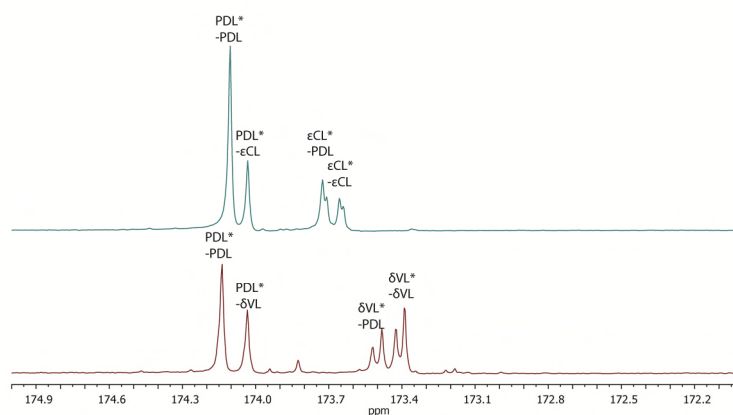


Figure 3.8 Quantitative ^{13}C NMR spectra of the carbonyl region after 24 h of transesterification of PPDL with PCL (top) and PVL (bottom) (125 MHz, CDCl_3 , 298 K).

The copolymerisation of ηCL and PDL was performed with an overall monomer concentration of 2 M in toluene at 80 °C. As a consequence of lower ring strain, the consumption of ηCL is not as rapid as δVL or ϵCL , allowing PDL to be incorporated into the polymer chain from the start of the copolymerisation of ηCL and PDL. However, the consumption of ηCL is still more rapid than PDL consumption as indicated by ^1H NMR spectroscopy through the faster reduction of the ηCL α -methylene resonance ($\delta = 4.31$ ppm) compared to the α -methylene resonance of PDL ($\delta = 4.15$ ppm). Furthermore, the overall rate of polymerisation progressed rapidly until all ηCL had been consumed, at which point the overall monomer conversion noticeably slowed as a consequence of only polymerising PDL (Figure 3.3b). Analysis of the polymerisation *via* quantitative ^{13}C NMR spectroscopy initially revealed prominent $\eta\text{CL}^*\text{-}\eta\text{CL}$ diad resonances, with the other diad resonances ($\text{PDL}^*\text{-PDL}$, $\text{PDL}^*\text{-}\eta\text{CL}$ and $\eta\text{CL}^*\text{-PDL}$) increasing in intensity once all of the ηCL monomer was consumed. Thus, all ηCL is consumed before the complete consumption PDL (Figure 3.9). Integration of the diad resonances showed that at all time points sampled, the materials formed were random copolymers where the relative integral of each diad was proportional to monomer composition (Table 3.3). SEC analysis showed a monomodal molecular weight distribution, with large dispersities ($D_M > 2$) as a consequence of low molecular weight cyclic species (Figure 3.10). A linear increase in molecular weight growth

over conversion determined by SEC is also observed as a consequence of the low molecular weight cyclic species lowering the determined M_n values.

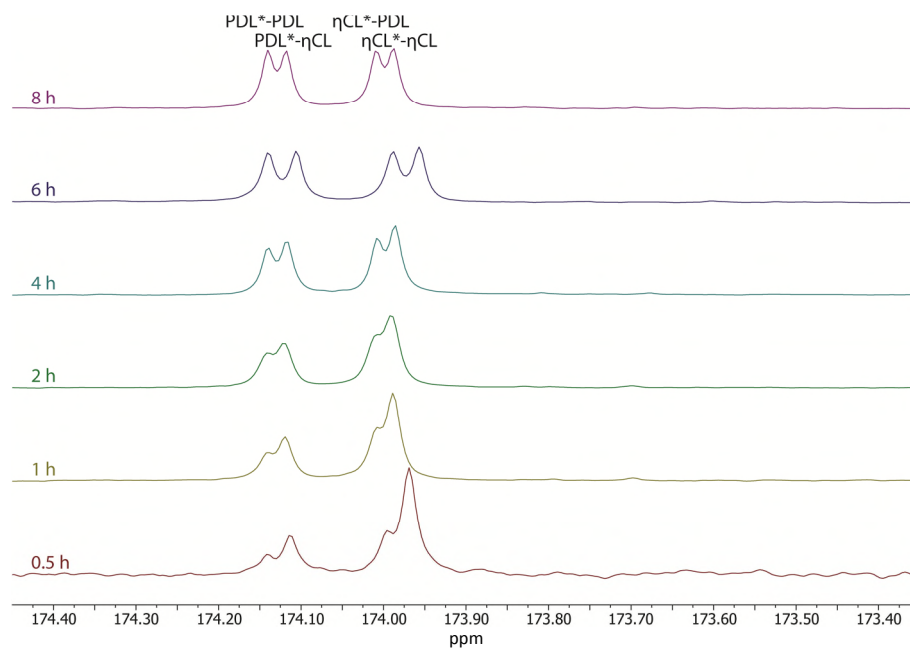


Figure 3.9 Quantitative ^{13}C NMR spectra of the carbonyl region during copolymerisations of ω -pentadecalactone with η -capryl lactone (125 MHz, CDCl_3 , 298 K).

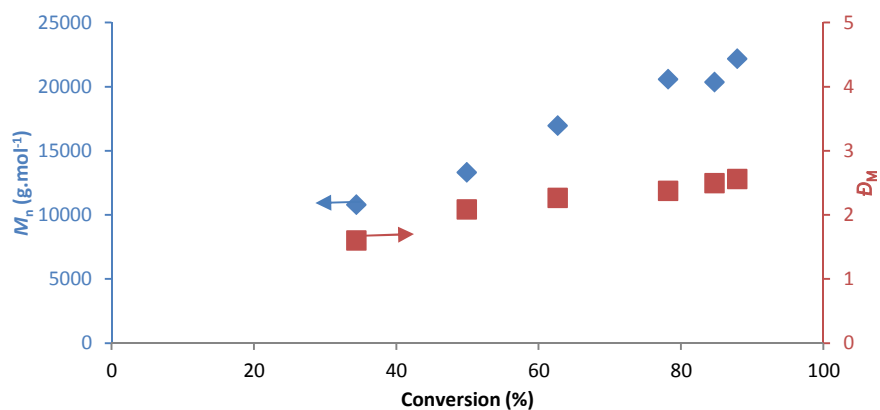


Figure 3.10 M_n against conversion for the copolymerisation of η -capryl lactone and ω -pentadecalactone at 2 M in toluene at 80 °C with $[\eta\text{CL}]_0:[\text{PDL}]_0:[\text{BnOH}]_0:[\text{Mg}(\text{BHT})_2(\text{THF})_2]_0$ of 50:50:1:1. M_n and D_m determined by SEC against poly(styrene) standards.

Table 3.3 Copolymerisation of PDL and η CL at 1:1 mol% targeting DP100.

Time (h)	Conversion (%)	M_n^a (GPC) (kDa)	M_w^a (GPC) (kDa)	D_M^a	M_n^b (NMR) (kDa)	Diads ^c			
						PDL*- PDL	PDL*- η CL	η CL*- PDL	η CL*- η CL
0.5	34	10.8	17.2	1.60	5.8	0.08 (0.04)	0.19 (0.16)	0.17 (0.16)	0.56 (0.64)
1	50	13.3	27.8	2.09	8.5	0.11 (0.07)	0.23 (0.19)	0.19 (0.19)	0.47 (0.55)
2	63	17.0	38.4	2.26	11.0	0.14 (0.10)	0.24 (0.22)	0.22 (0.22)	0.40 (0.47)
4	78	20.6	48.9	2.38	14.2	0.17 (0.16)	0.26 (0.24)	0.23 (0.24)	0.33 (0.36)
6	85	20.4	50.7	2.49	15.6	0.25 (0.18)	0.24 (0.24)	0.25 (0.24)	0.25 (0.33)
8	88	22.2	56.7	2.56	16.5	0.23 (0.20)	0.25 (0.25)	0.25 (0.25)	0.27 (0.31)

^aDetermined by SEC in CHCl_3 against poly(styrene) standards. ^bDetermined by end-group analysis by ^1H NMR spectroscopy. ^cDetermined by quantitative ^{13}C NMR spectroscopy, with * defining the carbonyl analysed and numbers in parentheses are theoretical values based on composition.

The copolymerisation of DDL and PDL at an overall concentration of 2 M in toluene at 80 °C targeting DP100 was found to be difficult to monitor *via* NMR spectroscopy and SEC analysis as a result of the similarity in the ring size of both monomers. ^1H NMR spectroscopic analysis revealed that chemical shifts which correspond to the α -methylene protons of both DDL and PDL overlap for both monomer and polymer resonances ($\delta = 4.15$ ppm and 4.05 ppm respectively). Kinetic plots of the copolymerisation showed only one linear progression as a result of both monomers being very similar in size, such that the catalyst does not differentiate between the two monomers (Figure 3.3a). This was further proven through the linear molecular weight growth observed throughout the polymerisation by SEC analysis (Figure 3.11). Similar to analysis by ^1H NMR spectroscopy, ^{13}C NMR spectroscopy revealed that the carbonyl peaks for DDL and PDL in the polymer have very similar chemical shifts (differing by ~ 0.02 ppm) (Figure 3.12). Throughout the polymerisation, the carbonyl resonances that correspond to DDL* and PDL* had equivalent

relative integrals by deconvolution, which indicates equal incorporation into the polymer chain. The sequencing of the copolymers is hard to define as a result of the similar chemical shifts, but was assumed to be random as a consequence of the equal incorporation of PDL and DDL over time (Table 3.4).

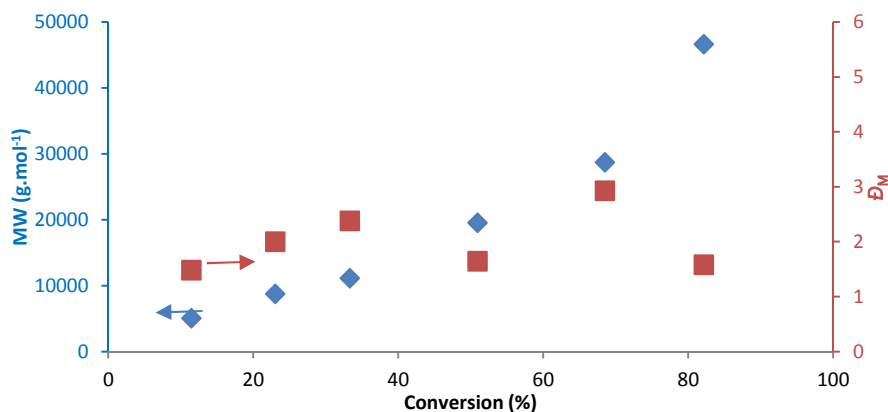


Figure 3.11 M_n against conversion for the copolymerisation of dodecalactone and ω -pentadecalactone at 2 M in toluene at 80 °C with $[DDL]_0:[PDL]_0:[BnOH]_0:[Mg(BHT)_2(THF)_2]_0$ of 50:50:1:1. M_n and \bar{M}_w determined by SEC against poly(styrene) standards.

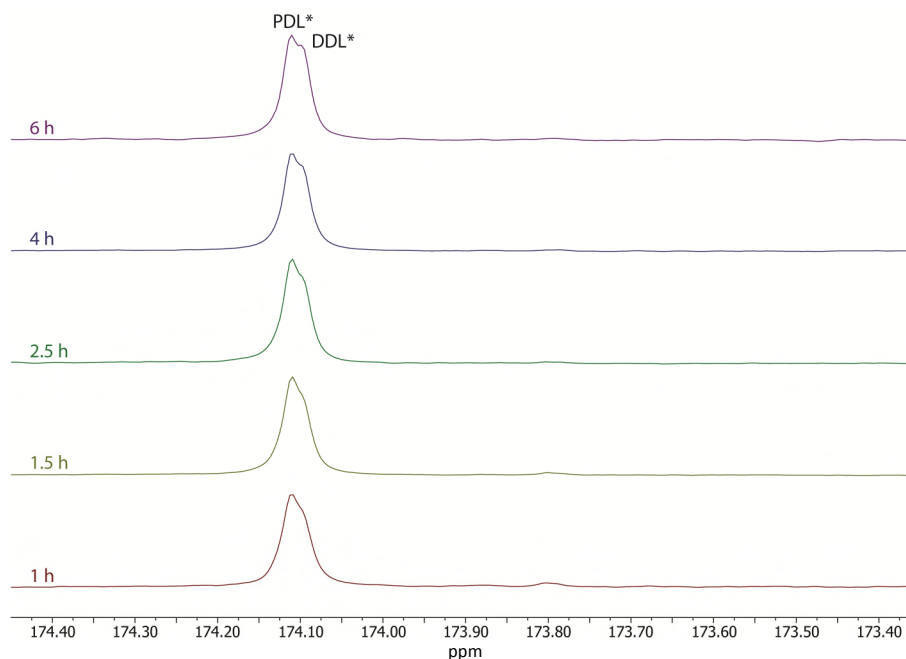


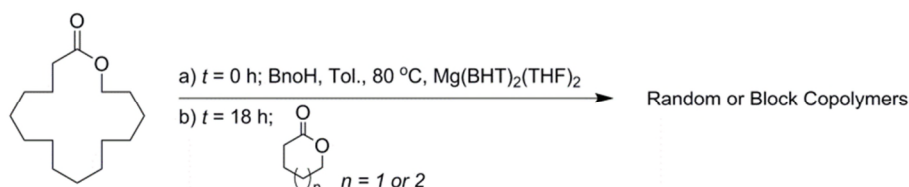
Figure 3.12 Quantitative ^{13}C NMR spectra of the carbonyl region during copolymerisations of ω -pentadecalactone with dodecalactone (125 MHz, $CDCl_3$, 298 K).

Table 3.4 Copolymerisation of PDL and DDL at 1:1 mol% targeting DP100.

Time (h)	Conversion (%)	M_n^a (kDa)	M_w^a (kDa)	PDI^a	M_n^b (kDa)
0.5	12	5.1	7.5	1.48	2.6
1.0	23	8.8	17.5	2.00	5.2
1.5	33	11.1	26.5	2.38	7.4
2.5	51	19.5	47.2	1.64	11.2
4.0	69	28.7	57.1	2.93	15.1
6.0	82	46.6	73.7	1.58	18.1

^aDetermined by SEC in CHCl₃ against poly(styrene) standards. ^bDetermined by end-group analysis by ¹H NMR spectroscopy. ^cDetermined by quantitative ¹³C NMR spectroscopy, with * defining the carbonyl analysed and numbers in parentheses are theoretical values based on composition.

3.2.3 Sequential Polymerisation



Scheme 3.3 Sequential polymerisation of ω -pentadecalactonee, followed by δ -valerolactone or ϵ -caprolactone.

One-pot copolymerisations of PDL with δ VL or ϵ CL have been shown to produce random copolymers. However, the polymerisation of one monomer with the injection of a second monomer either during or at the end of the polymerisation of the first monomer could produce gradient-block or block copolymers respectively (Scheme 3.3). Indeed, a recent study using a Zn catalyst system has shown that through sequential polymerisation of PDL followed by ϵ CL, only block copolymers were achieved and transesterification side reactions to form random copolymers were absent.²⁹

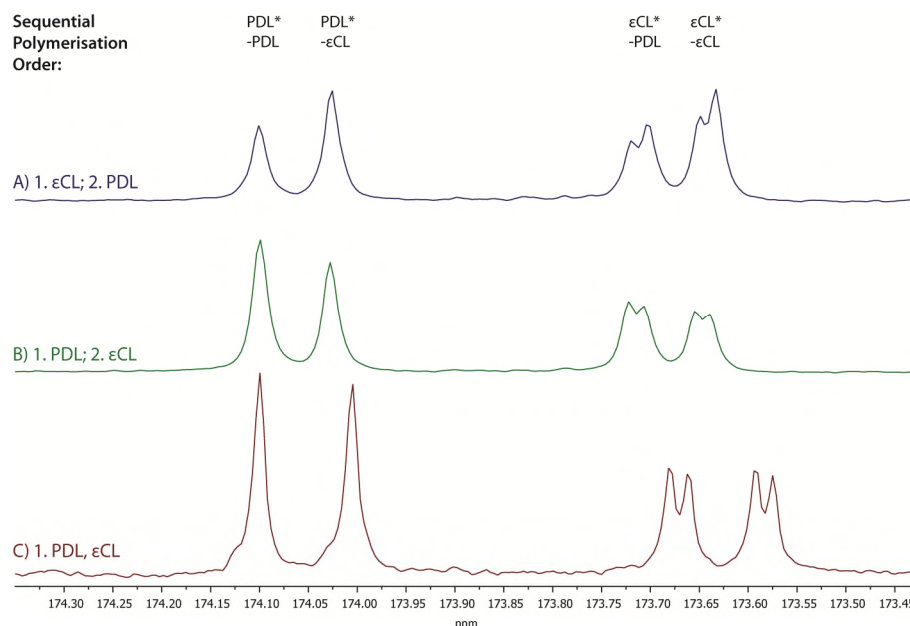


Figure 3.13 Quantitative ^{13}C NMR spectra of the carbonyl region during the sequential polymerisation of a) ϵ -caprolactone followed by ω -pentadecalactone and b) ω -pentadecalactone followed by ϵ -caprolactone compared to c) the one-pot copolymerisation of ϵ -caprolactone and ω -pentadecalactone (125 MHz, CDCl_3 , 298 K).

The sequential polymerisation of ϵCL followed by PDL was attempted at 1 M in toluene at 80 °C, using benzyl alcohol as initiator, $\text{Mg}(\text{BHT})_2(\text{THF})_2$ as catalyst and a targeted DP of 50 for both ϵCL and PDL (overall target of DP 100). After 1 h of ϵCL polymerisation, PDL at 1 M in toluene was injected into the reaction mixture and the polymerisation allowed to continue overnight. The resulting polymer was analysed by ^1H NMR and quantitative ^{13}C NMR spectroscopy. Overall monomer conversion, as determined by ^1H NMR spectroscopy was found to be 96% and analysis of the carbonyl region by quantitative ^{13}C NMR spectroscopy showed four carbonyl diad resonances corresponding to PDL*-PDL, PDL*- ϵCL , ϵCL *-PDL and ϵCL *- ϵCL (where * is the observed carbonyl) (Figure 3.13a). The relative integrals of each of the carbonyl diad resonances were equivalent, indicating a randomly sequenced copolymer. Therefore transesterification side reactions still occurred during the polymerisation of ϵCL and the formation of block copolymers cannot be achieved through this method.

The sequential polymerisation of PDL followed by ϵ CL was attempted at 1 M in toluene at 80 °C, using benzyl alcohol as initiator, $\text{Mg}(\text{BHT})_2(\text{THF})_2$ as catalyst and a targeted DP of 50 for both PDL and ϵ CL. The homopolymerisation of PDL progressed for 18 h before the injection of ϵ CL stock solution (1 M in toluene), after which the experiment was left to continue for a further 5 h. Quantitative ^{13}C NMR spectroscopy of the resulting polymer showed all four carbonyl diad resonances were present with relative integrals indicating a randomly sequenced copolymer, similar to the sequential polymerisation of ϵ CL followed by PDL (Figure 3.13b). This shows that transesterification side reactions occur alongside polymerisation of PDL, preventing the formation of block copolymers.

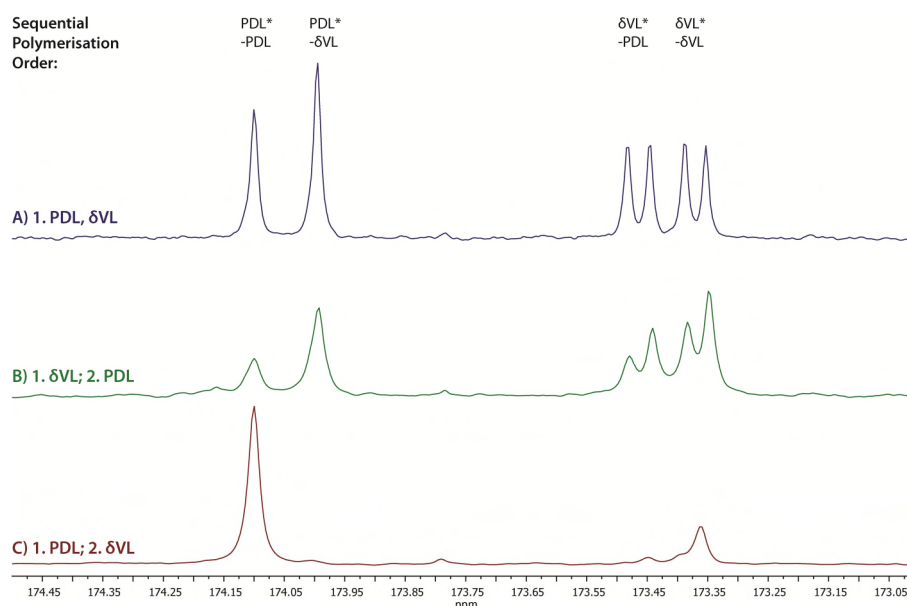


Figure 3.14 Quantitative ^{13}C NMR spectra of the carbonyl region of polymers formed by a) the one-pot copolymerisation of δ -valerolactone and ω -pentadecalactone compared to the sequential polymerisation of b) δ -valerolactone followed by ω -pentadecalactone and c) ω -pentadecalactone followed by δ -valerolactone (125 MHz, CDCl_3 , 298 K).

The sequential polymerisation of δ VL followed by PDL was attempted at 1 M in toluene at 80 °C, using benzyl alcohol as initiator, $\text{Mg}(\text{BHT})_2(\text{THF})_2$ as catalyst and a targeted DP of 50 for both δ VL and PDL. Analysis of the resultant polymer by quantitative ^{13}C NMR spectroscopy showed the presence of four carbonyl diad resonances corresponding to $\text{PDL}^*\text{-PDL}$, $\text{PDL}^*\text{-}\delta\text{VL}$, $\delta\text{VL}^*\text{-PDL}$ and $\delta\text{VL}^*\text{-}\delta\text{VL}$ of equivalent relative integrals, suggesting the formation of a randomly sequenced copolymer (Figure 3.14b). As a consequence of the

greater affinity $\text{Mg}(\text{BHT})_2(\text{THF})_2$ exhibits towards δVL compared to PDL, this result is unsurprising. Reversal of the sequential addition may therefore form block copolymers as the catalyst should show greater affinity to the formation of δVL chain segments over transesterification of the PDL block. Hence, the sequential polymerisation of PDL followed by δVL was attempted at 1 M in toluene at 80 °C, using benzyl alcohol as initiator, $\text{Mg}(\text{BHT})_2(\text{THF})_2$ as catalyst and a targeted DP of 50 for both δVL and PDL. Injection of the δVL stock solution (1 M in toluene) proceeded after 18 h of PDL homopolymerisation and the reaction continued for a further 5 h before termination. Analysis of the final mixture by ^1H NMR spectroscopy showed a significant reduction in the rapid consumption of δVL compared to one-pot copolymerisations of δVL and PDL. Integration of the carbonyl diad resonances observed by quantitative ^{13}C NMR spectroscopy showed two strong integrals corresponding to $\text{PDL}^*\text{-PDL}$ and $\delta\text{VL}^*\text{-}\delta\text{VL}$, with only very small integrals corresponding to $\text{PDL}^*\text{-}\delta\text{VL}$ and $\delta\text{VL}^*\text{-PDL}$, which is indicative of the formation of a block copolymer (Figure 3.14b). Therefore, polymerisation post-injection of δVL occurs without transesterification side reactions, avoiding randomisation of the polymer sequence. As the activation energy for the ROP of δVL is lower than the activation energy for the transesterification of PVL, it can be assumed that the block sequencing is maintained in the polymer to high conversions. The reduction in the consumption of δVL observed in the sequential polymerisation is likely a consequence of the entanglement of the polymer chain end, as the catalyst shows high affinity towards δVL . Hence, when a chain end comes into proximity of the catalyst, ring-opening addition is preferred over transesterification of the chain end. If the polymerisation is allowed to progress to a low concentration of δVL , less monomer is available for polymerisation and transesterification will likely occur, causing sequence randomisation.

3.2.4 Thermal Analysis

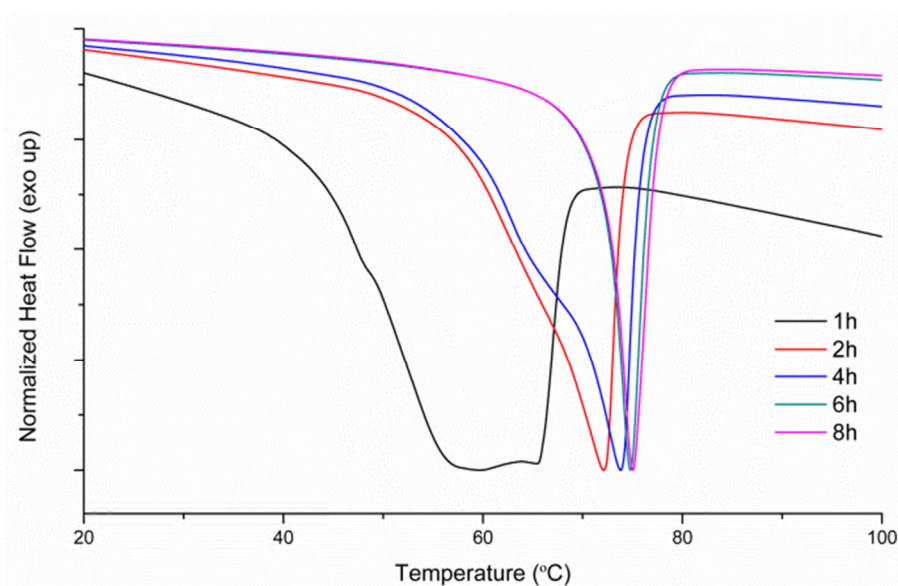


Figure 3.15 DSC thermograms of poly(ω -pentadecalactone-*co*- ϵ -caprolactone) T_m at 1, 2, 4, 6 and 8 h during copolymerisation of an equimolar mixture of ϵ -caprolactone and ω -pentadecalactone.

Differential scanning calorimetry (DSC) was used to measure the melting and crystallisation temperatures (T_m and T_c respectively) of the samples taken during the copolymerisation of an equimolar mixture of ϵ CL and PDL (Figure 3.15). As with previous reports, the glass transition temperature (T_g) is masked by the intensity of the T_m and T_c peaks in the trace, with fast cooling methods to overcome crystallisation in order to facilitate the appearance of the T_g curve proved fruitless.¹ During a typical 10 °C min⁻¹ heating cycles, it was observed that the T_m increased from a temperature of 60.1 °C, similar to the T_m of pure PCL, at low overall monomer conversion to a maximum of 75.0 °C, which corresponds to the mid-point between the T_m of pure PCL and pure PPDL. The copolymer has been previously shown to melt at a T_m proportional to the ratio of comonomers present.¹⁹ Furthermore, the increase in T_m is directly proportional to the overall monomer conversion above 50%, which corresponds to the incorporation of higher melting PDL into the chain. These trends are further observed for the crystallisation temperatures (T_c) of the polymers, which are also directly related to the ratio and conversion of comonomers used.

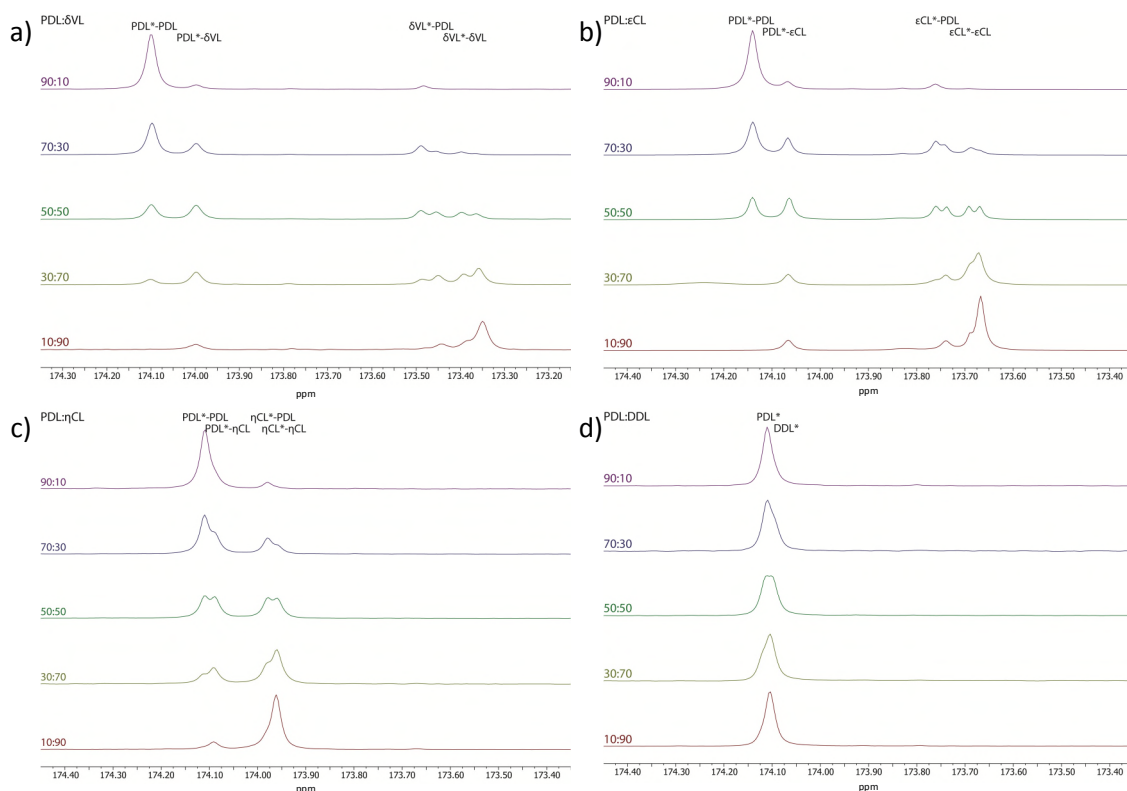


Figure 3.16 Quantitative ^{13}C NMR spectra of DP100 PDL copolymers with varying PDL mol% a) P(PDL-co- δVL), b) P(PDL-co- ϵCL), c) P(PDL-co- ηCL) and d) P(PDL-co-DDL) (125 MHz, CDCl_3 , 298 K).

To further investigate the thermal properties of the copolymers, PDL was copolymerised with δVL , ϵCL , ηCL and DDL with varying monomer feed ratios and analysed by DSC in order to discover whether this trend continued throughout the lactone range (Table 3.5). Ratio feeds of 10:90, 30:70, 50:50, 70:30 and 90:10 mol% for each lactone copolymerised with PDL, at a targeted DP of 100, were produced for analysis by quantitative ^{13}C NMR spectroscopy (Figure 3.16a) and DSC (Figure 3.18). Integration of the carbonyl diad resonances showed a random architecture for all copolymers at all molar ratios, where the relative integrals of each carbonyl diad resonance were proportional to the molar ratios of the comonomers (Table 3.5). In a comparable manner to the determination of copolymer T_g in the Flory-Fox equation, DSC thermograms obtained for each copolymer showed the observed copolymer T_m or T_c was dependent on the ratio of comonomers and their respective T_m or T_c . In order to eliminate the degree of polymerisation (DP) of PDL as the cause of the trend, a number of PPDL homopolymers were produced that ranged from

DP20 to DP100. DSC analysis of these materials showed PDDL ranging from DP20 to DP100 had the same T_m of 93 °C, which did not increase with increasing chain length (Figure 3.19).

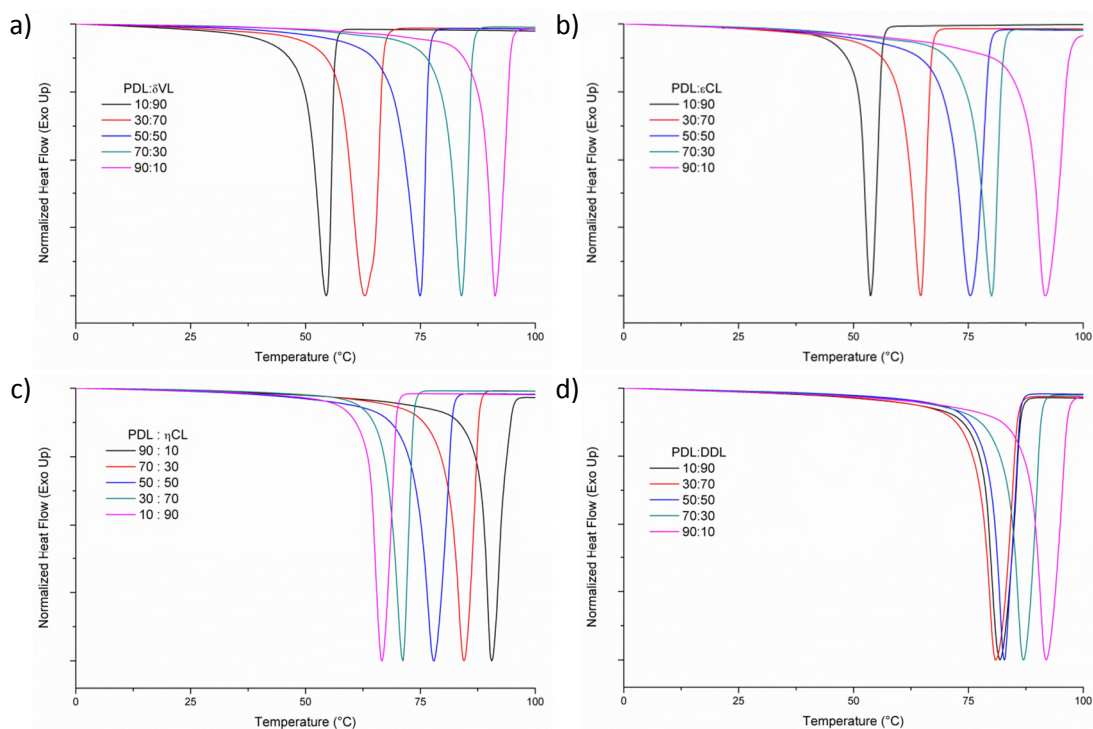


Figure 3.17 DSC thermograms (second heating curve, between 0 and 100 °C) showing the T_m for a) P(PDL-co- δ VL), b) P(PDL-co- ϵ CL), c) P(PDL-co- η CL) and d) P(PDL-co-DDL) at various molar ratios of PDL at DP100.

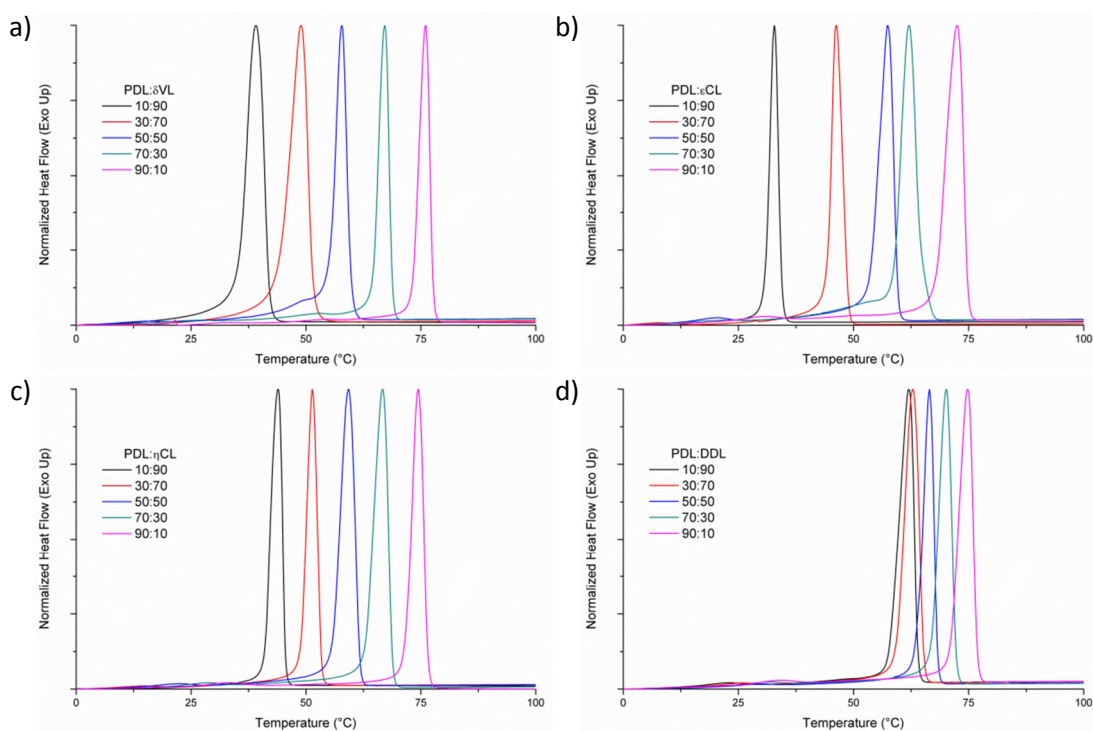


Figure 3.18 DSC thermograms (second cooling curve, between 0 and 100 °C) showing the T_c for a) P(PDL-co- δ VL), b) P(PDL-co- ϵ CL), c) P(PDL-co- η CL) and d) P(PDL-co-DDL) at various molar ratios of PDL at DP100.

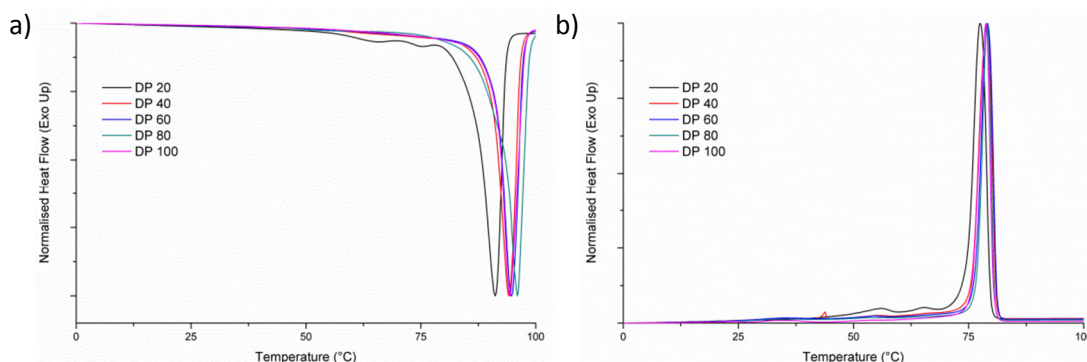


Figure 3.19 DSC thermograms showing a) the T_m (second heating curve, between 0 and 100 °C) and b) the T_c (second cooling curve, between 0 and 100 °C) for PPDL at various DPs.

Table 3.5 Copolymerisation of PDL with another lactone at varied monomer ratio feeds targeting DP100.

Lactone	[PDL] : [Lactone]	M_n^a (GPC) (kDa)	M_w^a (GPC) (kDa)	\bar{D}_M^a	M_n^b (NMR) (kDa)	T_m^c (°C)	T_c^c (°C)
δ VL	10 : 90	8.8	12.2	1.38	9.6	54.1	39.7
	30 : 70	8.8	15.8	1.80	11.7	62.5	49.6
	50 : 50	9.5	22.6	2.39	15.2	74.1	58.9
	70 : 30	12.1	34.7	2.88	18.5	83.0	68.5
	90 : 10	14.3	44.1	3.08	22.9	90.4	77.4
ϵ CL	10 : 90	12.8	23.7	1.85	22.3	53.2	33.5
	30 : 70	9.9	20.7	2.09	16.8	64.2	47.0
	50 : 50	10.8	27.4	2.54	16.8	74.9	58.2
	70 : 30	12.8	35.0	2.74	12.3	79.5	62.8
	90 : 10	14.7	43.7	2.96	12.0	91.2	73.4
η CL	10 : 90	14.7	38.3	2.61	13.8	66.0	44.9
	30 : 70	16.2	49.3	3.04	15.9	70.5	52.5
	50 : 50	18.9	64.5	3.42	18.2	77.7	60.2
	70 : 30	18.3	66.6	3.64	20.4	84.1	67.5
	90 : 10	21.9	72.3	3.30	22.3	90.9	75.6
DDL	10 : 90	23.0	78.2	3.40	21.5	80.2	63.0
	30 : 70	21.6	71.6	3.32	21.4	81.2	63.9
	50 : 50	19.9	67.5	3.39	21.5	82.3	67.8
	70 : 30	19.1	61.0	3.20	20.9	86.4	71.2
	90 : 10	19.0	57.7	3.04	20.7	91.0	76.0

^aDetermined by SEC in CHCl_3 against poly(styrene) standards. ^bDetermined by end-group analysis by ^1H NMR spectroscopy. ^cDetermined by DSC, with heating and cooling rates of $10\text{ }^\circ\text{C}\cdot\text{min}^{-1}$ against a blank reference sample.

3.2.5 Crystallographic Analysis

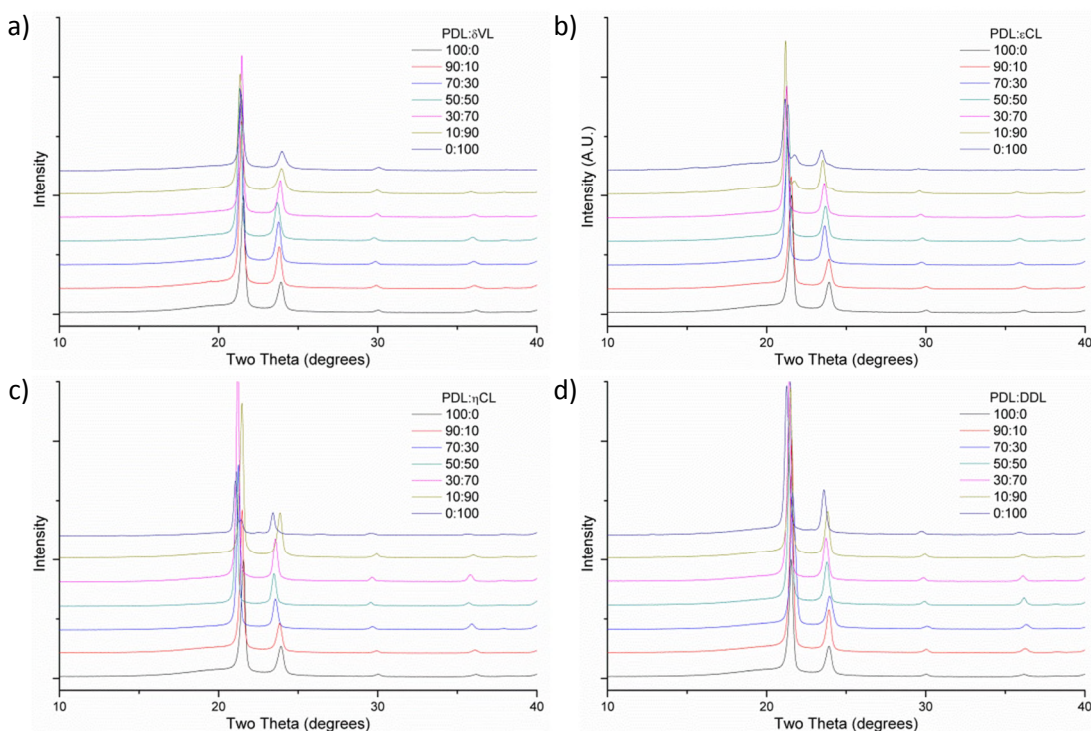


Figure 3.20 WAXD diffractograms of DP100 a) P(PDL-co- δ VL), b) P(PDL-co- ϵ CL), c) P(PDL-co- η CL) and d) P(PDL-co-DDL) with varying molar ratio feed of monomers.

The observation of a single T_m and T_c for each copolymer provided strong evidence of the randomisation of the polymer chain. As a consequence of the semi-crystalline nature of many unsubstituted poly(lactone)s, wide angle x-ray diffraction (WAXD) was employed to measure the crystallinity of the copolymers with different feed ratios and determine if cocrystallisation of the random copolymers occurred (Figure 3.20). Each copolymer was melted and pressed into a disc (*ca.* 100 mg) and standard “powder” 2θ - ϑ diffraction scans were carried out at room temperature in the angular range between 5° and 60° 2θ . All copolymers analysed displayed a high degree of crystallinity ($>70\%$), with distinct reflections of (110) and (200) at $2\theta = 21.5^\circ$ and 23.0° respectively. The lack of unique reflections between lactone copolymers and therefore the similar crystal packing of these copolymers shows strong cocrystallisation of PDL with all lactones tested. Crystallisation was also observed to be higher for all copolymers than for the homopolymer of the corresponding smaller lactone (*i.e.* PVL, PCL, P(η CL) or PDDL), which suggests that

incorporation of PDL into the chain could significantly alter the mechanical properties when compared to the homopolymers of the smaller lactones.

3.2.6 Degradation Studies

In order to measure the effect of cocrystallinity on the degradation of PDL copolymers, PDL copolymers with different comonomers, but identical T_m and T_c were tested. To this end, PDL was copolymerised with δ VL, ϵ CL and η CL at molar ratios of 42:58 (PDL: δ VL), 41:59 (PDL: ϵ CL) and 25:75 (PDL: η CL) to achieve copolymers with a targeted $T_m = 70$ °C and $T_c = 54$ °C but with differing compositions. These copolymers were pressed into discs and subjected to accelerated degradation in 5 M NaOH solutions at 37 °C (Figure 3.21). Accelerated degradation methods were used as a consequence of the slow degradation exhibited by PCL reported previously.³⁰ The degradation of P(PDL-co- δ VL) is rapid compared to the other two copolymers, with structural disc collapse occurring after *ca.* 90 days. The rapid degradation of P(PDL-co- δ VL) occurs as a consequence of the low hydrophobicity of the short alkyl chain length of a δ VL repeat unit backbone allowing protic sources near the hydrophilic ester linkage, unlike the highly hydrophobic long alkyl chain backbone of PDL repeat units. Furthermore, only P(PDL-co- δ VL) visibly swelled during the study, with a maximum mass gain of *ca.* 10% shortly before rapid mass loss occurred. The swelling and mass gain is likely a consequence of the relative hydrophilicity of the PVL carbonyl allowing water to penetrate the polymer network and swell the material. P(PDL-co-CL) discs fragmented after around 100 days as a consequence of the ϵ CL repeat unit being only slightly more hydrophobic than the δ VL repeat unit. P(PDL-co- η CL) was the slowest copolymer to degrade with only 10% mass loss occurring after 120 days. This is likely a consequence of the greater hydrophobicity of the alkyl chain backbone of η CL compared to δ VL or ϵ CL. The concentration of ester groups within the copolymers tested account for 30 ± 3 mol.% of the entire copolymer for each of the copolymers tested and as a consequence the hydrophilicity of the copolymer can be excluded as a factor for the

change in degradation behavior. Overall, the results show that the longer the alkyl chain repeat unit, the longer the degradation time hence, PDL copolymers can be prepared that display hydrolytic degradation behaviour independent of processing temperature (T_m and T_c).

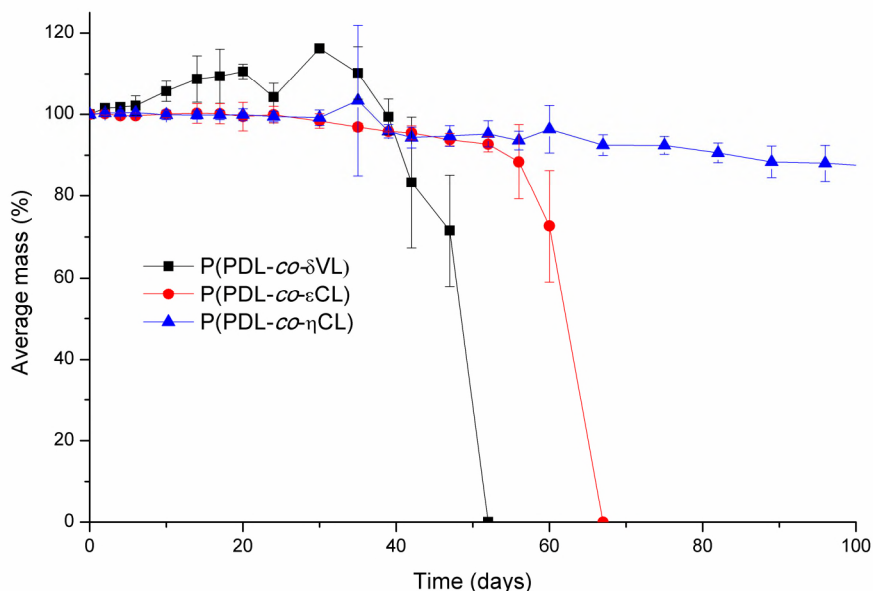


Figure 3.21 Average mass loss of PDL copolymers studied in accelerated degradation conditions (5 M NaOH, 38 °C).

3.3 Conclusion

ω -Pentadecalactone (PDL) was copolymerised with lactones of smaller ring size using $\text{Mg}(\text{BHT})_2(\text{THF})_2$ as a catalyst. Through quantitative ^{13}C NMR spectroscopy, it was shown that the smaller lactones (δ -valerolactone and ϵ -caprolactone) polymerised rapidly, followed by addition of PDL to the chain. Transesterification side reactions occurred more rapidly than addition of PDL, leading to randomisation of the chain architecture. Copolymerisation of PDL with η -caprylolactone (η CL) showed more rapid consumption of η CL than PDL, with transesterification side reactions again resulting in random copolymers. Copolymerisation of PDL and dodecalactone occurred simultaneously and is also thought to produce random copolymers. All copolymers exhibited values of T_m and T_c that followed a trend comparable to Flory-Fox theory. This trend was exploited to produce PDL copolymers

that exhibited the same processing temperature but that exhibited significantly different degradation rates.

3.4 References

1. M. L. Focarete, M. Scandola, A. Kumar and R. A. Gross, *J. Polym. Sci., Part B: Polym. Phys.*, 2001, **39**, 1721-1729.
2. J. Cai, C. Liu, M. Cai, J. Zhu, F. Zuo, B. S. Hsiao and R. A. Gross, *Polymer*, 2010, **51**, 1088-1099.
3. Z. Jiang, H. Azim, R. A. Gross, M. L. Focarete and M. Scandola, *Biomacromolecules*, 2007, **8**, 2262-2269.
4. L. Mazzocchi, M. Scandola and Z. Jiang, *Macromolecules*, 2009, **42**, 7811-7819.
5. B. Kalra, A. Kumar, R. A. Gross, M. Baiardo and M. Scandola, *Macromolecules*, 2004, **37**, 1243-1250.
6. G. Ceccorulli, M. Scandola, A. Kumar, B. Kalra and R. A. Gross, *Biomacromolecules*, 2005, **6**, 902-907.
7. I. van der Meulen, M. de Geus, H. Antheunis, R. Deumens, E. A. J. Joosten, C. E. Koning and A. Heise, *Biomacromolecules*, 2008, **9**, 3404-3410.
8. I. van der Meulen, Y. Li, R. Deumens, E. A. J. Joosten, C. E. Koning and A. Heise, *Biomacromolecules*, 2011, **12**, 837-843.
9. M. Bouyahyi, M. P. F. Pepels, A. Heise and R. Duchateau, *Macromolecules*, 2012, **45**, 3356-3366.
10. M. Eriksson, L. Fogelstrom, K. Hult, E. Malmstrom, M. Johansson, S. Trey and M. Martinelle, *Biomacromolecules*, 2009, **10**, 3108-3113.
11. N. Simpson, M. Takwa, K. Hult, M. Johansson, M. Martinelle and E. Malmström, *Macromolecules*, 2008, **41**, 3613-3619.

12. M. Claudino, I. van der Meulen, S. Trey, M. Jonsson, A. Heise and M. Johansson, *J. Polym. Sci., Part A: Polym. Chem.*, 2012, **50**, 16-24.
13. J. Zotzmann, M. Behl, Y. Feng and A. Lendlein, *Adv. Funct. Mater.*, 2010, **20**, 3583-3594.
14. Y. Nakayama, N. Watanabe, K. Kusaba, K. Sasaki, Z. Cai, T. Shiono and C. Tsutsumi, *J. Appl. Polym. Sci.*, 2011, **121**, 2098-2103.
15. A. Nakayama, N. Kawasaki, Y. Maeda, I. Arvanitoyannis, S. Aiba and N. Yamamoto, *J. Appl. Polym. Sci.*, 1997, **66**, 741-748.
16. I. Castilla-Cortázar, J. Más-Estellés, J. M. Meseguer-Dueñas, J. L. Escobar Ivirico, B. Marí and A. Vidaurre, *Polym. Degrad. Stab.*, 2012, **97**, 1241-1248.
17. L. M. Orozco-Castellanos, A. Marcos-Fernández and A. Martínez-Richa, *Polym. Adv. Technol.*, 2011, **22**, 430-436.
18. G. G. Pitt, M. M. Gratzl, G. L. Kimmel, J. Surles and A. Sohindler, *Biomaterials*, 1981, **2**, 215-220.
19. A. Kumar, B. Kalra, A. Dekhterman and R. A. Gross, *Macromolecules*, 2000, **33**, 6303-6309.
20. L. van der Mee, F. Helmich, R. de Bruijn, J. A. J. M. Vekemans, A. R. A. Palmans and E. W. Meijer, *Macromolecules*, 2006, **39**, 5021-5027.
21. H. Uyama, H. Kikuchi, K. Takeya and S. Kobayashi, *Acta Polym.*, 1996, **47**, 357-360.
22. I. van der Meulen, E. Gubbels, S. Huijser, R. Sablong, C. E. Koning, A. Heise and R. Duchateau, *Macromolecules*, 2011, **44**, 4301-4305.
23. L. Mazzocchetti, M. Scandola and Z. Jiang, *Eur. Polym. J.*, 2012, **48**, 1883-1891.
24. A. Kumar, K. Garg and R. A. Gross, *Macromolecules*, 2001, **34**, 3527-3533.
25. J. Calabrese, M. A. Cushing and S. D. Ittel, *Inorg. Chem.*, 1988, **27**, 867-870.
26. J. A. Wilson, S. A. Hopkins, P. M. Wright and A. P. Dove, *Polym. Chem.*, 2014, **5**, 2691-2694.

27. M. P. F. Pepels, P. Souljé, R. Peters and R. Duchateau, *Macromolecules*, 2014, **47**, 5542-5550.
28. M. T. Hunley, N. Sari and K. L. Beers, *ACS Macro Lett.*, 2013, **2**, 375-379.
29. M. Bouyahyi and R. Duchateau, *Macromolecules*, 2014, **47**, 517-524.
30. X. F. L. Christopher, M. S. Monica, T. Swee-Hin and W. H. Dietmar, *Biomed. Mater.*, 2008, **3**, 034108.

4 Synthesis and post-polymerisation

modification of one-pot ω -pentadecalactone

block-*like* copolymers

4.1 Introduction

Over the last decade, poly(ω -pentadecalactone) (PPDL) has attracted a lot of interest as a consequence of the long aliphatic backbone giving the material high crystallinity and tensile strength similar to that of low-density poly(ethylene) (LDPE).¹⁻³ As a monomer, ω -pentadecalactone (PDL) is an ideal candidate for 'green' methods of producing LDPE-like materials; the monomer is very common in nature and can be commercially produced from a renewable source. The repeat ester linkage in the PPDL backbone is an ideal source for degradation, which is not present in LDPE and therefore makes PPDL a renewable, degradable polymer. Hydrolysis is, however, difficult as a consequence of the long alkyl chain backbone being highly hydrophobic and preventing attack on the ester linkage.⁴ PPDL is biocompatible when implanted into the body, although it cannot be degraded by the body and therefore the homopolymer is not ideal as a biomaterial.

Through the use of γ -substituted ϵ -lactones, the production of PDL copolymers with side functionalities has been realised. Copolymers have been produced that introduce methyl, methacryloyl and benzoyl side chain functionalities into a P(PDL-*co*- ϵ CL) backbone. In each case, the crystallinity of the copolymer is greatly reduced as a consequence of the random sequencing of the polymer preventing cocrystallisation.⁵ While the methacryloyl- and benzoyl-functionalized P(PDL-*co*-CL) may provide opportunity for post-polymerization modification of the side-chain functionalities, this was not demonstrated. The scope of available γ -substituted ϵ CL monomers is limited due to rearrangement side reactions producing γ -lactones that cannot be polymerised, as observed with γ -acetyloxy- ϵ -caprolactone and γ -acryloyloxy- ϵ -caprolactone.

The use of unsaturated PDL monomers, such as globalide (Gbl), to produce functional PPDL has also been researched.⁶ Post-polymerisation modification of Gbl, a sixteen-membered ring lactone with one unsaturated linkage, has produced crosslinked materials through thiol-ene addition of trimercapto propionate (TMP). When copolymerised with 4-

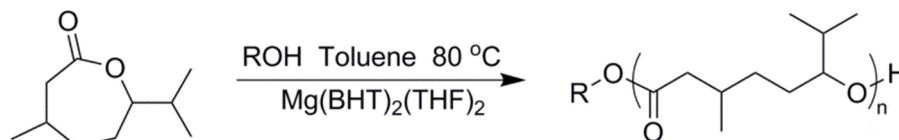
methylocaprolactone (4MeCL) and crosslinked *via* thermal radical crosslinking, the resulting material was completely amorphous and still showed high tensile strengths.

In all of these cases, the PDL copolymers were all completely randomly sequenced. Block copolymers of PDL and ϵ CL have recently been discovered through sequential polymerisation using a Zn or Ca catalyst, however the properties were very similar to random copolymers as a consequence of cocrystallisation.⁷ Furthermore, there is still no functionality in the polymer for post-polymerisation modification. The introduction of alkyl side-chain functionalities has been realised in the use of an ϵ -substituted ϵ -lactone (ϵ SL), ϵ -decalactone (ϵ DL), to produce one-pot PDL block copolymers.^{8, 9} Block copolymerisation occurs as a consequence of the thermodynamic preference for polymerisation of ϵ DL over PDL, meaning PDL would initiate from a secondary alcohol only after complete consumption of ϵ DL. Transesterification of the ϵ DL block is sterically unfavourable as a consequence of the side chain next to the ester and therefore mixing of the block by transesterification side reactions is not achievable. As with P(PDL-*co*- ϵ CL), P(PDL-*co*- ϵ DL) does not contain a region for post-polymerisation modification.

This chapter aims to explore whether PDL can form block copolymers with any ϵ SL or whether a certain degree of substitution is required to form block copolymers. Furthermore we aim to explore a method for the production of PDL copolymers with both monomers derived from renewable resources, as well as containing functional side chains accessible for post-polymerisation modification. It should be noted that the work by Duchateau and coworkers on the copolymerisation of PDL and ϵ DL was published during this chapter of work.⁷

4.2 Results and Discussion

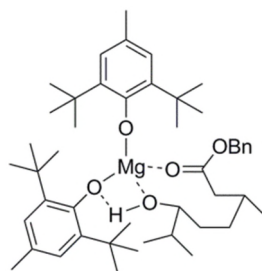
4.2.1 Homopolymerisation of menthide



Scheme 4.1 Polymerisation of menthide catalysed by $\text{Mg(BHT)}_2(\text{THF})_2$.

In order to introduce side-chain functionality into a PDL copolymer, menthide (MI) was produced by the Baeyer-Villiger oxidation of menthone using *m*-chloroperoxybenzoic acid (mCPBA). Initially, the homopolymerisation of MI catalysed by $\text{Mg(BHT)}_2(\text{THF})_2$ was attempted at a monomer concentration of 1 M in toluene at 80 °C, with benzyl alcohol as initiator and a targeted degree of polymerisation (DP) of 50 (Scheme 4.1). Polymerisation of menthide has been shown to progress at lower temperatures (25 °C), however in order to compare rates of polymerisation all experiments were conducted at 80 °C.¹⁰ Aliquots were taken periodically and monomer conversion was monitored by ^1H NMR spectroscopy and molecular weight growth followed by size-exclusion chromatography (SEC). The conversion of MI was observed by ^1H NMR spectroscopy through the reduction of the proton resonance attributable to the proton adjacent to the acyl oxygen of the ester of the monomer ($\delta = 4.05$ ppm), which coincided with the appearance of a resonance at $\delta = 4.74$ ppm, attributable to the proton adjacent to the linking oxygen of the ester of poly(menthide) (PMI). Interestingly, only 1% monomer conversion was observed for the initial 45 min of polymerisation, after which polymerisation occurred at a faster rate, exhibiting first order kinetics with respect to the monomer (Figure 4.2a). The initial pause in polymerisation is likely a consequence of the formation of a complex between the catalyst and the ring-opened MI unit with a benzyl alcohol initiating group attached. This could then chelate to the catalyst to form an 8-membered ring exhibiting a highly sterically blocked active site as a consequence of the isopropyl and methyl side groups (Scheme 4.2). Once the second MI unit is able to ring-open onto the newly forming chain, the polymerisation

progresses without hindrance to the active site and at an observed propagation rate of $k_p = 0.297 \text{ s}^{-1}$.



Scheme 4.2 Potential complex formed by $\text{Mg}(\text{BHT})_2(\text{THF})_2$ and the first ring-opened unit of MI using BnOH as an initiator (298 K, CDCl_3 , 298 K).

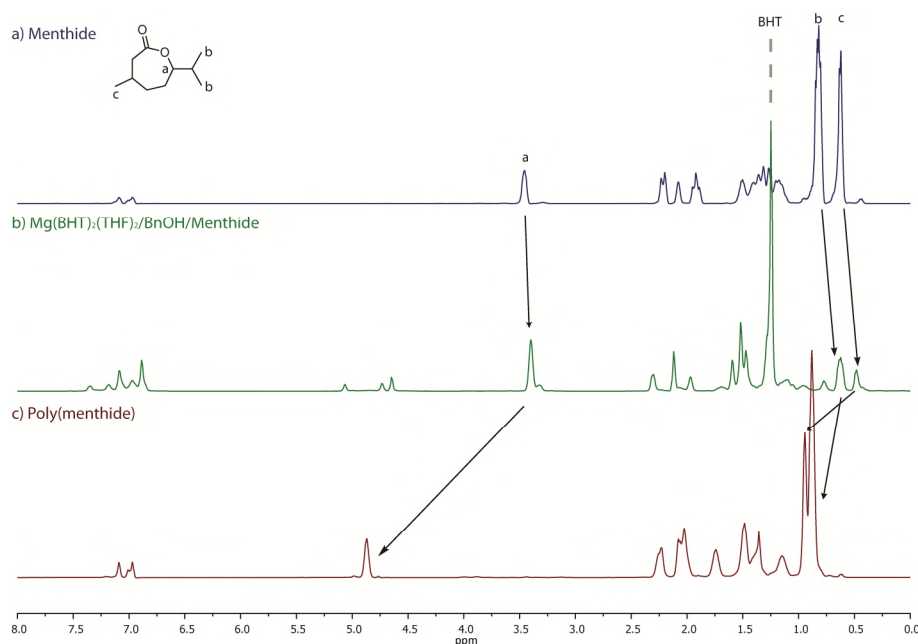


Figure 4.1 ^1H NMR spectra showing significant chemical shift changes between a) menthide, b) $\text{Mg}(\text{BHT})_2(\text{THF})_2/\text{BnOH}/\text{menthide}$ complex and c) poly(menthide) (400 MHz, $\text{toluene-}d_8$, 298 K).

In order to prove the formation of an initial complex between the catalyst and monomer, an equimolar solution of $\text{Mg}(\text{BHT})_2(\text{THF})_2$, MI and benzyl alcohol was prepared at 0.5 M in $\text{toluene-}d_8$. The solution was analysed by ^1H NMR spectroscopy before being heated for 1 h at 80 °C and analysed again. By analysing the chemical shift of the proton attached to the tertiary carbon adjacent to the ester of MI, a change in resonance from the monomer ($\delta = 3.46 \text{ ppm}$) to a shift of $\delta = 3.40 \text{ ppm}$ is observed (Figure 4.1). Comparison to the same proton resonance of the terminal monomer unit of PMI ($\delta = 3.43 \text{ ppm}$) shows only a slight difference in chemical shift. This indicates that the MI has been ring-opened,

however the monomer unit is still coordinated to the metal centre, resulting in a different chemical shift. This is further demonstrated by an upfield shift of each methyl group observed in the ^1H NMR spectrum for the complex but not in either spectra for the monomer or the polymer. ^1H NMR spectra recorded immediately before and after heating, as well as another 24 h after heating, returned identical results, which indicates that the complex formation occurs before heating and the complex is stable when heated and over an extended period of time.

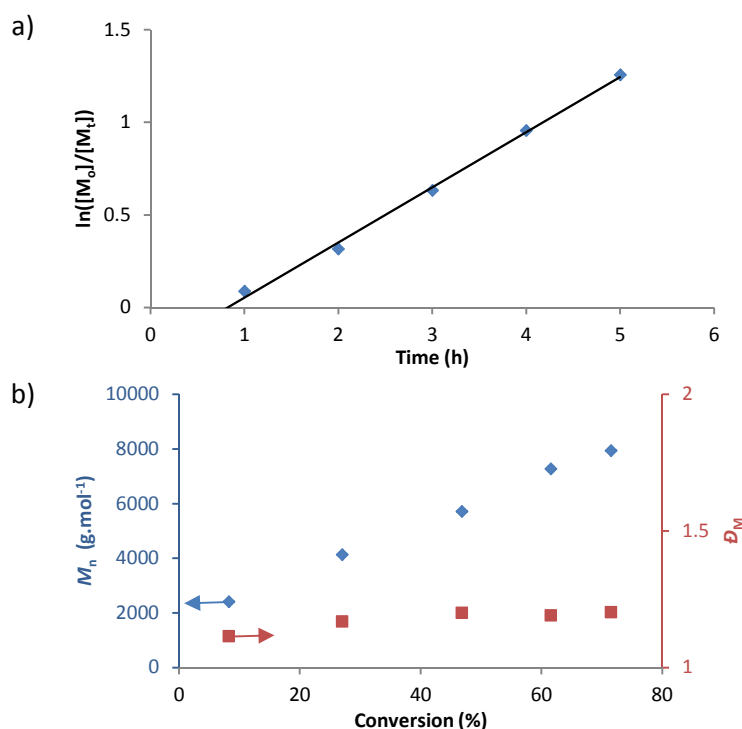


Figure 4.2 a) Kinetic plot for the homopolymerisation of menthide using $\text{Mg}(\text{BHT})_2(\text{THF})_2$ as a catalyst at 80°C in toluene with $[\text{M}]_0 : [\text{BnOH}]_0 : [\text{cat.}]_0 = 50 : 1 : 1$, total monomer concentration = 1 M. b) Changes in M_n and \bar{D}_M over monomer conversion for the same reaction. M_n and \bar{D}_M determined by SEC against poly(styrene) standards.

Monitoring the growth of molecular weight with respect to monomer conversion by SEC using CHCl_3 as an eluent, showed linear growth over increasing conversion and therefore good control over the polymerisation with negligible termination side reactions was achieved (Figure 4.2b). The molecular weight dispersity (\bar{D}_M) of PMI remained relatively low throughout the polymerisation compared to non-substituted lactones ($\bar{D}_M = \sim 1.2$), which indicates a lack of transesterification side reactions (Figure 4.3). Transesterification side

reactions in the ROP of lactones can occur, which cause large dispersities in the material produced (approaching 2). To investigate, an aliquot was left to polymerise for an extended amount of time (96 h) in order to see whether transesterification side reactions occurred after polymerisation was complete. The reaction was quenched with acidified (5% HCl) methanol, solvents removed by rotary evaporation and the polymer washed with cold hexanes. SEC analysis of the polymer showed that after 96 h, transesterification did not occur as D_M remained low (1.26 compared to a $D_M = 1.20$ after 5 h; 71% monomer conversion). A slight broadening of dispersity is expected at high conversions as a consequence of low monomer concentrations preventing every chain end from propagating equally. The lack of transesterification is likely a consequence of the substituted group present on the ϵ -carbon preventing transesterification side reactions through steric hindrance. When compared to the homopolymerisation of PDL as previously reported (Chapter 2), the consumption of MI is more rapid and therefore the copolymerisation would be expected to occur with rapid consumption of MI and slower consumption of PDL to produce either a block or gradient copolymer.

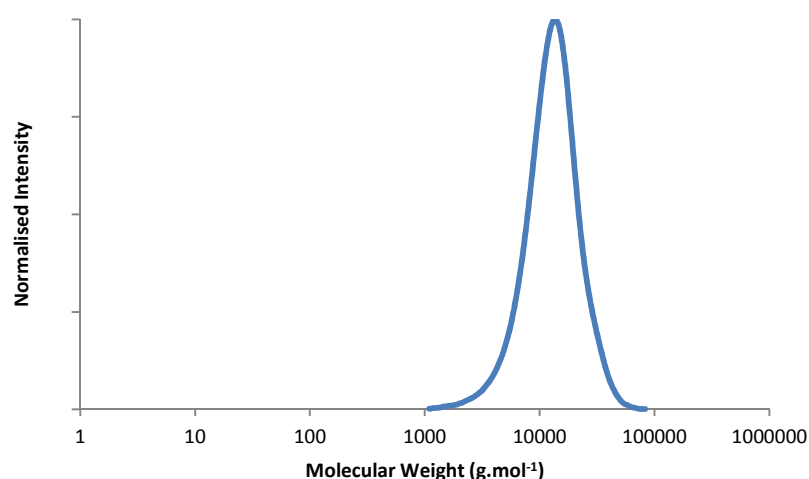
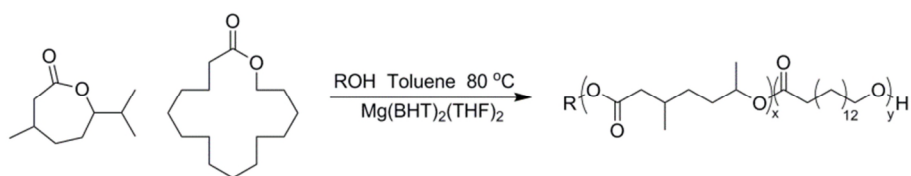


Figure 4.3 SEC chromatogram of the molecular weight distribution of the resultant polymer from the homopolymerisation of menthide at 1 M in toluene at 80 °C, with $[MI]_0 : [BnOH]_0 : [cat.]_0 = [50] : 1 : 1$. Molecular weight determined against poly(styrene) standards and $CHCl_3$ (0.5% Net_3) as eluent.

4.2.2 Copolymerisation of PDL and MI



Scheme 4.3 Copolymerisation of menthide and pentadecalactone in catalysed by $\text{Mg}(\text{BHT})_2(\text{THF})_2$.

The copolymerisation of an equimolar mixture of PDL and MI was undertaken at an overall monomer concentration of 2 M in toluene at 80 °C, with a targeted degree of polymerisation (DP) of 100 and benzyl alcohol as an initiator (Scheme 4.3). Aliquots were taken periodically and the conversion of each monomer was followed by ^1H NMR spectroscopy and molecular weights determined by SEC. As a consequence of an overlap in ^1H NMR spectroscopy for the resonances of the MI monomer and the PPDL α -methylene at $\delta = 4.05$ ppm, an initial sample was taken before polymerisation in order to integrate the total quantity of each monomer. Conversion could then be determined through subtraction of the unreacted MI from the total peak integral (Figure 4.4). This meant that the consumption of each monomer could be seen individually, unlike copolymerisations on non-substituted lactones (Figure 4.5).

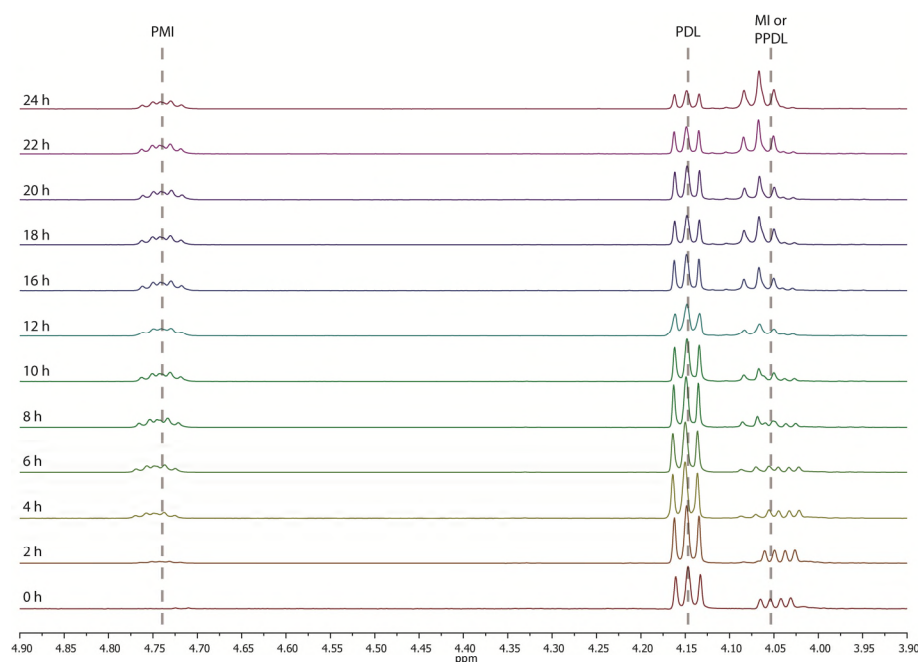


Figure 4.4 ^1H NMR spectra of the α -methylene signals observed during the copolymerisation of menthide and pentadecalactone at 1 : 1 mol%, targeting a total DP of 100 (400 MHz, 298 K, CDCl_3).

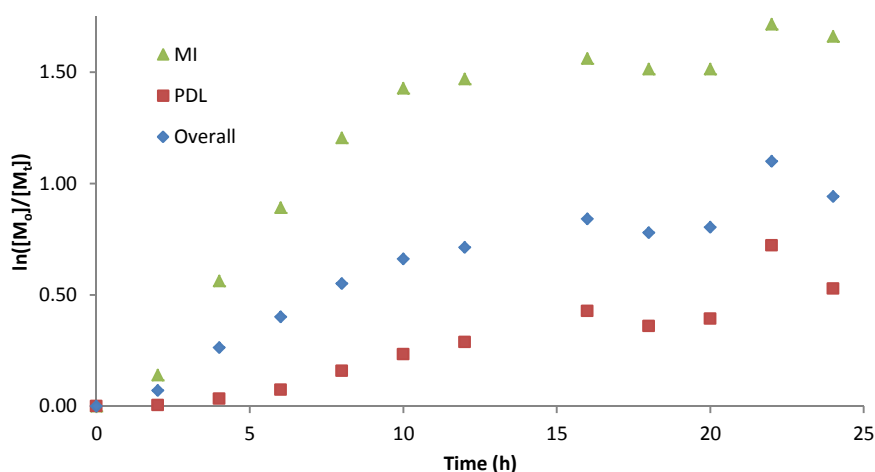


Figure 4.5 Kinetic plot for the copolymerisation of menthide and pentadecalactone, conducted at 80 °C in toluene with $[\text{PDL}]_0 : [\text{MI}]_0 : [\text{BnOH}]_0 : [\text{cat.}]_0 = 50 : 50 : 1 : 1$, total monomer concentration = 2 M.

As observed in the homopolymerisation of MI, the copolymerisation halted at 1% conversion for the first 45 min as a consequence of steric blockage to the catalyst. Once polymerisation recommenced, MI was preferentially consumed with limited consumption of PDL (< 7%) until 70% of MI was consumed, after 8 h. PDL was then consumed at a much slower rate than observed during homopolymerisation, with only 40% PDL consumption after 24 h of polymerisation. The slow consumption of PDL after the polymerisation of

another monomer in a copolymerisation is expected, as previous work on the copolymerisation of PDL with δ -valerolactone (δ VL) showed slow PDL incorporation after all δ VL had been consumed (Chapter 3). In this case the affinity of the catalyst towards δ VL was demonstrated to be higher than the affinity towards PDL, which is potentially the same reason for slower incorporation of PDL in this copolymerisation. SEC analysis showed linear growth of the molecular weight with conversion similar to MI homopolymerisation until 70% MI consumption, with a low dispersity characteristic of MI homopolymer formation (Figure 4.6). As the incorporation of PDL began, the molecular weight growth increased more rapidly as a consequence of the larger PDL molecular weight. Dispersities also began to increase as a consequence of low molecular weight cyclic species forming due to the thermodynamics of PDL polymerisation, from $\mathcal{D}_M = 1.29$ after 6 h of polymerisation to $\mathcal{D}_M = 1.93$ after 22 h of polymerisation. Throughout the copolymerisation, the \mathcal{D}_M remained less than 2, which is uncharacteristic of PDL copolymerisations where transesterification side reactions occur. However, as PDL begins to be incorporated into the polymer chain, there is a notable increase in dispersity. As the menthide block originally formed is unlikely to transesterify but transesterification side reactions can still progress in the PDL-rich regions, the sequencing of the copolymers formed are likely to be block or gradient copolymers.

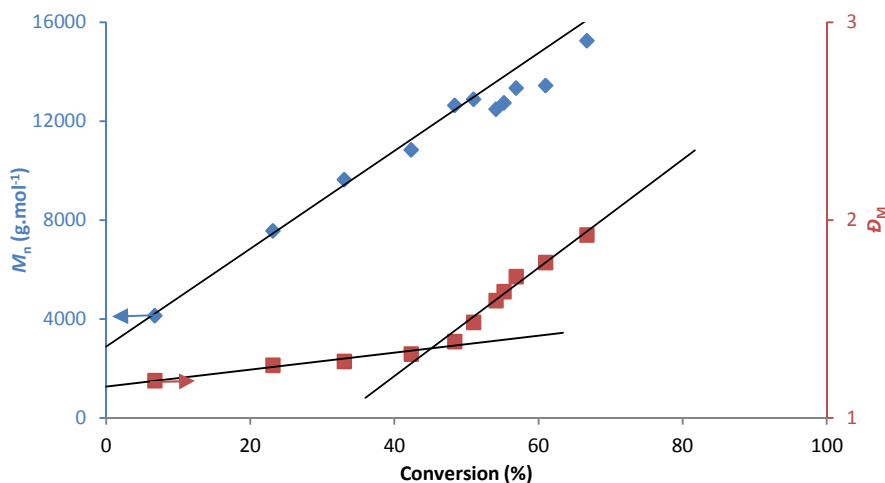


Figure 4.6 Changes in M_n and \overline{DP}_n over total monomer conversion for the copolymerisation of menthide and ω -pentadecalactone using $\text{Mg}(\text{BHT})_2(\text{THF})_2$ as a catalyst at 80 °C in toluene with $[\text{MI}]_0 : [\text{BnOH}]_0 : [\text{cat.}]_0 = 50 : 1 : 1$, total monomer concentration = 2 M. M_n and \overline{DP}_n determined by SEC against poly(styrene) standards.

In order to determine the monomer sequencing in the chain, each sample was analysed by quantitative ^{13}C NMR spectroscopy in order to integrate the carbonyl diad resonances. After 4 h, one prominent carbonyl diad resonance was present at $\delta = 173.0$ ppm, which corresponds to a MI carbonyl adjacent to a MI repeat unit ($\text{MI}^*\text{-MI}$, where * denotes the observed carbonyl), with three other carbonyl diad resonances of significantly lower integrals at $\delta = 173.2$, 173.8 and 174.1 ppm that correspond to $\text{MI}^*\text{-PDL}$, $\text{PDL}^*\text{-MI}$ and $\text{PDL}^*\text{-PDL}$ respectively (Figure 4.7). The carbonyl diad resonance attributable to $\text{MI}^*\text{-MI}$ is usually observed with a small shoulder peak upfield of the main resonance, which is a consequence of the menthide being produced from a mixture of menthone isomers, the isomerisation is preserved during the Baeyer-Villiger oxidation and thus affects the carbonyl diad resonances. Over the first 8 h of copolymerisation, the integral of the $\text{MI}^*\text{-MI}$ carbonyl diad resonance increased regularly when compared to the other carbonyl diad resonances present. This is a clear representation of MI being preferentially consumed throughout this part of the copolymerisation, with no growth in resonance attributable to PDL. Once the concentration of MI monomer became too low, PDL began to be incorporated into the polymer, observed by the integral of the $\text{PDL}^*\text{-PDL}$ carbonyl diad

resonance increasing, with no change observed in the other three carbonyl diad resonance integrals. As a consequence of the lack of a high quantity of MI*-PDL and PDL*-MI resonances, it can be assumed the polymers formed are block-like copolymers. A small amount of MI*-PDL and PDL*-MI resonances are present and therefore there is a slight gradation when one block ends and another begins resulting in 4 regions of monomer sequence switching. This occurs over a short amount of overall monomer conversion and the gradation is likely to be very short as a consequence. Quantitative ^{13}C NMR spectroscopy of the extended time period copolymerisation (186 h) did not show any difference in the relative integrals of the carbonyl diad resonances from analysis conducted immediately after copolymerisation had finished, therefore transesterification side reactions to form random copolymers do not occur. DOSY NMR spectroscopy showed the presence of only one polymer species, which indicates that one copolymer species had formed and not two species of homopolymers (Figure 4.8). SEC analysis of the polymerisation after 186 h did not show further increase in \bar{D}_m , thus it can be assumed transesterification side reactions at the polymerisation equilibrium is limited as a consequence of the catalyst affinity toward the menthide repeat units. These repeat units cannot transesterify, likely as a consequence of the steric bulk surrounding the ester linkage and lack of enthalpic gain from no ring-strain to further promote breaking the ester bond.

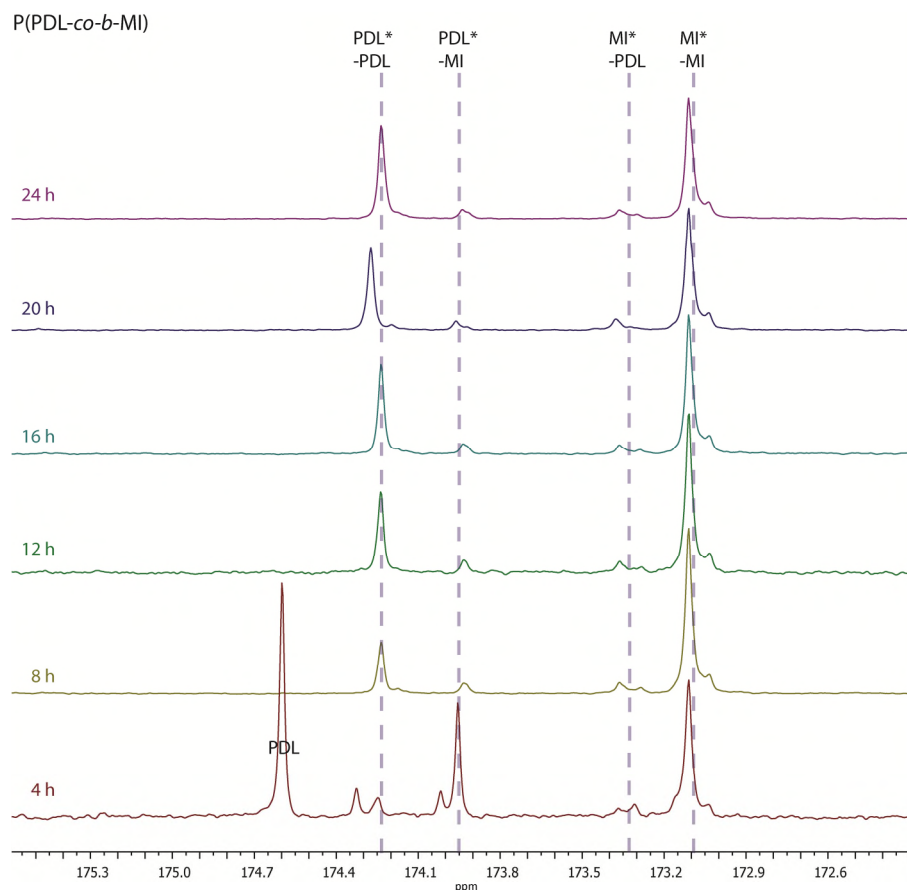


Figure 4.7 Quantitative ^{13}C NMR spectra of the carbonyl region during copolymerisation of ω -pentadecalactone with menthede (125 MHz, CDCl_3 , 298 K)

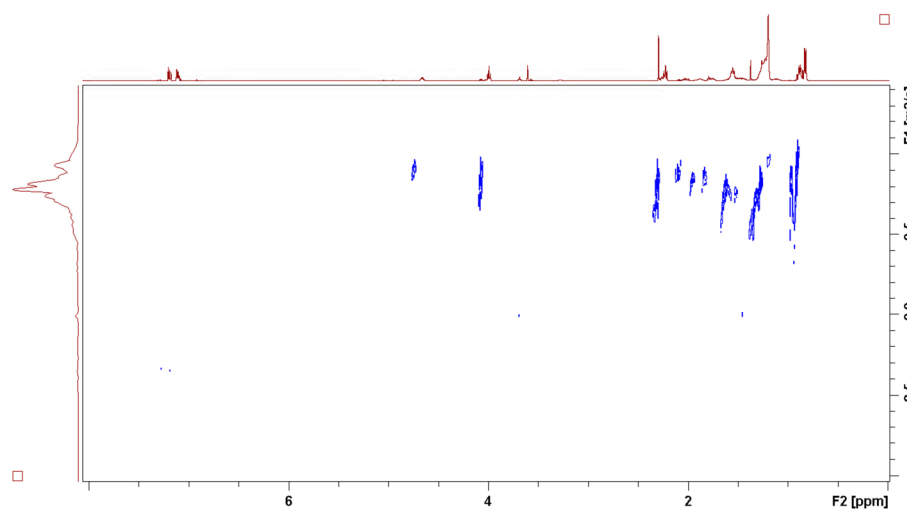


Figure 4.8 DOSY NMR spectra of P(PDL-co-MI) (500 MHz, 298 K, CDCl_3).

As further proof of the inability of PMI to transesterify, a mixture of PMI ($M_n = 10.7$ kDa, $5.4 \mu\text{mol}$) and PPDL ($M_n = 10.1$ kDa, $10.1 \mu\text{mol}$) was dissolved into toluene, with a large quantity of $\text{Mg}(\text{BHT})_2(\text{THF})_2$ ($16.5 \mu\text{mol}$) as a catalyst for transesterification. After 24 h, the resultant material was analysed by quantitative ^{13}C NMR spectroscopy and SEC in order to

determine whether any transesterification had taken place. As expected, the predominant carbonyl diad resonances observed by quantitative ^{13}C NMR spectroscopy were PDL*-PDL and MI*-MI, indicating the materials were either block-like copolymers or homopolymers and had not become randomly sequenced as a consequence of transesterification (Figure 4.9). The minimal evolution of carbonyl diad resonances corresponding to PDL*-MI and MI*-PDL in the presence of a large quantity of catalyst further demonstrates the poor ability of PMI to transesterify. SEC analysis of the resultant material showed no growth in molecular weight or broadening of dispersity that would be expected if the chain ends had undergone transesterification to produce a block copolymer (Figure 4.10). Furthermore, there was no significant broadening of the molecular weight distribution, further indicating low amounts of transesterification side reactions.

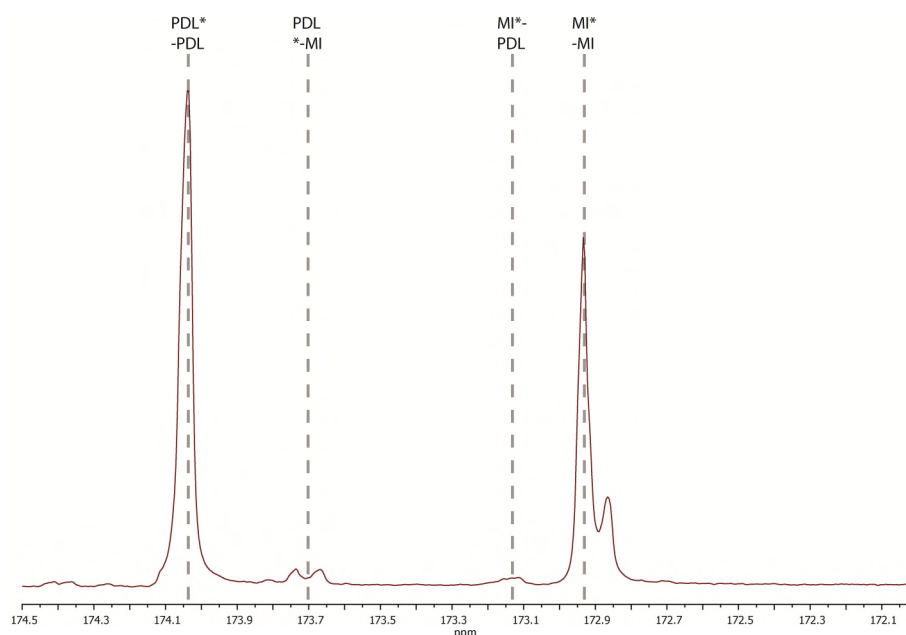


Figure 4.9 Quantitative ^{13}C NMR spectra of the carbonyl region for the transesterification of PPDL and PMI (125 MHz, CDCl_3 , 298 K).

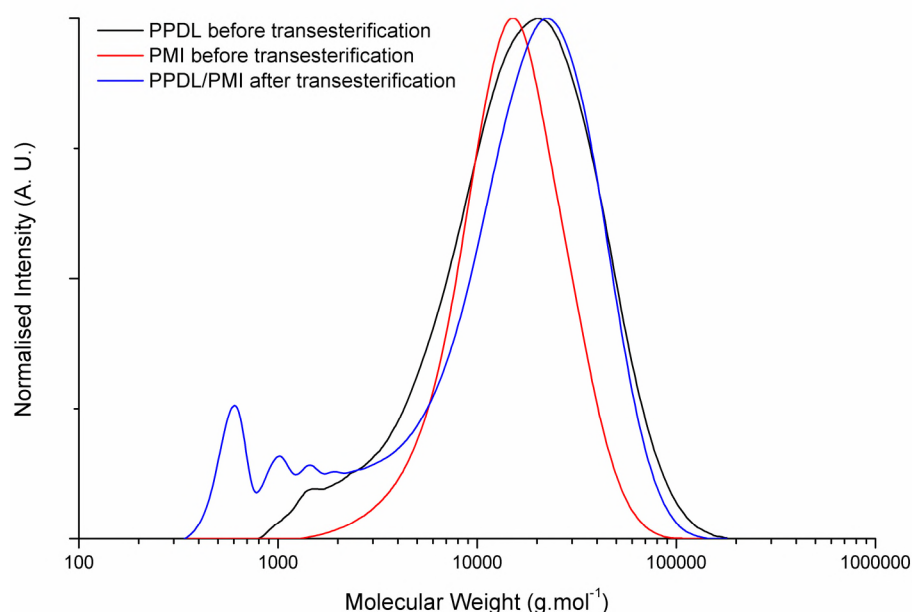


Figure 4.10 SEC chromatograms for the molecular weight distribution of PPDL, PMI and the resultant material from the attempted transesterification of both polymers. Molecular weights determined by poly(styrene) standards and CHCl_3 (0.5% Net_3) as eluent.

In order to determine whether the copolymerisation of PDL and MI can target specific molecular weights, an equimolar mixture of PDL and MI was undertaken at an overall monomer concentration of 2 M in toluene at 80 °C, with benzyl alcohol as initiator and $\text{Mg}(\text{BHT})_2(\text{THF})_2$ as catalyst, targeting total DPs of 20, 50 and 250 (Table 4.1). By ^1H NMR spectroscopy analysis of the final polymer, it was observed that each polymerisation progressed to $\geq 90\%$ total monomer conversion. Quantitative ^{13}C NMR spectroscopy proved that in each copolymerisation a largely block-like sequence was formed, with a slight gradation between blocks. The length of the gradation increased with increasing DP, indicating it is likely a thermodynamic effect of the monomer concentration, where the concentration of MI is low enough for PDL polymerisation to be equally preferable and polymerisation of both monomers occurs until the remaining MI is consumed.

Table 4.1 Copolymerisation of 1 : 1 mol% [PDL]₀ : [MI]₀ targeting various DPs

Target DP	Conversion ^a (%)	M_n^b (GPC) (kDa)	M_w^b (GPC) (kDa)	\mathcal{D}_M^b	M_n^c (NMR) (kDa)	Diads ^d			
						PDL*-PDL	PDL*-MI	MI*-PDL	MI*-MI
20	96	6.0	16.0	2.65	3.8	0.36	0.13	0.09	0.42
50	93	8.6	33.2	3.84	7.3	0.41	0.07	0.08	0.44
100	91	23.6	40.7	1.72	21.4	0.44	0.04	0.03	0.49
250	90	9.8	78.4	8.04	24.7	0.45	0.04	0.05	0.47

^aOverall monomer conversion determined by ¹H NMR spectroscopy. ^bDetermined by SEC in CHCl₃ against poly(styrene) standards. ^cDetermined by end-group analysis by ¹H NMR spectroscopy. ^dDetermined by quantitative ¹³C NMR spectroscopy, with * defining the carbonyl analysed.

The copolymerisation of MI and PDL with varying monomer feed ratios was attempted using ratio feeds of 10 : 90, 30 : 70, 50 : 50, 70 : 30 and 90 : 10 mol% for molar ratio of PDL : MI at an overall targeted DP of 100, with Mg(BHT)₂(THF)₂ as catalyst and benzyl alcohol as initiator. After 24 h of polymerisation, samples were analysed by ¹H and quantitative ¹³C NMR spectroscopy and differential scanning calorimetry (DSC). All copolymers showed high final overall monomer conversions indicating block lengths were formed similar to the initial monomer feed ratio (Table 4.2). This was confirmed through analysis by ¹H NMR spectroscopy of the polymer after remaining monomers were removed by precipitation. Therefore specific block lengths for either monomer can be targeted with a high degree of accuracy through varying the monomer feed ratio. Integration of the carbonyl diad resonances produced by quantitative ¹³C NMR spectroscopy showed a block-like architecture for all copolymers (Figure 4.11). Analysis of the carbonyl diad resonance integrals corresponding to PDL*-MI and MI*-PDL showed some gradation between blocks in each copolymer, however with increasing PDL content, the gradation length decreased; from 11 changes in the chain end to 2 between 10 : 90 and 90 : 10 mol% PDL : MI respectively (11% to 2% respectively of the entire polymer chain), as indicated by the quantitative ¹³C NMR spectroscopy integrals corresponding to PDL*-MI and MI*-PDL carbonyl diad resonances. As demonstrated during the kinetic study of the copolymerisation of MI and PDL, transesterification side reactions are not observed until PDL conversion begins, evidenced by the increase in dispersities during PDL conversion.

Analysis of the varied monomer ratio DP100 copolymers by SEC showed that with increasing PDL content, the D_M also broadened as a consequence of transesterification side reactions occurring concurrently with PDL polymerisation but not MI polymerisation. That is, the longer the PDL block length, the more transesterification side reactions occur, leading to increased D_M for high PDL content copolymer.

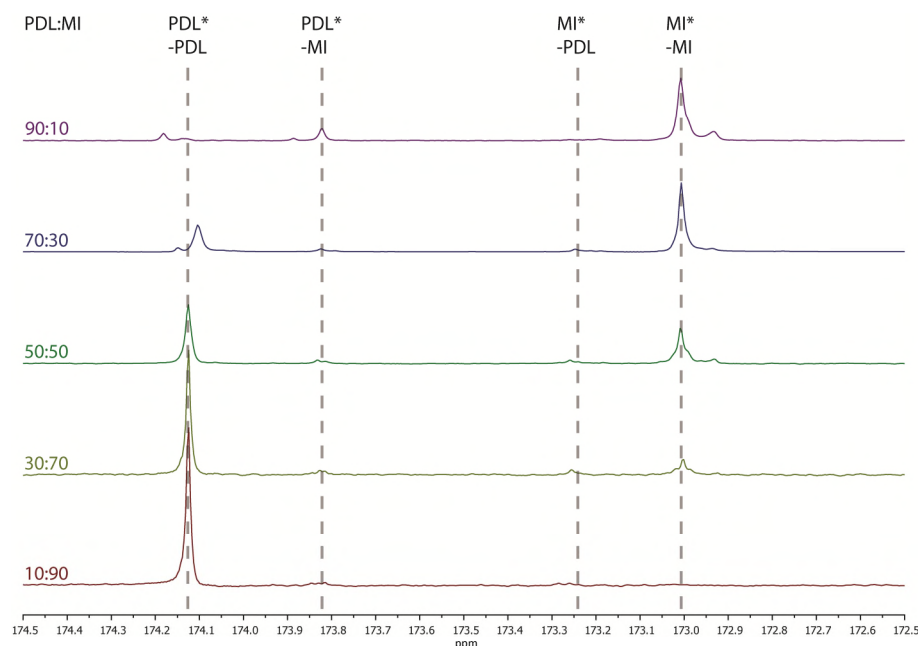


Figure 4.11 Quantitative ^{13}C NMR spectra of DP100 P(PDL-co-MI) copolymers with varying PDL mol% (125 MHz, CDCl_3 , 298 K).

Table 4.2 Copolymerisation of PDL and MI at varying monomer molar feed ratio targeting DP 100

[PDL]:[MI]	Conversion ^a (%)	M_n^b	M_w^b	D_M^b	M_n^c	Diad ^d			
		(GPC) (kDa)	(GPC) (kDa)		(NMR) (kDa)	PDL*- PDL*	PDL*- MI	MI*- PDL	MI*- MI
10:90	89	15.4	20.0	1.30	15.0	0.07	0.11	0.04	0.78
30:70	86	21.3	34.1	1.60	16.3	0.30	0.05	0.04	0.61
50:50	81	13.8	33.3	2.41	16.6	0.49	0.04	0.05	0.42
70:30	94	18.0	56.5	3.14	26.4	0.77	0.04	0.03	0.16
90:10	94	21.6	78.6	3.65	24.3	0.95	0.02	0.02	0.01

^aOverall monomer conversion determined by ^1H NMR spectroscopy. ^bDetermined by SEC in CHCl_3 against poly(styrene) standards. ^cDetermined by end-group analysis by ^1H NMR spectroscopy. ^dDetermined by quantitative ^{13}C NMR spectroscopy, with * defining the carbonyl analysed.

The thermal properties of P(PDL-co-MI) were investigated to monitor the effect of each block on the T_m and T_c through DSC analysis of the copolymers formed by varying molar ratio feed (Figure 4.12). Unlike PDL copolymers that exhibit cocrystallisation, no linear

relationship was found between the quantity of either monomer and the T_m or T_c . Some crystallinity was observed in the samples, further proving a block-like sequencing as a random copolymer would be prevented from crystallising as a consequence of the side chains preventing crystallisation packing of the polymer chains. The copolymer containing 10 : 90 mol% PDL : MI did not exhibit either T_m or T_c when analysed by DSC and remained liquid throughout the entire range of temperatures (-150 to 100 °C), caused by the prevention of packing by the side chain functionalities. With decreasing mole fraction of MI, the crystallisation of the polymer increased quickly, with an observed $T_m = 59.2$ °C for the 30 : 70 mol% PDL : MI copolymer. Samples of 30 : 70 and 50 : 50 mol% PDL : MI showed several minima within the melting curve towards lower temperatures as a consequence of smaller crystalline regions of PDL being dispersed within the amorphous MI region. As the MI block is already above the T_m of PMI ($T_g < -150$ °C), the smaller crystalline regions of PDL require a lower temperature to melt before the large bulk crystalline regions of PDL block, which melted at the observed T_m minimum. A small, secondary T_c is observed in the cooling cycle for both 30 : 70 and 50 : 50 mol%, which indicates a secondary crystallisation, indicating the crystallisation of PDL in a largely amorphous MI region. A single sharp T_c is observed for copolymers with $\geq 50\%$ PDL content, indicating that only the PDL block is crystallising. Increasing the ratio of MI lowers the observed T_c away from the T_c of pure PPDL as a consequence of dispersed pockets of the MI block preventing full crystallisation. Dynamic mechanical and temperature analysis (DMTA) was also performed on the 30 : 70 mol% PDL : MI copolymer in order to ascertain a glass transition temperature (T_g) for both blocks. Analysis showed a distinct T_g at -24 °C that corresponds to the T_g of a PPDL block and a small, broad peak at -130 °C that potentially corresponds to the T_g of a PMI block and therefore shows phase separation of PDL and MI regions of the polymer.

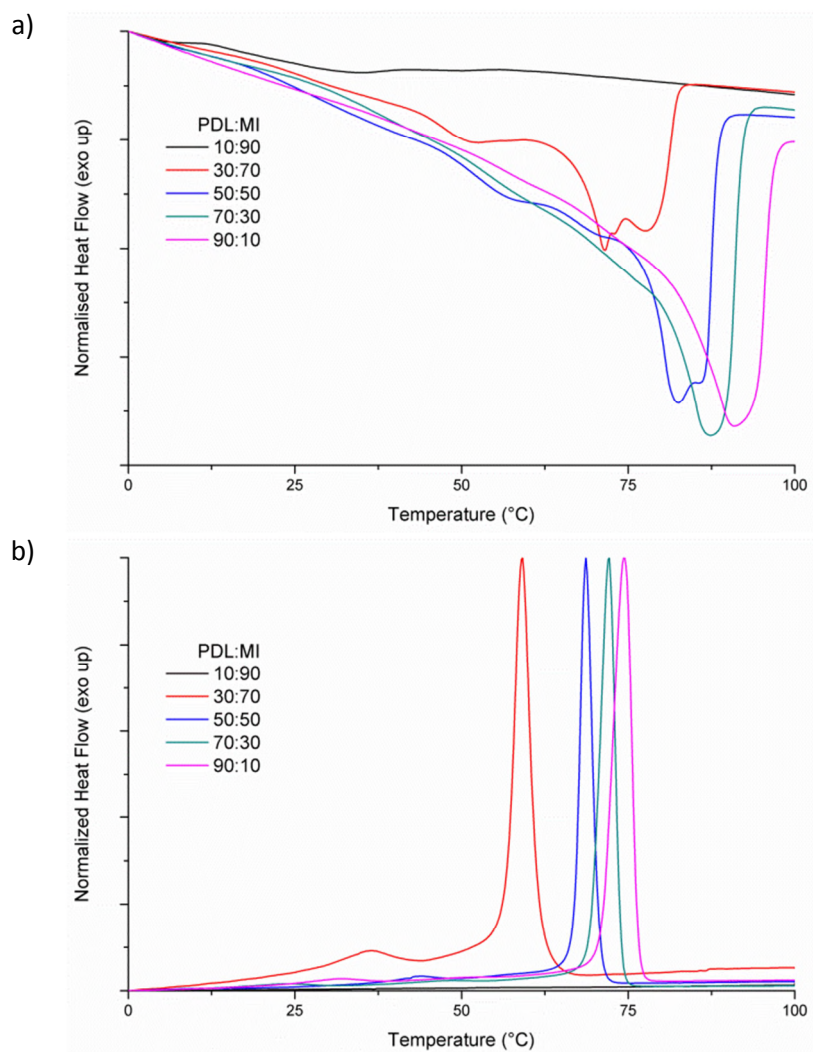
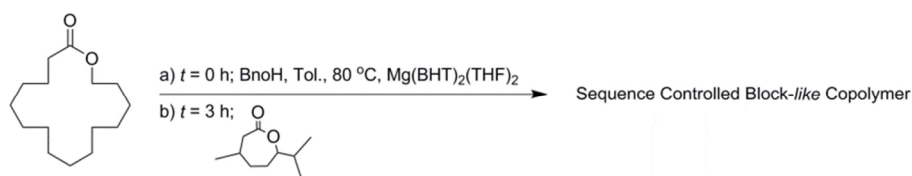


Figure 4.12 a) DSC thermograms (second heating curve, between 0 °C and 100 °C) of the T_m at various molar ratios of DP 100 P(ω -pentadecalactone-*co*- menthide). b) DSC thermograms (second cooling curve, between 0 °C and 100 °C) of the T_m at various molar ratios of DP 100 P(ω -pentadecalactone-*co*- menthide).

4.2.3 Triblock copolymers of PDL and MI



Scheme 4.4 Sequence controlled copolymerisation of PDL and MI through the timed injection of MI into a PDL homopolymerisation.

Through this ‘one-pot’ method of copolymerisation, the formation of one-pot PDL block copolymers is achieved. However, MI can initiate from a primary alcohol and therefore could potentially initiate from the end-chain alcohol of PPDL. Addition of MI during a polymerisation of PDL should mean the polymerisation switches in favour of MI, once all the MI is consumed the polymerisation would revert back to the consumption of PDL and the resulting material would be a triblock copolymer. To this end, the polymerisation of PDL at a concentration of 1 M in toluene at 80 °C, to a targeted DP of 50, was attempted (Scheme 4.4). Once conversion reached 50% by ^1H NMR spectroscopy ($t = 3$ h), a solution of MI at a concentration of 1 M in toluene was injected into the reaction.

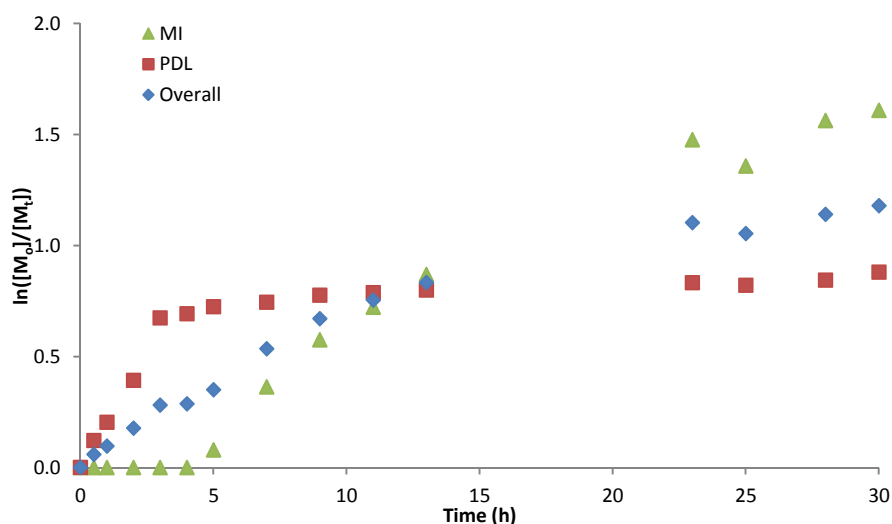
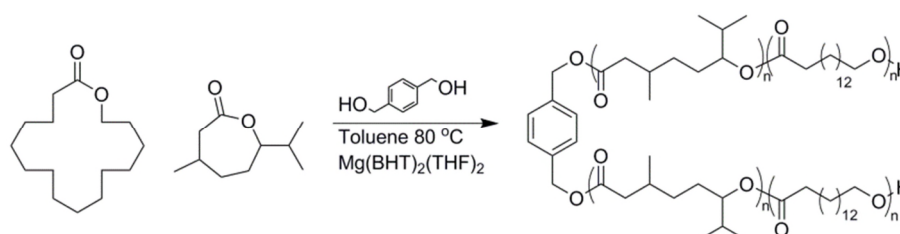


Figure 4.13 Kinetic plot for the sequence controlled copolymerisation of menthide and pentadecalactone, conducted at 80 °C in toluene with $[\text{PDL}]_0 : [\text{MI}]_0 : [\text{BnOH}]_0 : [\text{cat.}]_0 = 50 : 50 : 1 : 1$, total monomer concentration = 1 M, MI injected into reaction mixture at $t = 3$ h.

Similarly to the one-pot copolymerisation of MI and PDL, the sequential addition paused once MI was added for a period of 45 min before recommencing, with incorporation at a

similar rate to the homopolymerisation and one-pot copolymerisation (Figure 4.13). However, once all MI was consumed, the consumption of PDL was much slower than previously observed with 1% of the total PDL consumed every 18 h, which resulted in only 63% conversion of PDL after 100 h of polymerisation. This could be a consequence of either the catalyst becoming poisoned by H₂O introduced during the injection of MI into the system, or the catalyst having greater affinity for the MI and attaching to the MI block rather than chain end to polymerise PDL. Thus, sequential polymerisation may not be a viable method of production of P(PDL-co-MI-co-PDL) triblock copolymers. In order to maintain the polymerisation after the injection of MI, a second experiment was attempted with addition of Mg(BHT)₂(THF)₂ catalyst at the same time as the injection of menthide. The presence of the additional catalyst slowed the polymerisation even further as a consequence of the MI forming a complex with the catalyst, resulting in a longer inhibition time of 4 h before the addition of MI onto the polymer chain at a greatly reduced rate. This is likely a consequence of the complexation effect between menthide and the excess catalyst now present in the reaction mixture.



Scheme 4.5 Copolymerisation of MI and PDL with bifunctional initiator 1,4-benzenedimethanol.

The use of a bifunctional initiator should allow for one-pot triblock copolymers to be realised. Thus, an equimolar mixture of MI and PDL at a total monomer concentration of 2 M in toluene at 80 °C, with targeted total DPs of 100 and 200, were polymerised by Mg(BHT)₂(THF)₂ using 1,4-benzenedimethanol (BDM) as initiator (Scheme 4.5). The resulting materials were analysed by quantitative ¹³C NMR spectroscopy and determined to have block-like architecture (Figure 4.14). Interestingly, the integrals of MI*-PDL and PDL*-

MI carbonyl diad resonances in the total DP 100 copolymerisation, $P(\text{PDL}_{25}\text{-co-MI}_{50}\text{-co-PDL}_{25})$, were twice the integrals of the same carbonyl diad resonances in DP 100 $P(\text{PDL-co-MI})$, which indicates two gradation regions are present and a triblock copolymer has been formed. As expected, doubling the molar ratio of PDL and MI to initiator in the copolymerisation, to produce $P(\text{PDL}_{50}\text{-co-MI}_{100}\text{-co-PDL}_{50})$, displayed the same carbonyl diad resonances as observed in DP 100 $P(\text{PDL-co-MI})$ determined by quantitative ^{13}C NMR spectroscopy. Analysis of the triblock copolymers by SEC showed a significant increase in the \bar{M}_w when compared to the diblock copolymers produced above (Table 4.3). This is likely a consequence of the presence of two PDL blocks on either chain end that can both undergo transesterification side reactions that broaden \bar{M}_w , as opposed to the diblock copolymer that contains only one PDL block that can undergo transesterification side reactions (Figure 4.15).

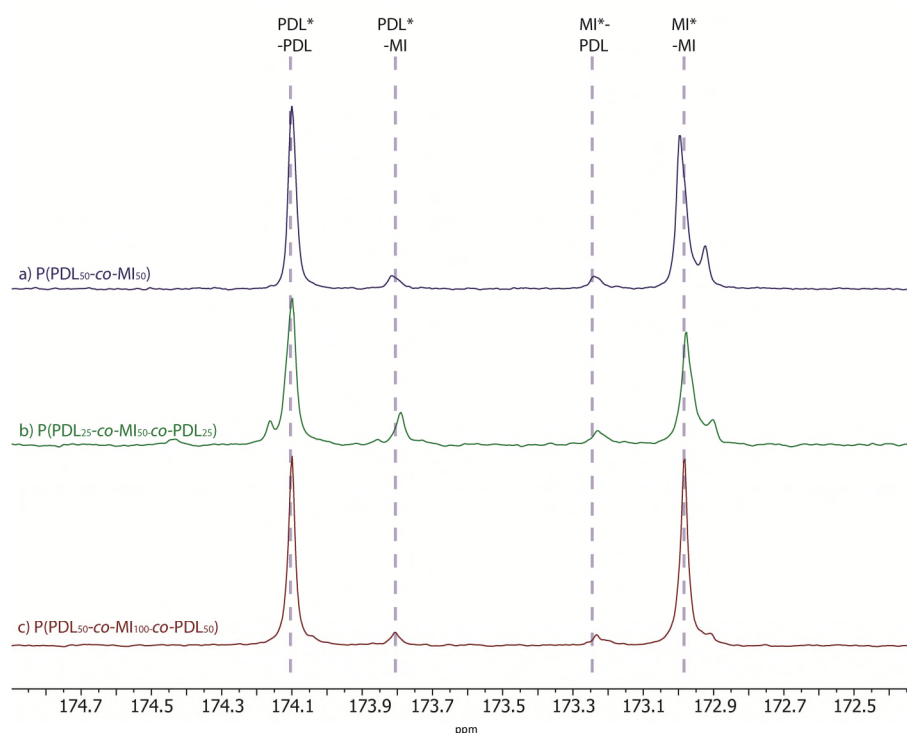


Figure 4.14 Quantitative ^{13}C NMR spectra of the carbonyl region of the diblock copolymer $P(\text{PDL}_{50}\text{-co-MI}_{50})$ and triblock copolymers $P(\text{PDL}_{25}\text{-co-MI}_{50}\text{-co-PDL}_{25})$ and $P(\text{PDL}_{50}\text{-co-MI}_{100}\text{-co-PDL}_{50})$ respectively (125 MHz, CDCl_3 , 298 K).

Table 4.3 Copolymerisations of PDL and MI at 1 : 1 mol% with varying DP and initiator.

Polymer	M_p^a (kDa)	M_n^a (kDa)	M_w^a (kDa)	\mathcal{D}_M^a	Diads ^b			
					PDL* -PDL	PDL* -MI	MI* -PDL	MI* -MI
P(PDL ₅₀ -co-MI ₅₀) ^c	20.7	13.4	24.0	1.79	0.44	0.04	0.03	0.49
P(PDL ₂₅ -co-MI ₅₀ -co-PDL ₂₅) ^d	15.7	5.7	16.3	2.87	0.46	0.09	0.05	0.41
P(PDL ₅₀ -co-MI ₁₀₀ -co-PDL ₅₀) ^d	72.7	15.6	67.1	4.29	0.41	0.04	0.04	0.51

^aDetermined by SEC in CHCl₃ against poly(styrene) standards. ^bDetermined by quantitative ¹³C NMR spectroscopy, with * defining the carbonyl analysed. Polymerisations conducted at 80 °C, 1 M in toluene and [I]₀ : [cat.]₀ = 1 : 1, where I is ^cbenzyl alcohol and ^d1,4-benzenedimethanol.

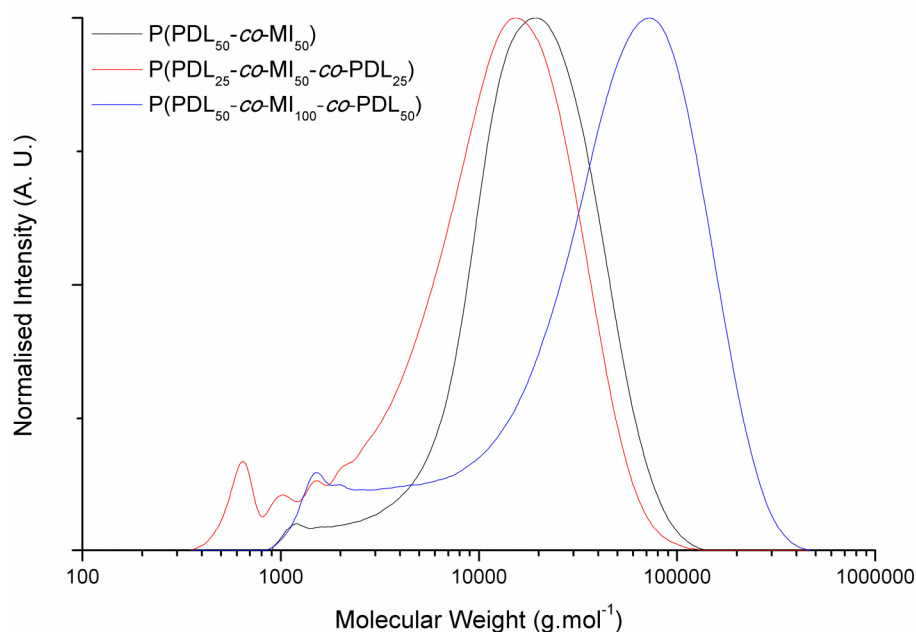
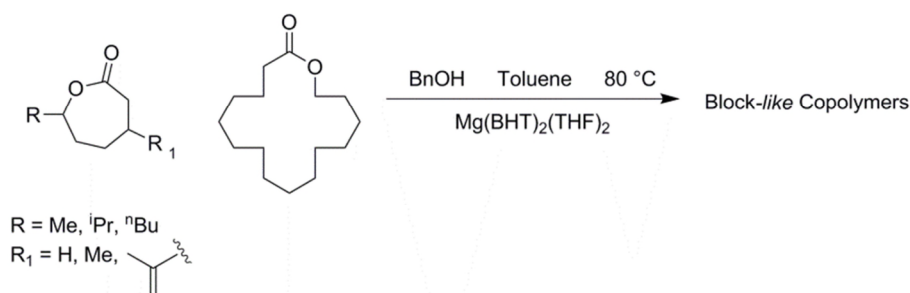


Figure 4.15 SEC chromatograms of the molecular weight distribution of a) P(PDL₅₀-co-MI₅₀), b) P(PDL₂₅-co-MI₅₀-co-PDL₂₅) and c) P(PDL₅₀-co-MI₁₀₀-co-PDL₅₀). Molecular weights determined by poly(styrene) standards and CHCl₃ (0.5% Net₃) as eluent.

4.2.4 PDL block copolymers



Scheme 4.6 Copolymerisation of an ϵ -substituted ϵ -lactone (ϵ SL) with ω -pentadecalactone using $\text{Mg}(\text{BHT})_2(\text{THF})_2$ as a catalyst to form block-like copolymers.

PDL copolymers with MI and ϵ DL are both block-like; in order to determine whether this is true for other ϵ -lactones with ϵ -substitutions (ϵ SL), lactones ϵ -heptalactone (ϵ HL), 3-bromocamphide and dihydrocarvide (DHC) were synthesised by Baeyer-Villiger oxidation of 2-methylcyclohexanone, 3-bromocamphor and dihydrocarvone respectively, for copolymerisation with PDL. The use of 3-bromocamphide and dihydrocarvide in copolymerisation with PDL, would introduce blocks with functionalities for post-polymerisation modification, which have not yet been demonstrated in PDL copolymerisations with other lactones. Copolymerisations using 3-bromocamphide were unsuccessful, producing only PPDL as a consequence of large steric hindrance blocking the catalyst from accessing the lactone. An equimolar mixture of ϵ HL and PDL at a total concentration of 2 M in toluene was successfully polymerised at 80 °C to a targeted total DP of 100 from a benzyl alcohol initiator (Scheme 4.6). The resultant polymer was analysed by ^1H NMR spectroscopy and showed high conversions. Dispersities similar to those observed in PDL and MI copolymers were confirmed by SEC analysis of the polymer (Table 4.4). Analysis by quantitative ^{13}C NMR spectroscopy showed that the copolymer of PDL and ϵ HL was block-like, with a carbonyl diad resonance distribution similar to $\text{P}(\text{PDL-co-MI})$ (Figure 4.16a). Analysis of the polymer by DOSY NMR spectroscopy showed the presence of only one polymer species, which indicates the formation of a copolymer (Figure 4.17a).

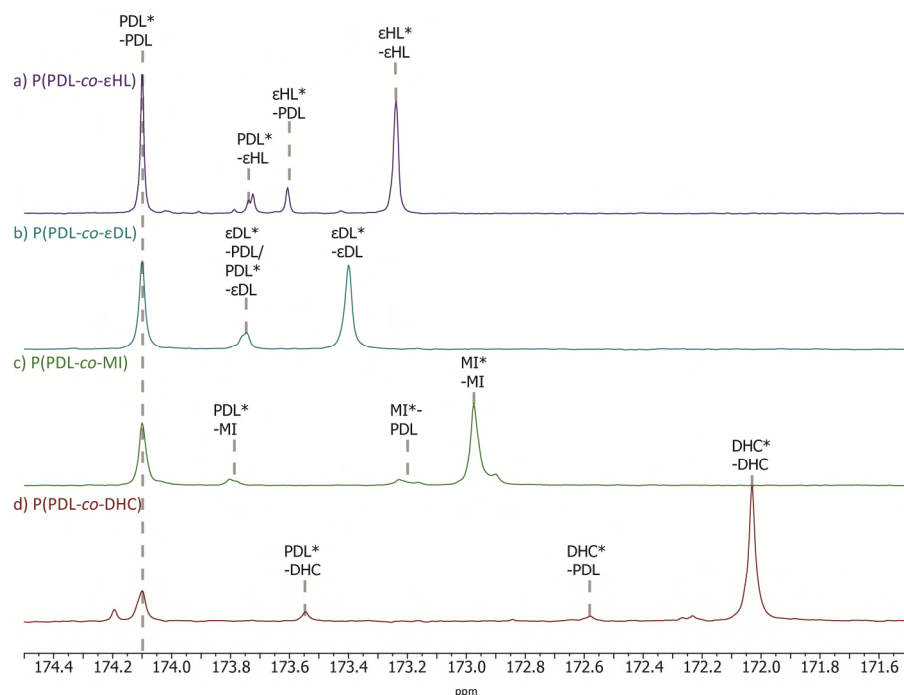


Figure 4.16 Quantitative ^{13}C NMR spectra of the carbonyl region of copolymerisations of ω -pentadecalactone with a) ϵ -heptalactone; b) ϵ -decalactone; c) menthine and d) dihydrocarvide at 1 : 1 mol% monomers and total DP of 100 (125 MHz, CDCl_3 , 298 K).

The copolymerisation of an equimolar mixture of PDL and ϵ DL was similarly achieved at 2 M in toluene at 80 °C, using benzyl alcohol as initiator, $\text{Mg}(\text{BHT})_2(\text{THF})_2$ as a catalyst and targeting a total DP of 100. The resultant polymer was characterised by ^1H NMR spectroscopy and SEC analysis. High monomer conversions and narrow D_M were determined, in line with previous literature.⁹ Quantitative ^{13}C NMR spectroscopy similarly showed the polymer sequencing was block-like, with only a relatively small carbonyl diad resonance integral corresponding to both $\text{PDL}^*\text{-}\epsilon\text{DL}$ and $\epsilon\text{DL}^*\text{-PDL}$ carbonyls compared to significantly larger $\text{PDL}^*\text{-PDL}$ and $\epsilon\text{DL}^*\text{-}\epsilon\text{DL}$ carbonyl diad resonance integrals (Figure 4.16b). DOSY NMR spectroscopy confirmed no formation of homopolymer species during the copolymerisation, with only one polymer species present (Figure 4.17b).

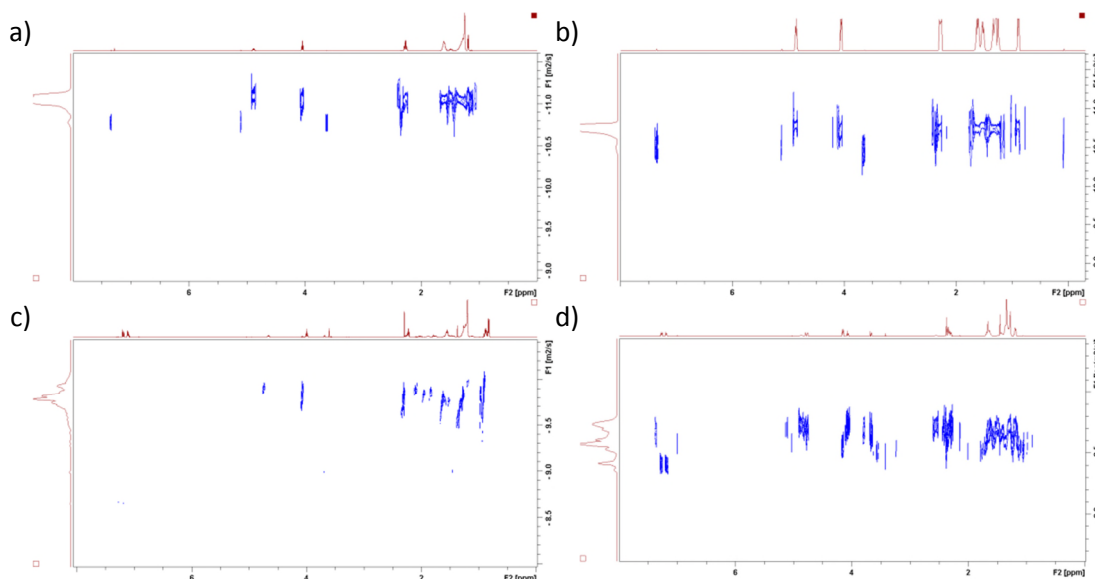


Figure 4.17 DOSY NMR spectra of a) P(PDL-*co*- ϵ HL), b) P(PDL-*co*- ϵ DL), c) P(PDL-*co*-MI) and d) P(PDL-*co*-DHC) (500 MHz, 298 K, CDCl_3).

The copolymerisation of an equimolar mixture of PDL and DHC at 2 M in toluene was achieved at 80 °C, using benzyl alcohol as initiator, $\text{Mg}(\text{BHT})_2(\text{THF})_2$ as a catalyst and targeting a total DP of 100. Analysis by ^1H NMR spectroscopy showed a maximum overall monomer conversion of 55% was achievable after 5 days of polymerisation as a consequence of only ~40% PDL polymerisation before copolymerisation halted. This could be a consequence of impurities present from production of the monomer. Quantitative ^{13}C NMR spectroscopy showed the copolymer formed was block-like as expected (Figure 4.16 d). Only one polymer species was determined by DOSY NMR spectroscopy, attributable to the formation of only copolymer species (Figure 4.17d). Analysis of P(PDL-*co*-DHC) by ^1H NMR spectroscopy showed that no side reactions had occurred during the polymerisation and all alkene functionalities remained intact on the polymer, as evidenced through comparative integration of the terminal methylene resonance of the alkene ($\delta = 4.79$ ppm) and the α -methylene resonance of poly(dihydrocarvide) ($\delta = 4.88$ ppm) (Figure 4.18). The presence of an alkene functionality could be used in post-polymerisation modification reactions, such as thiol-ene addition.¹⁰ Therefore, the production of one-pot functionalised PDL block-like copolymers is achievable.

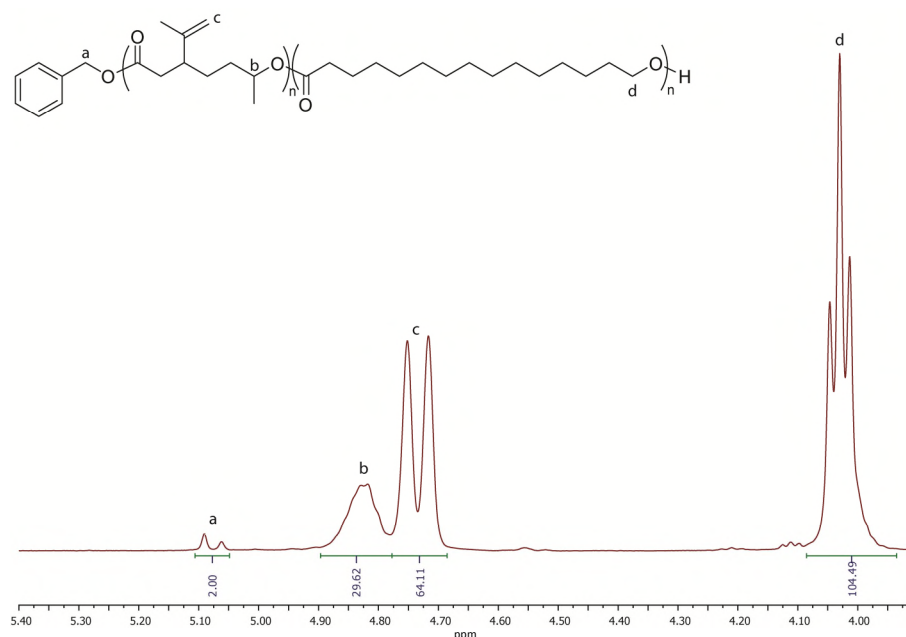


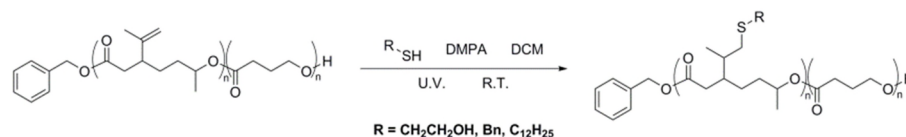
Figure 4.18 ^1H NMR spectrum for P(PDL-co-DHC) in the region of $\delta = 5.4$ - 3.9 ppm illustrating preservation of the alkene post-polymerisation (400 MHz, CDCl_3 , 298 K).

Table 4.4 Copolymerisation of pentadecalactone with an equimolar ratio of ϵ -substituted ϵ -lactone monomer, targeting a total DP of 100.

Monomer (ϵSL)	Conversion ^a (%)			M_n^b (GPC) (kDa)	M_w^b (GPC) (kDa)	\bar{D}_M^b	M_n^c (NMR) (kDa)	Diads ^d			
	PDL	ϵSL	Total					PDL* -PDL	PDL* - ϵSL	ϵSL * -PDL	ϵSL * - ϵSL
ϵHL	97	99	98	17.0	46.9	2.8	13.2	0.40	0.08	0.08	0.44
ϵDL	98	99	99	21.4	56.5	2.6	20.8	0.42	0.11 ^e		0.47
MI	85	94	90	20.9	54.9	2.6	14.5	0.35	0.04	0.05	0.56
DHC	45	99	57	6.1	9.7	1.6	9.6	0.16	0.04	0.03	0.77

^aDetermined by ^1H NMR spectroscopy. ^bDetermined by SEC in CHCl_3 against poly(styrene) standards. ^cDetermined by end-group analysis by ^1H NMR spectroscopy. ^dDetermined by quantitative ^{13}C NMR spectroscopy, with * defining the carbonyl analysed. ^eJoint integral as a consequence of low resolution between peaks.

4.2.5 Post polymerisation modification of P(PDL-co-DHC)



Scheme 4.7 Thiol-ene addition of a thiol onto P(PDL-co-DHC).

As a consequence of the pendent alkene functionality of DHC, a site is available for functionalisation either pre- or post-polymerisation using techniques such as thiol-ene addition, atom transfer radical addition, metathesis or Pd-catalysed coupling.¹¹ The copolymerisation of PDL and DHC is shown above to preserve the alkene functionality and could therefore be used to functionalise the polymer post-polymerisation. The thiol-ene

addition of mercaptoethanol onto P(PDL-co-DHC) was conducted following a previously reported technique at 2.5 M in DCM, using 2,2-dimethoxy-2-phenylacetophenone (DMPA) as a radical photoinitiator and a thiol : olefin ratio of 11 : 1 (Scheme 4.7).¹² After 4 h of exposure to UV light, the resultant polymer (P(PDL-co-DHCME)) was washed to remove excess thiol and analysed by ^1H NMR spectroscopy and SEC. A significant decrease in the proton resonances attributable to the alkene ($\delta = 4.76$ ppm) was observed, which indicates a conversion of 92% of all alkene groups has occurred. This corresponded with a new resonance at $\delta = 2.70$ ppm, which is attributable to $-\text{SCH}_2\text{CH}_2\text{OH}$ (Figure 4.19). Through the integration of this resonance, it was determined that thiol-ene addition had occurred in the case of all converted alkenes. SEC analysis of the final polymer showed only a slight decrease in molecular weight distribution, an expected consequence of altered Mark-Houwink parameters, and almost identical \bar{M}_w (Figure 4.20). These combined results show thiol-ene addition has occurred to the same extent on all polymer chains (Table 4.5).

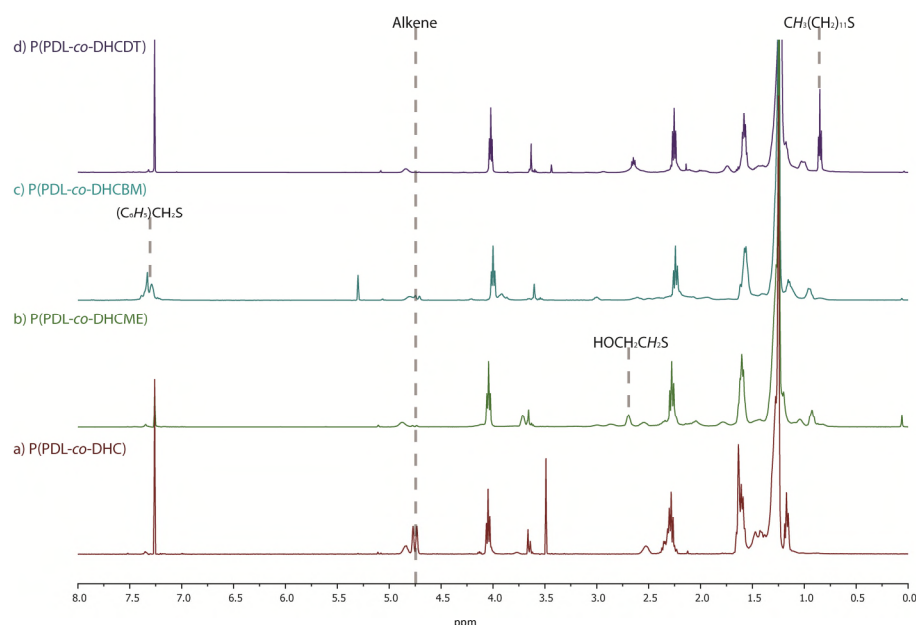


Figure 4.19 ^1H NMR spectra for a) P(PDL-co-DHC) and thiol-ene addition products b) P(PDL-co-DHCME), c) P(PDL-co-DHCBM) and P(PDL-co-DHCDT), with unique resonances highlighted to show conversion (a, b, d; 400 MHz, CDCl_3 , 298 K. c; 400 MHz, CD_2Cl_2 , 298 K).

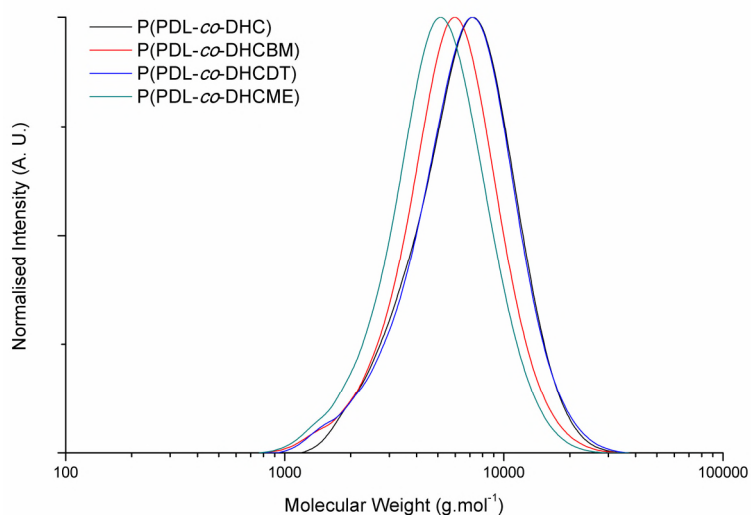


Figure 4.20 SEC chromatograms of P(PDL-*co*-DHC) and the resultant polymers from thiol-ene addition of benzyl mercaptan (P(PDL-*co*-DHCBM)), dodecanethiol (P(PDL-*co*-DHCDT)) and mercaptoethanol (P(PDL-*co*-DHCME)).

The addition of benzyl mercaptan to the polymer chain was also attempted, using DMPA as a photoinitiator, a thiol : olefin ratio of 11 : 1 and a total concentration of 2.5 M in DCM. The reaction mixture was degassed, placed under an argon environment and exposed to UV light for 4 h. After the excess thiol had been removed, analysis of the alkene resonance by ^1H NMR spectroscopy revealed that 56% of alkene had been consumed in the reaction and coincided with the appearance of a resonance attributable to BnCH_2S - ($\delta = 3.60$ ppm). Integration of the thiol ether resonance of the polymer (P(PDL-*co*-DHCBM)) showed that thiol-ene addition had occurred on all reacted alkenes. The lower addition of benzyl mercaptan compared to mercaptoethanol over the same period is most likely a consequence of the electron withdrawing effect of the aromatic ring on the thiol, making the thiol less active towards thiol-ene addition.

Table 4.5 Thiol-ene addition to P(PDL-*co*-DHC)

Polymer	Thiol Added	Conversion ^a (%)	M_n^b (GPC) (kDa)	M_w^b (GPC) (kDa)	D_M^b
P(PDL- <i>co</i> -DHC)	-	-	4.1	5.4	1.32
P(PDL- <i>co</i> -DHCME)	$\text{HOCH}_2\text{CH}_2\text{SH}$	92	4.4	5.7	1.30
P(PDL- <i>co</i> -DHCBM)	BnSH	56	5.0	6.5	1.30
P(PDL- <i>co</i> -DHCDT)	$\text{CH}_3(\text{CH}_2)_{11}\text{SH}$	>99	5.3	7.1	1.35

^aDetermined by ^1H NMR spectroscopy. ^bDetermined by SEC in CHCl_3 against poly(styrene) standards. ^cDetermined by end-group analysis by ^1H NMR spectroscopy.

The use of a more activated thiol in the thiol-ene addition to P(PDL-co-DHC) could result in a higher rate of conversion over the same period of time. To this end, the addition of dodecanethiol to the polymer chain was attempted, using DMPA as a photoinitiator, a thiol : olefin ratio of 11 : 1 and a total concentration of 2.5 M in DCM. The reaction mixture was degassed, placed under an argon environment and exposed to UV light for 4 h. After the removal of excess thiol, the resultant polymer (P(PDL-co-DHCDT)) was analysed by ^1H NMR spectroscopy, which revealed > 99% conversion of all alkene functionalities and coincided with the appearance of the terminal methyl resonance of dodecanethiol at $\delta = 0.85$ ppm that showed thiol-ene addition on each reacted alkene.

4.3 Conclusion

The production of one-pot block-like PDL copolymers has been shown to occur through the use of an ϵ -substituted ϵ -lactone (ϵSL) and a magnesium catalyst ($\text{Mg}(\text{BHT})_2(\text{BHT})_2$). The copolymers formed exhibit a largely block-like sequencing, with a short gradation between blocks. Analysis by quantitative ^{13}C NMR spectroscopy has demonstrated this effect occurs at any molar ratio of comonomers. Transesterification side reactions resulting in block mixing and sequence randomisation have also been shown to be negligible. This technique has also been expanded to demonstrate the production of triblock copolymers through the use of a bifunctional initiator. Furthermore, when using an alkene functionalised ϵSL , the alkene functionality has been shown to be preserved and able to undergo post-polymerisation modification through thiol-ene addition.

4.4 References

1. M. L. Focarete, M. Scandola, A. Kumar and R. A. Gross, *J. Polym. Sci., Part B: Polym. Phys.*, 2001, **39**, 1721-1729.
2. J. Cai, C. Liu, M. Cai, J. Zhu, F. Zuo, B. S. Hsiao and R. A. Gross, *Polymer*, 2010, **51**, 1088-1099.
3. H. Uyama, H. Kikuchi, K. Takeya and S. Kobayashi, *Acta Polym.*, 1996, **47**, 357-360.

4. Y. Nakayama, N. Watanabe, K. Kusaba, K. Sasaki, Z. Cai, T. Shiono and C. Tsutsumi, *J. Appl. Polym. Sci.*, 2011, **121**, 2098-2103.
5. C. Vaida, H. Keul and M. Moeller, *Green Chem.*, 2011, **13**, 889-899.
6. M. Claudino, I. van der Meulen, S. Trey, M. Jonsson, A. Heise and M. Johansson, *J. Polym. Sci., Part A: Polym. Chem.*, 2012, **50**, 16-24.
7. M. Bouyahyi and R. Duchateau, *Macromolecules*, 2014, **47**, 517-524.
8. L. Jasinska-Walc, M. Bouyahyi, A. Rozanski, R. Graf, M. R. Hansen and R. Duchateau, *Macromolecules*, 2015, **48**, 502-510.
9. L. Jasinska-Walc, M. R. Hansen, D. V. Dudenko, A. Rozanski, M. Bouyahyi, M. Wagner, R. Graf and R. Duchateau, *Polym. Chem.*, 2014.
10. D. Zhang, M. A. Hillmyer and W. B. Tolman, *Biomacromolecules*, 2005, **6**, 2091-2095.
11. K. A. Günay, P. Theato and H.-A. Klok, *J. Polym. Sci., Part A: Polym. Chem.*, 2013, **51**, 1-28.
12. S. C. Knight, C. P. Schaller, W. B. Tolman and M. A. Hillmyer, *RSC Adv.*, 2013, **3**, 20399-20404.

5 Towards sequence control of lactone ROP:

Copolymers from ϵ -substituted ϵ -lactones

5.1 Introduction

The use of lactones in ring-opening polymerisation (ROP) has been well documented and implemented in a range of applications, including biomedical materials,¹⁻⁶ polymer brushes,^{7, 8} crosslinked networks,⁹⁻¹¹ telechelic polymers^{12, 13} and self-assembling copolymers^{14, 15}. However, a major drawback in the production of useful one-pot copolymer materials from lactones has been transesterification side reactions, including inter- and intra-molecular transesterification, which has been shown to produce random copolymers and broad dispersities.¹⁶⁻²⁴ This has made defined polymer architectures such as multi-block copolymers or sequence-controlled block copolymers difficult to achieve. Whilst one-pot lactone copolymerisations have been shown to polymerise each monomer at a time in multiple literature sources (as a consequence of extremely different reactivity ratios), concurrent transesterification side reactions alongside the ROP of the second monomer invariably lead to the formation of randomly sequenced copolymers (Chapter 3).²²⁻²⁶

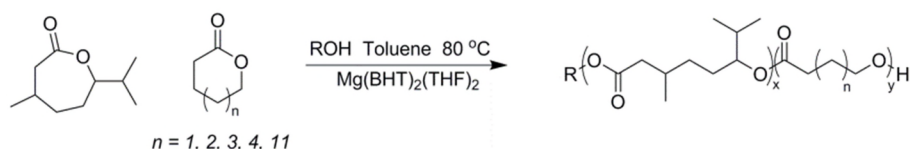
Naturally, the amount of transesterification side reactions can be curbed through careful choice of monomer. For example, small ring lactones polymerise rapidly and can be terminated before transesterification side reactions can occur. However, in order to produce a block copolymer through differences in reactivity ratios, the comonomer must have a much slower rate of polymerisation and during which competitive transesterification side reactions frequently occur to randomise the polymer chain sequence. An intrinsic part of the polymerisation of large ring (macro)lactones, such as ambrettolide (Amb), is the formation of low molecular weight cyclic species through ring-expansion transesterification before linear polymer species can form.²⁷ Transesterification side reactions are also noticeable throughout the remaining polymerisation, making defined block copolymers extremely difficult to produce.

Examples have been shown in the past involving the one-pot copolymerisation of a lactone with another monomer, such as a vinyl alcohol or a carbon dioxide/epoxy mixture, which rely on different polymerisation techniques to produce block copolymers.²⁸⁻³⁰ Block copolymers of lactones have also been produced through sequential polymerisation of each monomer, most frequently implemented in copolymerisations of lactide and ϵ -caprolactone (ϵ CL).^{3-5, 19, 20, 25, 31, 32} However, the only one-pot macrolactone copolymerisation in literature to produce block copolymers is between ϵ -decalactone (ϵ DL) and ω -pentadecalactone (PDL).^{21, 22}

As demonstrated in the previous chapter, block-like copolymers are achievable with the use of ϵ -lactones that are functionalised on the ϵ -carbon as a consequence of hindered transesterification on the ester linkage that is formed. This chapter aims to demonstrate that the formation of block copolymers is not unique to ϵ -substituted ϵ -lactones (ϵ SLs) copolymerised with PDL, but to any copolymer involving one or more ϵ SL and/or non-substituted lactone of ring size 8 or above.

5.2 Results and Discussion

5.2.1 MI copolymerisation with other lactones



Scheme 5.1 Copolymerisation of menthide with non-substituted lactones catalysed by $\text{Mg}(\text{BHT})_2(\text{THF})_2$.

The copolymerisation of menthide (MI) with PDL has been shown to produce copolymers with a block-like sequencing as a consequence of the rapid polymerisation of MI followed by the incorporation of PDL, with no transesterification side reactions occurring in the MI block (Chapter 4). In order to determine whether all MI copolymers are block-like, the copolymerisation of MI was tested with other non-substituted lactones; δ VL, ϵ CL, ζ -heptalactone (ζ HL) and η -caprylolactone (η CL) (Scheme 5.1). For each non-

substituted lactone, an equimolar mixture of MI and non-substituted lactone was polymerised by $\text{Mg}(\text{BHT})_2(\text{THF})_2$ catalyst from a benzyl alcohol initiator, at a total monomer concentration of 2 M in toluene at 80 °C with a targeted total DP of 100. In each copolymerisation, the final polymer was analysed by ^1H , quantitative ^{13}C and DOSY NMR spectroscopy and SEC in order to determine the sequencing and molecular weight distributions of the resultant polymers (Table 5.1). All polymerisations proceeded to high conversions ($\geq 75\%$), however \bar{D}_M for each copolymer was high, indicating transesterification side reactions of the non-substituted lactones occurred in each case, as observed with the copolymerisation of MI and PDL (Chapter 4). DOSY NMR spectroscopy confirmed that in each copolymerisation, only one polymer species had been formed, *i.e.* only copolymers were produced in the copolymerisation and no homopolymer species were found (Figure 5.1).

Table 5.1 Copolymerisations of menthide with a linear lactone at 1 : 1 mol% targeting an overall DP of 100

Lactone (L)	Ring size	Conversion ^a (%)			M_p^b (GPC) (kDa)	M_n^b (GPC) (kDa)	M_w^b (GPC) (kDa)	\bar{D}_M^b	M_n^c (NMR) (kDa)
		MI	L	Total					
δVL	6	60	90	75	5.8	23.9	5.5	2.29	9.7
ϵCL	7	60	97	79	37.7	28.0	40.9	1.46	10.7
ζHL	8	74	87	81	11.6	3.8	11.9	3.13	11.9
ηCL	9	57	94	76	19.2	18.4	28.1	1.52	10.9
PDL	16	85	94	90	39.7	19.1	40.9	2.14	20.3

^aDetermined by SEC in CHCl_3 against poly(styrene) standards. ^bDetermined by quantitative ^{13}C NMR spectroscopy, with * defining the carbonyl analysed.

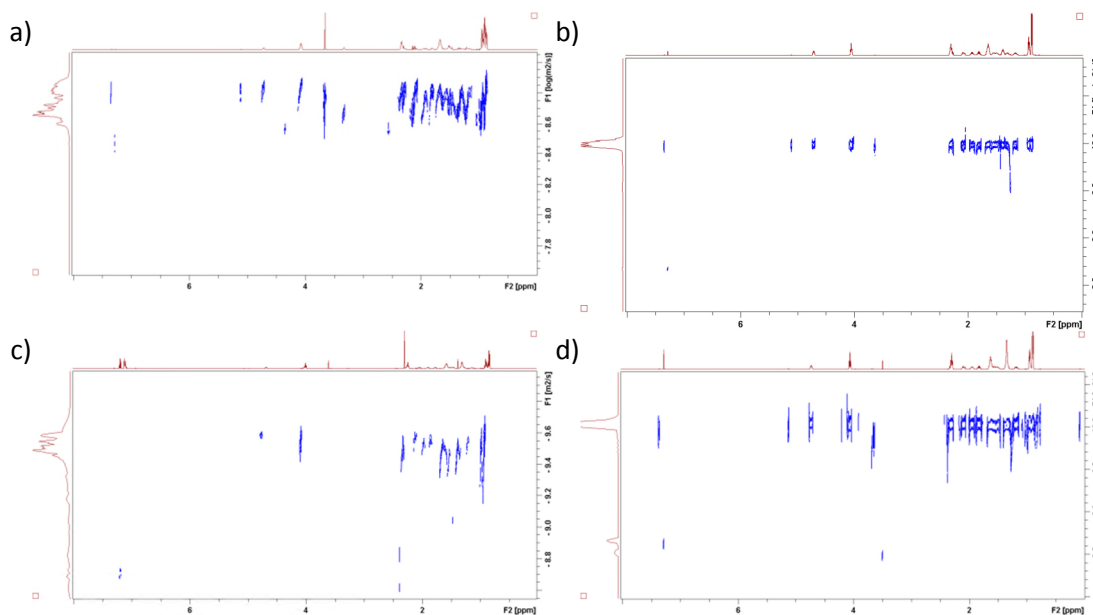


Figure 5.1 DOSY NMR spectra of a) P(MI-co- δ VL), b) P(MI-co- ϵ CL), c) P(MI-co- ζ HL) and d) P(MI-co- η CL) (500 MHz, 298 K, CDCl_3).

The resultant polymer from the copolymerisation of MI with the six-membered ring lactone, δ VL, was analysed by quantitative ^{13}C NMR spectroscopy. Each carbonyl diad resonance observed (MI*-MI, MI*- δ VL, δ VL*-MI, δ VL*- δ VL) had equivalent integrals and therefore equal quantities of each type of carbonyl with the copolymer, which is characteristic of a random copolymer (Table 5.2). In a previous study, it was determined that when using $\text{Mg}(\text{BHT})_2(\text{THF})_2$ as a catalyst, the homopolymerisation of δ VL to DP50 is extremely rapid (under 5 min) (Chapter 3).¹⁶ Hence, the copolymerisation of MI and δ VL, may occur in a similar method to the copolymerisation of PDL and δ VL. That is, the copolymerisation of MI with δ VL could progress through the initial rapid polymerisation of δ VL and, as a MI unit is incorporated onto the chain end, rapid transesterification side reactions move the MI repeat unit into the middle of the chain before another MI unit is added to the chain end. As the transesterification side reactions are randomly placed, the final copolymer would be completely random in sequence once all MI has been incorporated. This is the opposite to the copolymerisation of MI and PDL, where the unsaturated lactone polymerises after the substituted lactone, and is a consequence of the higher affinity of δ VL to the catalyst as well as the lower energy requirement for ROP to

occur compared to MI and PDL. As PMI is thought to exhibit little to no transesterification, the ester linkage in PMI could be 'locked' against transesterification side reactions. This is probably a consequence of the pendant isopropyl group adjacent to the acyl oxygen sterically blocking any attack on the ester carbonyl. MI polymerises primarily as a consequence of the ring-strain present in a 7-membered ring contributing a high enthalpy once broken; with no ring-strain in the polymer chain, an ester with a pendant side chain adjacent to the acyl oxygen effectively 'locks' the ester and prevents transesterification. Therefore, in the copolymerisation of δ VL and MI, the prevention of transesterification side reactions by the isopropyl group in esters MI*-MI and δ VL*-MI (where * denotes the observed carbonyl), means transesterification only occurs on the esters, δ VL*- δ VL and MI*- δ VL (Figure 5.2).

Table 5.2 Relative integrals of carbonyl diad resonances for copolymers of menthide and a linear lactone at 1 : 1 mol% targeting an overall DP of 100

Lactone (L)	Ring size	Diads ^b				Sequence
		L*-L	L*-MI	MI*-L	MI*-MI	
δ VL	6	0.22	0.28	0.26	0.25	Random
ϵ CL	7	0.24	0.24	0.25	0.27	Random
ζ HL	8	0.45	0.05	0.09	0.42	Block-like
η CL	9	0.40	0.08	0.09	0.43	Block-like
PDL	16	0.52	0.04	0.04	0.40	Block-like

^aDetermined by SEC in CHCl_3 against poly(styrene) standards. ^bDetermined by quantitative ^{13}C NMR spectroscopy, with * defining the carbonyl analysed.

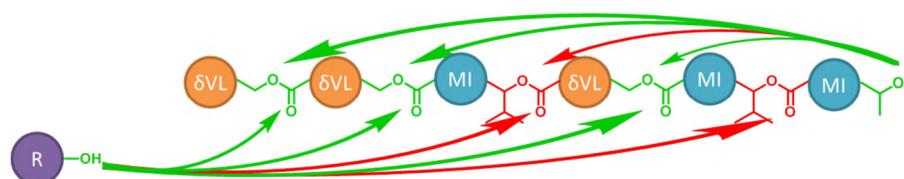


Figure 5.2 Possible transesterification side reactions in the copolymerisation of δ -valerolactone and menthide.

Copolymerisation of MI and ϵ CL (a 7-membered ring lactone) was also determined to produce randomly sequenced materials when analysed by quantitative ^{13}C NMR spectroscopy (Figure 5.3b). This is to be expected as a consequence of the homopolymerisation of ϵ CL being significantly faster than the homopolymerisation of MI under identical conditions, with the polymerisation of ϵ CL reaching completion before the

end of the inhibition period observed during the polymerisation of MI. Poly(ϵ -caprolactone) (PCL) is known to transesterify once polymerisation is complete, hence as MI is added to the chain-end, transesterification side reactions occur before the addition of another MI unit (*i.e.* the rate of transesterification of PCL is greater than the rate of ROP of MI), which causes a random copolymer to form as discussed above.

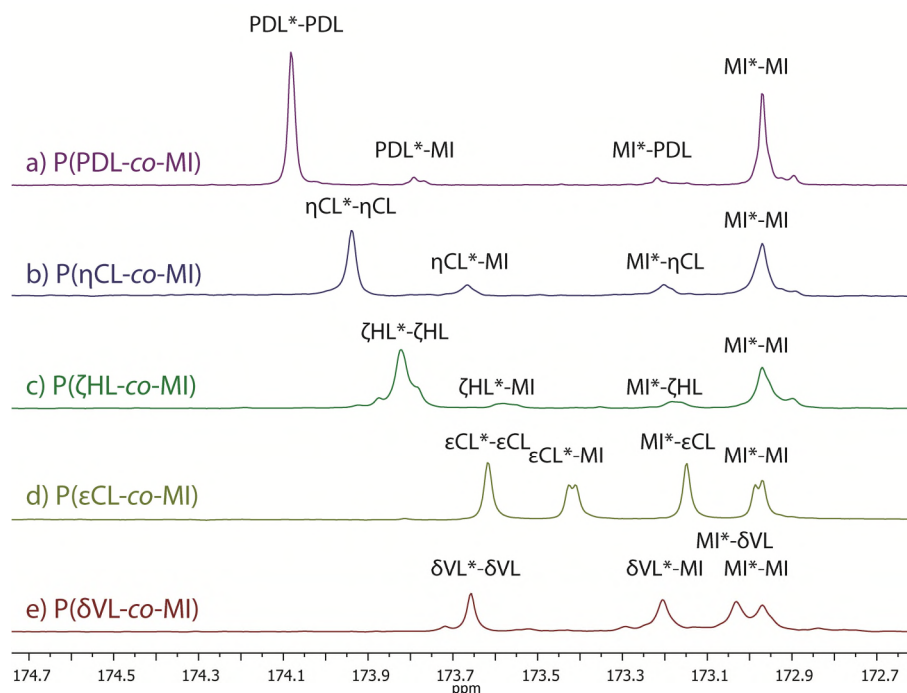


Figure 5.3 Quantitative ^{13}C NMR spectra of the carbonyl region for copolymers of menthede with a) ω -pentadecalactone; b) η -caprylactone; c) ζ -heptalactone; c) ϵ -caprolactone and d) δ -valerolactone at 1 : 1 mol% monomers with an total DP of 100 (125 MHz, CDCl_3 , 298 K).

The copolymerisation of MI with ζ HL (an 8-membered ring lactone) was analysed by quantitative ^{13}C NMR spectroscopy. The carbonyl diad resonances were found to have unequal integrals, with larger resonances observed for ζ HL*- ζ HL and MI*-MI carbonyl diad resonances than ζ HL*-MI and MI*- ζ HL carbonyl diad resonances. The sequencing of the polymer chain is therefore block-like and not random as observed with a linear lactone only one methylene smaller (ϵ CL). Copolymerisation of MI with η CL (a 9-membered ring lactone), similarly produced copolymers that exhibited the same block-like behaviour as P(ζ HL-co-MI). Thus, copolymerisations of MI with lactones containing larger ring size than 7

(ϵ CL) have been found to only form block-like copolymers, which is potentially a consequence of the activity of the catalyst towards lactones of different sizes. δ VL and ϵ CL both show high activity with $\text{Mg}(\text{BHT})_2(\text{THF})_2$ and can polymerise without the requirement of heat (Chapter 2). However, as demonstrated in all previous chapters, lactones with a ring size ≥ 8 and ϵ SLs all require heat in order to polymerise. In a copolymerisation of MI with either δ VL or ϵ CL, $\text{Mg}(\text{BHT})_2(\text{THF})_2$ readily polymerises δ VL or ϵ CL before MI as a consequence of high activity and therefore forming random copolymers, but readily polymerises MI before ζ HL, η CL and PDL (8-, 9- and 16-membered rings respectively) and therefore forms block copolymers. Whilst all non-substituted lactones do transesterify at some point in the copolymerisation, as evidenced by a broad \mathcal{D}_M in each case, the effect on the polymer sequencing is dependent on whether MI has already been polymerised. This is a consequence of the inability of MI to transesterify because of steric hindrance on the ester linkage. If the MI block is already formed, a block of linear lactone is formed that can transesterify within itself; however if the block is not formed, transesterification side reactions in conjunction with MI incorporation forms randomly sequenced copolymers.

5.2.2 *Transesterification of ϵ -substituted ϵ -lactones*

The transesterification of menthide has been previously shown to be extremely low, with little increase in \mathcal{D}_M over extended homopolymerisation time (96 h) and no transesterification with poly(pentadecalactone) (PPDL) in the presence of $\text{Mg}(\text{BHT})_2(\text{THF})_2$ catalyst (Chapter 4). The low rate of transesterification is likely a consequence of the presence of a functional group on adjacent to the acyl oxygen, sterically blocking the catalyst from facilitating transesterification. In order to determine whether or not transesterification does occur, homopolymerisations of several ϵ -substituted ϵ -lactones were studied over an extended period of time. The homopolymerisations of ϵ -heptalactone (ϵ HL), ϵ -decalactone (ϵ DL) and MI were all carried out at 80 °C in a 1 M solution in toluene, using benzyl alcohol as initiator and $\text{Mg}(\text{BHT})_2(\text{THF})_2$ as a catalyst. After 1 week of

polymerisation, the resultant homopolymers were analysed by SEC in order to monitor dispersity. The transesterification of ϵ HL was found to have occurred through the appearance of a broad, multimodal molecular weight distribution with $\mathcal{D}_M = 3.8$ compared to $\mathcal{D}_M = 1.3$ after 24 h of homopolymerisation. The dispersities of both poly(ϵ -decalactone) (P ϵ DL) and poly(menthide) (PMI) remained relatively low and monomodal after 1 week of homopolymerisation ($\mathcal{D}_M = 1.4$ and 1.3 respectively), which indicates few transesterification side reactions had occurred (Table 5.3).

After 2 weeks of homopolymerisation, P ϵ DL and PMI samples were again analysed by SEC. The molecular weight distribution of P ϵ DL was found to have significantly broadened, with new distribution peaks emerging and an increased \mathcal{D}_M (4.6) that indicates transesterification side reactions had become more prevalent. A decrease in the M_n was also observed as a consequence of a low molecular weight shoulder formed by intramolecular transesterification side reactions producing oligomeric cyclic species. During the same time period, the dispersity of PMI was found to only slightly increase ($\mathcal{D}_M = 1.5$), which shows that transesterification side reactions are occurring, though not to the same extent as observed with P ϵ HL and P ϵ DL. This is an effect of the ϵ -substituent sterically hindering the transesterification of the polymer, as larger, bulky functionalities significantly hinder transesterification compared to smaller functionalities, which only partially slow the rate of transesterification.

Table 5.3 Homopolymerisations of ϵ -substituted ϵ -lactones targeting an overall DP of 50

Lactone (ϵ SL)	Time (weeks)	Conversion ^a (%)	M_p^b (GPC) (kDa)	M_n^b (GPC) (kDa)	M_w^b (GPC) (kDa)	\mathcal{D}_M^b
ϵ HL	1	93	16.0	4.0	15.0	3.8
ϵ HL	2	94	12.4	3.4	12.4	3.7
ϵ DL	1	97	14.0	11.2	15.4	1.4
ϵ DL	2	98	20.8	4.1	19.0	4.6
MI	1	90	13.5	10.8	14.5	1.3
MI	2	92	15.2	11.9	17.5	1.5

^aDetermined by SEC in CHCl_3 against poly(styrene) standards. ^bDetermined by quantitative ^{13}C NMR spectroscopy, with * defining the carbonyl analysed.

In order to determine whether transesterification of adjacent MI units (MI*-MI) were involved in the randomisation of the polymer chain in the copolymerisation of MI and a small non-substituted lactone (*i.e.* δ VL or ϵ CL), the transesterification of PCL and PMI was tested. Different molecular weight DP 5 PCL and DP 50 PMI ($M_n = 650 \text{ g.mol}^{-1}$ and 8400 g.mol^{-1} respectively) were mixed in a 1 M solution in toluene, with $\text{Mg}(\text{BHT})_2(\text{THF})_2$ as a transesterification catalyst at 80°C . After 72 h, the resultant polymer was precipitated into hexane and analysed by ^1H NMR spectroscopy and SEC. Whilst both PCL and PMI were confirmed to still be present by ^1H NMR spectroscopy, SEC analysis showed two distinct molecular weight peaks corresponding to the original molecular weight peaks of the homopolymers tested (Figure 5.4). Analysis of the final material by quantitative ^{13}C NMR spectroscopy showed less than 1% of carbonyl diad resonances attributable to adjacent ϵ CL and MI repeat units were present (Figure 5.5). Thus, transesterification occurs at an extremely reduced rate, with no randomisation between two different homopolymer chains compared to the much more rapid intermolecular transesterification of PPDL and PCL or PVL observed after 24 h (Chapter 3). As PCL is known to transesterify readily from previous literature, the lack of transesterification between PCL and PMI is therefore a consequence of the inability of PMI to readily undergo transesterification side reactions.

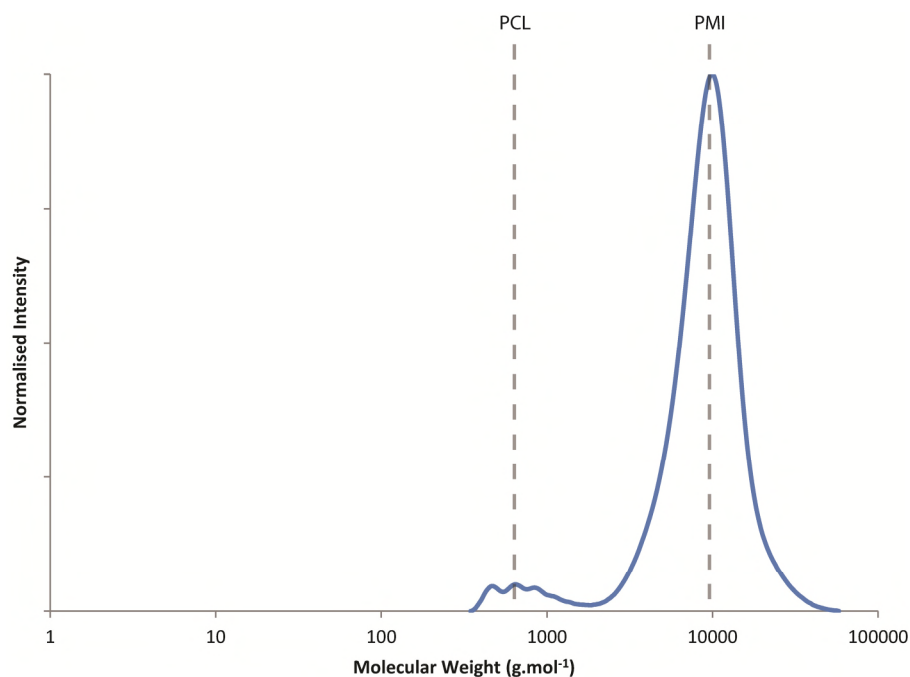


Figure 5.4 SEC chromatogram of the resultant polymer mixture of the transesterification of DP 5 PCL and DP 50 PMI at 1 M in toluene at 80 °C, using $\text{Mg}(\text{BHT})_2(\text{THF})_2$ as a catalyst. Molecular weight determined against poly(styrene) standards using CHCl_3 (0.5% NEt_3) as eluent.

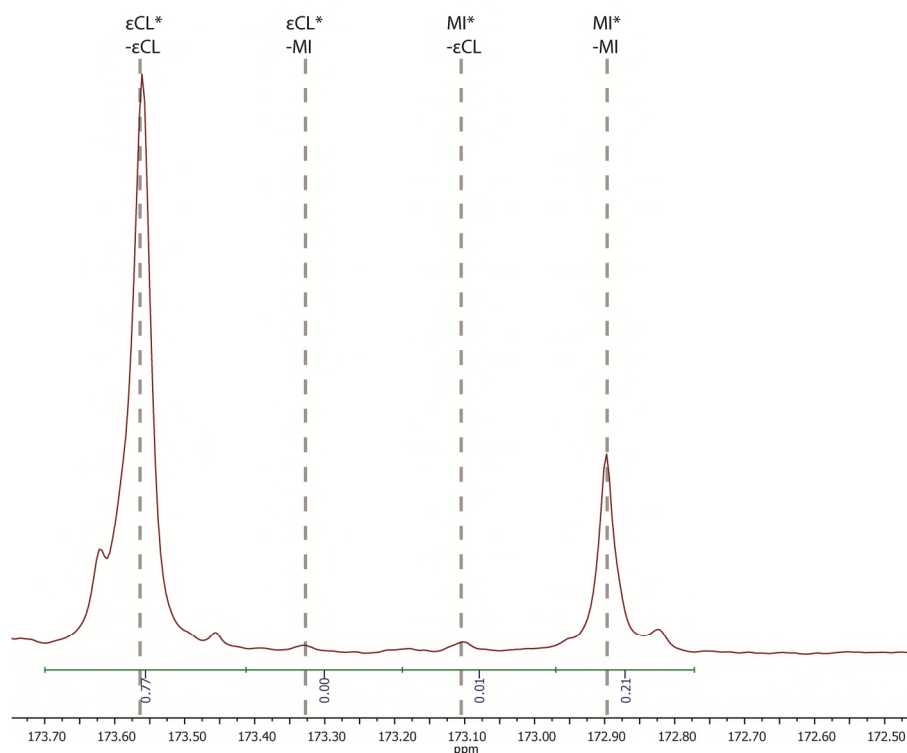


Figure 5.5 Quantitative ^{13}C NMR spectra of the carbonyl region for the resultant material from the transesterification of poly(ϵ -caprolactone) and poly(menthene) (125 MHz, CDCl_3 , 298 K).

As further demonstration of the lack of significant transesterification in poly(ϵ SL), different molecular weight DP 50 P ϵ HL and DP 50 PMI homopolymers (M_n = 4000 g.mol⁻¹ and 10800 g.mol⁻¹ respectively) were mixed in a 1 M solution in toluene, with Mg(BHT)₂(THF)₂ as a transesterification catalyst at 80 °C. After 24 h, the reaction was quenched with acidified (5% HCl) methanol and washed with cold hexane in order to remove the catalyst. The resultant polymer was analysed by quantitative ¹³C NMR spectroscopy and SEC. The molecular weight distribution observed by SEC analysis did not show significant broadening of dispersity or significant change in the distribution peak; however as a consequence of the final distribution, covering both initial distributions of the two homopolymers, transesterification side reactions cannot be ruled out (Figure 5.6). Analysis of the carbonyl diad resonances by quantitative ¹³C NMR spectroscopy for the final material showed that transesterification between the two homopolymers had been extremely low with the evolution of a small ϵ HL*-MI and no carbonyl diad resonance observed corresponding to MI*- ϵ HL (Figure 5.7). This may be a consequence of a small amount of chelation of the PMI chain end to the catalyst, which then undergoes intermolecular transesterification onto a neighbouring P ϵ HL chain. This further demonstrates the inability of poly(ϵ SL) ester linkage transesterification, further proving the more block-like sequencing of copolymers of ϵ SLs.

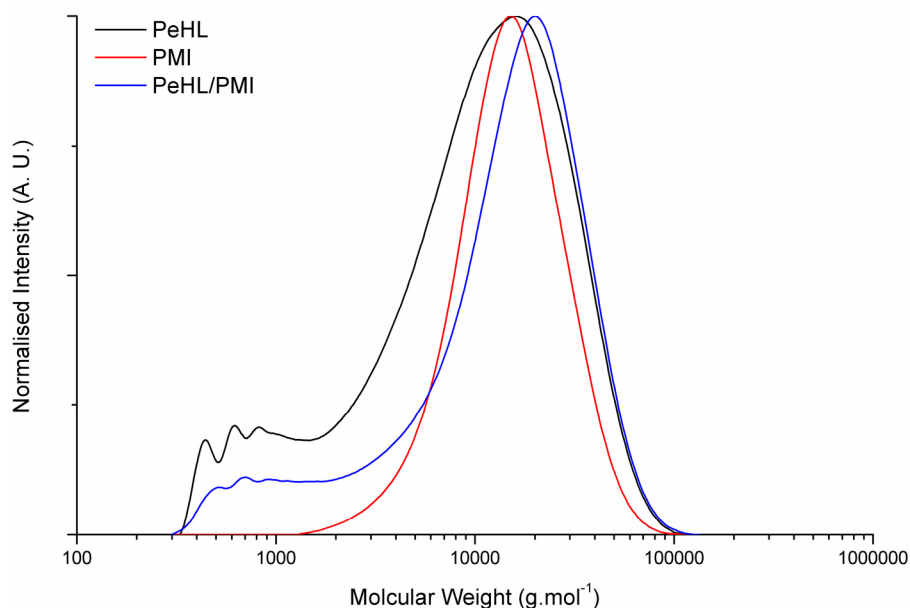


Figure 5.6 SEC chromatograms for the molecular weight distribution of P ϵ HL, PMI and the resultant material from the attempted transesterification of both polymers. Molecular weights determined by poly(styrene) standards and CHCl_3 (0.5% NEt_3) as eluent.

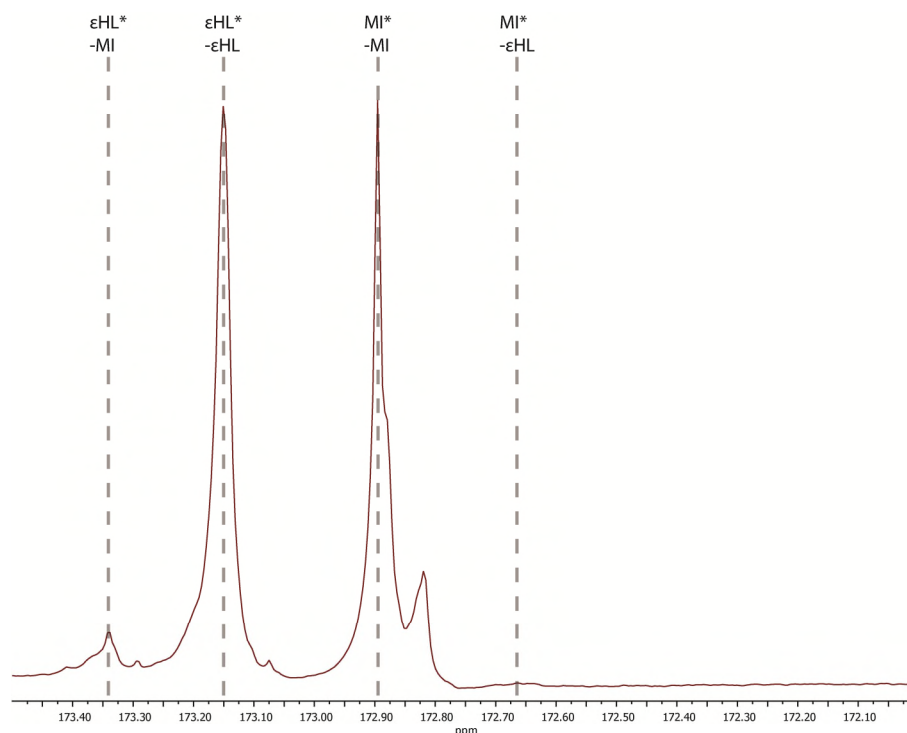


Figure 5.7 Quantitative ^{13}C NMR spectra of the carbonyl region for the resultant material from the transesterification of poly(ϵ -heptalactone) and poly(menthicle) (125 MHz, CDCl_3 , 298 K).

5.2.3 Terpolymerisation of ϵ -caprolactone, menthicle and ω -pentadecalactone

As a consequence of the unique behaviour of copolymerising ϵ SL monomers with large non-substituted lactones, the production of random copolymers is difficult to achieve

(Chapter 4). Both ϵ SL monomers and macrolactones are known to produce random copolymers with small non-substituted lactones, therefore a terpolymerisation of an ϵ SL monomer with a macrolactone and smaller lactone could produce polymers with random sequencing. From the above results and the previous chapter, it can be assumed that the rate of consumption of each monomer will be ϵ CL \gg MI $>$ PDL and as shown, transesterification of ϵ CL will occur whilst MI is consumed to form a random copolymer. Once the MI is transesterified from the chain end into the middle of the chain, the ester linkage is effectively 'locked-in' and transesterification is unlikely to occur on this site. Hence, when PDL is added to the chain end, transesterification of 'unlocked' esters (ϵ CL*- ϵ CL and MI*- ϵ CL) are still occurring, randomising the polymer sequence. However, as a consequence of MI*-MI and ϵ CL*-MI carbonyls being 'locked', PDL cannot transesterify from the chain end into these positions and thus a carbonyl corresponding to PDL*-MI cannot be formed.

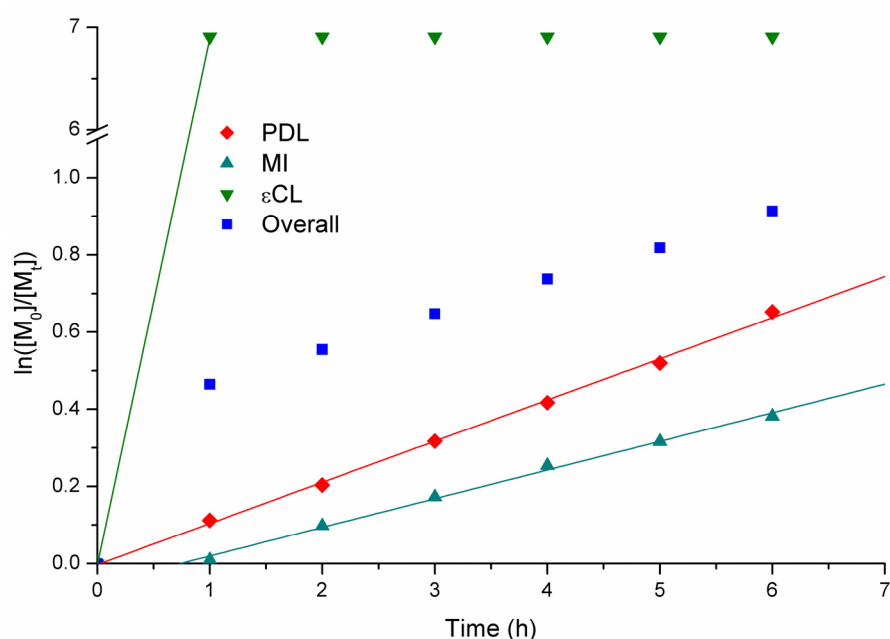


Figure 5.8 Kinetic plot for the terpolymerisation of ϵ -caprolactone, menthide and pentadecalactone, conducted at 80 °C in toluene with $[\epsilon\text{CL}]_0 : [\text{PDL}]_0 : [\text{MI}]_0 : [\text{BnOH}]_0 : [\text{cat.}]_0 = 50 : 50 : 50 : 1 : 1$, total monomer concentration = 1 M.

Table 5.4 Terpolymerisations of ϵ CL, PDL and MI

ϵ CL : PDL : MI	Diads ^a			ϵ CL*-PDL	ϵ CL*- ϵ CL	ϵ CL*-MI	MI*-PDL	PDL*- ϵ CL	MI*-MI
	PDL*-PDL	PDL*- ϵ CL	PDL*-MI						
50 : 50 : 50	0.21 (0.17)	0.18 (0.14)	0.02 (0.10)	0.10 (0.14)	0.10 (0.12)	0.15 (0.08)	0.08 (0.10)	0.07 (0.08)	0.09 (0.06)
10 : 50 : 50	0.38 (0.25)	0.03 (0.05)	0.06 (0.20)	0.09 (0.05)	0.01 (0.01)	0.02 (0.04)	0.03 (0.20)	0.06 (0.04)	0.31 (0.16)

^aDetermined by quantitative ^{13}C NMR spectroscopy, with * defining the carbonyl analysed and theoretical value for random sequencing in parentheses.

In order to confirm this theory, the terpolymerisation of equimolar quantities of ϵ CL, MI and PDL at 1 M in toluene was conducted at 80 °C, using benzyl alcohol as an initiator and $\text{Mg}(\text{BHT})_2(\text{THF})_2$ as catalyst. The polymerisation was followed by ^1H NMR spectroscopy, which showed complete consumption of ϵ CL within 1 h of polymerisation, with PDL consumed more rapidly than MI over the next 5 h (Figure 5.8). The quicker consumption of PDL compared to MI is possibly a consequence of the preference of MI for propagation from a menthide chain end as observed from slow initiation from benzyl alcohol or an active PPDL chain end. Analysis of the final copolymer by quantitative ^{13}C NMR spectroscopy showed that the final copolymer contained all 9 possible carbonyl diad resonances (PDL*-PDL, PDL*- ϵ CL, PDL*-MI, ϵ CL*-PDL, ϵ CL*- ϵ CL, ϵ CL*-MI, MI*-PDL, MI*- ϵ CL and MI*-MI) (Figure 5.9). The relative integrals for each of the ϵ CL carbonyl diad resonances were all equivalent, suggesting random sequencing of ϵ CL throughout the polymer chain and the same was observed for the relative integrals of MI carbonyl diad resonances (Table 5.4). However, in the case of PDL carbonyl diad resonances only PDL*-PDL and PDL*- ϵ CL diad resonances exhibited similar integrals and the integral corresponding to the PDL*-MI carbonyl diad resonance accounted for less than 1% of all observed carbonyl diad resonances. PDL and MI polymerisation is shown to occur at the same time (but differing rates of conversion) through ^1H NMR spectroscopy, though very few PDL*-MI carbonyl diad resonances are formed as a consequence of the transesterification of ϵ CL incorporating the chain end into the middle of the chain more rapidly than the consumption of both MI and PDL. The appearance of a small PDL*-MI is

therefore a consequence of a PDL monomer being added to the chain end immediately after a MI monomer is added and before transesterification side reactions have occurred. As carbonyl diad resonances corresponding to PDL*-MI are still present, if somewhat minimal, the 'locking' effect of the isopropyl group in MI is not permanent and will transesterify at a significantly slower rate than other esters. It would be expected that the sequential addition of ϵ CL into a copolymerisation of PDL and MI would result in a completely random copolymer if transesterification side reactions did occur at a similar rate for all comonomers (*i.e.* with no steric hindrance affecting transesterification). The sequential addition would need to be during the incorporation of PDL, after full MI conversion, in order to prove the inability of the MI*-MI to readily polymerise.

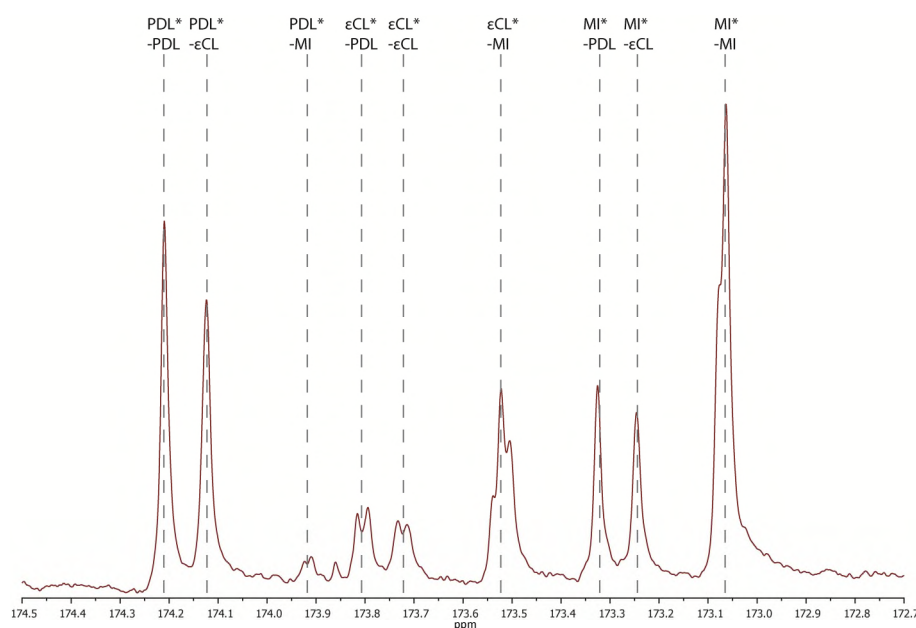


Figure 5.9 Quantitative ^{13}C NMR spectra of the carbonyl region for the one-pot terpolymerisation of equimolar quantities of ϵ -caprolactone, menthide and pentadecalactone with an initial concentration of $[\epsilon\text{CL}]_0 : [\text{MI}]_0 : [\text{PDL}]_0 : [\text{BnOH}]_0 : [\text{cat.}]_0 = 50 : 50 : 50 : 1 : 1$, total initial monomer concentration = 1 M (125 MHz, CDCl_3 , 298 K).

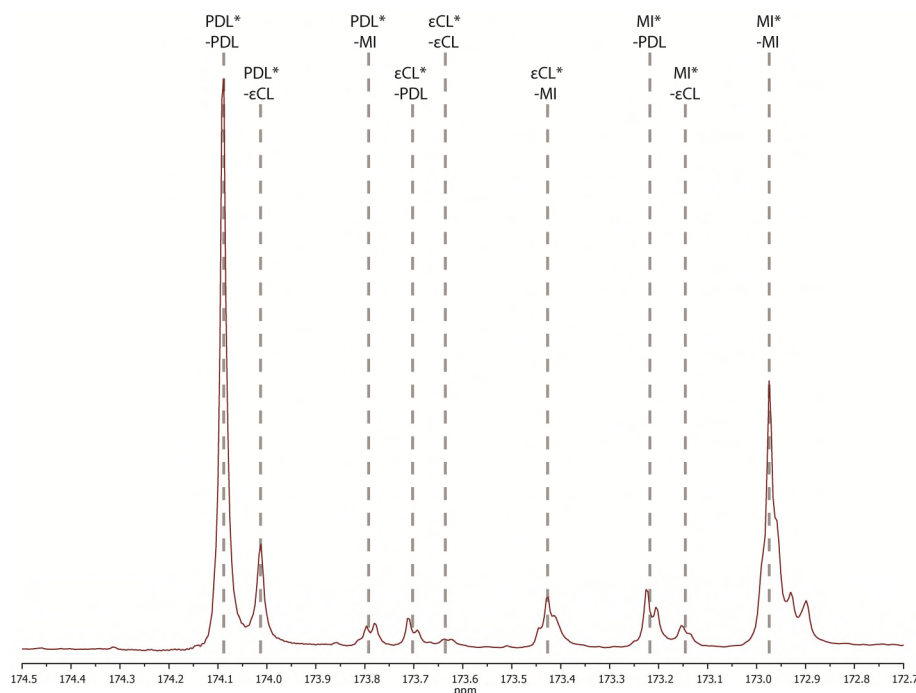
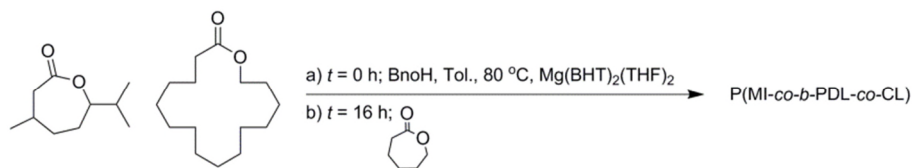


Figure 5.10 Quantitative ^{13}C NMR spectra of the carbonyl region for the one-pot terpolymerisation of equimolar quantities of ϵ -caprolactone, menthide and pentadecalactone with an initial concentration of $[\epsilon\text{CL}]_0 : [\text{MI}]_0 : [\text{PDL}]_0 : [\text{BnOH}]_0 : [\text{cat.}]_0 = 10 : 50 : 50 : 1 : 1$, total initial monomer concentration = 1 M (125 MHz, CDCl_3 , 298 K).

As the terpolymerisation of ϵCL , MI and PDL is shown to occur with more rapid PDL incorporation than MI incorporation, reducing the molar ratio of ϵCL with respect to PDL and MI should allow for more transesterification during MI incorporation, producing a more prevalent PDL*-MI carbonyl diad resonance and therefore closer to random polymer sequencing. The terpolymerisation of ϵCL , MI and PDL was carried out at a molar ratio of 10 : 50 : 50 $\epsilon\text{CL} : \text{MI} : \text{PDL}$ at 1 M in toluene at 80 °C, using benzyl alcohol as initiator and $\text{Mg}(\text{BHT})_2(\text{THF})_2$ as a catalyst. Analysis of the resultant material by quantitative ^{13}C NMR spectroscopy revealed the presence of all nine expected carbonyl diad resonances, however two carbonyl diad resonances (PDL*-PDL and MI*-MI) appear prominently and with larger relative integrals than would be expected with a randomly sequenced terpolymer (Figure 5.10). The sequencing of the terpolymer is therefore much more block-like in sequencing as a consequence of the low quantity of ϵCL not transesterifying at a more rapid rate than the incorporation of MI. The secondary alcohol chain end of ring-

opened MI is then unfavourable for PDL incorporation and greatly favoured by MI monomer, thus forming block-like sequences.



Scheme 5.2 Copolymerisation of menthide and pentadecalactone with timed injection of ϵ -caprolactone.

The introduction of caprolactone into a P(MI-co-PDL) prepolymer could randomise the chain through transesterification side reactions during ϵ CL incorporation, similar to the sequential polymerisation of PDL followed by ϵ CL (Chapter 3). This could then be used to produce a MI block-like copolymer with a tunable, degradable segment. The copolymerisation of equimolar quantities of PDL and MI at 1 M in toluene was conducted at 80 °C, using benzyl alcohol as an initiator and $\text{Mg}(\text{BHT})_2(\text{THF})_2$ as catalyst. After 8 h of polymerisation, a 1 M solution of ϵ CL in toluene was injected into the polymerisation at an equimolar quantity of initial PDL or MI monomer (Scheme 5.2). After 24 h of polymerisation, the resultant polymer was analysed by quantitative ^{13}C NMR spectroscopy and SEC analysis. As expected, the presence of carbonyl diad resonances corresponding to PDL*-PDL, PDL*-MI, MI*-PDL and MI*-MI was observed at relative intensities indicative of a block-like sequencing (Figure 5.11). Interestingly, the only carbonyl diad resonances observed relating to ϵ CL were PDL*- ϵ CL, ϵ CL*-PDL and ϵ CL*- ϵ CL, with no carbonyl diad resonances corresponding to ϵ CL*-MI or MI*- ϵ CL observed as would be expected if no 'locking' of the -MI ester had occurred and transesterification side reactions between all lactones had occurred. Furthermore, the significant difference in integration between the large PDL*-PDL and ϵ CL*- ϵ CL carbonyl diad resonances compared to the smaller PDL*- ϵ CL and ϵ CL*-PDL carbonyl diad resonances is indicative of a more block-like sequencing with a gradation between blocks (Table 5.5). This is unexpected given previous sequential

additions of ϵ CL to PDL polymerisations (Chapter 3), however this does provide a method for the one-pot production of a ϵ CL block-like terpolymer with two other lactones.

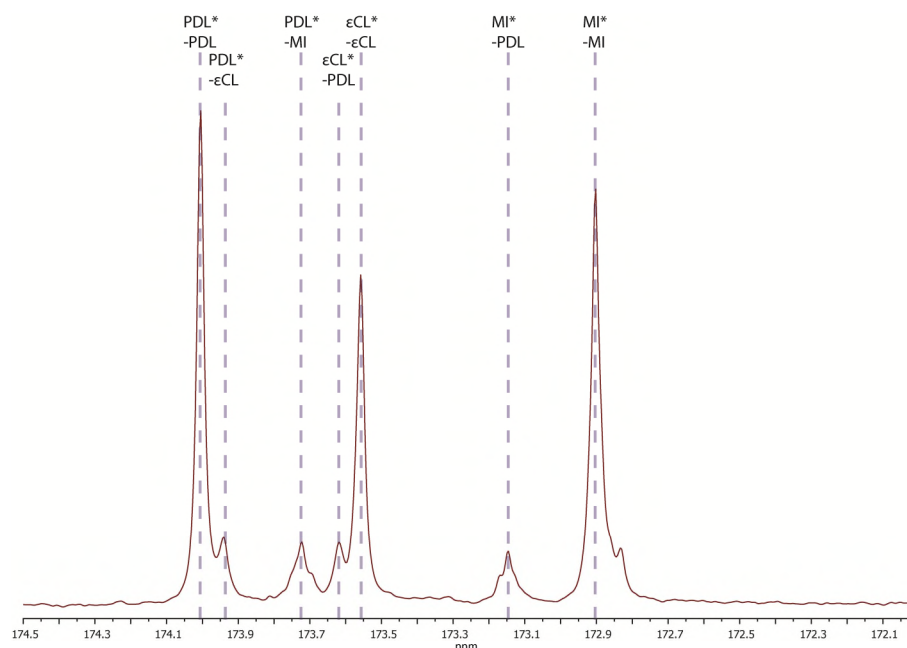
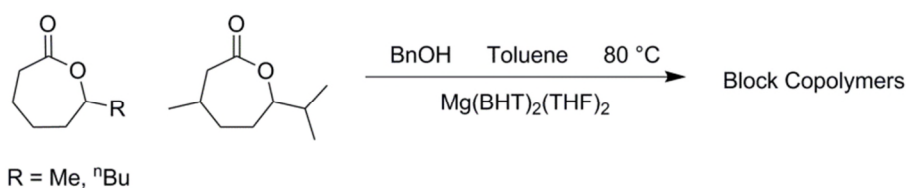


Figure 5.11 Quantitative ^{13}C NMR spectra of the carbonyl region for the copolymerisation of equimolar quantities of menthide and pentadecalactone with a timed injection of ϵ -caprolactone and an initial concentration of $[\epsilon\text{CL}]_0 : [\text{MI}]_0 : [\text{PDL}]_0 : [\text{BnOH}]_0 : [\text{cat.}]_0 = 50 : 50 : 50 : 1 : 1$. Injection of ϵ CL at $t = 16$ h and total initial monomer concentration = 1 M (125 MHz, CDCl_3 , 298 K).

Table 5.5 Terpolymer carbonyl diads formed from the sequential polymerisation of PDL and MI followed by ϵ CL.

$\epsilon\text{CL} : \text{PDL} : \text{MI}$	Diads ^a								
	PDL* -PDL	PDL* - ϵCL	PDL* -MI	ϵCL^* - PDL	ϵCL^* - ϵCL	ϵCL^* -MI	MI* -PDL	PDL* - ϵCL	MI* -MI
50 : 50 : 50	0.29 (0.16)	0.05 (0.10)	0.07 (0.14)	0.04 (0.10)	0.21 (0.06)	0.00 (0.09)	0.05 (0.14)	0.00 (0.10)	0.30 (0.12)

^aDetermined by quantitative ^{13}C NMR spectroscopy, with * defining the carbonyl analysed and theoretical value for random sequencing in parentheses.

5.2.4 ϵ SL block copolymers

Scheme 5.3 Copolymerisation of menthide with an ϵ -substituted ϵ -lactone.

During the copolymerisations of PDL with ϵ HL or ϵ DL (Chapter 4), it was observed that the reaction solution increased in viscosity within the first hour, indicating a high degree of conversion during this time. Hence, an inhibition period before the polymerisation is unlikely to occur with the less bulky methyl or butyl ϵ -substitution of ϵ HL and ϵ DL respectively. The polymerisation of MI, unlike the polymerisation of ϵ HL and ϵ DL, does require an induction period in order for the polymerisation to occur. Transesterification side reactions do not readily occur in ϵ SL polymers (P ϵ SLs) until after polymerisation as a consequence of steric hindrance to the ester caused by the presence of the ϵ -substituent; hence one-pot copolymerisation between MI and another ϵ SL could produce block or gradient copolymers depending on the difference in reactivity of the comonomers.

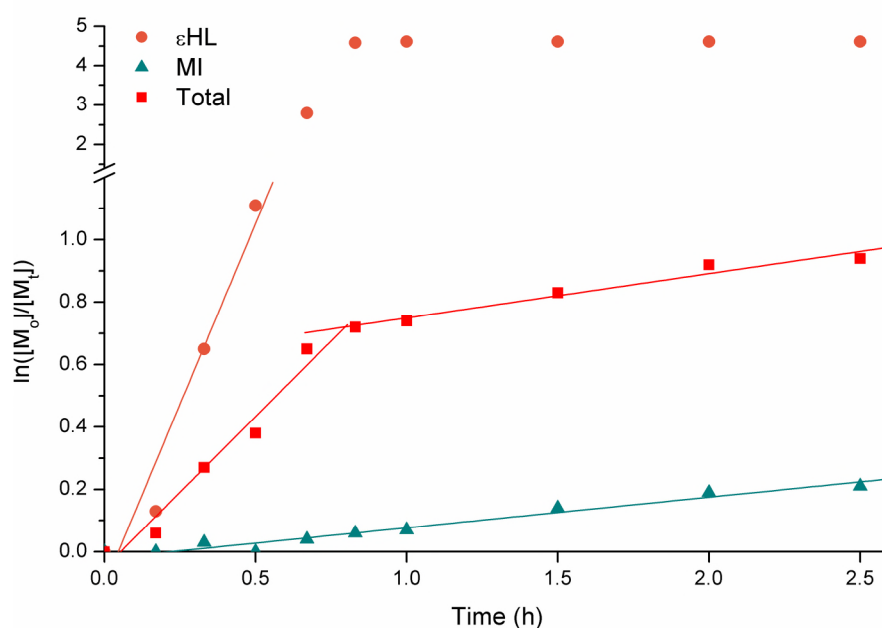


Figure 5.12 Kinetic plot for the copolymerisation of ϵ -heptalactone and menthide at 80 °C in toluene with $[\epsilon\text{HL}]_0 : [\text{MI}]_0 : [\text{BnOH}]_0 : [\text{cat.}]_0 = 50 : 50 : 1 : 1$, total initial monomer concentration = 1 M.

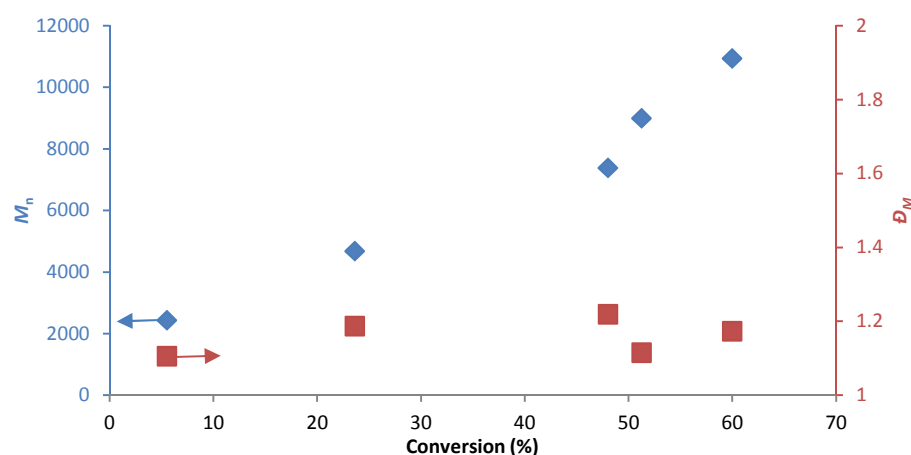


Figure 5.13 Evolution of M_n and D_M over total monomer consumption for the copolymerisation of ϵ -heptalactone and menthide at 80 °C in toluene with $[\epsilon\text{HL}]_0 : [\text{MI}]_0 : [\text{BnOH}]_0 : [\text{cat.}]_0 = 50 : 50 : 1 : 1$, total initial monomer concentration = 1 M. M_n and D_M determined by SEC against poly(styrene) standards.

The copolymerisation of an equimolar mixture of ϵ HL and MI at a concentration of 2 M in toluene at 80 °C, with benzyl alcohol as initiator, $\text{Mg}(\text{BHT})_2(\text{THF})_2$ as catalyst and a targeted DP of 100 was performed (Scheme 5.3). Aliquots were taken at different time intervals and analysed by ^1H NMR spectroscopy and SEC. As expected, the polymerisation started with the rapid consumption of ϵ HL as observed by ^1H NMR spectroscopy with a rapid reduction of the proton resonance attributable to the proton adjacent to the linking oxygen of the ester of the monomer ($\delta = 4.43$ ppm), which coincided with the appearance of a resonance at $\delta = 4.92$ ppm, attributable to the proton adjacent to the linking oxygen of the ester of poly(ϵ -heptalactone) (P ϵ HL). After a period of 40 min of polymerisation, MI monomer consumption was observed at a slower speed than previous polymerisations that continued throughout the remainder of the polymerisation (Figure 5.12). At 1 h, no ϵ HL monomer was present in the reaction, with only MI consumed throughout the remaining reaction. SEC analysis showed an initial slow growth in molecular weight up to 50% of overall monomer conversion, after which a more rapid increase in molecular weight gain over conversion was observed, corresponding to the initial conversion of a low molecular weight monomer (*i.e.* ϵ HL) and followed by conversion of a higher molecular weight monomer (MI) (Figure 5.13). Dispersities remained low throughout the copolymerisation,

indicating very few termination or transesterification side reactions occurred during the polymerisation (Figure 5.14).

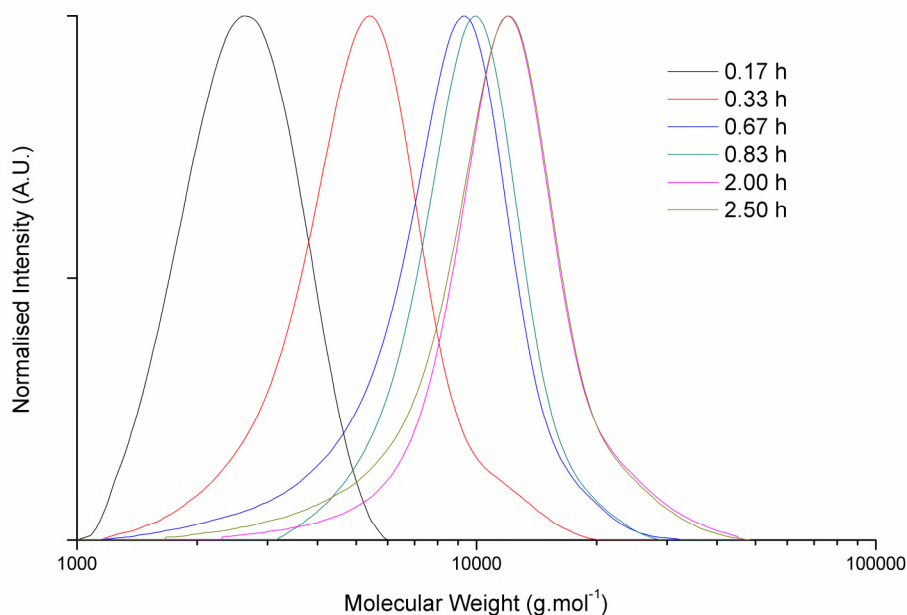


Figure 5.14 Molecular weight distribution of polymeric species in the copolymerisation of ϵ -heptalactone and menthide at 80 °C in toluene with $[\epsilon\text{HL}]_0 : [\text{MI}]_0 : [\text{BnOH}]_0 : [\text{cat.}]_0 = 50 : 50 : 1 : 1$, total initial monomer concentration = 1 M.

Analysis through quantitative ^{13}C NMR spectroscopy showed that the copolymer carbonyl diad resonances were majority $\epsilon\text{HL}^*-\epsilon\text{HL}$ and MI^*-MI , however the carbonyl diad resonances $\epsilon\text{HL}^*-\text{MI}$ and $\text{MI}^*-\epsilon\text{HL}$ were significantly higher in integration than previous copolymerisations, indicating a larger gradation between the two blocks of roughly 20 repeat units (Figure 5.15). This could be a consequence of the reactivity ratios of the comonomers; as ϵHL has low steric hindrance as a consequence of the methyl group being smaller, the monomer is preferable to the catalyst for polymerisation over MI. As the concentration of ϵHL becomes too low, MI becomes marginally preferential for polymerisation over ϵHL and both monomers polymerise dependent on vicinity to the catalyst. Once complete consumption of the ϵHL has occurred, the MI continues to add to the polymer chain and a gradient copolymer is formed. Using the same conditions the polymerisation was conducted at a lower temperature (40 °C) in order to polymerise only ϵHL to full conversion, then raising the temperature to 80 °C to polymerise MI onto the

active chain end, in order to access a more discrete block copolymer. This proved fruitless as a consequence of the complexation of menthide with the catalyst leading to incomplete conversion of ϵ HL.

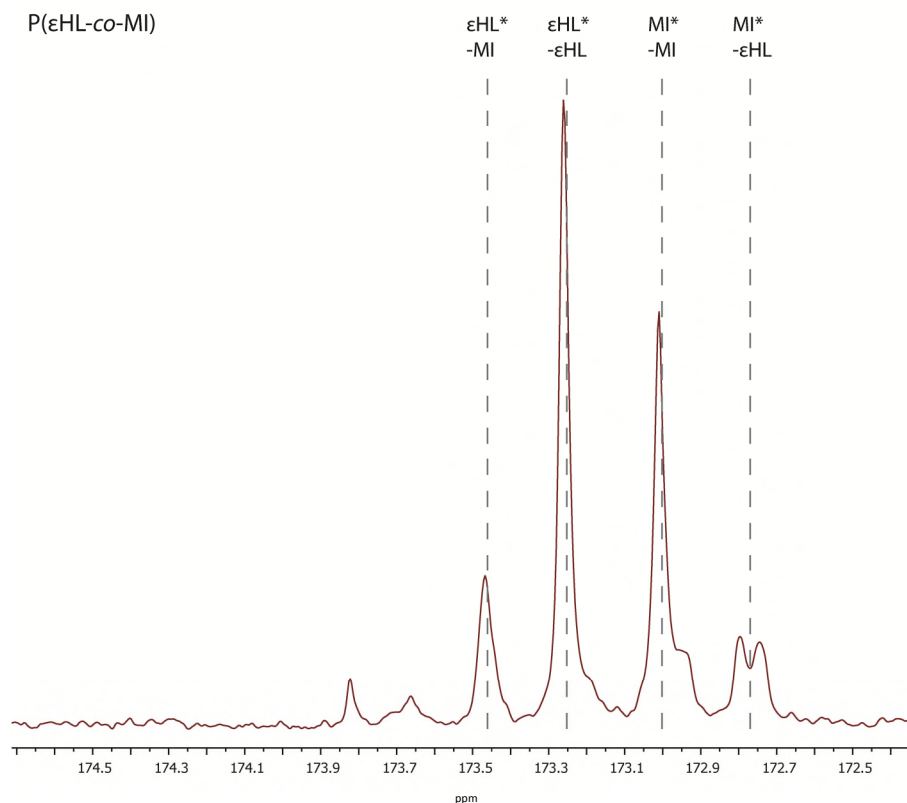


Figure 5.15 Quantitative ^{13}C NMR spectra of the carbonyl region for the one-pot copolymerisation of ϵ -heptalactone and menthide at 1 : 1 mol% with initial concentration of $[\epsilon\text{HL}]_0$: $[\text{MI}]_0$: $[\text{BnOH}]_0$: $[\text{cat.}]_0 = 50 : 50 : 1 : 1$, total initial monomer concentration = 1 M (125 MHz, CDCl_3 , 298 K).

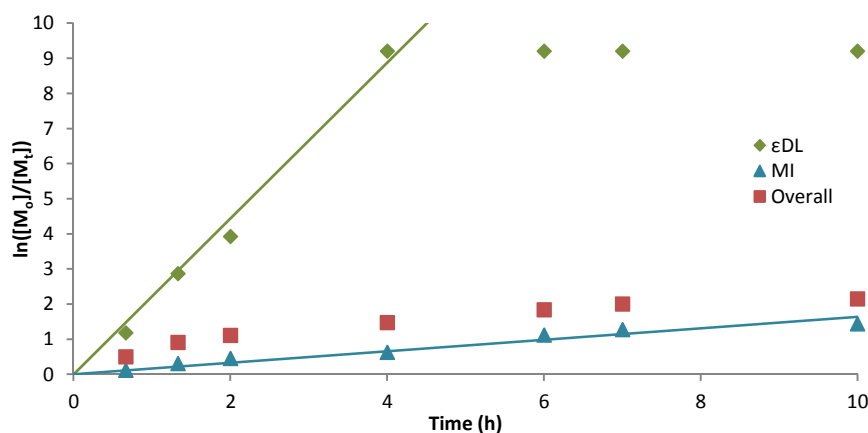


Figure 5.16 Kinetic plot for the copolymerisation of ϵ -decalactone and menthide at 80 °C in toluene with $[\epsilon\text{DL}]_0$: $[\text{MI}]_0$: $[\text{BnOH}]_0$: $[\text{cat.}]_0 = 50 : 50 : 1 : 1$, total initial monomer concentration = 1 M.

The copolymerisation of an equimolar mixture of ϵ DL and MI at a concentration of 1 M in toluene at 80 °C, with benzyl alcohol as initiator, $\text{Mg}(\text{BHT})_2(\text{THF})_2$ as catalyst and a targeted DP of 100 was also performed. Again, aliquots were taken at different time intervals and analysed by ^1H NMR spectroscopy and SEC. Similarly to the copolymerisation of ϵ HL and MI, the consumption of ϵ DL occurred rapidly before the consumption of MI (Figure 5.16). As the conversion of ϵ DL reached completion, MI began to be consumed and continued polymerising at a much slower rate than observed with ϵ DL. SEC analysis of samples taken during the polymerisation revealed a quick increase in molecular weight during the conversion of ϵ DL, followed by a much slower increase over time once only MI was being incorporated into the polymer chain. All molecular weight distributions were monomodal (Figure 5.17), with narrow dispersities ($\mathcal{D}_M = 1.22$ after 2.5 h), which shows no low molecular weight cyclic species formation or separate polymer species for each monomer (Table 5.6).

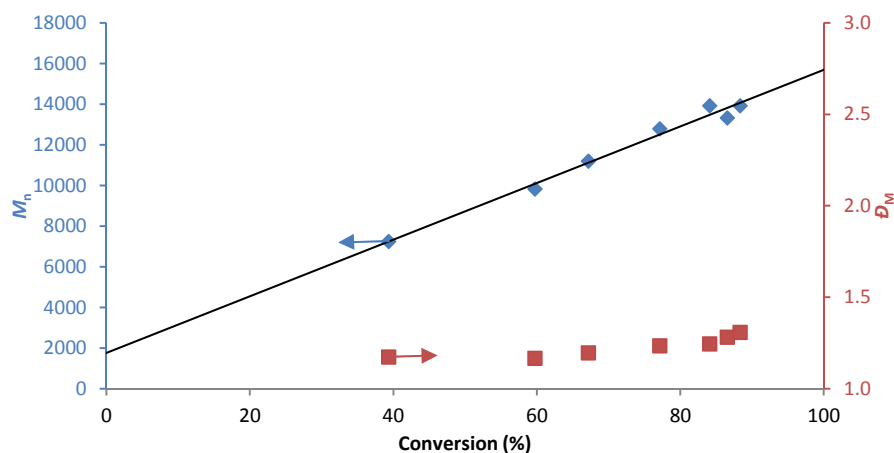


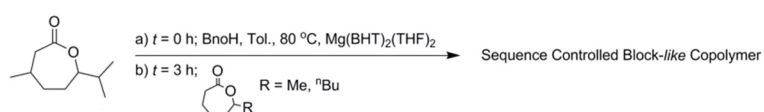
Figure 5.17 Evolution of M_n and \mathcal{D}_M over total monomer consumption for the copolymerisation of ϵ -heptalactone and menthide at 80 °C in toluene with $[\epsilon\text{HL}]_0 : [\text{MI}]_0 : [\text{BnOH}]_0 : [\text{cat.}]_0 = 50 : 50 : 1 : 1$, total initial monomer concentration = 1 M. M_n and \mathcal{D}_M determined by SEC against poly(styrene) standards.

Table 5.6 Copolymerisation of MI with an equimolar ratio of ϵ -substituted ϵ -lactone monomer, targeting a total DP of 100.

Monomer (ϵ L)	Conversion ^a (%)	M_n^b (GPC) (kDa)	M_w^b (GPC) (kDa)	D_M^b	M_n^c (NMR) (kDa)	Diads ^d			
						ϵ L* -MI	ϵ L* - ϵ L	MI* -MI	MI* - ϵ L
ϵ HL	95 (91, 99)	9.1	19.2	2.12	16.5	0.13	0.36	0.33	0.17
ϵ DL	93 (87, 99)	16.7	26.4	1.57	19.2	0.18	0.36	0.27	0.19

^aOverall monomer conversion determined by ^1H NMR spectroscopy, numbers in parenthesis indicate conversion (%) for MI and monomer respectively. ^bDetermined by SEC in CHCl_3 against poly(styrene) standards. ^cDetermined by end-group analysis by ^1H NMR spectroscopy. ^dDetermined by quantitative ^{13}C NMR spectroscopy, with * defining the carbonyl analysed. ^eJoint integral as a consequence of low resolution between peaks.

5.2.5 Sequence control of ϵ -substituted ϵ CLs

**Scheme 5.4** Sequence control polymerisation of ϵ -substituted ϵ CLs.

The rapid consumption of ϵ HL compared to MI leads to the potential of inserting a short ϵ HL block at a given point in the polymerisation of MI and achieve sequential control. In order to demonstrate this, a homopolymerisation of MI at 1 M in toluene with benzyl alcohol as initiator, $\text{Mg(BHT)}_2(\text{THF})_2$ as catalyst and a targeted DP of 100 was started. After 3 h of polymerisation 10 eq. ϵ HL at 1 M in toluene was injected into the polymerisation and consumption of both monomers was followed by ^1H NMR spectroscopy (Scheme 5.4). Monitoring the reaction by ^1H NMR spectroscopy revealed that within 30 minutes, all ϵ HL had been consumed with only 2% monomer conversion of MI occurring within this time period (Figure 5.18). SEC analysis of the final copolymer exhibited a monomodal molecular weight distribution with low dispersity ($D_M = 1.20$), which indicates that the ϵ HL had been incorporated successfully into the polymer chain without causing partial or full termination of existing chain ends, as well as no new chain or cyclic species formation (Figure 5.19). Analysis by DOSY NMR spectroscopy confirmed only one polymer species was present at the end of the polymerisation, which indicates that the formation of two separate homopolymer species had not occurred (Figure 5.20).

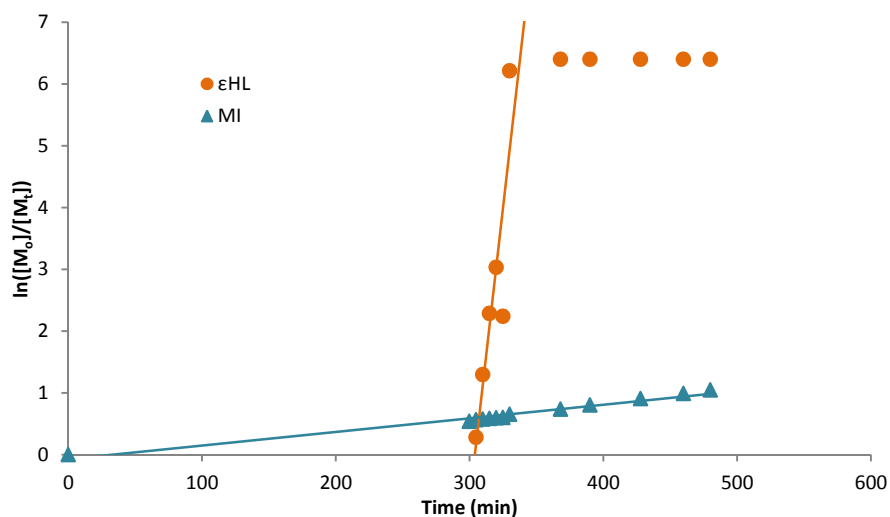


Figure 5.18 Kinetic plot for the sequence controlled copolymerisation of menthide and ϵ -heptalactone, conducted at 80 °C in toluene with $[MI]_0 : [\epsilon HL]_0 : [BnOH]_0 : [cat.]_0 = 100 : 10 : 1 : 1$, total monomer concentration = 1 M, ϵHL injected into reaction mixture at $t = 3$ h.

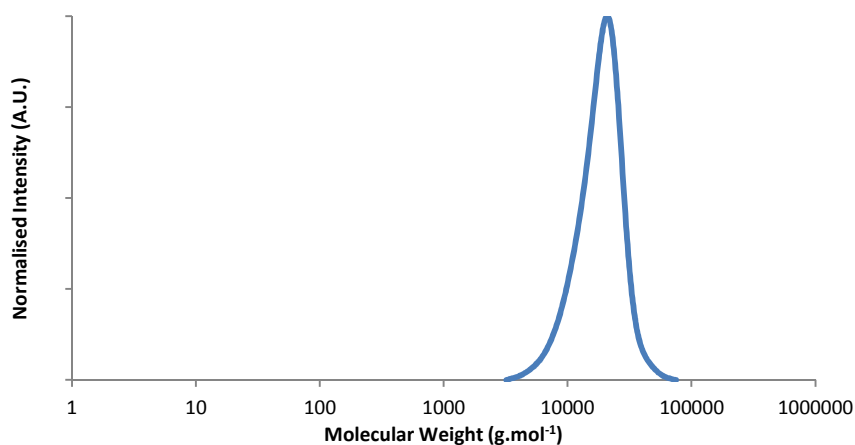


Figure 5.19 SEC chromatogram for poly(ϵ -heptalactone-co-menthide) in $CHCl_3$. Molecular weight determined against poly(styrene) standards.

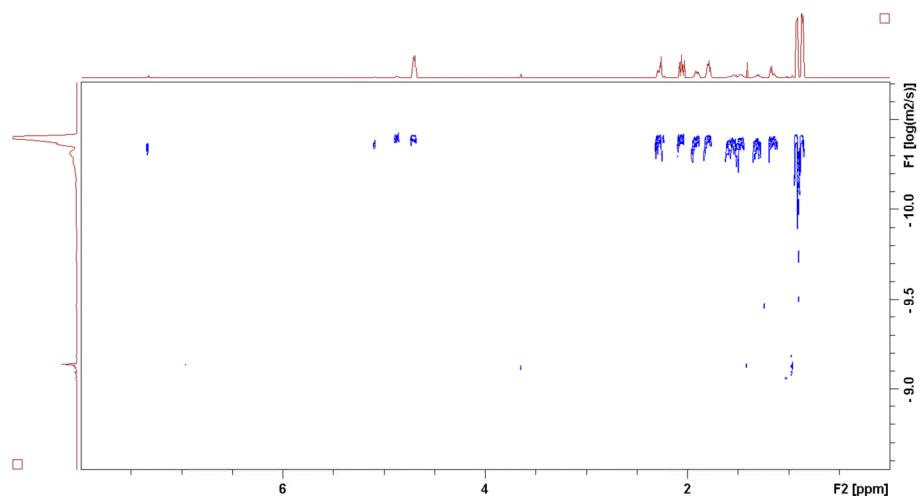


Figure 5.20 DOSY NMR spectra of the resultant polymer from sequence controlled injection of 10 eq. ϵHL into a DP 100 homopolymerisation of MI at 50% MI conversion (500 MHz, 298 K, $CDCl_3$).

^1H NMR spectroscopic analysis of purified polymer samples taken during the incorporation of ϵHL into the polymer chain, allowed for the DP of the polymer to be determined during this stage as well as the quantities of each type of repeat unit (ϵHL or MI) (Figure 5.21). The incorporation of ϵHL was observed to be very rapid with an average of 0.5 MI repeat units being incorporated during the same time period, suggesting block formation as a consequence of the difference in reactivity between the monomers with the catalyst. Analysis of the resultant copolymer by quantitative ^{13}C NMR spectroscopy could not confirm the formation of a block copolymer as a consequence of the gradation between blocks producing carbonyl diad resonances for $\epsilon\text{HL}^*\text{-MI}$ and $\text{MI}^*\text{-}\epsilon\text{HL}$ equivalent to the carbonyl diad resonance of $\epsilon\text{HL}^*\text{-}\epsilon\text{HL}$ (Figure 5.22).

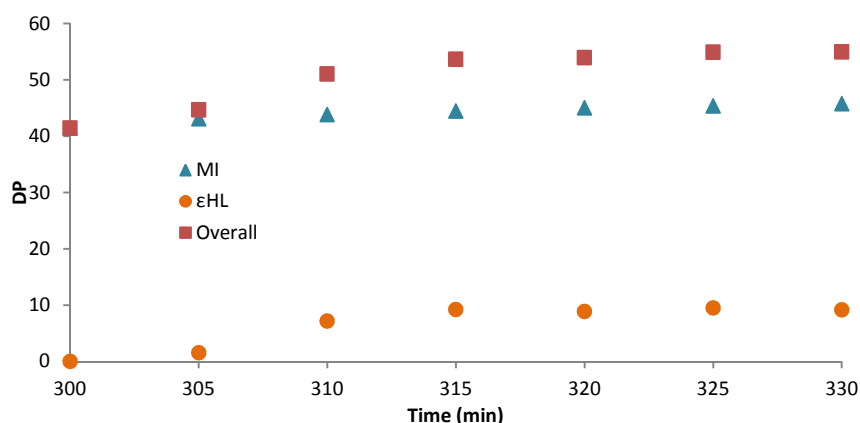


Figure 5.21 Increase in DP over 30 min after injection of ϵHL for the copolymerisation of MI and ϵHL , conducted at 80 °C in toluene with $[\text{MI}]_0 : [\epsilon\text{HL}]_0 : [\text{BnOH}]_0 : [\text{cat.}]_0 = 100 : 10 : 1 : 1$, total monomer concentration = 1 M, ϵHL injected into reaction mixture at $t = 3$ h.

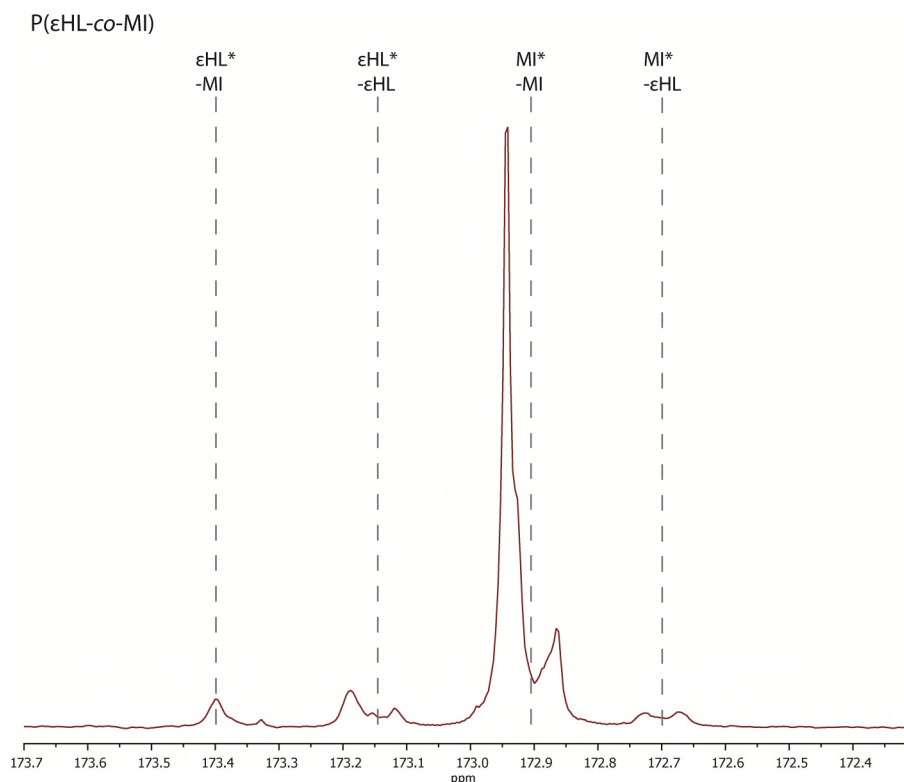


Figure 5.22 Quantitative ^{13}C NMR spectra of the carbonyl region for the sequential control copolymerisation of ϵ HL and MI with $[\epsilon\text{HL}]_0 : [\text{MI}]_0 : [\text{BnOH}]_0 : [\text{cat.}]_0 = 10 : 100 : 1 : 1$, with ϵ HL injection after 3 h and a total initial monomer concentration of 1 M (125 MHz, CDCl_3 , 298 K).

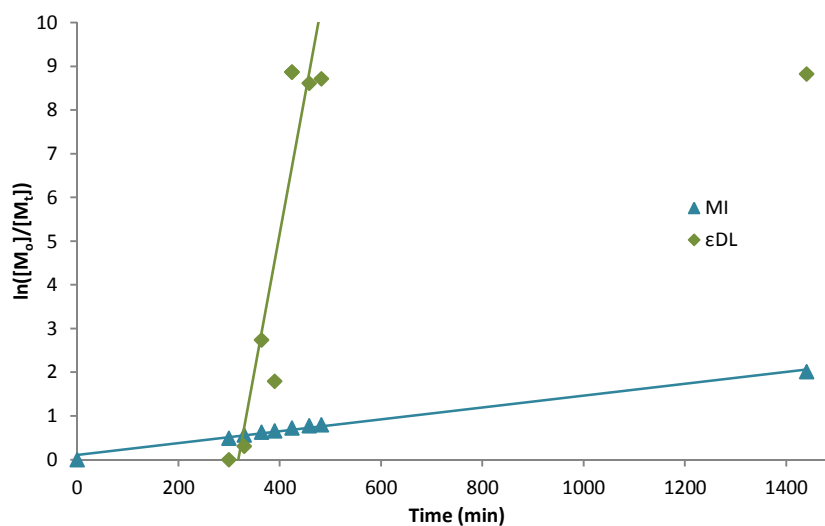


Figure 5.23 Kinetic plot for the sequence controlled copolymerisation of menthide and ϵ -decalactone, conducted at 80 °C in toluene with $[\text{MI}]_0 : [\epsilon\text{DL}]_0 : [\text{BnOH}]_0 : [\text{cat.}]_0 = 100 : 10 : 1 : 1$, total monomer concentration = 1 M, ϵ DL injected into reaction mixture at $t = 3$ h.

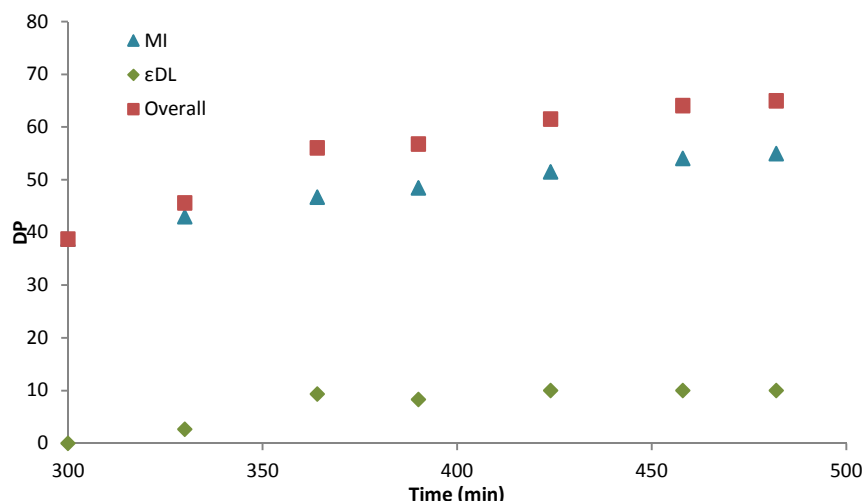


Figure 5.24 Increase in DP over 200 min after injection of ϵ DL for the copolymerisation of MI and ϵ DL, conducted at 80 °C in toluene with $[MI]_0 : [\epsilon DL]_0 : [BnOH]_0 : [cat.]_0 = 100 : 10 : 1 : 1$, total monomer concentration = 1 M, ϵ DL injected into reaction mixture at $t = 3$ h.

In order to clarify whether the ability to sequentially control block formation in poly(menthide) (PMI) is achievable with other ϵ SL monomers, a sequential control experiment was conducted with ϵ DL replacing ϵ HL as comonomer. Hence, the homopolymerisation of MI at 1 M in toluene with benzyl alcohol as initiator, $Mg(BHT)_2(THF)_2$ as catalyst and a targeted DP of 100 was started, with the injection of 10 eq. ϵ DL at 1 M in toluene after 3 h of polymerisation and consumption of both monomers followed by 1H NMR spectroscopy. As a consequence of the longer alkyl side chain of ϵ DL, the incorporation of ϵ DL into the polymer chain was observed to be slower than ϵ HL in the same conditions (Figure 5.23). However, the incorporation of ϵ DL into the polymer chain was achieved, with full monomer conversion occurring within 2 h post-injection. MI conversion also persisted during the consumption of ϵ DL with 18% monomer conversion during this time (Figure 5.24). As transesterification side reactions do not occur in this polymerisation, consumption of both monomers over this period of time should form a randomly sequenced section of the polymer chain. SEC analysis of the final copolymer showed a monomodal distribution indicative of successful incorporation of both monomers into the polymer chain, with no termination side reactions or new chain formation occurring as a consequence of monomer injection (Figure 5.25). A low dispersity ($\mathcal{D}_M = 1.18$)

in the final copolymer also shows good control over the polymerisation with few side reactions broadening the molecular weight distribution. However, a slight low molecular weight tail is observed, likely as a consequence of a small quantity of water being introduced into the system during the injection of ϵ DL that poisons the catalyst and terminates some active chains.

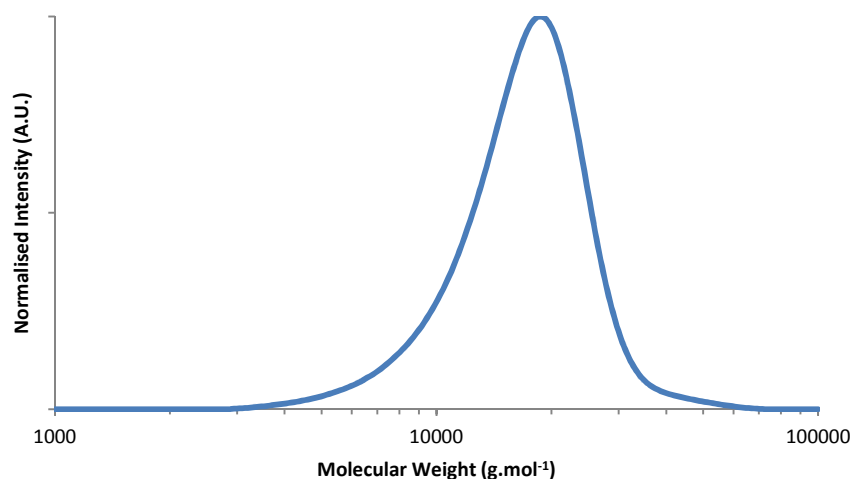


Figure 5.25 SEC chromatogram for poly(ϵ -decalactone-*co*-menthilde). Molecular weight determined against poly(styrene) standards.

In order to determine the polymer sequencing, quantitative ^{13}C NMR spectroscopy of the final copolymer was implemented in order to integrate the carbonyl region. Three carbonyl diad resonance representing $\epsilon\text{DL}^*\text{-}\epsilon\text{DL}$, $\epsilon\text{DL}^*\text{-MI}$ and $\text{MI}^*\text{-}\epsilon\text{DL}$, and $\text{MI}^*\text{-MI}$ ($\delta = 173.46$, 173.23 and 172.99 respectively) were present (Figure 5.26). As expected, the integration for the $\text{MI}^*\text{-MI}$ carbonyl diad resonance was significantly greater than other carbonyl diad resonances. However, the integrals for the remaining carbonyl diad resonances were equivalent, indicative of a randomly sequenced segment of copolymer. As a consequence of low quantities of transesterification side reactions, the random segment is known to begin and end at a specific place within the polymer chain (in this case starting at 36% menthilde conversion and ending at 55% overall monomer conversion) as well as maintaining a low dispersity despite having a randomly sequenced section of copolymer.

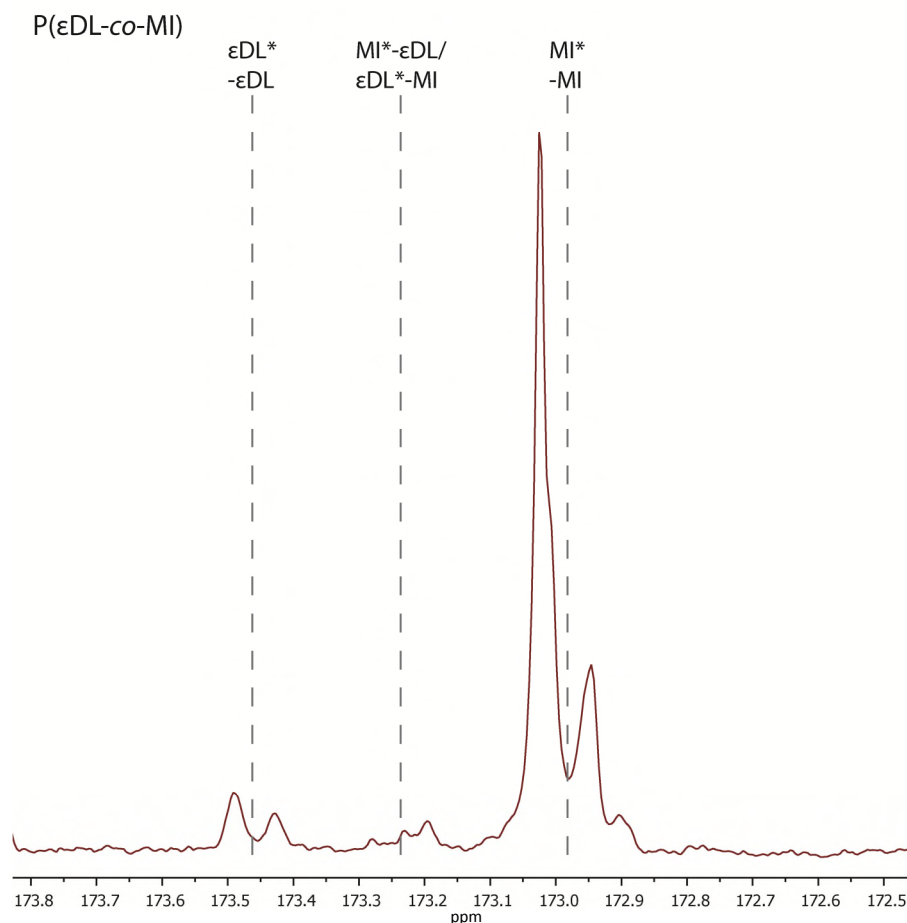
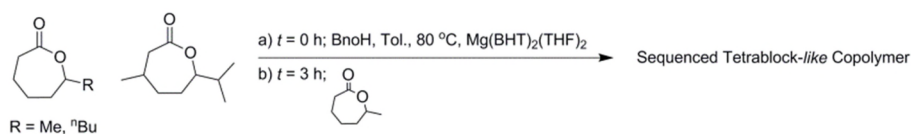


Figure 5.26 Quantitative ^{13}C NMR spectra of the carbonyl region for the sequential control copolymerisation of ϵDL and MI with $[\epsilon\text{DL}]_0 : [\text{MI}]_0 : [\text{BnOH}]_0 : [\text{cat.}]_0 = 10 : 100 : 1 : 1$, with ϵDL injection after 3 h and a total initial monomer concentration of 1 M (125 MHz, CDCl_3 , 298 K).

Overall, the ability to produce block-like lactone copolymers that do not exhibit transesterification side reactions is achievable with the use of ϵSLs as a one-pot reaction and potentially obtainable through the sequential addition of a rapidly polymerising low-substituted lactone (*e.g.* ϵHL) into a slowly polymerising highly-substituted lactone (*e.g.* MI). The use of ϵDL to produce a block-like copolymer is only achieved in a one-pot copolymerisation with MI as sequential control *via* monomer injection produces a randomly copolymerised block. Combination of the two methods could be used in order to produce alternating tetra-block copolymers of controlled block length.



Scheme 5.5 Copolymerisation of menthide with an ϵ -substituted ϵ -lactone with sequential addition of ϵ -heptalactone to produce a tetrablock-like copolymer.

To this end, a one-pot copolymerisation of ϵ HL and MI at a 20 : 50 molar equivalent ratio respectively at a total monomer concentration of 1 M in toluene, with 1 molar equivalent of benzyl alcohol as initiator, 1 molar equivalent of $\text{Mg}(\text{BHT})_2(\text{THF})_2$ as catalyst and a total targeted DP of 70 was conducted at 80 °C (Scheme 5.5). After 5 h of polymerisation, a 1 M solution of ϵ HL in toluene containing another 20 molar equivalents of monomer with respect to initiator was injected into the polymerisation mixture and the polymerisation continued for another 5 h (10 h total polymerisation time). Samples were taken at time intervals consistent with the completion of one block in the polymerisation and characterised using ^1H and quantitative ^{13}C NMR spectroscopy and SEC analysis. Analysis of samples by ^1H NMR spectroscopy showed complete conversion of ϵ -heptalactone had occurred within 1 h from the beginning of the reaction or within 30 min post-injection into the reaction mixture (Figure 5.27). Conversion of MI equivalent to the formation of a block of DP 20 was found to occur after a period of 5 h, after which ϵ HL could be injected to form another block segment. Polymer samples were washed with cold hexanes in order to remove monomer and catalyst. Analysis of the resultant polymers by ^1H NMR spectroscopy clearly showed the rapid increase of ϵ HL incorporated into the polymer chain at the start of the polymerisation, followed by the slower evolution of a MI block (Figure 5.28). Once more ϵ HL monomer was added into the reaction mixture, another rapid incorporation of ϵ HL into the polymer chain was observed, followed again by slow incorporation of MI. A minimal amount of MI (~2%) was shown to be consumed during the rapid consumption of ϵ HL, reaffirming the strong affinity of the catalyst towards the ROP of ϵ HL over MI observed in previous copolymerisations.

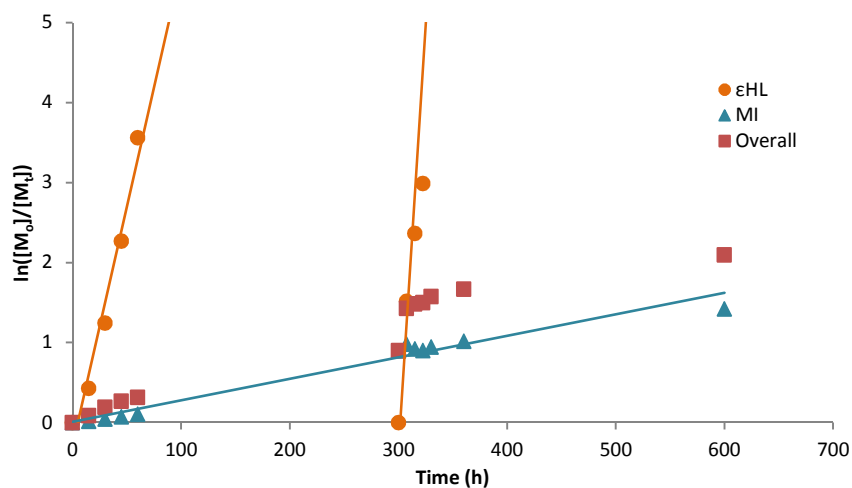


Figure 5.27 Kinetic plot for the sequence-controlled block copolymerisation of menthide and ϵ -heptalactone, conducted at 80 °C in toluene with $[MI]_0 : [\epsilon HL]_0 : [BnOH]_0 : [cat.]_0 = 50 : 50 : 1 : 1$, with a further 20 eq. ϵHL added at $t = 5.33$ h and total initial monomer concentration = 1 M.

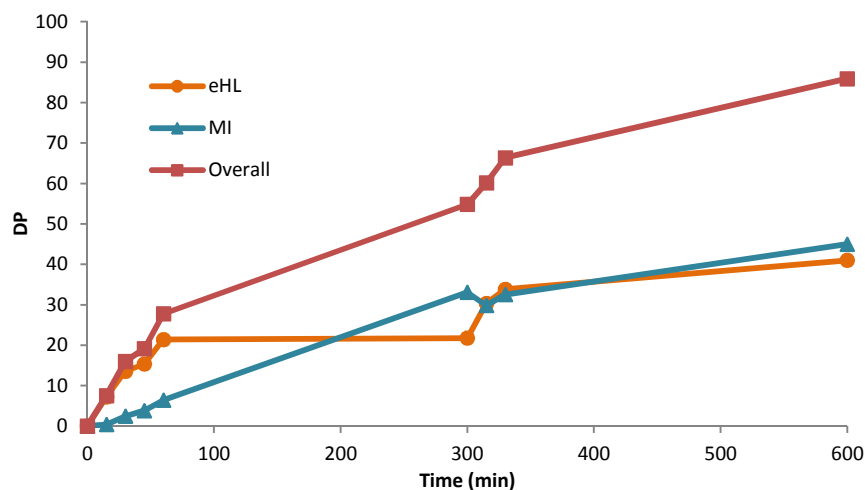


Figure 5.28 Increase in DP throughout the sequence-controlled block copolymerisation of MI and ϵHL , conducted at 80 °C in toluene with $[MI]_0 : [\epsilon HL]_0 : [BnOH]_0 : [cat.]_0 = 50 : 20 : 1 : 1$, with a further 20 eq. ϵHL added at $t = 5.33$ h and total monomer concentration = 1 M.



Figure 5.29 Quantitative ^{13}C NMR spectra of the carbonyl region for the sequence-controlled block copolymerisation of menthide and ϵ -heptalactone using $\text{Mg}(\text{BHT})_2(\text{THF})_2$ as a catalyst at 80°C in toluene with $[\text{MI}]_0 : [\epsilon\text{HL}]_0 : [\text{BnOH}]_0 : [\text{cat.}]_0 = 50 : 20 : 1 : 1$, with a further 20 eq. ϵHL added at $t = 5$ h and total monomer concentration = 1 M. (125 MHz, CDCl_3 , 298 K).

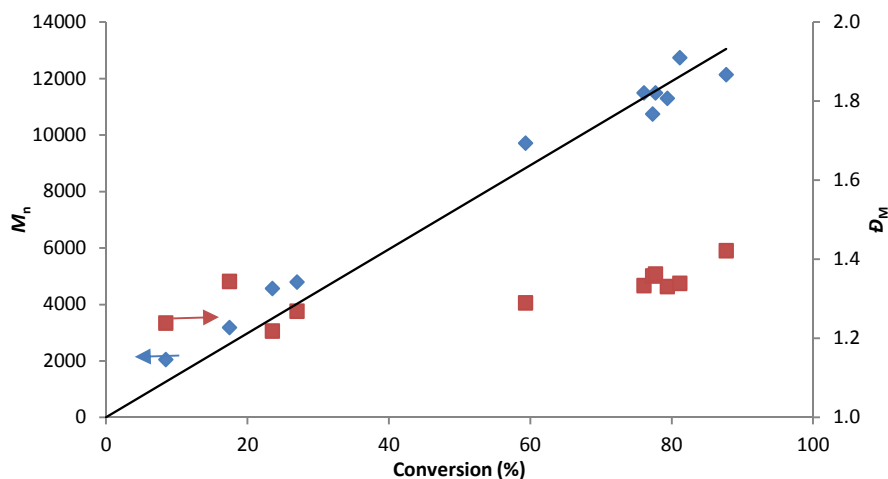


Figure 5.30 Changes in M_n and \bar{D}_M over total monomer conversion for the sequence-controlled block copolymerisation of menthide and ϵ -heptalactone using $\text{Mg}(\text{BHT})_2(\text{THF})_2$ as a catalyst at 80 °C in toluene with $[\text{MI}]_0 : [\epsilon\text{DL}]_0 : [\text{BnOH}]_0 : [\text{cat.}]_0 = 50 : 20 : 1 : 1$, with a further 20 eq. ϵHL added at $t = 5$ h and total monomer concentration = 1 M. M_n and \bar{D}_M determined by SEC against poly(styrene) standards.

Polymer sequencing was confirmed by quantitative ^{13}C NMR spectroscopy which showed large integrals for carbonyl diad resonances corresponding to $\epsilon\text{HL}^*-\epsilon\text{HL}$ and MI^*-MI carbonyls and smaller integrals corresponding to $\epsilon\text{HL}^*-\text{MI}$ and $\text{MI}^*-\epsilon\text{HL}$ carbonyl diad resonances, indicative of a largely block-like copolymer with small gradient transition between blocks (Figure 5.29). Furthermore, the evolution of each block can be observed by quantitative ^{13}C NMR spectroscopy; after 1 h, the majority of carbonyl diad resonances are attributable to $\epsilon\text{HL}^*-\epsilon\text{HL}$ as a consequence of the first block formation. This is followed by the evolution of the MI^*-MI carbonyl diad resonance which increases in integration to match the integration of $\epsilon\text{HL}^*-\epsilon\text{HL}$ before more ϵHL is injected into the polymerisation. After the injection, a rapid increase in the integral for the $\epsilon\text{HL}^*-\epsilon\text{HL}$ carbonyl diad resonance is observed again. During the final 4 h of polymerisation, the integral for the MI^*-MI carbonyl diad resonance again increases to match the integral for $\epsilon\text{HL}^*-\epsilon\text{HL}$. Given the extremely slow transesterification of the system, this is a good indication of the formation of a tetrablock copolymer consisting of equal alternating blocks of ϵHL and MI . It should be noted that although the peak intensity of the final MI^*-MI carbonyl diad resonance does not appear to increase over the final 4 h of polymerisation, the integration

and breadth of the peak increase as a consequence of the different stereoisomers of MI exhibiting slight differences in carbonyl diad resonances.

Analysis of the polymers by SEC showed a steady increase in molecular weight throughout polymerisation, similar to that observed in the one-pot copolymerisation of ϵ HL and MI (Figure 5.30). Dispersity was observed to increase slightly during the polymerisation from $\mathcal{D}_M = 1.3$ after the complete consumption of the initial ϵ HL to $\mathcal{D}_M = 1.4$ after formation of the second MI block (Figure 5.31). However transesterification side reactions are minimal in poly(ϵ SL)s (PeSLs), as shown previously. A slight low molecular weight tail is observed by SEC analysis post-injection of ϵ HL and is therefore likely a consequence of a small quantity of termination side reactions caused by the slight poisoning of the catalyst from water addition during monomer injection.

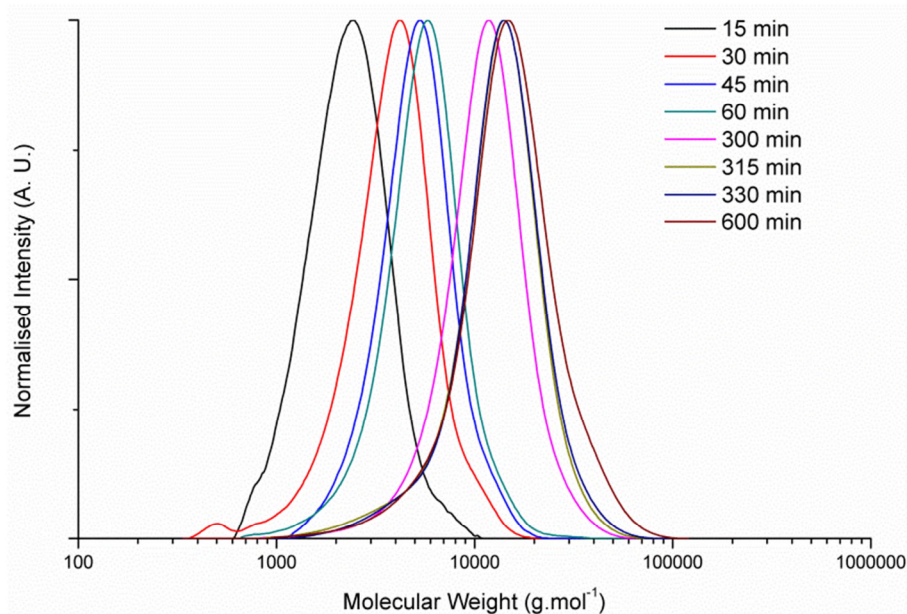


Figure 5.31 Molecular weight distribution of polymeric species in the the sequence-controlled block copolymerisation of menthide and ϵ -heptalactone using $\text{Mg}(\text{BHT})_2(\text{THF})_2$ as a catalyst at 80 °C in toluene with $[\text{MI}]_0 : [\epsilon\text{DL}]_0 : [\text{BnOH}]_0 : [\text{cat.}]_0 = 50 : 20 : 1 : 1$, with a further 20 eq. ϵ HL added at $t = 5$ h and total monomer concentration = 1 M. Molecular weights determined by SEC against poly(styrene) standards.

5.3 Conclusion

ϵ -Substituted ϵ -lactones (ϵ SLs) have been shown to exhibit unique ROP behaviour compared to other non-substituted lactones, producing new sequencing that has so far proven extremely difficult in one-pot copolymerisations. The presence of the ϵ -substitution has been shown to severely hinder transesterification side reactions, leading to homopolymers of relatively low dispersities. Copolymerisation of ϵ SLs with small non-substituted lactone, such as δ -valerolactone or ϵ -caprolactone, produce random copolymers as a consequence of the rapid transesterification side reactions of the non-substituted lactone during incorporation of the ϵ SL. However, when copolymerised with a non-substituted lactone of ring size of 8 or larger, ϵ SLs have been found to produce block-like copolymers as a consequence of the ϵ SL polymerising first and being unable to readily transesterify during the incorporation of the second monomer. A short gradation between blocks is observed as a consequence of competition between the lower concentration of the more reactive monomer and high concentration of the less reactive monomer. The same behaviour is also observed in the copolymerisation of ϵ SLs with different reactivities, which has been implemented in the demonstration of block-like copolymers to form a tetrablock-like copolymer with low dispersity. Dependent on the combination of monomers copolymerised the gradation between blocks can vary significantly, however there remains potential for optimised conditions or improved catalysts to reduce the gradation to a lower degree.

5.4 References

1. I. van der Meulen, M. de Geus, H. Antheunis, R. Deumens, E. A. J. Joosten, C. E. Koning and A. Heise, *Biomacromolecules*, 2008, **9**, 3404-3410.
2. S. Blanquer, J. Tailhades, V. Darcos, M. Amblard, J. Martinez, B. Nottelet and J. Coudane, *J. Polym. Sci., Part A: Polym. Chem.*, 2010, **48**, 5891-5898.
3. F. Fay, E. Renard, V. Langlois, I. Linossier and K. Vallee-Rehel, *Eur. Polym. J.*, 2007, **43**, 4800-4813.
4. A. Nakayama, N. Kawasaki, Y. Maeda, I. Arvanitoyannis, S. Aiba and N. Yamamoto, *J. Appl. Polym. Sci.*, 1997, **66**, 741-748.
5. G. G. Pitt, M. M. Gratzl, G. L. Kimmel, J. Surles and A. Sohindler, *Biomaterials*, 1981, **2**, 215-220.
6. D. Zhang, M. A. Hillmyer and W. B. Tolman, *Biomacromolecules*, 2005, **6**, 2091-2095.
7. B. Kalra, A. Kumar, R. A. Gross, M. Baiardo and M. Scandola, *Macromolecules*, 2004, **37**, 1243-1250.
8. F. Suriano, O. Coulembier and P. Dubois, *React. Funct. Polym.*, 2010, **70**, 747-754.
9. M. Claudino, d. M. I. van, S. Trey, M. Jonsson, A. Heise and M. Johansson, *J. Polym. Sci., Part A: Polym. Chem.*, 2012, **50**, 16-24.
10. I. van der Meulen, Y. Li, R. Deumens, E. A. J. Joosten, C. E. Koning and A. Heise, *Biomacromolecules*, 2011, **12**, 837-843.
11. X. F. L. Christopher, M. S. Monica, T. Swee-Hin and W. H. Dietmar, *Biomed. Mater. (Bristol, U. K.)*, 2008, **3**, 034108.
12. M. Eriksson, L. Fogelstrom, K. Hult, E. Malmstrom, M. Johansson, S. Trey and M. Martinelle, *Biomacromolecules*, 2009, **10**, 3108-3113.
13. N. Simpson, M. Takwa, K. Hult, M. Johansson, M. Martinelle and E. Malmström, *Macromolecules*, 2008, **41**, 3613-3619.

14. A. P. Dove, *Chem. Commun.*, 2008, 6446-6470.
15. S. Cui, X. Wang, Z. Li, Q. Zhang, W. Wu, J. Liu, H. Wu, C. Chen and K. Guo, *Macromol. Rapid Commun.*, 2014, **35**, 1954-1959.
16. J. A. Wilson, S. A. Hopkins, P. M. Wright and A. P. Dove, *Macromolecules*, 2015, **48**, 950-958.
17. G. Ceccorulli, M. Scandola, A. Kumar, B. Kalra and R. A. Gross, *Biomacromolecules*, 2005, **6**, 902-907.
18. Z. Jiang, H. Azim, R. A. Gross, M. L. Focarete and M. Scandola, *Biomacromolecules*, 2007, **8**, 2262-2269.
19. A. Kumar, K. Garg and R. A. Gross, *Macromolecules*, 2001, **34**, 3527-3533.
20. M. Bouyahyi and R. Duchateau, *Macromolecules*, 2014, **47**, 517-524.
21. L. Jasinska-Walc, M. Bouyahyi, A. Rozanski, R. Graf, M. R. Hansen and R. Duchateau, *Macromolecules*, 2015, **48**, 502-510.
22. L. Jasinska-Walc, M. R. Hansen, D. V. Dudenko, A. Rozanski, M. Bouyahyi, M. Wagner, R. Graf and R. Duchateau, *Polym. Chem.*, 2014.
23. M. Bouyahyi, M. P. F. Pepels, A. Heise and R. Duchateau, *Macromolecules*, 2012, **45**, 3356-3366.
24. A. Kumar, B. Kalra, A. Dekhterman and R. A. Gross, *Macromolecules*, 2000, **33**, 6303-6309.
25. M. Basko, A. Duda, S. Kazmierski and P. Kubisa, *J. Polym. Sci., Part A: Polym. Chem.*, 2013, **51**, 4873-4884.
26. A. Pilone, N. De Maio, K. Press, V. Venditto, D. Pappalardo, M. Mazzeo, C. Pellecchia, M. Kol and M. Lamberti, *Dalton Trans.*, 2015, **44**, 2157-2165.
27. M. P. F. Pepels, P. Souljé, R. Peters and R. Duchateau, *Macromolecules*, 2014, **47**, 5542-5550.
28. Y. C. Yu, S. J. Shin, K. D. Ko, W.-R. Yu and J. H. Youk, *Polymer*, 2013, **54**, 5595-5600.

29. Y. Li, J. Hong, R. Wei, Y. Zhang, Z. Tong, X. Zhang, B. Du, J. Xu and Z. Fan, *Chem. Sci.*, 2015, **6**, 1530-1536.
30. R. Mahadev Patil, A. A. Ghanwat, S. Ganugapati and R. Gnaneshwar, *J. Macromol. Sci., Part A: Pure Appl. Chem.*, 2015, **52**, 114-123.
31. C. G. Jaffredo, J.-F. Carpentier and S. M. Guillaume, *Macromolecules*, 2013, **46**, 6765-6776.
32. N. Ajellal, J.-F. Carpentier, C. Guillaume, S. M. Guillaume, M. Helou, V. Poirier, Y. Sarazin and A. Trifonov, *Dalton Trans.*, 2010, **39**, 8363-8376.

6 Conclusions

6.1 Conclusions

The use of the catalyst, magnesium 2,6-di-tert-butyl-4-methylphenoxide ($\text{Mg}(\text{BHT})_2(\text{THF})_2$), has been demonstrated to effectively polymerise ω -pentadecalactone (PDL) through 'immortal' ring-opening polymerisation (iROP). Furthermore, the catalyst is shown to polymerise PDL in a non-inert environment and maintain high end-group fidelity, with no side reactions with water observed. The catalyst is also shown to polymerise other smaller lactones 'immortally' and at much greater rates than can be achieved with macrolactone polymerisation.

The copolymerisations of PDL with other non-substituted lactones were investigated with $\text{Mg}(\text{BHT})_2(\text{THF})_2$ as a catalyst as a consequence of the high activity found. Following the kinetics by ^1H and ^{13}C NMR spectroscopy showed that in each copolymerisation, the smaller ring lactone polymerised faster than PDL and that during the incorporation of PDL, transesterification side reactions randomised the polymer sequencing to produce a statistically random copolymer regardless of the molar ratio of the monomers. A direct relationship between the molar ratio of the comonomers and the melting and crystallisation temperatures (T_m and T_c respectively) of the resultant copolymers was established. The different rates of degradation between PDL copolymers was shown to be dependent on the smaller ring lactone used, with smaller lactone comonomers degrading more rapidly. The thermal and degradative properties of the PDL copolymers could therefore be independently tuned in order to produce tailor-made PDL copolymers.

Unlike PDL copolymerisations with non-substituted lactones, the copolymerisation of PDL with ϵ -substituted ϵ -lactones (ϵSLs) was shown to produce block-like copolymers. Following the kinetics of the copolymerisation revealed that the sequencing was a consequence of the smaller, substituted lactone polymerising before PDL polymerisation. However, transesterification side reactions involving the ϵSL block were not observed during the subsequent incorporation of PDL into the polymer chain and a copolymer with a

small gradient between blocks was formed. The use of an alkene functionalised ϵ SL resulted in a one-pot block-like PDL copolymer with a functional group that was used for the post-polymerisation modification by thiol-ene addition in order to attach thiols onto the polymer chain.

The relative inability of ϵ SLs to undergo transesterification side reactions compared to non-substituted counterparts was also investigated. As a consequence of the lack of transesterification side reactions involving ϵ SLs, particularly menthide (MI), the copolymerisation of MI with a range of non-substituted lactones of different ring-size was tested. The results showed that MI copolymers with a lactone of ring-size ≥ 8 produces block-like copolymers in a similar method observed in the copolymerisation of PDL and MI. As a consequence of the more rapid polymerisation of non-substituted lactones of ring-size < 8 , transesterification side reactions occurred during the incorporation of MI and random copolymers were formed. Terpolymerisations involving small ring lactones, macrolactones and ϵ SLs were shown to produce a range of sequences depending on the technique used.

The large differences in rates of polymerisation for ϵ SLs were then used to produce more one-pot block-like lactone copolymers. The sequential addition of a more rapid polymerising ϵ SL monomer into the polymerisation of a slower polymerising ϵ SL monomer allowed for the realisation of the potential for sequence control of lactone copolymers and production of multi-block lactone copolymers in one-pot.

The work outlined by this thesis has demonstrated the basic considerations in producing lactone copolymers with defined sequencing. This can be implemented to produce macrolactone or ϵ SL copolymers with any basic sequence; block, random, block terpolymer and more. However, with the formation of block-like copolymers, a gradation still remains between the blocks. The gradation can be limited with fine control over the polymerisation and efforts are currently underway to further minimise the gradation.

7 Experimental

7.1 Materials

All reagents were purchased from Sigma Aldrich, except 2,6-di-*tert*-4-methylphenol was purchased from Alfa Aesar and ϵ -caprolactone was purchased from Acros. All solvents were supplied by Fisher and dried using an Innovative Technology Inc. Pure Solv MD-4-EN solvent purification system. Benzyl alcohol, δ -valerolactone, ϵ -caprolactone, ζ -heptalactone, η -caprylolactone, ω -dodecalactone, menthide, dihydrocarvide, 3-bromocamphide and pulegide were dried over calcium hydride for 24 hours before vacuum distillation. ω -Pentadecalactone was dissolved in 75 wt.% toluene and dried overnight on molecular sieves. All other reagents were used as received.

7.2 Instrumental methods

Proton (^1H) NMR spectra were recorded using a Bruker DPX-300 spectrometer or Bruker DPX-400 spectrometer. Carbon (^{13}C) NMR spectra were recorded using a Bruker DPX-400 spectrometer, Bruker DRX-500 spectrometer or Bruker AV-II-700 spectrometer. All chemical shifts were recorded in parts per million (ppm) relative to a reference peak of chloroform solvent at $\delta = 7.26$ ppm and 77.16 ppm for ^1H and ^{13}C NMR spectra respectively. Molecular weights were determined through size exclusion chromatography (SEC) using an Agilent 390-MDS on PLgel Mixed-D type columns in series with refractive index (RI) detection. Weights were calculated using a calibration curve determined from poly(styrene) standards with chloroform (0.5% NEt_3) as eluent flowing at $1.0 \text{ mL}\cdot\text{min}^{-1}$ and sample concentration $3 \text{ mg}\cdot\text{mL}^{-1}$. Wide-angle X-ray diffraction (WAXD) was performed on a Panalytical X'Pert Pro MPD equipped with a Cu $K\alpha_1$ hybrid monochromator as the incident beam optics and PiXcel detector. MALDI-ToF (matrix assisted laser desorption ionisation – time of flight) spectra were recorded using a Bruker Daltronics Ultraflex II MALDI-ToF mass spectrometer, equipped with a nitrogen laser delivering 2 ns laser pulses at 337 nm with a positive ion ToF detection performed using an accelerating voltage of 25 kV. Samples were spotted onto a Bruker ground steel MALDI-ToF analytical plate through application of a small portion of a solution containing trans-2-[3-(4-*tert*-butylphenyl)-2-methyl-2-propylidene]malonitrile (DCTB) as a matrix (20

μL of a 10 mg mL^{-1} solution in THF), sodium trifluoroacetate as a cationisation agent ($5\text{ }\mu\text{L}$ of a 10 mg mL^{-1} solution in THF), and analyte ($5\text{ }\mu\text{L}$ of a 10 mg mL^{-1} solution in THF) followed by solvent evaporation. The samples were measured in reflectron ion mode and calibrated by comparison to 2×10^3 poly(ethylene oxide) standards. Differential scanning calorimetry (DSC) was obtained from using a Mettler Toledo DSC1 star system. DSC heating and cooling curves were run in triplicate in series under a nitrogen atmosphere at a heating rate of $\pm 10\text{ }^\circ\text{C}\cdot\text{min}^{-1}$ in a $40\text{ }\mu\text{L}$ aluminum crucible. Thiol-ene reactions were performed in a Metalight QX1 lightbox.

7.3 Experimental procedures for Chapter 1

7.3.1 Synthesis of $\text{Mg}(\text{BHT})_2(\text{THF})_2$

Using a modified version of the previously reported procedure,¹ 2,6-di-*tert*-butyl-4-methylphenol (4.407 g, 20.0 mmol) was dissolved in dry toluene (20 mL). Di-*n*-butylmagnesium 1 M in heptane (10 mL, 10.0 mmol) was added dropwise with stirring at room temperature. The exotherm raised the temperature of the flask and did not peak above $60\text{ }^\circ\text{C}$. The solution was stirred for a further 2 hours before removing solvent under vacuum. The remaining white solid was dissolved in dry pentane (25 mL), before dry tetrahydrofuran (5 mL) was added dropwise with stirring. The reaction was stirred for a further 2 hours before removing solvent to yield a white solid (5.96 g, 9.8 mmol, 98%). The product was dried under vacuum overnight and stored in a glovebox. Characterising data was consistent with the previous report.¹

^1H NMR (400 MHz, 298 K, C_6D_6): $\delta = 7.01$ (s, BHT Ar), 3.59 (t, $^3J_{\text{H-H}} = 6.4$, THF $\text{CH}_2\text{CH}_2\text{O}$), 2.30 (s, BHT CH_3Ar), 1.48 (s, BHT $(\text{CH}_3)_3\text{CAr}$), 1.20 (m, THF $\text{CH}_2\text{CH}_2\text{O}$). ^{13}C NMR (125 MHz, 298 K, C_6D_6): $\delta = 159.0$, 154.4, 139.5, 139.3, 130.0, 127.2, 123.1 (BHT Ar C), 72.6 (THF $\text{CH}_2\text{CH}_2\text{O}$), 37.5 (BHT ArCH_3), 34.0 (BHT $\text{ArC}(\text{CH}_3)_3$), 27.0 (THF $\text{CH}_2\text{CH}_2\text{O}$), 23.7 (BHT $\text{ArC}(\text{CH}_3)_3$) ppm.

7.3.2 General procedure of δ -valerolactone polymerisation

Using standard glovebox techniques, an ampoule was filled with $\text{Mg}(\text{BHT})_2(\text{THF})_2$ (10.0 mg, 16.4 μmol), benzyl alcohol (1.70 μL , 16.4 μmol), δ -valerolactone (0.082 g, 823.4 mmol) and toluene (0.74

mL). The ampoule was sealed and heated at 80 °C for a defined time period. The reaction was quenched with the addition of acidified (5 % HCl) methanol. Chloroform was added to dissolve any solids and the polymer was precipitated in excess methanol.

^1H NMR (400MHz, 298K, CDCl_3): δ = 7.34 (s, Ar), 5.13 (s, $\text{C}=\text{OOCH}_2\text{Ar}$), 4.10 (t, $^3J_{\text{H-H}} = 5.9$ Hz, $\text{CH}_2\text{OC}=\text{O}$), 2.54 (t, $^3J_{\text{H-H}} = 7.0$ Hz, $\text{CH}_2\text{C}=\text{OO}$), 1.85 and 1.69 (all remaining hydrogens) ppm. ^{13}C NMR (125MHz, 298K, CDCl_3): δ = 173.40 ($\text{CH}_2\text{C}=\text{OO}$), 128.69, 128.33 (aromatic CH), 69.57 (Bn $\text{COC}=\text{O}$), 64.04 ($\delta\text{VL COC}=\text{O}$), 33.81 ($\text{CH}_2\text{C}=\text{OO}$), 28.20 ($\text{CH}_2\text{CH}_2\text{C}=\text{O}$) and 21.54 ($\text{CH}_2\text{CH}_2\text{O}$) ppm.

7.3.3 General procedure of ϵ -caprolactone polymerisation

Using standard glovebox techniques, an ampoule was filled with $\text{Mg}(\text{BHT})_2(\text{THF})_2$ (21.3 mg, 35 μmol), benzyl alcohol (3.63 μL , 35 μmol), ϵ -caprolactone (0.4 g, 3.5 mmol) and toluene (1.4 mL). The ampoule was sealed and heated at 80 °C for a defined time period. The reaction was quenched with the addition of acidified (5 % HCl) methanol. Chloroform was added to dissolve any solids and the polymer was precipitated in excess methanol.

^1H NMR (400MHz, 298K, CDCl_3): δ = 7.29 (s, Ar), 5.06 (s, $\text{C}=\text{OOCH}_2\text{Ar}$), 4.01 (t, $^3J_{\text{H-H}} = 6.7$ Hz, $\text{CH}_2\text{OC}=\text{O}$), 2.25 (t, $^3J_{\text{H-H}} = 6.4$ Hz, $\text{CH}_2\text{C}=\text{OO}$), 1.60 and 1.33 (all remaining hydrogens) ppm. ^{13}C NMR (125MHz, 298K, CDCl_3): δ = 173.51 ($\text{CH}_2\text{C}=\text{OO}$), 128.55, 128.18 (aromatic CH), 66.13 (Bn $\text{COC}=\text{O}$), 64.12 ($\epsilon\text{CL COC}=\text{O}$), 34.11 ($\text{CH}_2\text{C}=\text{OO}$), 28.35, 25.53 and 24.57 (all other carbons) ppm.

7.3.4 General procedure of ω -pentadecalactone polymerisation

Using standard glovebox techniques, an ampoule was filled with $\text{Mg}(\text{BHT})_2(\text{THF})_2$ (10 mg, 16.5 μmol), benzyl alcohol (1.7 μL , 16.5 μmol) and ω -pentadecalactone stock solution (75 wt.% toluene, 824.0 μmol). The ampoule was sealed and heated at 80 °C for a defined time period. The reaction was quenched with the addition of acidified (5 % HCl) methanol. Chloroform was added to dissolve any solids and the polymer was precipitated in excess methanol.

Note: For polymerisations in non-inert atmospheres, no glovebox techniques were used to measure reagents and stock solutions were prepared without drying techniques.

^1H NMR (300MHz, 298K, CDCl_3): δ = 7.35 (s, Ar), 5.20 (s, $\text{C}=\text{OOCH}_2\text{Ar}$), 5.11 (s, $\text{C}=\text{OOCH}_2\text{Ar}$), 4.05 (t, $^3J_{\text{H-H}} = 6.8$ Hz, $\text{CH}_2\text{OC}=\text{O}$), 2.28 (t, $^3J_{\text{H-H}} = 7.5$ Hz, $\text{CH}_2\text{C}=\text{OO}$), 1.61 and 1.25 (all remaining hydrogens) ppm. ^{13}C NMR (125MHz, 298K, CDCl_3): δ = 174.12 ($\text{CH}_2\text{C}=\text{OO}$), 128.59, 128.21 (aromatic CH), 66.10 (Bn $\text{COC}=\text{O}$), 64.45 (PDL $\text{COC}=\text{O}$), 34.47 ($\text{CH}_2\text{C}=\text{OO}$), 30-28, 26-24 (all other carbons) ppm. Yield in inert conditions: 76%. Yield in non-inert conditions: 72%.

7.4 Experimental procedures for Chapter 2

7.4.1 Synthesis of η -caprylolactone

Using a modified version of the previously reported procedure,² cyclooctanone (12.8 g, 101.6 mmol) was dissolved in CH_2Cl_2 (150 mL) and cooled in an ice bath. *m*-Chloroperoxybenzoic acid (50 g, 203.2 mmol) was slowly added to the solution before heating to reflux at 70 °C for 10 days. The solution was then cooled back to 0 °C before removal of salts over Celite® and washing with CH_2Cl_2 (2 × 75 mL). The combined solutions were then washed with 10% $\text{Na}_2\text{S}_2\text{O}_5$ solution (2 × 300 mL), saturated Na_2CO_3 solution (2 × 300 mL) and saturated NaCl (2 × 300 mL). The organic layer was dried with MgSO_4 before removal of solvent through rotary evaporation. Purification was achieved through silica gel chromatography using 10 : 1 petroleum ether (40-60 °C) : ethyl acetate as eluent and yielded a transparent liquid (9.0 g, 63.7 mmol, 62%). Characterising data was consistent with the previous report.²

^1H NMR (400 MHz, 298 K, CDCl_3): δ = 4.12 (m, $\text{CH}_2\text{OC}=\text{O}$), 2.39 (m, $\text{CH}_2\text{C}=\text{OO}$), 1.87, 1.55 and 1.25 (all remaining hydrogens) ppm. ^{13}C NMR (125 MHz, 298 K, CDCl_3): δ = 173.90 (OCOCH_2), 64.54 (OCH_2), 34.65 (OCOCH_2), 29.55, 27.83, 25.16, 25.63 and 24.73 (CH_2) ppm.

7.4.2 Synthesis of ω -dodecalactone

Using a modified version of the previously reported procedure,² cyclododecanone (12.7 g, 69.6 mmol) was dissolved in CH_2Cl_2 (90 mL) and cooled in an ice bath. *m*-Chloroperoxybenzoic acid (30 g, 139.2 mmol) was slowly added to the solution before heating to reflux at 70 °C for 7 days. The solution was then cooled back to 0 °C before removal of salts over Celite® and washing with CH_2Cl_2

(2 × 45 mL). The combined solutions were then washed with 10% Na₂S₂O₅ solution (2 × 180 mL), saturated Na₂CO₃ solution (2 × 180 mL) and saturated NaCl (2 × 180 mL). The organic layer was dried with MgSO₄ before removal of solvent through rotary evaporation. Purification was achieved through silica gel chromatography using 10 : 1 petroleum ether (40-60 °C) : ethyl acetate as eluent and yielded a transparent liquid (9.3 g, 469 mmol, 67%). Characterising data was consistent with the previous report.²

¹H NMR (400 MHz, 298 K, CDCl₃): δ = 4.15 (m, CH₂OC=O), 2.35 (m, CH₂C=OO), 1.70 and 1.32 (all remaining hydrogens) ppm. ¹³C NMR (125 MHz, 298 K, CDCl₃): δ = 174.33 (OCOCH₂), 64.73 (OCH₂), 34.82 (OCOCH₂), 27.56, 26.76, 26.56, 25.54, 25.50, 25.09, 24.64 and 24.35 (CH₂) ppm.

7.4.3 General procedure of lactone and ω-pentadecalactone copolymerization

Using standard glovebox techniques, an ampoule was filled with Mg(BHT)₂(THF)₂ (10 mg, 16.5 μmol), benzyl alcohol (1.7 μL, 16.5 μmol), lactone (824.0 μmol) and ω-pentadecalactone stock solution (75 wt.% toluene, 824.0 μmol). The ampoule was sealed and heated at 80 °C for a defined time period. The reaction was quenched with the addition of acidified (5% HCl) methanol.

Chloroform was added to dissolve any solids and the polymer was precipitated in excess methanol.

P(δVL-co-PDL):

¹H NMR (400 MHz, 298 K, CDCl₃): δ = 7.35 (s, Ar), 5.11 (s, C=OOCH₂Ar), 4.06 (m, CH₂OC=O), 2.33 (m, CH₂C=OO), 2.28 (m, CH₂C=OO), 1.67, 1.60, 1.27 and 1.24 (all remaining hydrogens) ppm. ¹³C NMR (500 MHz, 298 K, CDCl₃): δ = 174.16 (PDL*-PDL, OCOCH₂), 174.05 (PDL*-VL, OCOCH₂), 173.54 (PDL-VL*-PDL, OCOCH₂), 173.50 (VL-VL*-PDL, OCOCH₂), 173.44 (PDL-VL*-VL, OCOCH₂), 173.41 (VL-VL*-VL, OCOCH₂), 64.73 (PDL*-VL, OCH₂), 64.52 (PDL*-PDL, OCH₂), 64.05 (VL*-VL, OCH₂), 63.86 (VL*-PDL), 34.54 (PDL*-PDL, OCOCH₂), 34.45 (PDL*-VL, OCOCH₂), 33.93 (PDL-VL*-PDL, OCOCH₂), 33.90 (VL-VL*-PDL, OCOCH₂), 33.85 (PDL-VL*-VL, OCOCH₂), 33.82 (VL-VL*-VL, OCOCH₂), 29.80-29.54, 29.41 (PDL, CH₂), 28.77 (VL, OCH₂CH₂), 26.05 (VL, OCOCH₂CH₂), 25.86 (PDL, CH₂), 25.13 (VL, OCOCH₂CH₂CH₂) ppm. SEC (CHCl₃): *M*_n = 14.2 kDa, *M*_w = 31.7 kDa, *D*_M = 2.23.

P(εCL-co-PDL):

^1H NMR (400 MHz, 298 K, CDCl_3): δ = 7.35 (s, Ar), 5.19 (s, $\text{C=OOCH}_2\text{Ar}$), 5.11 (s, $\text{C=OOCH}_2\text{Ar}$), 4.06 (t, $^3J_{\text{H-H}} = 4.2$ Hz, $\text{CH}_2\text{OC=O}$), 2.30 (m, $\text{CH}_2\text{C=OO}$), 1.64, 1.38 and 1.21 (all remaining hydrogens) ppm.

^{13}C NMR (700 MHz, 298 K, CDCl_3): δ = 174.13 (PDL*-PDL, OCOCH_2), 174.06 (PDL*- ϵCL , OCOCH_2), 173.75 (PDL- ϵCL^* -PDL, OCOCH_2), 173.73 (ϵCL - ϵCL^* -PDL, OCOCH_2), 173.68 (PDL- ϵCL^* - ϵCL , OCOCH_2), 173.66 (ϵCL - ϵCL^* - ϵCL , OCOCH_2), 64.67 (PDL*- ϵCL , OCH_2), 64.55 (PDL*-PDL, OCH_2), 64.29 (ϵCL^* - ϵCL , OCH_2), 64.17 (ϵCL^* -PDL), 34.56 (PDL*-PDL, OCOCH_2), 34.51 (PDL*- ϵCL , OCOCH_2), 34.34 (PDL- ϵCL^* -PDL, OCOCH_2), 34.32 (ϵCL - ϵCL^* -PDL, OCOCH_2), 34.29 (PDL- ϵCL^* - ϵCL , OCOCH_2), 34.27 (ϵCL - ϵCL^* - ϵCL , OCOCH_2), 29.80-29.64, 29.44 (PDL, CH_2), 28.50 (ϵCL , OCH_2CH_2), 25.69 (ϵCL , $\text{OCOCH}_2\text{CH}_2$), 25.63 (PDL, CH_2), 24.73 (ϵCL , $\text{OCOCH}_2\text{CH}_2\text{CH}_2$) ppm. SEC (CHCl_3): M_n = 25.5 kDa, M_w = 69.1 kDa, \bar{D}_M = 2.12.

P(ηCL-co-PDL):

^1H NMR (400 MHz, 298 K, CDCl_3): δ = 7.37 (s, Ar), 5.13 (s, $\text{C=OOCH}_2\text{Ar}$), 5.03 (s, $\text{C=OOCH}_2\text{Ar}$), 4.07 (t, $^3J_{\text{H-H}} = 6.7$ Hz, $\text{CH}_2\text{OC=O}$), 2.33 (m, $\text{CH}_2\text{C=OO}$), 1.65, 1.34 and 1.28 (all remaining hydrogens) ppm.

^{13}C NMR (500 MHz, 298 K, CDCl_3): δ = 174.10 (PDL*-PDL, OCOCH_2), 174.08 (PDL*- ηCL , OCOCH_2), 173.96 (ηCL^* -PDL, OCOCH_2), 173.95 (ηCL^* - ηCL , OCOCH_2), 64.54 (PDL*- ηCL , OCH_2), 64.50 (PDL*-PDL, OCH_2), 64.42 (ηCL^* - ηCL , OCH_2), 64.38 (ηCL^* -PDL), 34.50 (PDL*-PDL, OCOCH_2), 34.48 (PDL*- ηCL , OCOCH_2), 34.39 (ηCL^* -PDL, OCOCH_2), 34.38 (ηCL^* - ηCL , OCOCH_2), 29.80-29.50, 29.40 (PDL, CH_2), 29.08 (ηCL , OCH_2CH_2), 28.74 (ηCL , $\text{OCOCH}_2\text{CH}_2$), 25.94 (PDL, CH_2), 25.07 (ηCL , $\text{OCOCH}_2\text{CH}_2\text{CH}_2$) ppm. SEC (CHCl_3): M_n = 20.1 kDa, M_w = 56.4 kDa, \bar{D}_M = 2.80.

P(DDL-co-PDL):

^1H NMR (300 MHz, 298 K, CDCl_3): δ = 7.34 (s, Ar), 5.10 (s, $\text{C=OOCH}_2\text{Ar}$), 4.04 (t, $^3J_{\text{H-H}} = 6.7$ Hz, $\text{CH}_2\text{OC=O}$), 2.27 (t, $^3J_{\text{H-H}} = 7.5$ Hz, $\text{CH}_2\text{C=OO}$), 1.60, 1.24 (all remaining hydrogens) ppm. ^{13}C NMR (500 MHz, 298 K, CDCl_3): δ = 174.08 (PDL*, OCOCH_2), 174.07 (DDL*, OCOCH_2), 64.49 (OCH_2), 34.50 (OCOCH_2), 29.80-29.64, 29.38 (PDL, CH_2), 29.28 (DDL, CH_2), 28.77 (CL , OCH_2CH_2), 26.04 (DD, CH_2), 25.13 (PDL, CH_2) ppm. SEC (CHCl_3): M_n = 46.6 kDa, M_w = 73.7 kDa, \bar{D}_M = 1.58.

7.4.4 General Procedure of Degradation Studies

Polymer samples were pressed into 3 x Ø10 mm x 1mm discs whilst in the melt and cooled gently in order to remove air bubbles. In the case of P(PDL-*co*-δVL) only 2 discs were studied. The discs were submerged in 20 mL 5 M NaOH and heated in an incubator, with shaking, at 37 °C. The discs were removed at a weekly time point, rinsed with deionized water and the surface dried on blotting paper. The mass of each disc was recorded, before placing in 20 mL of fresh 5 M NaOH solution and repeating.

7.5 Experimental procedures for Chapter 3

7.5.1 Synthesis of menthide

Using a modified version of the previously reported procedure,³ menthone (16.0 mL, 92.8 mmol) was dissolved in CH₂Cl₂ (120 mL) and cooled in an ice bath. *m*-Chloroperoxybenzoic acid (40 g, 185.6 mmol) was slowly added to the solution before stirring at room temperature for 5 days. The solution was then cooled back to 0 °C before removal of salts over Celite® and washing with CH₂Cl₂ (2 × 60 mL). The combined solutions were then washed with 10% Na₂S₂O₅ solution (2 × 240 mL), saturated Na₂CO₃ solution (2 × 240 mL) and saturated NaCl (2 × 240 mL). The organic layer was dried with MgSO₄ before removal of solvent through rotary evaporation. Purification was achieved through silica gel chromatography using 6 : 4 petroleum ether (40-60 °C) : ethyl acetate as eluent. Yield = 11.4 g (66.8 mmol, 72%). Characterising data was consistent with the previous report.³

¹H NMR (400 MHz, 298 K, CDCl₃): δ = 4.04 (m, CH₂CH(^{*i*}Pr)OC=O), 2.51 (m, CH₂C=OO), 1.95 and 1.85 (m, CH₂), 1.59 (m, CH(CH₃)₂C), 1.29 (m, CH(CH₃)(CH₂)₂), 1.03 (d, CH₃C(CH₂)₂), 0.96 (dd, (CH₃)₂C(CH)) ppm. ¹³C NMR (125 MHz, 298 K, CDCl₃): δ = 175.02 (OCOCH₂), 84.78 (OCOCH(^{*i*}Pr)CH₂), 42.64 and 40.80 (CH₂COO), 37.52 and 34.34 (CH₂CH₂C(CH₃)H), 33.40 and 30.49 (CH₂C(CH₃)HCH₂), 31.02 and 26.76 (CH(^{*i*}Pr)CH₂CH₂), 26.73 and 24.03 (CHCH(CH₃)₂), 18.46 (CH₃CH(CH₂)₂), and 17.17 ((CH₃)₂CHCH) ppm.

7.5.2 Synthesis of dihydrocarvide

Using a previously reported procedure,⁴ (+)-dihydrocarvone (10.3 g, 67.8 mmol) was dissolved into a mixture of 200 mL water and 200 mL methanol and stirred at room temperature. Over the course of 24 h, oxone (7.4 g, 24.1 mmol) and sodium bicarbonate (5.3 g, 63.0 mmol) were added four times into the mixture. The reaction was continued for a further 24 h before salts were filtered off and methanol removed by rotary evaporation. Extraction of the product was carried out using diethyl ether (3 x 60 mL). The organic layer was washed with sodium metabisulfite solution (4 g in 70 mL) and water (2 x 70 mL). The solution was dried over magnesium sulphate before removal of solvent by rotary evaporation and purification on a silica column using 10 : 1 petroleum ether : ethyl acetate. Yield = 4.7 g (27.7 mmol, 41%). Characterising data was consistent with the previous report.⁴

¹H NMR (400 MHz, 298 K, CDCl₃): δ = 4.66 (d, CH₂=CH(CH₃)CH), 4.41 (m, CH₂CH(CH)OC=O), 2.69-2.48 (m, CH₂C=OO), 2.21 (m, (CH₂)₂CH(CH)), 1.86 (d, CH₂CH₂CH), 1.65 (s, CH₃C(CH)=CH₂), 1.57 (m, CH₂), 1.28 (d, CH₃CH(CH₂)O) ppm. ¹³C NMR (125 MHz, 298 K, CDCl₃): δ = 174.57 (OCOCH), 148.41 (CH₂=CH(CH₃)CH), 110.08 (CH₂=CH(CH₃)CH), 76.56 (OCOCH(CH₃)CH₂), 41.77 (CH(CH₂)₂C), 40.14 (CH₂COO), 35.79 (CH₂CH₂C(CH₃)HO), 34.21 (CH₂CH₂CH(C)), 22.55 (CH₃CH(CH₂)O) and 20.10 (CH₃C(=CH₂)C) ppm.

7.5.3 General procedure of menthide complexation

Using standard glovebox techniques, a vial was filled with Mg(BHT)₂(THF)₂ (30.0 mg, 49.4 μ mol), benzyl alcohol (5.1 μ L, 49.4 μ mol) and menthide (8.4 mg, 49.4 μ mol), before being dissolved into *d*-toluene. The solution was transferred into a Young's tap NMR tube and sealed. A ¹H NMR spectrum was recorded before the NMR tube was heated at 80 °C for 1 h and analysed again. A final ¹H NMR spectrum was recorded 24 h after heating.

¹H NMR (400 MHz, 298 K, CDCl₃): δ = 7.45, 7.19-6.99 (m, Ar), 5.17 (d, C=OOCH₂Ar), 4.75 (s, BHT ArOH), 3.52 (d, THF CH₂O), 3.45 (m, CH₂CH(ⁱPr)OC=O), 2.41, 2.23 (s, BHT ArCH₃), 2.08 (m, CH₂C=OO),

1.70 (m, CH_2), 1.62 (m, $\text{CH}(\text{CH}_3)_2\text{C}$), 1.58 (m, CH_2), 1.41 (m, $\text{CH}_3\text{CH}(\text{CH}_2)_2$), 1.36 (s, BHT $(\text{CH}_3)_3\text{C}$), 1.25 (m, $\text{CH}_3\text{CH}(\text{CH}_2)_2$), 0.88 (m, BHT ArCH_3), 0.74 (dd, $(\text{CH}_3)_2\text{C}(\text{CH})$) and 0.60 (d, $\text{CH}_3\text{CH}(\text{CH}_2)_2$) ppm. ^{13}C NMR (125 MHz, 298 K, CDCl_3): δ = 161.15 (MI, OCOCH_2), 152.06 (BHT, COH), 137.16 (BnOH, CCH_2), 135.96 (BHT, $\text{CC}(\text{CH}_3)_3$), 128.21 (BHT, CCH_3), 127.22 and 126.40 (BnOH), 125.80 (BHT, CCH_3), 68.04 ($\text{OCOCH}(\text{CH}_3)\text{CH}_2$), 42.24 (MI, CH_2COO), 37.03, 33.36 (MI, $\text{CH}_2\text{CH}_2\text{C}(\text{CH}_3)\text{H}$), 31.78 and 31.27 (BHT $\text{C}(\text{CH}_3)_3$), 29.84 (MI, $\text{CH}_2\text{CH}(\text{Pr})\text{COO}$), 25.71 (THF, CH_2), 20.42 (BHT, CCH_3), 19.96 (MI, $\text{CH}_2\text{CH}(\text{CH}_3)\text{CH}_2$), 18.21 and 14.35 (MI, $\text{CHCH}(\text{CH}_3)_2$) ppm.

7.5.4 General procedure of menthide homopolymerization

Using standard glovebox techniques, an ampoule was filled with $\text{Mg}(\text{BHT})_2(\text{THF})_2$ (10.0 mg, 16.5 μmol), benzyl alcohol (1.7 μL , 16.5 μmol), menthide (140.2 mg, 824.0 μmol) and toluene (0.857 mL). The ampoule was sealed, shaken until all solids dissolved and heated at 80 °C for a defined time period. The reaction was quenched with the addition of acidified (5% HCl) methanol. Polymer was recovered through the evaporation of solvents and purified through washing with cold hexanes.

^1H NMR (400 MHz, 298 K, CDCl_3): δ = 7.32 (m, Ar), 5.07 (d, $\text{C}=\text{OOCH}_2\text{Ar}$), 4.69 (m, $\text{CH}_2\text{CH}(\text{Pr})\text{OC}=\text{O}$), 2.30 (m, $\text{CH}_2\text{C}=\text{OO}$), 1.90 and 1.78 (m, CH_2), 1.62 (m, $\text{CH}(\text{CH}_3)_2\text{C}$), 1.13 (m, $\text{CH}(\text{CH}_3)(\text{CH}_2)_2$), 0.91 (m, $\text{CH}_3\text{C}(\text{CH}_2)_2$), 0.85 (dd, $(\text{CH}_3)_2\text{C}(\text{CH})$) ppm. ^{13}C NMR (125 MHz, 298 K, CDCl_3): δ = 173.02 (OCOCH_2), 78.36 ($\text{OCOCH}(\text{CH}_3)\text{CH}_2$), 41.98 (CH_2COO), 32.63 ($\text{CH}_2\text{CH}_2\text{C}(\text{CH}_3)\text{H}$), 28.48 ($\text{CH}_2\text{CH}(\text{Pr})\text{COO}$), 19.79 ($\text{CH}_2\text{CH}(\text{CH}_3)\text{CH}_2$), 18.69 and 17.58 ($\text{CHCH}(\text{CH}_3)_2$) ppm. SEC (CHCl_3): M_n = 7.9 kDa, M_w = 9.5 kDa, D_M = 1.20.

7.5.5 General procedure of menthide and ω -pentadecalactone copolymerization

Using standard glovebox techniques, an ampoule was filled with $\text{Mg}(\text{BHT})_2(\text{THF})_2$ (10.0 mg, 16.5 μmol), initiator (16.5 μmol), menthide (140.2 mg, 824.0 μmol) and ω -pentadecalactone stock solution (75 wt.% toluene, 824.0 μmol). The ampoule was sealed and heated at 80 °C for a defined time period. The reaction was quenched with the addition of acidified (5% HCl) methanol. Polymer was recovered through the evaporation of solvents and purified through washing with cold hexanes.

^1H NMR (400 MHz, 298 K, CDCl_3): δ = 7.33 (s, Ar), 5.09 (s, $\text{C}=\text{OOCH}_2\text{Ar}$), 4.70 (m, MI $\text{CH}_2\text{OC}=\text{O}$), 4.03 (m, PDL $\text{CH}_2\text{OC}=\text{O}$), 2.26 (m, PDL $\text{CH}_2\text{C}=\text{OO}$), 2.06 (m, MI $\text{CH}_2\text{C}=\text{OO}$), 0.91 (s, MI $\text{CH}_3\text{CH}(\text{CH}_2)_2$), 0.86 (s, MI $(\text{CH}_3)_2\text{CHCH}$), 2.15, 1.91, 1.79, 1.54, and 1.23 (all remaining hydrogens) ppm. ^{13}C NMR (125 MHz, 298 K, CDCl_3): δ = 174.15 (PDL*-PDL, OCOCH_2), 173.85 (PDL*-MI, OCOCH_2), 173.24 (MI*-PDL, OCOCH_2), 173.02 (MI*-MI, OCOCH_2), 78.37 (MI*-MI, OCH_2), 64.51 (PDL*-PDL, OCH_2), 42.01 (MI, CH_2COO) 34.54 (PDL CH_2COO), 32.66 (MI, $\text{CH}_2\text{CH}_2\text{CH}(\text{CH}_3)$) 31.20 (MI, $\text{CH}_2\text{CH}(\text{CH}_3)\text{CH}_2$), 30.40 (MI, $\text{CH}(\text{Pr})\text{CH}_2\text{CH}_2$), 19.81 (MI $\text{CH}_3\text{CH}(\text{CH}_2)_2$), 18.72 and 17.60 (MI $(\text{CH}_3)_2\text{CHCH}$), 29.80-29.27, 28.75, 28.51, 26.04 and 25.23 (all other carbons) ppm. SEC (CHCl_3): M_n = 13.4 kDa, M_w = 24.0 kDa, \mathcal{D}_M = 1.79.

7.5.6 General procedure of ω -pentadecalactone and ϵ -substituted ϵ -lactone copolymerization

Using standard glovebox techniques, an ampoule was filled with $\text{Mg}(\text{BHT})_2(\text{THF})_2$ (10.0 mg, 16.5 μmol), benzyl alcohol initiator (1.7 μL , 16.5 μmol), ϵ -substituted ϵ -lactone (824.0 μmol) and ω -pentadecalactone stock solution (75 wt.% toluene, 824.0 μmol). The ampoule was sealed and heated at 80 °C for a defined time period. The reaction was quenched with the addition of acidified (5% HCl) methanol. Polymer was recovered through the evaporation of solvents and purified through washing with cold hexanes.

P(PDL-co- ϵ HL):

^1H NMR (400 MHz, 298 K, CDCl_3): δ = 7.32 (s, Ar), 5.09 (s, $\text{C}=\text{OOCH}_2\text{Ar}$), 4.87 (m, ϵDL $\text{CH}_2\text{OC}=\text{O}$), 4.03 (m, PDL $\text{CH}_2\text{OC}=\text{O}$), 3.61 (m, CH_2OH), 2.26, 1.59, 1.47, 1.27 and 1.17 (all remaining hydrogens) ppm. ^{13}C NMR (125 MHz, 298 K, CDCl_3): δ = 174.09 (PDL*-PDL, OCOCH_2), 173.71 (PDL*- ϵHL , OCOCH_2), 173.59 (ϵHL *-PDL, OCOCH_2), 173.22 (ϵHL *- ϵHL , OCOCH_2), 128.62 and 128.25 (Aromatic C), 70.65 (ϵHL *- ϵHL , OCH_2), 70.50 (PDL*- ϵHL , OCH_2), 64.58 (ϵHL *- ϵHL , OCH_2), 64.49 (PDL*-PDL, OCH_2), 35.67 (ϵHL , CH_2COO) 34.58 (PDL CH_2COO), 34.50 (ϵHL , $\text{CH}_2\text{CH}_2\text{CH}(\text{CH}_3)$) 34.28 (ϵHL , $\text{CH}_2\text{CH}(\text{CH}_3)\text{CH}_2$), 20.05 (ϵHL $(\text{CH}_3)_2\text{CHCH}$), 29.74-29.27, 28.75, 26.05 and 25.17-24.88 (all other carbons) ppm. SEC (CHCl_3): M_n = 23.6 kDa, M_w = 40.7 kDa, \mathcal{D}_M = 2.70.

P(PDL-co-εDL):

^1H NMR (400 MHz, 298 K, CDCl_3): δ = 7.33 (s, Ar), 5.09 (s, $\text{C}=\text{OOCH}_2\text{Ar}$), 4.84 (m, $\epsilon\text{DL CH}_2\text{OC}=\text{O}$), 4.03 (m, PDL $\text{CH}_2\text{OC}=\text{O}$), 3.63 (m, CH_2OH), 0.87 (s, $\epsilon\text{DL CH}_3(\text{CH}_2)_3$), 2.26, 1.59, 1.50, 1.26 and 0.87 (all remaining hydrogens) ppm. ^{13}C NMR (125 MHz, 298 K, CDCl_3): δ = 174.10 (PDL*-PDL, OCOCH_2), 173.75 (PDL*- ϵDL and ϵDL *-PDL, OCOCH_2), 173.40 (ϵDL *- ϵDL , OCOCH_2), 128.64 and 128.26 (Aromatic C), 73.97 (ϵDL *- ϵDL , OCH_2), 73.83 (PDL*- ϵDL , OCH_2), 64.59 (ϵDL *-PDL, OCH_2), 64.50 (PDL*-PDL, OCH_2), 34.60 (ϵDL , CH_2COO) 34.51 (PDL CH_2COO), 33.92 (ϵDL , $\text{CH}_2\text{CH}_2\text{CH}(\text{Bu})$) 33.84 (ϵDL , $\text{CH}_2\text{CH}(\text{Bu})\text{CH}_2$), 14.11 ($\epsilon\text{DL CH}_3(\text{CH}_2)_3$), 29.75-29.27, 28.77, 27.57, 26.05, 25.25-25.04 and 22.68 (all other carbons) ppm. SEC (CHCl_3): M_n = 21.4 kDa, M_w = 56.5 kDa, \mathcal{D}_M = 2.6.

P(PDL-co-DHC):

^1H NMR (400 MHz, 298 K, CDCl_3): δ = 7.33 (s, Ar), 5.09 (s, $\text{C}=\text{OOCH}_2\text{Ar}$), 4.82 (m, DHC $\text{CH}_2\text{OC}=\text{O}$), 4.73 (d, $\text{CH}_2=\text{C}(\text{CH}_3)\text{CH}$) 4.03 (m, PDL $\text{CH}_2\text{OC}=\text{O}$), 3.63 (m, CH_2OH), 2.51 (m, PDL $\text{CH}_2\text{C}=\text{OO}$), 2.26 (m, DHC $\text{CH}_2\text{C}=\text{OO}$), 1.15 (m, DHC $\text{CH}_3\text{CHO}(\text{CH}_2)$), 1.59, 1.40 and 1.23 (all remaining hydrogens) ppm. ^{13}C NMR (125 MHz, 298 K, CDCl_3): δ = 174.33 (PDL*-PDL, OCOCH_2), 173.78 (PDL*-DHC, OCOCH_2), 172.81 (DHC*-PDL, OCOCH_2), 172.26 (DHC*-DHC, OCOCH_2), 145.53 (DHC, $\text{CH}_2=\text{C}(\text{CH}_3)\text{CH}$), 128.57 and 128.32 (Aromatic C), 112.72 (DHC, $\text{CH}_2=\text{C}(\text{CH}_3)\text{CH}$), 70.99 (DHC*-DHC, OCH_2), 70.77 (PDL*-DHC, OCH_2), 64.64 (DHC*-PDL, OCH_2), 64.55 (PDL*-PDL, OCH_2), 50.54 (DHC, $(\text{CH}_2)_2\text{CHC}(\text{CH}_3)=\text{CH}_2$), 43.84 (DHC, $(\text{CH}_2)_2\text{CHC}(\text{CH}_3)=\text{CH}_2$) 39.44 (DHC, CH_2COO), 34.46 (PDL, CH_2COO), 33.54 (DHC, $\text{CH}_2\text{CH}_2\text{CH}(\text{CH}_3)$), 19.94 (DHC $\text{CH}_3\text{CH}(\text{CH}_2)\text{O}$), 18.45 (DHC, $\text{CH}_3\text{C}(\text{CH}_2)=\text{CH}$), 29.68-29.20, 28.68, 28.40, 27.89, 27.15, 26.93, 26.69, 26.37, 25.97 and 25.06 (all other carbons) ppm. SEC (CHCl_3): M_n = 6.1 kDa, M_w = 9.7 kDa, \mathcal{D}_M = 1.6.

7.5.7 General procedure for the transesterification of poly(menthide) and poly(ω -pentadecalactone)

Using standard glovebox techniques, an ampoule was filled with $\text{Mg}(\text{BHT})_2(\text{THF})_2$ (10.0 mg, 16.5 μmol), poly(menthide) ($M_n = 10.7$ kDa, 57.5 mg, 5.4 μmol), poly(ω -pentadecalactone) ($M_n = 10.1$ kDa, 102.2 mg, 10.1 μmol) and toluene (2 mL). The ampoule was sealed and heated at 80 °C for a defined time period. The reaction was quenched with the addition of acidified (5% HCl) methanol. Polymer was recovered through the evaporation of solvents and purified through washing with cold hexanes.

7.5.8 General procedure for thiol-ene addition to P(PDL-co-DHC)

Using a previously reported procedure,⁴ P(PDL-co-DHC) (134.3 mg, 12.5 μmol , 432.6 μmol olefin), thiol (4.8 mmol, 11 equivalents per olefin) and 2,2-dimethoxy-2-phenylacetophenone (25.5 mg, 99.5 μmol) were dissolved in CH_2Cl_2 to a total concentration of 2.5 M. The solution was transferred into an ampoule and oxygen removed by freeze-pump-thawing three times. The ampoule was refilled with argon and subjected to a UV source for 4 h. The solution was diluted with 25 mL chloroform and washed three times with 25 mL aqueous bleach solution to remove unused thiol. Polymer was purified through precipitation out of excess methanol.

P(PDL-co-DHCME):

¹H NMR (400 MHz, 298 K, CDCl_3): δ = 7.35 (s, Ar), 5.10 (s, $\text{C}=\text{OOCH}_2\text{Ar}$), 4.94 (m, DHCME $\text{CH}_2\text{OC}=\text{O}$), 4.75 (d, $\text{CH}_2=\text{C}(\text{CH}_3)\text{CH}$), 4.04 (m, PDL $\text{CH}_2\text{OC}=\text{O}$), 3.72 (m, CH_2OH), 3.66 (m, CH_2OH), 2.99 and 2.86 (m, DHCME $\text{SCH}_2\text{CH}(\text{CH}_3)\text{CH}$), 2.69 (m, DHCME $\text{SCH}_2\text{CH}_2\text{OH}$), 2.56 (m, PDL $\text{CH}_2\text{C}=\text{OO}$), 2.28 (m, DHCME $\text{CH}_2\text{C}=\text{OO}$), 0.93 (m, DHC $\text{CH}_3\text{CH}(\text{CH}_2)\text{O}$), 2.10, 1.78, 1.70-0.98 (all remaining hydrogens) ppm. ¹³C NMR (125 MHz, 298 K, CDCl_3): δ = 174.16 (PDL*-PDL, OCOCH_2), 173.70 (PDL*-DHCME, OCOCH_2), 173.36 (DHCME*-PDL, OCOCH_2), 172.26 (DHCME*-DHCME, OCOCH_2), 145.66 (DHC, $\text{CH}_2=\text{C}(\text{CH}_3)\text{CH}$), 128.66 and 128.28 (Aromatic C), 112.81 (DHC, $\text{CH}_2=\text{C}(\text{CH}_3)\text{CH}$), 71.15 (DHCME*-DHCME, OCH_2), 70.69 (PDL*-DHCME, OCH_2), 70.60 (PDL*-DHC, OCH_2), 64.87 (DHC*-PDL, OCH_2),

64.54 (PDL*-PDL, OCH₂), 63.19 (DHCME, CH₂CH₂OH), 51.56 (DHCME, (CH₂)₂CHC(CH₃)CH₂S), 43.88 (DHC, (CH₂)₂CHC(CH₃)=CH₂), 38.39 (DHCME, CH₂COO), 34.54 (PDL, CH₂COO), 33.66 (DHCME, CH₂CH₂CH(CH₃)), 29.68-29.30, 28.78, 26.07 and 25.15 (all other carbons) ppm. SEC (CHCl₃): M_n = 4.4 kDa, M_w = 5.7 kDa, \mathcal{D}_M = 1.30.

P(PDL-co-DHCBM):

¹H NMR (400 MHz, 298 K, CDCl₃): δ = 7.39-7.28 (m, Ar), 5.07 (s, C=OOCH₂Ar), 4.81 (m, DHCBM CH₂OC=O), 4.73 (d, CH₂=C(CH₃)CH), 3.99 (m, PDL CH₂OC=O), 3.66 (m, CH₂OH), 3.60 (s, DHCBM SCH₂Bn), 2.24 (m, DHC CH₂C=OO), 0.96 (m, DHC CH₃CHO(CH₂)), 2.61-2.31, 1.94, 1.57, 1.42, 1.23 and 1.16 (all remaining hydrogens) ppm. ¹³C NMR (125 MHz, 298 K, CDCl₃): δ = 174.08 (PDL*-PDL, OCOCH₂), 173.55 (PDL*-DHCBM, OCOCH₂), 172.93 (DHCBM*-PDL, OCOCH₂), 172.35 (DHCBM*-DHCBM, OCOCH₂), 130.22, 130.12, 129.05 and 128.47 (Aromatic C), 112.78 (DHC, CH₂=C(CH₃)CH), 71.29 (DHCBM*-DHCBM, OCH), 70.65 (PDL*-DHCBM, OCH), 64.91 (DHCBM*-PDL, OCH₂), 64.47 (PDL*-PDL, OCH₂), 51.51 (DHCBM, (CH₂)₂CHC(CH₃)CH₂S), 43.81 (DHC, CH₂COO), 34.48 (PDL, CH₂COO), 33.54 (DHC, CH₂CH₂CH(CH₃)), 30.08-29.18, 28.74, 26.02, 25.11, 20.05 and 18.56 (all other carbons) ppm. SEC (CHCl₃): M_n = 5.0 kDa, M_w = 6.5 kDa, \mathcal{D}_M = 1.30.

P(PDL-co-DHCDT):

¹H NMR (400 MHz, 298 K, CDCl₃): δ = 7.32 (m, Ar), 5.08 (s, C=OOCH₂Ar), 4.84 (m, DHCDT CH₂OC=O), 4.73 (d, DHC CH₂=C(CH₃)CH), 4.02 (m, PDL CH₂OC=O), 3.63 (m, SCH₂CH₂), 3.60 (s, CH₂CH₂OH), 2.25 (m, DHC CH₂C=OO), 1.01 (m, DHCDT CH₃CHO(CH₂)), 0.85 (t, DHCDT CH₃(CH₂)₁₁, ³J_{H-H} = 6.9 Hz), 2.64, 1.74, 1.58 and 1.35-1.10 (all remaining hydrogens) ppm. ¹³C NMR (125 MHz, 298 K, CDCl₃): δ = 174.05 (PDL*-PDL, OCOCH₂), 173.52 (PDL*-DHCDT, OCOCH₂), 172.82 (DHCDT*-PDL, OCOCH₂), 172.55 (DHCDT*-DHCDT, OCOCH₂), 128.58 and 128.36 (Aromatic C), 112.76 (DHC, CH₂=C(CH₃)CH), 71.16 (DHCDT*-DHCDT, OCH₂), 70.56 (PDL*-DHCDT, OCH₂), 64.90 (DHC*-PDL, OCH₂), 64.45 (PDL*-PDL, OCH₂), 51.48 (DHCDT, (CH₂)₂CHC(CH₃)CH₂S), 39.27 (DHCDT, CH₂COO), 34.46 (PDL, CH₂COO), 19.95 (DHCDT, CH₃CH(CH₂)O), 14.19 (DHCDT, CH₃(CH₂)₁₁S), 34.73, 34.17, 33.98-33.34,

32.90, 31.98, 29.81-28.44, 26.01, 25.10, 26.37, 22.75 and 25.06 (all other carbons) ppm. SEC (CHCl_3):

$M_n = 5.3$ kDa, $M_w = 7.1$ kDa, $\mathcal{D}_M = 1.35$.

7.6 Experimental procedures for Chapter 4

7.6.1 Synthesis of ϵ -heptalactone

Using a modified version of the previously reported procedure,² 2-methylcyclohexanone (6.1 g, 54.4 mmol) was dissolved in CH_2Cl_2 (250 mL) and cooled in an ice bath. *m*-Chloroperoxybenzoic acid (30 g, 139.2 mmol) was slowly added to the solution before stirring at room temperature for 5 days. The solution was then cooled back to 0 °C before removal of salts over Celite® and washing with CH_2Cl_2 (2 × 125 mL). The combined solutions were then washed with 10% $\text{Na}_2\text{S}_2\text{O}_5$ solution (2 × 500 mL), saturated Na_2CO_3 solution (2 × 500 mL) and saturated NaCl (2 × 500 mL). The organic layer was dried with MgSO_4 before removal of solvent through rotary evaporation. Purification was achieved through silica gel chromatography using 6 : 4 petroleum ether (40-60 °C) : ethyl acetate as eluent. Yield = 5.1 g (40.1 mmol, 74%). Characterising data was consistent with the previous report.²

^1H NMR (400 MHz, 298 K, CDCl_3): δ = 4.42 (m, $\text{CH}_2\text{CH}(\text{CH}_3)\text{OC}=\text{O}$), 2.60 (m, $\text{CH}_2\text{C}=\text{OO}$), 1.87 and 1.57 (m, CH_2), 1.30 (d, CH_3) ppm. ^{13}C NMR (125 MHz, 298 K, CDCl_3): δ = 175.75 (OCOCH_2), 76.89 ($\text{OCOCH}(\text{CH}_3)\text{CH}_2$), 36.25 (CH_2COO), 35.06 ($\text{CH}_2\text{CH}_2\text{C}(\text{CH}_3)\text{H}$), 28.31 ($\text{CH}_2\text{CH}_2\text{COO}$), 22.94 ($\text{CH}(\text{CH}_3)\text{CH}_2\text{CH}_2$) and 22.64 (CHCH_3) ppm.

7.6.2 General procedure of menthide and non-substituted lactone copolymerization

Using standard glovebox techniques, an ampoule was filled with $\text{Mg}(\text{BHT})_2(\text{THF})_2$ (10.0 mg, 16.5 μmol), benzyl alcohol initiator (1.7 μL , 16.5 μmol), menthide (140.2 g, 824.0 μmol), lactone (824.0 μmol) and diluted to 2 M in toluene. The ampoule was sealed and heated at 80 °C for a defined time period. The reaction was quenched with the addition of acidified (5% HCl) methanol. Polymer was recovered through the evaporation of solvents and purified through washing with cold hexanes.

P(δVL-co-MI):

¹H NMR (400 MHz, 298 K, CDCl₃): δ = 7.32 (s, Ar), 5.07 (s, C=OOCH₂Ar), 4.69 (m, MI CH₂OC=O), 4.05 (m, δVL CH₂OC=O), 3.30 (m, CH₂OH), 2.32, 2.08, 1.90, 1.78, 1.65, 1.48, 1.30, 1.15 and 0.88 (all remaining hydrogens) ppm. ¹³C NMR (125 MHz, 298 K, CDCl₃): δ = 173.80 (δVL*-δVL, OCOCH₂), 173.35 (δVL*-MI, OCOCH₂), 173.17 (MI*-δVL, OCOCH₂), 173.11 (MI*-MI, OCOCH₂), 128.61 and 128.27 (Aromatic C), 78.46 (MI*-MI, OCH₂), 76.54 (δVL*-MI, OCH₂), 69.52 (MI*-δVL, OCH₂), 63.90 (δVL*-δVL, OCH₂), 41.69 (MI*-MI, CH₂COO), 41.50 (MI*-δVL, CH₂COO), 34.08 and 33.75 (δVL*-MI, CH₂COO), 33.43 (δVL*-δVL, CH₂COO), 32.51 (MI, CH₂CH(CH₃)CH₂), 31.48 and 31.19 (MI, CHCH(CH₃)₂), 18.96 and 18.71 (MI, CH₃CH(CH₂)₂), 17.50 and 17.05 (MI (CH₃)CHCH), 30.58, 30.38, 28.53, 28.17, 21.69, 21.50, 19.97 and 19.79 (all other carbons) ppm. SEC (CHCl₃): *M_n* = 23.9 kDa, *M_w* = 51.5 kDa, *D_M* = 2.29.

P(εCL-co-MI):

¹H NMR (400 MHz, 298 K, CDCl₃): δ = 7.33 (s, Ar), 5.05 (s, C=OOCH₂Ar), 4.77 (m, MI CH₂OC=O), 4.11 (m, εCL CH₂OC=O), 3.79 (m, CH₂OH), 0.93 (s, MI CH₃(CH₂)₃), 2.36, 2.24, 2.12, 1.98, 1.86, 1.69, 1.59, 1.44, 1.35, 1.21 and 0.98 (all remaining hydrogens) ppm. ¹³C NMR (125 MHz, 298 K, CDCl₃): δ = 173.57 (εCL*-εCL, OCOCH₂), 173.38 (εCL*-MI, OCOCH₂), 173.10 (MI*-εCL, OCOCH₂), 172.92 (MI*-MI, OCOCH₂), 128.60 and 128.23 (Aromatic C), 78.29 (MI*-MI, OCH₂), 73.36 (εCL*-MI, OCH₂), 64.19 (MI*-εCL, OCH₂), 64.09 (εCL*-εCL, OCH₂), 41.96 (MI*-MI, CH₂COO), 41.67 (MI*-εCL, CH₂COO), 34.46 (εCL*-MI, CH₂COO), 34.15 (εCL*-εCL, CH₂COO), 32.54 (MI, CH₂CH(CH₃)CH₂), 31.19 (MI, CHCH(CH₃)₂), 19.78 (MI, CH₃CH(CH₂)₂), 18.69 and 17.53 (MI (CH₃)₂CHCH), 28.44, 25.58, 24.81 and 24.62 (all other carbons) ppm. SEC (CHCl₃): *M_n* = 28.0 kDa, *M_w* = 40.9 kDa, *D_M* = 1.46.

P(ζHL-co-MI):

¹H NMR (400 MHz, 298 K, CDCl₃): δ = 7.34 (s, Ar), 5.10 (s, C=OOCH₂Ar), 4.71 (m, MI CH₂OC=O), 4.04 (m, ζHL CH₂OC=O), 3.62 (m, CH₂OH), 0.93 (d, MI CH₃(CH₂)₃), 0.87 (d, MI (CH₃)CHCH), 2.28, 2.07, 2.07, 1.92, 1.80, 1.66-1.44, 1.41, 1.40-1.22 and 1.16 (all remaining hydrogens) ppm. ¹³C NMR (125 MHz, 298 K, CDCl₃): δ = 173.88 (ζHL*-ζHL, OCOCH₂), 173.64 (ζHL*-MI, OCOCH₂), 173.23 (MI*-ζHL,

OCOCH₂), 173.01 (MI*-MI, OCOCH₂), 128.67 and 128.33 (Aromatic C), 78.37 (MI*-MI, OCH₂), 64.38 (ζHL*-ζHL, OCH₂), 42.03 (MI*-MI, CH₂COO), 41.79 (MI*-ζHL), 34.31 (ζHL*-MI, CH₂COO), 32.67 (MI, CH₂CH(CH₃)CH₂), 31.22 (MI, CHCH(CH₃)₂), 19.83 (MI, CH₃CH(CH₂)₂), 18.74 and 17.63 (MI (CH₃)CHCH), 28.88, 28.56, 25.74 and 24.94 (all other carbons) ppm. SEC (CHCl₃): M_n = 3.8 kDa, M_w = 11.9 kDa, \mathcal{D}_M = 3.13.

P(ηCL-co-MI):

¹H NMR (400 MHz, 298 K, CDCl₃): δ = 7.34 (s, Ar), 5.10 (s, C=OOCH₂Ar), 4.71 (m, MI CH₂OC=O), 4.04 (m, ηCL CH₂OC=O), 3.62 (m, CH₂OH), 0.93 (d, MI CH₃(CH₂)₃), 0.87 (d, MI (CH₃)CHCH), 2.28, 2.07, 1.92, 1.80, 1.66-1.41, 1.32 and 1.16 (all remaining hydrogens) ppm. ¹³C NMR (125 MHz, 298 K, CDCl₃): δ = 173.98 (ηCL*-ηCL, OCOCH₂), 173.71 (ηCL*-MI, OCOCH₂), 173.25 (MI*-ηCL, OCOCH₂), 173.02 (MI*-MI, OCOCH₂), 128.67 and 128.30 (Aromatic C), 78.38 (MI*-MI, OCH₂), 64.45 (εCL*-εCL, OCH₂), 42.04 (MI*-MI, CH₂COO), 41.79 (MI*-ηCL), 34.68 (ηCL*-MI, CH₂COO), 34.40 (ηCL*-ηCL, CH₂COO), 32.69 (MI, CH₂CH(CH₃)CH₂), 31.22 (MI, CHCH(CH₃)₂), 19.84 (MI, CH₃CH(CH₂)₂), 18.75 and 17.63 (MI (CH₃)CHCH), 29.10, 28.72, 28.61, 28.54, 25.88, 25.17 and 25.00 (all other carbons) ppm. SEC (CHCl₃): M_n = 18.4 kDa, M_w = 28.1 kDa, \mathcal{D}_M = 1.52.

7.6.3 General procedure of menthide and ε-substituted ε-lactone copolymerization

Using standard glovebox techniques, an ampoule was filled with Mg(BHT)₂(THF)₂ (10.0 mg, 16.5 μmol), benzyl alcohol initiator (1.7 μL, 16.5 μmol), menthide (140.2 mg, 824.0 μmol), ε-substituted ε-lactone (824.0 μmol) and diluted to 1 M in toluene. The ampoule was sealed and heated at 80 °C for a defined time period. The reaction was quenched with the addition of acidified (5% HCl) methanol. Polymer was recovered through the evaporation of solvents and purified through washing with cold hexanes.

P(εHL-co-MI):

¹H NMR (400 MHz, 298 K, CDCl₃): δ = 7.34 (s, Ar), 5.10 (s, C=OOCH₂Ar), 4.87 (m, εHL CH₂OC=O), 4.71 (m, MI CH₂OC=O), 3.66 (m, CH₂OH), 1.18 (d, εHL CH₃CH), 0.93 (d, MI CH₃(CH₂)₃), 0.87 (d, MI

(CH₃)CHCH), 2.27, 2.07, 1.92, 1.80 and 1.66-1.22 (all remaining hydrogens) ppm. ¹³C NMR (125 MHz, 298 K, CDCl₃): δ = 173.84 (ϵ HL*-OBn, OCOCH₂), 173.68 (MI*-OBn, OCOCH₃), 173.48 (ϵ HL*-MI, OCOCH₂), 173.27 (ϵ HL*- ϵ HL, OCOCH₂), 173.02 (MI*-MI, OCOCH₂), 172.59 (MI*- ϵ HL, OCOCH₂), 129.15 and 128.34 (Aromatic C), 78.38 (MI*-MI, OCH₂), 70.70 (ϵ HL*- ϵ HL, OCH₂), 50.96 (ϵ HL*- ϵ HL, CH₂COO), 42.04 (MI*-MI, CH₂COO), 35.69 (ϵ HL, CH₂CH₂COO), 34.61 (ϵ HL, CH₂CH₂CH(CH₃)), 32.68 (MI, CH₂CH(CH₃)CH₂), 31.22 (MI, CHCH(CH₃)₂), 20.06 (ϵ HL, (CH₃CH(CH₂)O), 19.84 (MI, CH₃CH(CH₂)₂), 18.75 and 17.63 (MI (CH₃)CHCH), 30.43, 28.53, 25.09, 24.97 and 21.57 (all other carbons) ppm. SEC (CHCl₃): M_n = 9.1 kDa, M_w = 19.2 kDa, \bar{D}_M = 2.12.

P(ϵ DL-co-MI):

¹H NMR (400 MHz, 298 K, CDCl₃): δ = 7.36 (s, Ar), 5.11 (s, C=OOCH₂Ar), 4.86 (m, ϵ DL CH₂OC=O), 4.72 (m, MI CH₂OC=O), 3.67 (m, CH₂OH), 0.94 (d, MI CH₃(CH₂)₃), 0.89 (d, MI (CH₃)CHCH), 2.28, 2.08, 1.93, 1.81 and 1.68-1.11 (all remaining hydrogens) ppm. ¹³C NMR (125 MHz, 298 K, CDCl₃): δ = 173.78 (ϵ DL*-OBn, OCOCH₂), 173.65 (MI*-OBn, OCOCH₃), 173.45 (ϵ DL*-MI, OCOCH₂), 173.39 (ϵ DL*- ϵ DL, OCOCH₂), 172.98 (MI*-MI, OCOCH₂), 172.89 (MI*- ϵ DL, OCOCH₂), 128.65 and 128.30 (Aromatic C), 78.38 (MI*-MI, OCH₂), 73.95 (ϵ DL*- ϵ DL, OCH₂), 51.49 (ϵ DL*- ϵ DL, CH₂COO), 42.01 (MI*-MI, CH₂COO), 34.58 (ϵ DL, CH₂CH₂CH(CH₃)), 19.82 (MI, CH₃CH(CH₂)₂), 18.72 and 17.61 (MI (CH₃)CHCH), 14.01 (ϵ DL, CH₃(CH₂)₃), 33.86, 32.63, 31.68, 31.20, 30.41, 28.56, 27.55, 25.10, 22.75 and 22.66 (all other carbons) ppm. SEC (CHCl₃): M_n = 16.7 kDa, M_w = 26.4 kDa, \bar{D}_M = 1.58.

7.6.4 General procedure for the transesterification of poly(menthide) and poly(ϵ -caprolactone)

Using standard glovebox techniques, an ampoule was filled with Mg(BHT)₂(THF)₂ (10.0 mg, 16.5 μ mol), poly(menthide) (M_n = 6.4 kDa, 140.0 mg, 22.0 μ mol), poly(ϵ -caprolactone) (M_n = 0.6 kDa, 99.0 mg, 165.0 μ mol) and toluene (2 mL). The ampoule was sealed and heated at 80 °C for a defined time period. The reaction was quenched with the addition of acidified (5% HCl) methanol. Polymer was recovered through the evaporation of solvents and purified through washing with cold hexanes.

7.6.5 General procedure for the transesterification of poly(menthide) and poly(ϵ -heptalactone)

Using standard glovebox techniques, an ampoule was filled with $\text{Mg}(\text{BHT})_2(\text{THF})_2$ (10.0 mg, 16.5 μmol), poly(menthide) ($M_n = 10.7$ kDa, 43.5 mg, 4.1 μmol), poly(ϵ -heptalactone) ($M_n = 3.4$ kDa, 37.0 mg, 10.9 μmol) and toluene (2 mL). The ampoule was sealed and heated at 80 °C for a defined time period. The reaction was quenched with the addition of acidified (5% HCl) methanol. Polymer was recovered through the evaporation of solvents and purified through washing with cold hexanes.

7.7 References

1. J. Calabrese, M. A. Cushing and S. D. Ittel, *Inorg. Chem.*, 1988, **27**, 867-870.
2. L. van der Mee, F. Helmich, R. de Bruijn, J. A. J. M. Vekemans, A. R. A. Palmans and E. W. Meijer, *Macromolecules*, 2006, **39**, 5021-5027.
3. D. Zhang, M. A. Hillmyer and W. B. Tolman, *Biomacromolecules*, 2005, **6**, 2091-2095.
4. S. C. Knight, C. P. Schaller, W. B. Tolman and M. A. Hillmyer, *RSC Adv.*, 2013, **3**, 20399-20404.